Investigating the Mechanisms of Neutrophil Recruitment to Head and Neck Cancers in vitro and in vivo

Hanan Abdulrauf Niaz

Unit of Oral and Maxillofacial Medicine and Surgery
School of Clinical Dentistry
University of Sheffield
United Kingdom

A thesis submitted for the degree of Doctor of Philosophy March 2017

This thesis is dedicated to my parents Abdulrauf and Najat, My husband Osama and my angels Jana and Joud , without whom none of my success would be possible

DECLARATION

No portion of the work referred to in this thesis has been submitted in support of an application for another qualification of this or any other University or Institute of Learning.

ACKNOWLEDGMENTS

The path towards this dissertation has been long and circuitous. I am deeply grateful to almighty GOD for the wisdom, the strength he bestowed upon me, peace of my mind and patience in order to accomplish a life changing experience.

I would like to express my very great appreciation to Dr Craig Murdoch for giving me the chance of exploring the fascinating world of immunology (Wonderland) and for his valuable constructive suggestions during the planning and development of this research work. I am particularly grateful for his understanding, patience, motivation and immense knowledge.

My sincere thanks also go to Dr Keith Hunter for his willingness to give his time so generously, and teaching me and assisting with histology. I am particularly grateful for the assistance given by Dr Simon Tazzyman for passing on all his neutrophil knowledge and all the support he provided throughout the years. My deep gratitude also goes to Dr Munitta Muthana for the assistance with the *in vivo* study. My thanks are also extended to Dr Helen Colley for access to patient biopsy material and to Dr Vanessa Henderson for her valuable advice when needed.

My Special thanks are extended to Mrs Brenka McCabe, Mr Jason Heath and Mr David Thompson for all their technical daily help. Also, I would like to thanks everyone in the School of Clinical Dentistry for providing such a friendly working environment, particularly my fellow colleagues in Unit of Oral and Maxillofacial Surgery, postgraduate office C45. I am indebted to Miss Diana Ferreira, Miss Priyanka Prajapati, Miss Lucie Hadley, Miss Silvia Caddeo and Miss Sofia Granados Aparici for all the love and care they provided through the long journey; I been so lucky to have friends like you.

Last but not least, I owe my deep gratitude towards my mom, Najat Abugiad, and my dad Abdulrauf Niaz, for their endless love and continued support, even if that meant travelling thousands of miles away from home. There is nothing I can say or do that can express my whole-hearted respect to what have you done and are still doing for me.

And finally my husband Dr Osama Al Amer, so much has happened in the past years, you always supported and believed in me; thanks for your understanding when I worked late. I can’t thank you enough for helping me making my dream come true.

ABSTRACT

Tumour-associated neutrophils (TAN) can have a significant impact on the tumour microenvironment via release of potent growth and angiogenic factors, chemokines and proteinases that can profoundly influence tumour progression. Moreover, several studies have shown that increased neutrophil numbers systematically or within the tumour correlate with an unfavourable prognosis in head and neck squamous cell cancer (HNSCC) patients. The aims of this study were to identify which factors are responsible for neutrophil recruitment into HNSCC and if TAN affect tumour growth in an *in vivo* model.

The number of TAN within human HNSCC tissue was evaluated by immunohistochemical staining for the neutrophil marker myeloperoxidase (MPO). The factors secreted by FaDu HNSCC multi-cellular tumour spheroids (MCTS) were analysed by cytokine array and ELISA. Neutrophils isolated from the peripheral blood of healthy volunteers were used to measure neutrophil migration to factors identified from the array, then the recruitment of neutrophils to MCTS was assessed overtime by flow cytometry in the absence and presence of small molecule inhibitors. FaDu xenograft mouse models were used to confirm the effect of these inhibitors on neutrophil recruitment *in vivo* and also on tumour growth.

MPO staining confirmed the presence of marked numbers of TAN in HNSCC compared to normal oral epithelium. HNSCC MCTS resemble *in vivo* tumours, displaying areas of hypoxia, necrosis and cell proliferation. Neutrophils migrated to recombinant CXCL8, CXCL1 and MIF and these chemoattractants were found in the conditioned medium of FaDu MCTS. The recruitment of neutrophils into FaDu MCTS was significantly inhibited when neutrophils were pre-treated with antagonists for CXCR2 and CXCR4, the receptors for CXCL8, CXCL1 and MIF respectively. Moreover, use of the MIF inhibitor, ISO-1 caused a dramatic reduction in the number of neutrophils recruited into FaDu MCTS. In addition, in vivo, ISO-1 significantly reduced the number of TAN by up to 80% in xenograft FaDu tumours. Collectively, these data suggest that CXCL8, CXCL1 and MIF in particular are important in the recruitment of TAN into HNSCC.

Table of Contents

LIST OF FIGURES

Abbreviation

ABC	Avidin/biotin complex
APC	Allophycocyanin
Arg-1	Arginase-1
BrdU	5-bromo-2-deoxyuridine
BSA	Bovine serum albumin
CAF	Cancer-associated fibroblasts
CD	Cluster of differentiation molecule
CM	Conditioned Media
CEACAM1	Carcinoembryonic antigen-related cell adhesion molecule
CORTACTIN	Cortical actin binding protein
CXCL	Chemokine Ligand
CXCL-8	Interleukin 8
DMSO	Dimethyl sulfoxide
DAB	3,3'-Diaminobenzidine
DAPI	4',6-diamidino-2-phenylindole
DARC	Duffy Ag receptor for chemokines
DR	Desmoplastic reaction
DW	Distal Water
EDTA	Ethylenediaminetetraacetic acid
EMT	Epithelial-to-mesenchymal transition
EC	Endothelial cells
ERK	Extracellular signal–regulated kinases
ECM	Extracellular matrix
ELISA	Enzyme-Linked Immunosorbent Assay
ELR	Glutamic acid-leucine-arginine
ENA-78	Epithelial-derived neutrophil-activating peptide 78 (CXCL-5)
FaDu	Hypopharyngeal squamous cell carcinoma
FFPE	Formalin Fixed Paraffin embedded
FITC	Fluorescein isothiocyanate
FMO	Fluorescence minus one
FSC	Forward scatter
GCP-2	Granulocyte chemotactic protein 2 (CXCL-6)
GPCR	G-protein-coupled receptor
GRO-α	Growth related oncogene-α (CXCL-1)
GRO-β	Growth related oncogene-β (CXCL-2)
GRO-γ	Growth related oncogene-γ (CXCL-3)
GrMDSC	Granulocytic Myeloid derived suppressor cells
H&E	Haematoxylin and eosin
HCC	Hepatocellular carcinoma
HIER	Heat-induced epitope retrieval
HIF	Hypoxia inducible factors
HNC	Head and neck cancer
HNSCC	Head and neck squamous carcinoma

HPV	Human Papillomavirus
HRP	Horseradish peroxidase
HMGB-1	High mobility group box 1 protein
HVD	High vascular density
IHC	Immunohistochemistry
ICAM-1	Intercellular adhesion molecule 1
IMF	Immunofluorescence
ISO-1	4,5-Dihydro-3-(4-hydroxyphenyl)-5-isoxazoleacetic acid methyl ester
KC	Neutrophil chemokine
LVD	low vascular density
MCTS	Multi-cellular Tumour Spheroid
MPO	Myeloperoxidase
MMP	Matrix metalloproteinase
MIF	Macrophage migration inhibitory factor
MIP-2α	Macrophage inflammatory protein-2α
MDSC	Myeloid derived suppressor cells
MoMDSC	Monocytic Myeloid derived suppressor cells
MAPK	Mitogen activated protein kinase
MVD	Microvessel density
NAP-2	Neutrophil activating peptide 2 (CXCL-7)
NET	Neutrophil extracellular trap
NLR	Neutrophil to lymphocyte ratio
NC	Necrotic centre
NOF	Normal oral fibroblast
OCT	Optimal cutting temperature compound
OIS	oncogene-induced cellular senescence
OSCC	Oral squamous cell carcinoma
OK	Oral keratinocyte
PBS	Phosphate buffer saline
PE	Phycoerythrin
PIMO	Pimonidazole hydrochloride
PI	Propidium iodide
PS	phosphatidylserine
PMN	Polymorphonuclear cells
PD-1	Programmed death 1
RAGE	Receptor for advanced glycation end products
ROS	Reactive oxygen species
ROI	Regions of interest
RNS	Reactive nitrogen species
SDF-1	Stromal cell-derived factor-1 (CXCL-12)
SSC	Side scatter
TAM	Tumour-associated macrophages
TAN	Tumour-associated neutrophils
TME	Tumour microenvironment
TB	Tumour body
TGF-ß	Transforming growth factor-ß

TS	Tumour stroma
TNF-α	Tumour necrosis factor-α
TSCC	Tongue squamous cell carcinoma
TIMP	Tissue inhibitor of metalloproteinases
TI	Tumour invasive front
VEGF	Vascular endothelial growth factor
VEGF-A	Vascular endothelial growth factor A
5FU	5-fluorouracil

Chapter 1: Introduction

1.1. Head and Neck Cancer

Head and neck cancers (HNCs) are a group of heterogeneous malignancies arising from many distinct anatomical sites of the head and neck region including the oral cavity, oropharynx, nasopharynx, hypopharynx, nasal cavity and para-nasal sinuses, ear, salivary glands and larynx. The majority (approximately 90%) of HNCs arise from the squamous epithelium and therefore, the term head and neck squamous cell carcinoma (HNSCC) is frequently used to describe these cancers.

1.1.1. Epidemiology of Head and Neck Cancer

According to the World Health Organization (WHO) approximately 600,000 new cases and 300,000 deaths of HNSCC are reported annually, making it the sixth most common cancer (Warnakulasuriya, 2009) and the eighth leading cause of cancer mortality worldwide (Ragin et al., 2007). These cancers also have a higher male to female ratio of approximately 4:1 (Ferlay et al., 2010). Although, there is a large variation in HNSCC incidence by both sex and geographic region, the highest incidences are found in the Indian subcontinent, Eastern Europe, Australia, Brazil, Southern Africa and parts of the Pacific region (Warnakulasuriya, 2009). In UK, there were a total of 7495 cases reported in 2015 with 54% of cases reported in people above 65 years of age (Globocan, 2012) (Fig. 1.1). Despite surgical and therapeutic advances, individuals with HNSCC have a poor 5-year survival rate that is a result of various factors including late stage of diagnosis (primarily due to the lack of pain at early stage of disease), high probability of recurrence and secondary metastasis (Ragin and Taioli, 2007, Ragin et al., 2007).

(A)

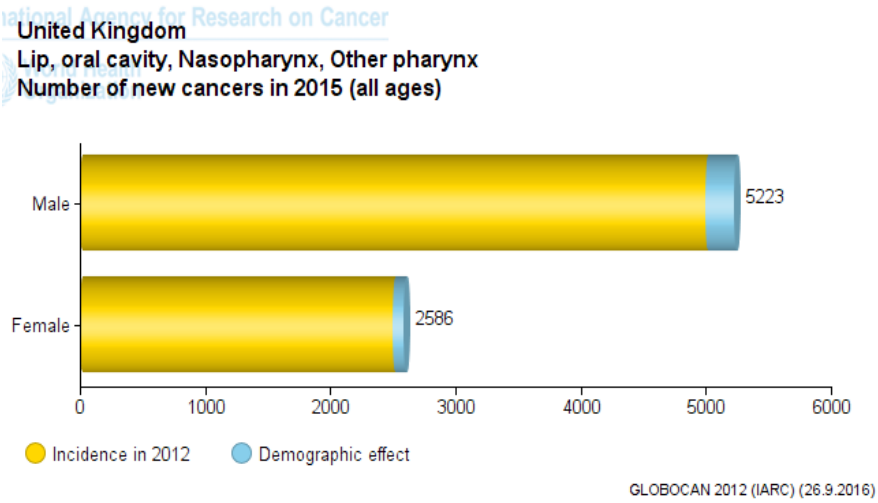

(B)

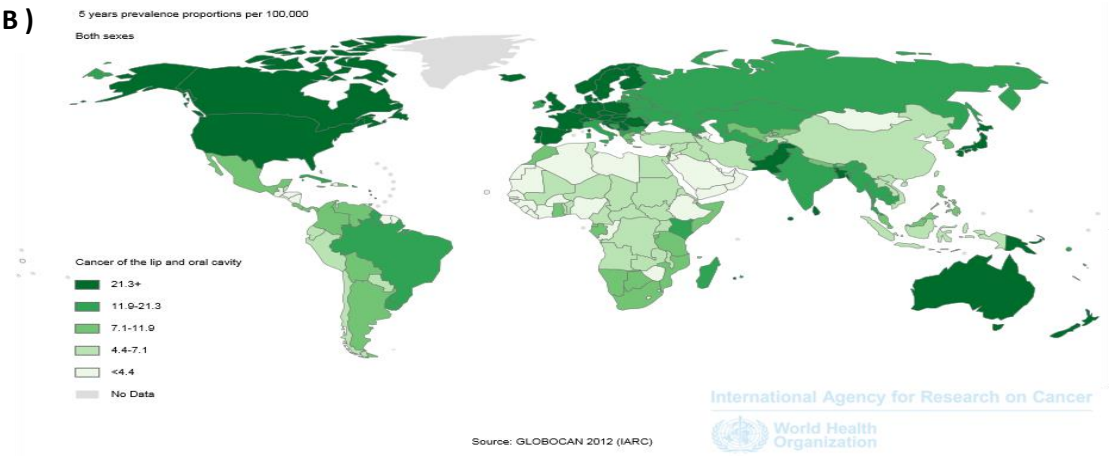

(C)

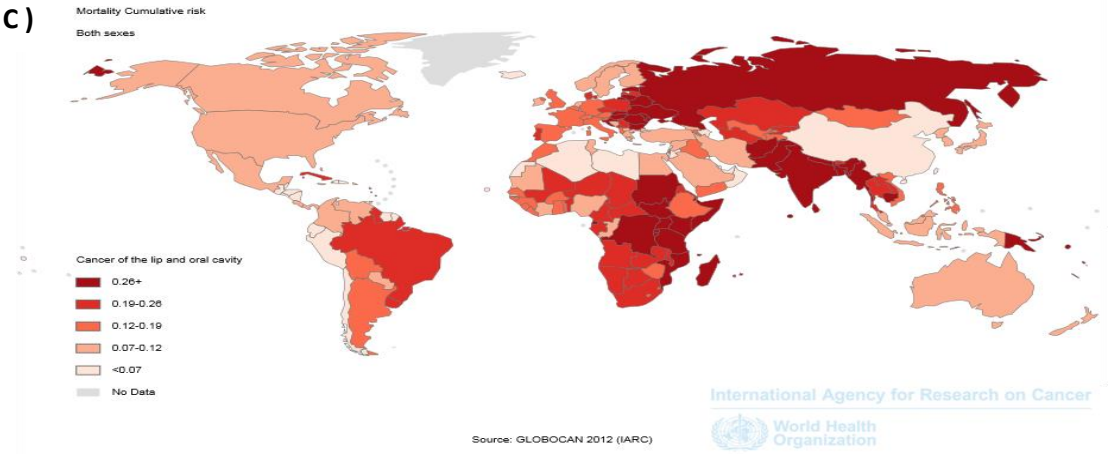

Figure 1.1 Incidence, prevalence and mortality rates for lip, oral cavity and pharynx in the UK and globally. (A) Bar chart shows the estimated age-standardized incidence of HNC in UK in 2015. **(B)** 5-year prevalence and **(C)** mortality rates of lip and oral cavity cancer worldwide in 2012. Data is shown as rates per 100, 000 of the global population in both sex (Data obtained from GLOBOCAN 2012).

1.1.2. Risk Factors

1.1.2.1. Smoking and alcohol consumption

The major risk factors identified for HNSCC are tobacco use and alcohol consumption. The increased risk is due to the genotoxic effects produced by carcinogen metabolites found in tobacco smoke including nitrosamines and polycyclic hydrocarbons, and acetaldehyde present in alcohol (Pai and Westra, 2009). Over a prolonged period of time these carcinogens irreversibly damage the DNA of key genes that regulate the cell cycle leading to altered gene expression and ultimately dysregulated mitosis. A study of the effect of possible risk factors for death from cancer in low and middle income countries showed that smoking accounts for 42% of deaths of people diagnosed with cancer of the oral cavity while heavy alcohol consumption accounts for 16% of deaths globally. In contrast, in high income countries deaths due to these risk factors are much higher with smoking accounting for 71% of deaths and 33% for alcohol consumption (Danaei et al., 2005).

1.1.2.2 Human Papillomavirus

Approximately, 20-25% of individuals with HNC contain DNA for the oncogenic Human Papillomavirus (HPV). HPV is a DNA virus known as the main causative agent of cervical cancer and it is increasingly being associated as a risk factor in the development of HNSCC, particularly in younger patients. HPV types 16 and 18 have been recognized as the predominant virus responsible for up to 70% of oropharyngeal cancers (Pai and Westra, 2009). Increasing evidence shows that HPV-associated HNSCCs strongly correlate with viral infection and sexual activity (Smith et al., 2004). In contrast to cancers arising from smoking and alcohol, HPV-positive HNSCC have been associated with better outcomes and a reduced risk of recurrence than HPV-negative HNSCC (Ragin and Taioli, 2007). Immune profiling of HPV-

positive and –negative tumours demonstrated an increased expression of immune-related genes such as the antigen presenting ligand (CD83), co-stimulatory molecules (GITRL), adhesion molecule (CD62L), chemokine receptor (CXCR3) and the NK cell marker (NKG2D) in HPV-positive compared to HPV-negative samples. This immune activation pattern was associated with accumulation of $CD20^{+}$B and $FoxP3^{+}$T-reg cells and was a predictor for improved survival (Russell et al., 2013), suggesting that differences between the aetiology of HPV-positive and –negative HNSCC leads to altered immune responses that ultimately affect patient outcome.

1.1.2.3 Other HNSCC aetiological factors

There is strong evidence to suggest that dietary factors also play an important role in the development of HNSCC. For example, there is an association between high intake of red meat and increased risk of oral cancer, while other studies show a protective effect of foods that contain vitamin C, E, and vegetable and fruit consumption (Saman, 2012). The precise mechanism of how these foods affect carcinogenesis is unknown and is a topic of much debate. However, several studies have now associated low folate status with cancer risk (George et al., 2009, Pelucchi et al., 2003). Folate is an essential dietary component required for production of nucleotides and therefore essential for DNA synthesis and repair. Low folate status has been shown to cause uracil mis-incorporation (Blount et al., 1997) and impaired DNA repair (Duthie et al, 2008) all of which increase the risk of cancer. Other exogenous risk factors include ultra-violet DNA damage upon exposure to sunlight (Weller et al., 2010), a particular risk for lip cancers, occupational exposure to carcinogens (Gustavsson et al., 1998) and poor oral hygiene (Orbak et al., 2005), although the latter may be associated with tumour progression rather than carcinogenesis.

1.1.3. Mechanisms of tumorigenesis

Mounting evidence accumulating over several decades indicates that HNSCC tumour development is a multistep process involving a number of genetic alterations over a long period of time. The route that normal cells take on their way to transformation into a neoplastic cell is highly diverse, but during this complex process impairment in function of critical genes, including oncogenes and tumour suppressor genes play a critical role in tumour initiation and progression (Kopnin, 2000). A prominent example is mutation in the p53 gene that occurs commonly in HNSCC and well as in many human cancers. This accounts for dysregulated function of the p53 tumour suppressor protein that results in inefficiency of DNA repair mechanisms and loss in apoptotic machinery (Levine, 1997). Mutation of p53 has been reported in 40%-60% of patients with HNSCC and is linked with progression from pre-malignancy to invasive disease (Shin et al., 2001, Cruz et al., 1998). Overexpression of Epidermal Growth Factor Receptor (EGFR) has been detected in 90% of HNSCC (Kalyankrishna and Grandis, 2006) and binding of receptor to any of its ligands initiates multiple layers of growth signalling and amplification that mediate uncontrolled cell growth. Other important signalling mechanism in HNSCC is the inhibitory transforming growth factor-ß (TGF-ß) pathway. TGF-ß binding to its receptors initiates phosphorylation of intracellular SMAD2, SMAD3 and SMAD 4 (Huntley et al., 2004), which governs target gene transcription and thus inhibits proliferation and induces apoptosis. Inactivation of TGF-ß has been detected in various cancers, including HNSCC (Wang et al., 1997). Oral squamous cell carcinoma (OSCC) cells have been shown to avoid apoptosis by the PI3K–PTEN–AKT pathway, and mutations of PIK3CA have been defined in 10-20% of patients (Kozaki et al., 2006).

As a result of this genetic instability and uncontrolled cell growth, tumours increase in size but cannot exceed 1-2 mm^3 in an avascular state. In order to maintain an adequate supply of oxygen and nutrients and diffusion of waste products the tumour requires the formation of new blood vessels – the process of angiogenesis (Folkman, 2002). Under normal physiological conditions, like wound healing, this process is tightly regulated, while during tumour progression the angiogenic switch, which controls the balance between pro- and anti-angiogenic molecules, is skewed to a pro-angiogenic state. This leads to multiple defects in tumour vascular shape, branching pattern, size and lack of normal arrangement of arterioles, capillaries and venules (Baluk et al., 2005). A tumour with a high tendency of forming a network of microvessels will mostly transfer from microscopic lesion to a rapidly expanding mass with metastatic spread (Zetter, 1998). For example, increased expression of the pro-angiogenic factor VEGF in HNSCC was associated with increased tumour vascularity and poor prognosis (Kyzas et al., 2005).

1.1.4. Clinical and histological pathogenesis of oral cancer

Most of the tumours that occur in the head and neck region are squamous cell in origin and the overwhelming majority of these are in the oral cavity (oral squamous cell carcinoma; OSCC). Clinically, the appearance of the normal oral mucosa is pink/red with smooth mucosal surfaces. Histologically, the tissue is typically comprised of a dense connective tissue containing fibroblasts, blood vessels and neuronal tissue. Stratified layers of epithelial cells are attached to the connective tissue via interactions between the basal cells and the basement membrane by hemi-desmosome contacts. The epithelial basal cells act as stem cells and are the only cells that have the ability to replicate (these are also cells that become malignant). As the cells divide they differentiate towards the apical surface of the epithelium,

firstly becoming spinous cells and then finally differentiating into the stratum corneum before desquamating into the oral cavity (Fig. 1.2). Some parts of the oral mucosa are highly keratinised (hard palate) whereas others are non-keratinised (buccal mucosa) depending on their function.

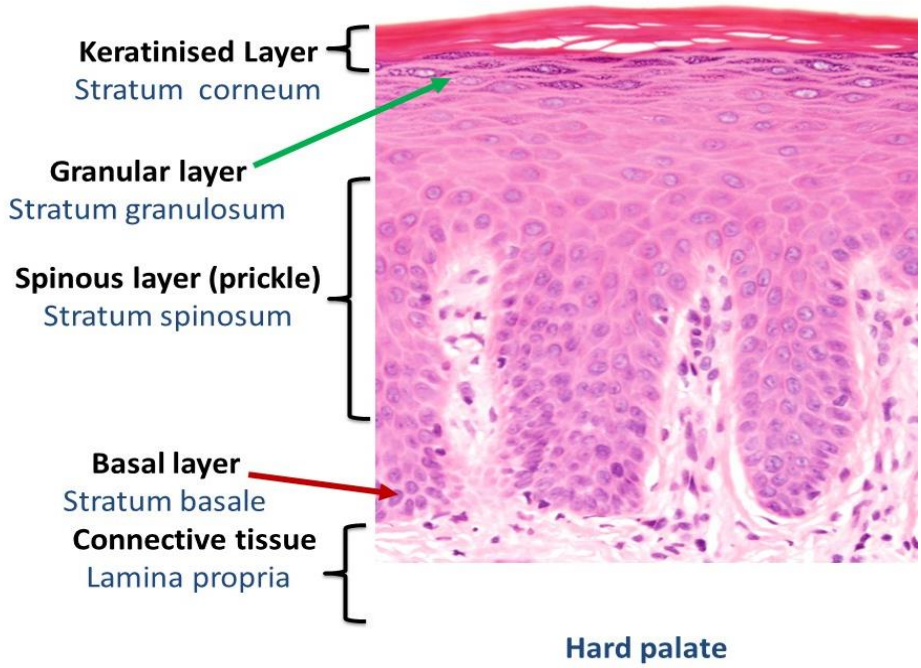

Figure 1.2 Histology of the oral mucosa. Histological micrograph showing the connective tissue and epithelium of the oral mucosa. The epithelium is further divided into distinct regions and can be keratinised or non-keratinised depending on location in the oral cavity.

At initial stages, lesions present clinically in the form of pre-malignant lesions such as leukoplakia (white plaque), erythroplakia (red plaque) or combination of both (erythroleukoplakia). Leukoplakia is the most frequently observed although erythroplakia tend to be more aggressive and these lesions are the ones most likely to progress to cancer. Lesions at that stage are usually small in size and mostly asymptomatic (Mashberg et al., 1989)

with little or no pain commonly experienced. Histological examination of leukoplakias can demonstrate thickening of the entire epithelium (acanthosis) and/or thickening of the surface, keratinised layers of the epithelium (hyperkeratosis) (Fig. 1.3). Not all leukoplakias continue to form tumours. In fact, the development of cancer is uncommon with only 8%-18% of patients going on to develop SCC within 8 years after the diagnosis of a pre-malignant lesion (Jr et al., 1984). Most pre-malignant lesions regress and the epithelium returns to a normal clinical appearance. Most people presenting at oral medicine clinics have high risk factors such as smoking and alcohol consumption and so the aetiology of many of the pre-malignant lesions that return to normal are unknown, likewise, there is currently no way to discriminate between those lesions that progress to cancer from those that do not. At the histological level these changes include drop-shaped rete ridges, nuclear enlargement, keratin pearls and irregular epithelial stratification and mitotic cells in the spinous (upper) layer of the epithelium (Fig. 1.3). Based on the severity of the cellular abnormalities, dysplasia is graded from mild dysplasia (abnormalities limited to the lower one-third of the epithelium), expanding of dysplastic lesion to the lower two-thirds in moderate dysplasia, and involvement of full thickness of the epithelium in severe dysplasia/carcinoma *in situ*. Once a pre-malignant lesion has progressed to cancer the characteristic clinical features include ulceration and sever pain of the lesion, and formation of a lump which is often hard on palpation (Bagan et al., 2010) (Fig. 1.3). As the tumour grows, it invades the connective tissue and it is at this stage that the tumour is considered as an invasive carcinoma. Histologically, this is characterized by increased cell nuclear to cytoplasmic ratio, varying degrees of keratinization intercellular bridges, increased atypical mitotic figures; hyperchromasia, basement membrane invasion, and an associated inflammatory response (Fig. 1.3) (Rivera and Venegas, 2014).

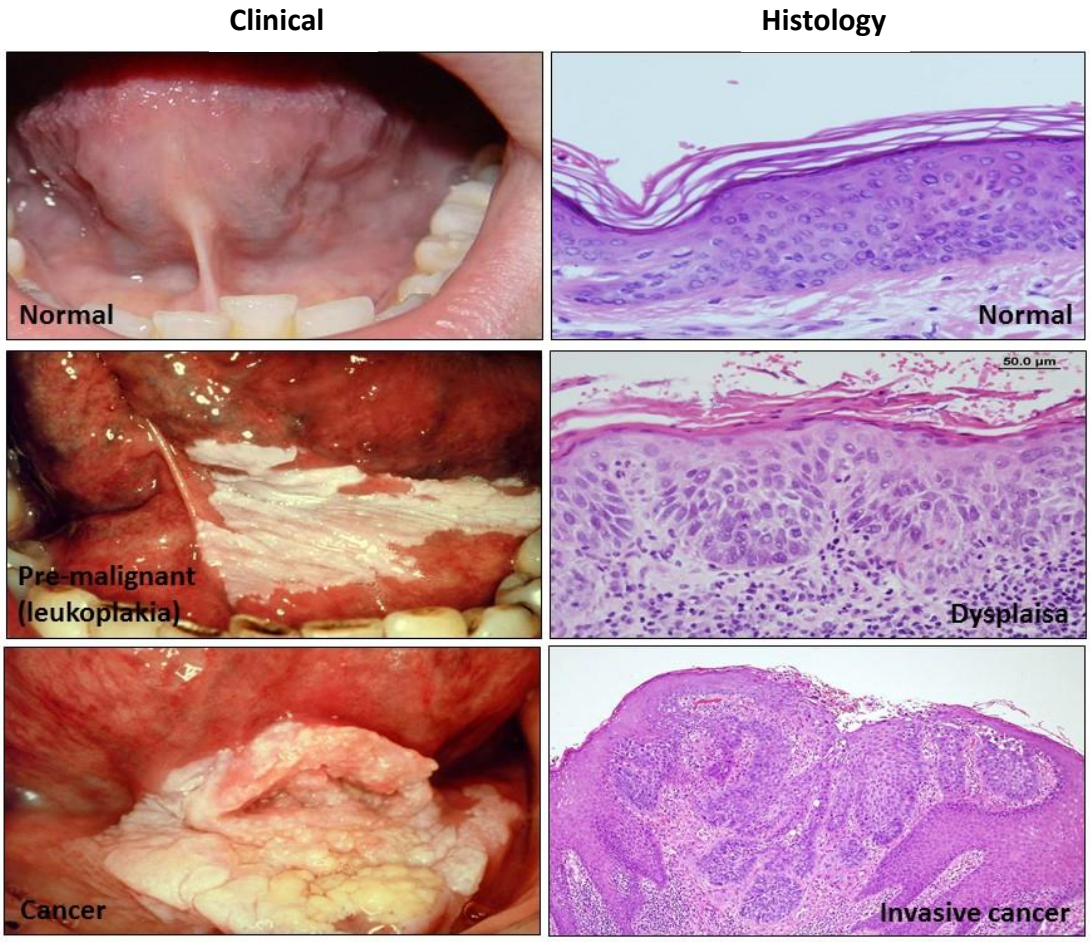

Figure 1.3 Clinical and histological images represent the change in oral mucosa in oral cancer progression

1.1.5. Insight into the HNSCC tumour microenvironment

For decades most cancers, including HNSCC, have been thought of and treated as if they are composed of a heterogeneous population of epithelial cells, but this concept has shifted because of the recognition of the active role that the stroma plays in cancer progression (Shekhar et al., 2001). The tumour stroma is comprised of endothelial cells (EC), neuronal cells, immune cells, cancer-associated fibroblasts (CAF) and their surrounding matrix. Collectively, these elements along with cancerous cells are commonly referred to as the tumour microenvironment (TME). The presence of most of these cellular components has been

reported in HNSCC and their contribution in the process required for tumour progression will be discussed briefly here.

The major cellular elements of TME are CAFs and these have been reported in HNSCC with an active myofibroblastic (MF)-like phenotype (Vered et al., 2010). Accumulating evidence has demonstrated that cross-talk between CAF and HNSCC cells enhance the neoplastic progression by facilitating connective tissue invasion (Daly et al., 2008), aiding epithelial cell proliferation (Lin et al., 2011), initiating the epithelial-to-mesenchymal transition (EMT) (Dudas et al., 2011a), producing angiogenic factors for tumour angiogenesis, regulating immune escaping processes (Dudas et al., 2011b, Alcolea et al., 2012) and promoting metastasis (Vered et al., 2010). Not surprisingly, the presence of myofibroblast CAFs have been associated with poor prognosis and mortality in OSCC (Marsh et al., 2011).

Along with CAF there has been much interest in the role that tumour-associated leukocytes play in cancer progression. Many different types of tumours have been shown to contain leukocytes populations such as lymphocytes, granulocytes and macrophages. In recent years tumour-associated macrophages (TAM) have received much attention and in some tumours these cells can make up to 50% of a cell population of the tumour mass (Van Overmeire et al., 2014). Infiltration of macrophages has been observed in numerous human cancers and their density has been correlated positively with poor prognosis (Takeya and Komohara, 2016), including in OSCC (Mori et al., 2011). TAM have been associated with increased secretion of factors that can affect tumour growth directly (Condeelis and Pollard, 2006), but their main influence seems to be on tumour angiogenesis (Murdoch et al., 2008). TAM have been shown to accumulate in hypoxic/necrotic areas of some tumours, most likely due to their role as scavenger phagocytes, where they secrete a number of factors that dramatically influence

vascularisation such as vascular endothelial growth factor (VEGF), matrix metalloproteinase 7 and MMP9 (Granata et al., 2010, Huang et al., 2002). TAM can also secrete immunomodulatory cytokines such as IL-10 that dampen down any T-cell response directed against tumour cells (Sica et al., 2000). The role that innate immune cells play in cancer progression has led to an increased interest in neutrophils. These are also phagocytic cells that are traditionally recognised as key players in the innate immunity to pathogens. This thesis examines the role that neutrophils play in HNSCC and so the following sections discuss this leukocyte in more detail.

1.2. Neutrophils

1.2.1. Origin and life cycle

Neutrophils are key players of the human innate immune system. They are derived from hematopoietic pluripotent stem cells in the bone marrow in a process known as myelopoiesis, which is a term used to describe the production of granulocytes and monocytes from progenitor cells. During granulopoiesis (production of granulocytes), the appearance of cytoplasmic granules marks the transition from myeloblasts to promyelocytes, myelocytes to metamyelocyte and continues until these cells differentiate into mature, segmented neutrophils also known as polymorphonuclear cells (PMN). Neutrophil granules have been classified based on their content and differentiation stage at which granule synthesis takes place. They are segregated as primary granules (azurophillic), secondary granules (specific) and tertiary granules (gelatinase). These granules house an array of toxic weaponry such as

antimicrobial agents, proteinases and reactive oxygen species (ROS), which can have a

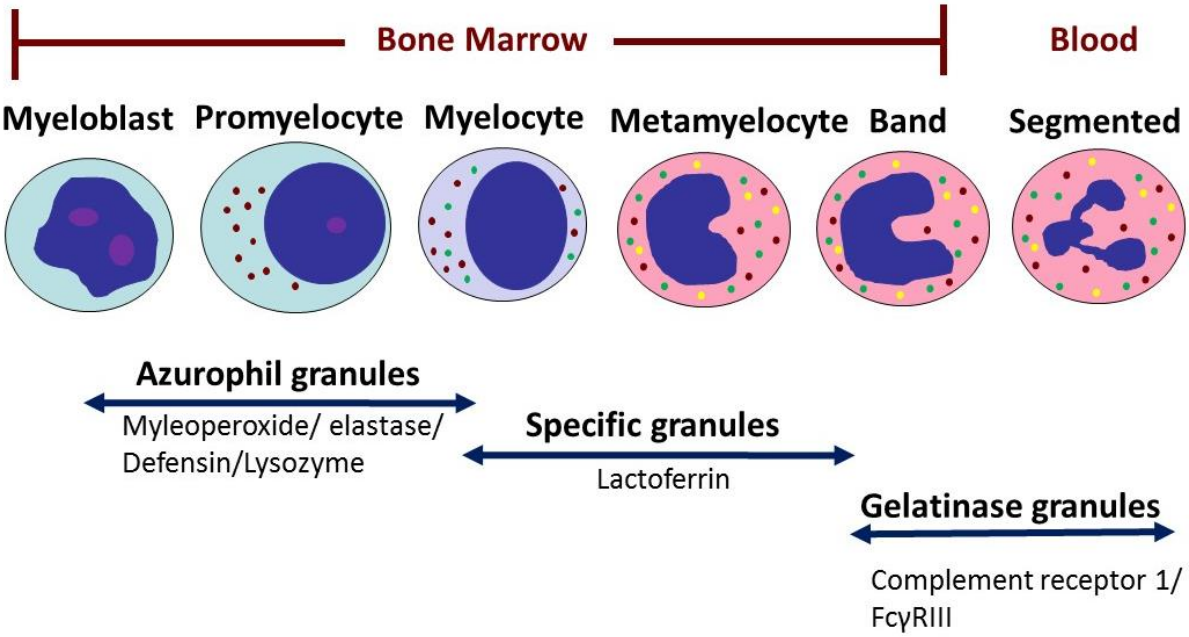

Figure 1.4 Development of neutrophils in the bone marrow and granule formation. A schematic representation of neutrophil maturation in the bone marrow during granulopoiesis that is characterized by appearance of granules. Neutrophil granules carry a rich variety of antimicrobials and signalling molecules that are divided into three types primary, secondary and tertiary granules during neutrophil maturation.

profound effect on host tissues (Fig. 1.4)

The bone marrow acts as a reservoir to hold the extensive high production rate of neutrophils (approximately 10^{11} cells per day) that is essential to meet the increased need during infection and explains the relatively short half-life of neutrophils (6-8 hours) compared to other leukocytes in the circulation. Migration of mature neutrophils from the bone marrow through trans-endothelial pores and into the bloodstream is tightly controlled by several factors. The most prominent cytokine is granulocyte colony stimulating factor (G-CSF) (Semerad et al., 2002) along with the balance in expression levels of chemokine receptors CXCR4 and CXCR2

on the surface of neutrophils that determines their retention or release from bone marrow into the circulation (Martin et al., 2003). Neutrophil release from bone marrow is CXCR2 dependent, the binding partner for CXCL1 and CXCL2 in human or neutrophil chemokine (KC) and macrophage inflammatory protein-2α (MIP-2α) in mice respectively, whereas, CXCR4 is essential for retention of neutrophils to bone marrow (Eash et al., 2010). Senescent neutrophils up-regulate CXCR4 expression and they home to the bone marrow from the circulation in CXCR4-dependnt manner (Martin et al., 2003). The use of the small molecule antagonist for CXCR4, AMD3100, in humans or mice results in the rapid mobilization of neutrophils from bone marrow to blood (Liles et al., 2003, Broxmeyer et al., 2005). Consistent with this finding, an *in vivo* study using transgenic mice carrying a myeloid specific deletion of CXCR4, showed a significant reduction in the number of neutrophils in the bone marrow and increased numbers in the circulation (Eash et al., 2009), confirming the key role for CXCR4 and its ligand CXCL12/SDF-1 in regulating neutrophil mobilization or retention in bone marrow.

1.2.2. Neutrophil recruitment cascade

Neutrophils are the most abundant white blood cell in the circulation and account for two thirds of all peripheral blood leukocytes. They are found in two different pools; the circulating pool, which are freely circulating in the peripheral blood and the marginated pool, which are neutrophils adhering to the endothelium of small vessels. It has been suggested that from the circulating pool neutrophils are recruited to sites of inflammation and tumours (Friedman, 2002).

It is well accepted that during transmigration into tissue neutrophils become activated as a result of their interaction with vascular walls that induce a number of functional and phenotypic changes (Beyrau et al., 2012). For example, a study compared changes in the expression of surface receptors of blood and bronchalveolar lavage fluid neutrophils between normal and patients with sarcoidosis and found that lung neutrophils switch to the activated phenotype in both the healthy and disease group. The key changes in activated phenotype were characterized by modulation of adhesion receptors (Mac-1/CD11b, L-selectin/CD62L, α_4 integrins /CD49d, ICAM-1/CD54) and the immunoglobulin receptor (FcγRII/CD32), but expression of the anaphylatoxin receptor (C5a/CD88) and CEACAM8/CD66b were independent of the disease state (Fortunati et al., 2009). Neutrophils use the increased expression and activation of adhesion molecules on their surface to bind to their counter-ligands expressed on the surface of activated endothelial cells such as E-selectin (CD62E) and intercellular adhesion molecule-1 (ICAM-1/CD54). These interactions allow tethering of neutrophils on the endothelium surface where they encounter specific chemokines (CXCL1-3, CXCL5 and CXCL8 amongst others) presented on glycosaminoglycan chains that decorate the endothelial cell surface. Chemokine binding to neutrophil cell surface receptors CXCR1 and

CXCR2 influence integrin avidity, which causes neutrophils to firmly adhere to the endothelial cell surface. Neutrophils then migrate between the endothelial cells in a PECAM-1/CD31-dependent mechanism and migrate towards the inflammatory site in a chemokine concentration-dependent manner (Chosay et al., 1998). The up-regulation of chemokine receptors (CCR1, CCR2, CCR3, CCR5, CXCR3 and CXCR4) on the surface of infiltrated neutrophils from patients with chronic inflammatory lung diseases and rheumatoid arthritis compared to circulating neutrophils from healthy individuals may account for the increased disease severity in these people (Hartl et al., 2008). During trans-endothelial migration neutrophil function was altered to prolong the survival of recruited neutrophils during inflammation *in vitro* (McGettrick et al., 2006). Moreover, using labelled neutrophils in a zebrafish model to measure the lifespan of tissue neutrophils *in vivo*, Dixon et al showed that tissue neutrophils had an extended half-life (around 120 hours) in comparison to circulating counterparts (Dixon et al., 2012). These data suggest that the tissue microenvironment contains factors that extended neutrophil life in order that they can exert their effects.

1.2.3. Neutrophils, inflammation and wound repair

During tissue-associated injury, inflammation is an essential event to protect the host from infection. Inflammatory mediators are released by injured or infected cells to defend against bacteria and facilitate the activation and directed migration of different leukocytes from the circulation to the site of damage. Neutrophils are the first recruited effectors cells to arrive at the site, followed by monocytes and lymphocytes. Neutrophils serve as a potent source of cytokines that can further mediate leukocyte adherence to the vascular endothelium (Werner and Grose, 2003). Once at sites of inflammation neutrophils can phagocytose microbes or necrotic cell debris to remove them from the environment. They can also degranulate to

release a plethora of molecules that act as antimicrobial peptides or directly kill organisms such as superoxide. Neutrophils store and secrete two important players in remodelling the extracellular matrix and re-vascularising of the damaged/infected area; MMP-9 and VEGF (Gaudry et al., 1997). They can release MMP-9 in active form (tissue inhibitor of metalloproteinases (TIMP)-free form), unlike other cells of body, indicating their potent proangiogenic activity (Ardi et al., 2007). The recently identified mechanism neutrophils use to defend against pathogens is neutrophil extracellular trap (NETs) (Brinkmann et al., 2004). As the name indicates, neutrophil trap pathogens via release of their core DNA and DNA binding proteins. Further analysis of NETs, identified 24 neutrophil proteins and enzymes, including elastase (proteases), histones (antimicrobial), cathepsins, and lactoferrins, MPO among many others toxic molecules that can induce host cell injury (Urban et al., 2009).

The most important regulatory mechanism is that normal inflammation is self-limiting and will diminish gradually after the causative agent is removed or repaired. This is in contrast to cancer that has been described as wounds that never heal (Dvorak, 1986), suggesting that normal inflammation and cancer share some common features.

Inflammation has emerged as a new hallmark of malignancy (Colotta et al., 2009) and there is an accumulating body of evidence to associate persistent infection and chronic inflammation with tumour formation. For instance, patients with chronic ulcerative colitis and Crohn's disease tend to be at a higher risk of developing colon carcinoma (Eaden et al., 2001, Ullman and Itzkowitz, 2011) whereas, *Helicobacter pylori* infection has been identified as the main causative agent of gastroduodenal ulcers and gastric cancer (Ernst and Gold, 2000). Evidence has also linked increased numbers of the oral microbe *Porphyromonas gingivalis* (*P. gingivalis*) with malignant OSCC (Gallimidi et al., 2015). This is because *P. gingivalis* is the main

causative agent of periodontitis that is associated with chronic oral inflammation with increased influx of neutrophils into the oral tissue (Lakschevitz et al., 2013) and poor oral hygiene and periodontitis has been linked with increased risk of oral cancer (Orbak et al., 2005).

A key feature of cancer-related inflammation includes infiltration of immune cells and such immune responses were firstly thought to reflect an attempt by the immune system to eliminate tumour cells. However, numerous studies have since showed that transformed tumour cells escape this immunosurveillance in order to initiate tumour progression (Sakakura and Chikamatsu, 2013).

The involvement of reactive oxygen species (ROS) in inducing DNA damage and promoting carcinogenesis has been reported in many cancer diseases (Kumar et al., 2008a). High levels of ROS were detected in the serum and neutrophils of advance stage OSCC when compared to controls (Das et al., 2007). Other neutrophil-secreted products such as neutrophil gelatinase–associated lipocalin (NGAL), a protein found in activated neutrophils have been correlated with HNSCC tumorigenesis (Wang et al., 2015).

1.2.4. The emerging role of neutrophils in cancer

Neutrophils have been observed in close association with tumour cells and within the tumour vasculature since the 1980s (Welch et al., 1989) but the exact role of neutrophils in human cancers is only just being unravelled. It is becoming clear that tumour-associated neutrophils (TAN) play an important role in malignant transformation, tumour progression, angiogenesis and immune surveillance (Mantovani et al., 2011) which will be discussed in the following section:

1.2.4.1. Tumour-infiltrating (associated) neutrophils

Although TANs make up only between 5-25% of cellular tumour mass (Eruslanov et al., 2014), a variety of human cancer studies have linked the number of neutrophils encountered within the tumour microenvironment with disease progression and clinical outcome, which suggests that these cells may have a role in tumour progression. For example, a study by Trellakis and colleagues in head and neck cancer showed a higher percentage of infiltrating neutrophils were associated with poor survival in advance disease compared to non-disease tissue (Trellakis et al., 2011b, Trellakis et al., 2011a). Similar findings have been observed in gastric adenocarcinoma patients, where immunohistochemical analysis determined that elevated level of CD15+ neutrophils correlated with poor patient survival (Zhao et al., 2012). The presence of increased numbers of neutrophils has also been observed in patients with renal cell carcinoma (Jensen et al., 2009a), and hepatocellular carcinoma (HCC) (Zhou et al., 2012, Kuang et al., 2011) and their levels related to reduced survival times in these patients (summarized in Table 1.1).

Tumour type	Neutrophils marker	Clinical outcome	Mechanism of recruitment	Ref.
Colorectal carcinoma	CD66b	Shortened patient survival	ND	(Rao et al., 2012)

Hepatocellular carcinoma (HCC)	CD66b CD15+ neutrophils	Poor patient survival	CXCL16 CXCL5 CXCL1 CXCL2 CXCL3 and CXCL8	(Gao et al., 2012) (Zhou et al., 2012) (Kuang et al., 2011)
Melanoma	CD66b	Poor prognosis	Expression of pSTAT3	(Jensen et al., 2012)
Head and neck squamous cell carcinoma (HNSCC)	CD66b MPO	Poor patient survival in advanced disease	CXCL8 MIF	(Trellakis et al., 2011a) (Dumitru et al., 2011)
Non small cell lung cancer (NSCLC)	CD66b	Poor clinical outcome	ND	(Ilie et al., 2012)
Broncheoalveolar adenocacinoma	Morphological identification	Poor patient survival	Correlated to high CXCL8 production	(Bellocq et al., 1998)
Renal Cell Carcinoma (RCC)	CD66b	Increased tumour size and short recurrence-free, cancer-specific and overall survival	ND	(Jensen et al., 2009a)
Breast Cancer	Neutrophil elastase	Lower recurrence free survival	ND	(Yamashita et al., 1995)
Non-Hodgkins lymphoma	CD15, elastase, nuclear morphology	Indirect link, neutrophils were main source of APRIL which is linked to patient survival	ND	(Schwaller et al., 2007)
Gastric adenocarcinoma	CD15	Lymph node/distant metastasis, tumour stage and patient prognosis	ND	(Zhao et al., 2012)

Table.1.1: Association of TAN with clinical outcome in human cancers. ND= not determined

1.2.4.2. Circulating neutrophils in cancer patients

Many studies have used the neutrophil to lymphocyte ratio in peripheral blood (NLR) as a predictor of mortality of patients with cancer. A negative impact of an elevated

neutrophils/lymphocyte ratio for patient survival was found in various cancers including breast (Azab et al., 2012), non-small cell lung cancer (Cedres et al., 2012), oral (Perisanidis et al., 2013), nasopharyngeal (An et al., 2011), ovarian cancer (Cho et al., 2009) and colon cancer (Ding et al., 2010). A more detailed analysis in HNSCCs showed that neutrophils not only increased in numbers NLR but also the presence of an immature population of CD16-positive neutrophils was detected in the peripheral blood of these patients. Functionally, these neutrophils had a reduced capability to release reactive oxygen species and reduced apoptosis in patients with HNSCC compared to controls (Trellakis et al., 2011b). Others have observed that peripheral blood neutrophils in oral cancer patients have a shortened life-span that may be due to an increase in activity of proteins participating in extrinsic apoptotic pathway; Fas-associated protein with death domain (FADD) and caspase-8 activity (Jablonska et al., 2009).

1.2.4.3. Neutrophil phenotype: N1 versus N2

Until recently, neutrophils were thought to be a short-lived homogeneous cell type that arrives rapidly at the site of an infection or injury as professional phagocytes. These cells then die and are then engulfed by macrophages, which is necessary for the resolution of inflammation. A growing body of evidence has challenged this notion and the presence of longer life-span (5.4 days) human neutrophils in tumours has been reported (Pillay et al., 2010), suggesting that the tumour microenvironment is capable of generating conditions that prolong TAN survival. Wislez *et al,* showed that tumour-derived GM-CSF and G-CSF from patients with bronchoalveolar adenocarcinoma inhibited 24-hour spontaneous neutrophil apoptosis *in vitro* (Wislez et al., 2001). Moreover, the ability of neutrophils within the tumour to develop a distinct phenotype that is polarized into two distinct sub-groups (N1 & N2)

similar to that described for tumour-associated macrophage (TAM) has been recently identified (Galdiero et al., 2012). Fridlender and colleagues found that TANs can present with a hyper-segmented, anti-tumorigenic (N1) phenotype, with enhanced ability to eradicate tumour cells, enable activation of cytotoxic T lymphocytes, and have increased expression of pro-inflammatory cytokines such as tumour necrosis factor-α (TNF-α) with a simultaneous reduction in immunosuppressive Arginase-1 (Arg-1) levels. The most characteristic features for N2 TAN are increased expression of the pro-angiogenic genes, c-myc and STAT3, known regulators of VEGF, MMP9, as well as increased secretion of CCL2, CCL5 that promote monocyte recruitment and Arg-1 from neutrophils, thus promoting immunosuppressive functions. Up-regulation of CXCR4 receptor expression on the surface of N2-TAN has also been reported (Jablonska et al., 2010). There is also evidence that N2 TAN display a ring-like nuclear structure that resembles an immature neutrophil morphology (Andzinski et al., 2016).

This immerging evidence has been obtained mainly from murine models of cancer and may not directly relate to human TAN because of species-specific differences. To date there are very few studies examining human TAN with just one describing TAN isolated from freshly removed early stage lung tumour tissue. Phenotypically, these TANs displayed the cell surface markers $CXCR1^{Lo}$, $CXCR2^{Lo}$, $CD62L^{Lo}$ and $CD54^{Hi}$ with a distinct CC and CXCR profile $CXCR4^{Hi}$, $CXCR3^{Hi}$, $CCR7^{Hi}$ and $CCR5^{Hi}$. Unexpectedly, this subset of neutrophils can induce T-cell proliferation and increase IFN-**γ** production, indicating that the early stages of tumour growth TAN display markers that have been previously described as an N1 phenotype (Eruslanov et al., 2014).

1.2.4.4. TAN or MDSC

It is worth noting the relationship between myeloid-derived suppressor cells (MDSC) and TANs. MDSC consist of a heterogeneous mixture of immature myeloid cells, immature granulocytes, monocytes-macrophages, dendritic cells and myeloid progenitor cells characterized by their immune suppressive behaviour. In contrast to tumour-bearing mice, where MDSC are well characterized based on the expression of myeloid cell markers Gr-1 and CD11b (markers also expressed by murine neutrophils), there is much controversy and lack of a uniform marker to identify human MDSC. Major markers employed for immune-phenotyping of human MDSC include the common myeloid markers CD11b and CD33 and HLA-DR$^{neg/low}$ but do not include markers for mature myeloid cells such as CD40, CD80 and CD83. MDSC can be subdivided to CD14^{+} monocytic MDSC (MoMDSC) (CD14^{high}, CD15^{neg}, CD16^{high}) or CD15^{+} granulocytic MDSC (GrMDSC) (CD14$^{neg/low}$, CD15^{+}, CD16^{neg}) (Greten et al., 2011). Both subsets have the ability to supress T-cell responses either via reactive oxygen species (ROS) from GrMDSC or depletion of L-arginine mediated by Arg1 and iNOS from MoMDSC. However, the differences between GrMDSC and neutrophils in cancer patients are less clear and are overlapping. A study in renal cell carcinoma (RCC) showed no morphological difference between MDSC and PMN isolated from the peripheral blood of patients, indeed the authors demonstrated that human MDSC resemble activated PMN. These CD15^{+}MDSC express high levels of CD11b, CD66b, and VEGFR1, while only a small amount of CD62L and CD16 was detected in peripheral blood of RCC patients in compared to control granulocytes. GrMDSC from RCC patients release high levels of arginase I, a cytokine that plays a significant role to impair T-cell function, similar observations have been found when neutrophils were activated *in vitro* (Rodriguez et al., 2009). Similarly, a subpopulation of CD66b^{+}PMN was identified from the peripheral blood of HNC patients using density gradient centrifugation. This neutrophilic MDSC population was found to have longer survival times in blood and lack

expression of CXCR1 and CXCR2, which diminished their migration property when compared to mature normal neutrophils of the same patients (Brandau et al., 2011). To further discriminate TAN from GrMDSC and naive bone marrow neutrophils (BMN) isolated from mice, Fridlender and co-workers used a transcriptomics approach to compare the three cell populations. They found that TAN are a distinct population of neutrophil and mRNA of BMN and GrMDSC are more closely related to each other than to TAN. The most significant difference between TAN and either GrMDSC or BMN can be summarized by the up-regulation of anti-apoptotic NF-κB genes (IEX-1, SOD-2, GADD-45B, BCL-2A1), cytokine and chemokine genes (CXCL1, CXCL2 and CCL3), genes related to proteolysis (MMP-13, MMP-14, TIMP-1), whereas the level of mRNA involved in cytoskeleton organization and biogenesis, granule protein and respiratory burst were notably down-regulated (Fridlender et al., 2012).

1.2.5. Tumour-derived factors mediating neutrophil recruitment to tumours

To be recruited to the tumour site, neutrophils must exit the vasculature and transmigrate into tissues. As described previously, neutrophil extravasation is a tightly regulated process that comprises capturing of free flowing neutrophils by the activated vascular endothelium, followed by firmer adhesion and rolling of neutrophils along the vessel wall that will allow interaction between chemokine and their receptor on the neutrophils surface, before the transmigration across the endothelial cell barrier into inflammatory tissue along a chemotactic gradient (reviewed in (Williams et al., 2011)). The following section will classify the potential tumour-derived chemotactic factors involved in neutrophil migration in to mediators that belonging to chemokine subfamily or non-chemokine inflammatory.

1.2.5.1. Chemokine and chemokine receptors

The role of chemokines in the pathogenesis of cancer is diverse but mainly they are known for their ability to induce cell migration. Chemokines are small chemoattractant peptides (8-17kDa) that are characterized by the presence or absence of the sequence motif glutamic acid-leucine-arginine (ELR) and by four conserved cysteine residues. Chemokines bind to seven-transmembrane G-protein-coupled receptors (GPCR). By far the most studied neutrophil attracting chemokines in human are CXCL8 (IL-8) and CXCL6 (GCP-2) that bind to both CXCR1 and CXCR2, whereas CXCL1 (GROα), CXCL2 (GROβ), CXCL3 (GROγ), CXCL5 (ENA-78) and CXCL7 bind to CXCR2 on the surface of neutrophils (Lee et al., 1992, Ahuja and Murphy, 1996a). In murine neutrophils, CXCR2 is very similar to human CXCR2 but binds to KC, a murine chemokine with CXCL-8 homology, (Cacalano et al., 1994), and MIP-2. Although the expression of CXCR1 has been detected in mice (Fan et al., 2007), data suggests that CXCR2 is predominantly responsible for neutrophil recruitment. As depletion of CXCR2 in inflammatory mice model resulted in significant inhibition of recruitment of neutrophils to the peritoneal cavity in response to LPS inoculation and $CXCR2^{-}/^{-}$ mice showed almost complete abrogated of neutrophils up to two weeks following mycobacterial infection (Gonçalves and Appelberg, 2002). The expression of CXCR2 has been detected in and non-leukocytic cells such as endothelial cell, epithelial cell as well as tumour cells (Murdoch et al., 1999, Desurmont et al., 2015). The importance of CXCR2 in tumour progression will be further discussed in section (1.2.5.1.1).

For some of these members of this family the biological activities have already been well established *in vitro* and *in vivo*. For example, the expression of CXCL8 has been found to be highly up-regulated in various human malignancies; for instance, brain, breast, colon, cervical, gastric, lung, melanoma, ovarian, Hodgkin's disease, prostate, renal cell carcinoma and B-cell

chronic lymphocytic leukaemia as well as by different cell lines (Xie, 2001). However, many studies point to the connection between CXCL8 secreted by tumour cells derived from several types of carcinomas or from cells within the tumour stroma and neutrophil infiltration, indicating that intratumoral CXCL8 expression is a potent neutrophil chemoattractant within the tumour micro-environment (Haqqani et al., 2000, Bellocq et al., 1998). A recent *in vitro* and *in vivo* study in HNSCC showed that $CD66b^+$ neutrophil infiltration was associated with high level of CXCL8, along with detection of high concentrations of CCL4 (MIP-1b) and CCL5 (RANTES) in the serum of patients (Trellakis et al., 2011a, Trellakis et al., 2011b). This result was confirmed by another group who showed that isolated neutrophils migrated towards conditioned media collected from the hypopharyngeal squamous cell carcinoma cells line (FaDu) that expresses considerable amounts of CXCL8 and CXCL1 (Bru et al., 2009). Overexpression of adhesion protein carcinoembryonic antigen-related cell adhesion molecule 1 (CEACAM1) in tongue squamous cell carcinoma (TSCC) has been linked with increased infiltration of neutrophils (Wang et al., 2014).

CXCL5 was identified as a potent chemoattractant of neutrophils *in vitro*. Furthermore, a murine tumour model and immunohistochemical studies showed a correlation between overexpression of CXCL5 and elevated numbers of $CD66b^+$ neutrophils infiltrating into HCC tissue that was associated with poor prognosis in HCC patients (Zhou et al., 2012). The role of other chemokines in neutrophil recruitment has been rarely studied, although an elevated level of CXCL6 was detected from an osteosarcoma cell line and in patients with gastrointestinal tumours that were associated with granulocyte neutrophilic recruitment (Proost et al., 1993, Gijsbers et al., 2005). A separate study also showed that administration of CXCL6 neutralizing antibodies in a melanoma mice model, injected subcutaneously with

GCP-2 overexpress melanoma cell, reduced tumour growth and metastasis when compared to un-treated mice, as well as inhabiting neutrophil migration *in vitro* (Verbeke et al., 2011).

Other inflammatory mediators can have an indirect effect on the recruitment of neutrophils. For instance, a clinical and experimental study in HCC showed that pro-inflammatory IL-17 in the peritumoral stroma of HCC is a critical mediator for the recruitment of neutrophils into tissues by up-regulating the expression levels of several chemokines including CXCL1, CXCL2, CXCL3 and CXCL8 from epithelial cells compared with intratumoral areas. The same study showed microlocalization of $CD15^{+}$ neutrophils and IL-17 in the peritumoral stroma by immunohistochemistry while only marginal levels of CD15 and IL-17 were detected in the cancer nest. Additionally, blocking of chemokine receptors CXCR1 and CXCR2 by specific monoclonal antibodies markedly reduced neutrophil migration induced by IL-17-treated liver epithelial cells L02 (Kuang et al., 2011). Similarly, a significant increase in TANs was observed in HCC cell line expressing high levels of CXCR6 receptor via producing pro-inflammatory cytokines, such as IL-1β, IL-6, CXCL8 and IL-17F secreted by this cell (Gao et al., 2012).

The common denominator among all the studies on ELR^{+} chemokines is that they mainly act by high-affinity binding to CXCR2 that is expressed abundantly by neutrophils and plays a role in tumour development. The effect of using a specific CXCR2 antagonist (AZ10397767) on neutrophils was demonstrated in a lung tumour model. A significant reduction in the number of TAN was observed in mice treated with the CXCR2 inhibitor and this was accompanied with retardation in tumour growth. The authors suggested that these infiltrating cells provide a secondary source of mediator that can stimulate tumour cell proliferation (Tazzyman et al., 2011). This notion is supported by the finding HCC cell proliferation, migration and metastatic potential can be induced by CXCL5 expression, a chemokine that also binds exclusively to

CXCR2. Further analysis for the mechanism underlying HCC proliferation and invasion indicated that CXCL5 induced several signalling pathways including PI3K-AkT and ERK1/2 pathway that was dependent on CXCR2 activation (Zhou et al., 2012).

1.2.5.1.1. Role of CXCR2 and other receptor in cancer

The chemokine receptor CXCR2 binds exclusively to ELR+ CXCL chemokines, including CXCL1-3 and CXCL5-8 (Ahuja and Murphy, 1996b). These ELR+ CXCL chemokines are generally considered chemoattractants for neutrophils, which are the major leukocyte cell population expressing the CXCR2 receptor. In addition to neutrophils, CXCR2 expression has also been found on several types of malignant cells where it has been associated with an aggressive phenotype. For example, overexpression of CXCR2 was detected on tumour cells in patients with metastatic colon cancer. Treatment of patients with 5-fluorouracil (5FU) chemotherapy induced CXCR2 transcripts levels in liver metastases that was associated with poor patient outcome (Desurmont et al., 2015). Treatment of HCT116 and Caco2 colorectal cancer cells with SCH-527123, a selective CXCR2 antagonist, inhibited phosphorylation of the NF-κB/MAPK/AKT pathway, and reduced cell migration and invasion by interfering with the CXCL8/CXCR2 axis (Ning et al., 2011). Moreover, blocking CXCR2 induced apoptosis in human colon carcinoma cells, whilst reducing their motility and proliferation in vitro (Varney et al., 2011). Administration of SCH-527123 in a murine colon cancer model showed no detectable difference on primary tumour growth between treated and untreated mice, but significantly reduced the number of metastases, highlighting the role of CXCR2 in tumour cell locomotion and angiogenesis. This anti-metastatic activity was found to be associated with diminished blood vessel formation within the metastatic lesion. In contrast, using a Lewis lung cancer (LLC) murine model, Keane and colleagues showed that depletion of CXCR2 had a significant

inhibitory effect on both primary tumour growth as well as lung metastases formation that was also associated with reduced angiogenesis (Keane et al., 2004).

CXCR2 activation may result in autocrine signalling, as CXCL8 gene transfectants in colorectal cancer cells increased cell proliferation and migration activity (Ning et al., 2011). Similar observations were demonstrated in other tumour cells, where elevated levels of CXCR2 and its ligands (CXCL1-3) were detected in oesophageal and lung cancer, further suggesting an autocrine loop to induce cell proliferation (Wang et al., 2006, Keane et al., 2004).

CXCR2 has been implicated indirectly in tumour growth via recruitment of leukocyte to tumour sites. As mentioned previously, accumulation of neutrophils has been reported in various malignancies (see section 1.2.4) and neutrophil migration to tumour sites was found to be CXCR2-dependent (Jablonska et al., 2014). The authors showed that administration of anti-CXCR2 antibodies in both melanoma and fibrosarcoma xenograft murine model supressed tumour growth by inhibiting neutrophil infiltration and tumour angiogenesis (Jablonska et al., 2014). Accumulating evidence has reported the ability of ELR+ CXCL chemokines to act as angiogenic agents in a direct or indirect manner. For example, increased expression of CXCL8 from malignant colonic epithelial stimulated chemotaxis of human microvascular endothelial cells that express CXCR2 (Heidemann et al., 2003). Therefore, it is not surprising that neutralizing CXCR2 with specific antibodies impaired angiogenesis in vivo (Addison et al., 2000).

Beside the well-described role of neutrophils as a mediator of angiogenesis, CXCR2 has been found to be responsible for recruitment of CXCR2+CD11b+Ly6Gh neutrophil-like MDSC that have immunosuppressive activity. Treatment targeting this CXCR2 MDSC population showed an enhanced response to checkpoint blockade treatment with anti-programmed death-1 (PD-

1) in a rhabdomyosarcoma (RMS) mouse model (Highfill et al., 2014, Katoh et al., 2013). Depletion of CXCR2 in a murine pancreatic cancer model, provided compelling evidence of the importance of CXCR2 signalling in neutrophil infiltration to tumours (Steele et al., 2016). Depletion of neutrophils using an anti-Ly6G strategy decreased metastasis and increased the recruitment of anti-tumour CD3+ T cells (Steele et al., 2016).

1.2.5.1.2. Duffy antigen receptor for chemokines binding to CXCR2 ligands

A protective role of CXCR2 in early tumorigenesis has been recently proposed. In a process known as oncogene-induced cellular senescence (OIS), activation of a specific oncogene results in the entry of cells into an irreversible growth arrest state known as cellular senescence. Here senescence cells were found to secrete CXCL6 and CXCL8 via NF-κB and C/EBPβ proinflammtory transcription factors. In addition, OIS was associated with overexpression of CXCR2 (Kuilman et al., 2008). Further evidence supports this notion, as inhibiting CXCR2 in tumour cells impaired cell cycle arrest and reduced the DNA-damage response, whilst overexpression of CXCR2 in cells restored the senescence phenotype (Acosta et al., 2008).

Some ELR+ CXC chemokines, such as CXCL8, CXCL1 and CXCL7 can bind to Duffy antigen receptor for chemokines (DARC), a seven transmembrane receptor expressed on erythrocytes and other cells that is structurally similar to chemokine receptors. Binding of these ELR+ CXC chemokines to DARC does not induce a downstream signalling event by either GPCR or Ca +2 flux (Neote et al, 1994), and this is proposed to be due to the absence of the highly conserved DRY motif from the intracellular loop of DARC that is essential for G protein binding and signal transduction (Hadley and Peiper, 1997).DARC are presumed to function as decoy receptors, mopping up excess chemokine in the microenvironment and therefore limiting their activity.

DARC that is expressed on erythrocytes can absorb CXCL8 from circulation to limit the stimulation of leukocytes (Darbonne et al., 1991) . Addsion et al, who demonstrated that expression of DARC within tumours could alter the progression of the disease, provided further evidence. The authors showed that overexpression of DARC in lung cancer cells resulted in enlarged tumours when implanted into a xenograft model, but histological examination showed significant increases in tumour necrosis, with reduced tumour cell viability and metastasis formation *in vivo* (Addison et al., 2004). The same negative regulatory affect was observed when DARC was overexpressed in a breast cancer model, where tumour growth and metastasis were also reduced (Wang et al., 2006).

1.2.5.2. Other molecules involves in neutrophil infiltration

Apart from ELR^+ chemokines there has been a number of studies describing other factors that support neutrophil recruitment to tumours. A recent *in vivo* study demonstrated a neuropeptide, gastrin-releasing peptide (GRP), induced neutrophil recruitment via a GPCR that was dependent on the PI3K and MAPKs signalling pathway, similarly to other chemoattractant molecules. This migration was abolished using RC-3095, specific inhibitor for GRP receptor (Czepielewski et al., 2012). High mobility group box 1 protein (HMGB1) is a highly conserved chromatin-binding factor that aids transcription. It is passively released from stressed or necrotic cells and acts as an alarm signal to activate innate immune responses, in particular phagocytes that can then clear the cell debris (Scaffidi et al., 2002). Orlova and colleagues found that HMGB1 injected into the peritoneum of mice rapidly recruited neutrophils that was dependent on co-expression of the integrin heterodimer CD11b/CD18 and the receptor for HMGB1, receptor for advanced glycation end products (RAGE) on neutrophils (Orlova et al., 2007).

1.2.5.3. Macrophage migration inhibitory factor

1.2.5.3.1. Characteristics and biological activity

As its name indicates macrophage migration inhibitory factor (MIF) was first described as an inhibitor of random macrophage migration and activation (David, 1966) from a study aimed at understanding delayed type hypersensitivity reactions. Subsequent studies have reported that MIF expression is ubiquitous in a variety of cells including monocyte/macrophages (Calandra et al., 1994), lymphocytes, eosinophils (Rossi et al.), neutrophils (Daryadel et al., 2006), and non-immune cells such as endothelial cells (Nishihira et al., 1998) and epithelial cells (Imamura et al., 1996). In addition, the expression of MIF has been detected in several tissues and cells, especially those tissues exposed to the environment; for example, lung, gastrointestinal and skin (Shimizu et al, 1996). The discovery that MIF is produced from corticotrophic cells of the pituitary gland, classify it as a hormone as well as cytokine. Another distinctive feature of MIF is that it can overcome the anti-inflammatory effect of glucocorticoids to enable a sustained inflammatory response (Bernhagen et al., 2007). There is much evidence to demonstrate that MIF plays a significant role in various inflammatory and autoimmune disease, such as sepsis (Bozza et al., 1999), acute respiratory distress syndrome (ARDS) (Lai et al., 2003), glomerulonephritis (Yang et al., 1998) atherosclerosis (Das et al., 2013), rheumatoid arthritis (Morand et al., 2006) and lupus (Foote et al., 2004). Unlike many other cytokines, pre-formed MIF can be stored intracellularly and expressed constitutively without *de novo* protein synthesis (Bacher et al., 1997).

X-ray crystallographic studies of human and rat MIF revealed a homotrimer structure, each monomer consisting of four β sheet and two α helices connected by hydrogen bonds (Suzuki et al., 1996). Although not directly related to the chemokine superfamily, MIF shares a structural similarity with chemokines as it contains a conserved Glu-Leu-Arg (ELR) motif that is present in many CXCL chemokines. However, in MIF an aspartic acid (Asp/D) amino acid residue replaces the glutamate (Glu/E) making the sequence DLR in MIF. This motif is consequently known as “pseudo-(E)LR” motif

(Hébert et al., 1991)Also, 3D structural analysis has revealed a striking similarity between the monomeric form of MIF and dimeric form of CXCL8 (Weber et al., 2008) (Fig.1.5).

MIF has unique enzymatic catalytic activity toward D-dopachrome or L-dopachrome tautomerase to give 5,6-dihydroxyindole-2-carboxylic acid (DHICA)(Rosengren et al., 1996). The MIF tautomerase site is located in the N-terminus with the proline motif being essential for activity as a single proline mutation at this site showed reduction in the catalytic activity along with impaired cytokine activity (Stamps et al., 1998). A significant reduction in the level of superoxide generated by neutrophils incubated with mutant MIF was observed compared to wild-type MIF, indicating the importance of the catalytic site for MIF's biological activity (Swope et al., 1998, Bendrat et al., 1997). Binding of MIF to its cell surface receptor, CD74 (also known as the MHC class II-associated invariant chain (II)), is not enough to initiate signal transduction mechanisms as CD74 has a short intracytoplasmic tail of only 46 amino acids (Shi et al., 2006). However, MIF mediates activation of signal-regulated kinase 1 (ERK1)/ERK2), members of the family of mitogen-activated protein kinases (MAPKs), by binding to a CD74/CD44 complex (Leng et al., 2003). MIF has also been reported to bind to CXCR2 and CXCR4 (Bernhagen et al., 2007). While it is predicated that there is a two site binding interaction between the N-loop of MIF with the N-terminal domain of CXCR2 and between the MIF pseudo (E)LR motif and extracellular loops of CXCR2 (Kraemer et al., 2011), the binding site of MIF with CXCR4 are still to be revealed.

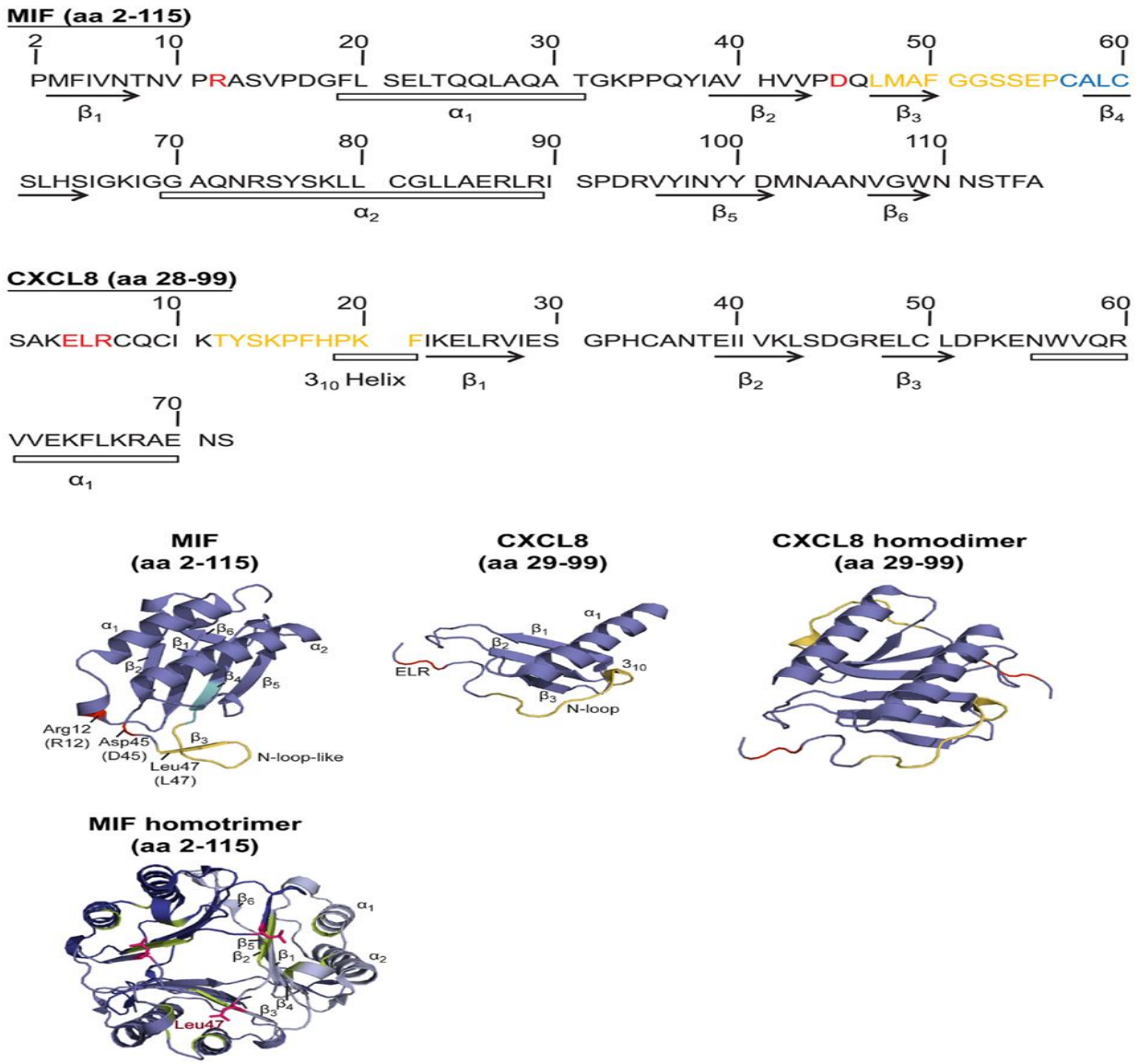

Figure 1.5 Crystal structure and amino acid sequence comparing MIF to CXCL8 (Tillmann et al., 2013)

1.2.5.3.2. MIF as inflammatory molecule and chemotactic cytokine

MIF has been recently classified as having "chemokine-like functions (CLF)" because some of its activity is similar to those observed in chemokines, leading to many changing its name from MIF to CLF. MIF is released from cells under inflammation, infection and in response to stress

and it is able to induce leukocyte recruitment (Gregory et al., 2004) .MIF has been identified as a non-cognate ligand of chemokine receptor CXCR2 and CXCR4 (Bernhagen et al., 2007). However, MIF lacks the critical cysteine residues in its N-terminus that is present in classical chemokines. The precise biological function of MIF has not yet been fully revealed but evidence suggest that MIF is capable of inducing an immune response either by acting directly on immune cells or indirectly by activating other stimuli to the immune system. For instance, MIF has been shown to act as inflammatory cytokine and that upon release can trigger cytokine production such as, CXCL8, CXCL6, TNF-α, INF-γ, IL-1β and IL-12 from macrophages (Onodera et al., 2004). These MIF-activated macrophages can induce further inflammatory stimuli by releasing free radicals (White et al, 2001). Beside macrophages, MIF has been reported to mediate the recruitment of monocytes, neutrophils (Dumitru et al., 2011, Trellakis et al., 2011a) and T-cells (Bernhagen et al., 2007). Interestingly, the presence of MIF in the tumour microenvironment has been reported to alter anti-cancer immunity response. MIF was found to have a direct inhibitory effect on NK cells, and the use of neutralizing antibodies against MIF abrogated this effect (Apte et al., 1998). Another study investigated the mechanism MIF employees to inhibit NK cell activity; the authors showed that MIF reduced the ability of NK cells to recognize tumour cells via downregulation of NK cell receptor, NKG2D (natural killer group 2D) (Krockenberger et al., 2008). In addition, high levels of MIF in a neuroblastoma model inhinited T lymphocyte activation, via the IFN-γ pathway, resulting in arrest of cell growth and increased cell death (Yan et al., 2006). MIF is also essential for the immunosuppressive activity of monocytic MDSCs in melanoma, and treatment with a small molecule MIF enzymatic antagonist, 4-IPP, significantly reduced T-cell activity (Yaddanapudi et al., 2016).

There is considerable evidence to demonstrate the central role that MIF plays in the inflammatory response indirectly. Deletion of MIF gene from macrophages impairs the response to pathogenic bacteria and lipopolysaccharide due to a significant downregulation of Toll-like receptor 4 (TLR4), the signal-transducing molecule of the LPS receptor complex (Roger et al., 2001).In addition, MIF has been found to downregulate the tumour suppressor p53 in fibroblast and macrophage, inducing cell survival (Hudson et al., 1999).

1.2.5.3.3. MIF in cancer

Clinical reports has described increased expression of MIF in variety of human tumours including breast (Xu et al., 2008), prostate (Meyer-Siegler et al., 2005), osteosarcoma (Han et al., 2008), colon (He et al., 2009), gastric (He et al., 2006), neuroblastoma and glioma (Mittelbronn et al., 2011). Recently, overexpression of MIF was detected from HNSCC patients and correlated with poor patient outcome and tumour progression (Kindt et al., 2013b).

MIF employs a variety of mechanisms that contribute in tumorigenesis and invasiveness of cancer. First, MIF can induce tumour cell survival via inducing the phosphoinositide-3-kinase (PI3K)/Akt signalling pathway, which leads to phosphorylation of the proapoptotic proteins BAD and Foxo3 supressing apoptosis (Lue et al., 2006) or via down-regulation of tumour suppressor gene p53 (Hudson et al., 1999). Second, MIF signalling via CD74 leads to sustained activation of MAPK extracellular-signal regulated kinase ERK 1/ERK 2 (Lue et al., 2006). MIF-induced phosphorylation of ERK1 and ERK2 is mediated by the CD74/CD44 complex has also been associated with cell proliferation (Shi et al., 2006). Inhibition of MIF or it is receptor using CD74 neutralizing antibodies significantly decreased the proliferation of DU-145 prostate cancer cell in vitro (Meyer-Siegler et al., 2006). Knockdown of MIF reduced the tumour growth rate in a xenograft model of hepatocellular carcinoma (Huang et al., 2014) ,while MIF

overexpression in vivo enhanced tumour growth and metastasis formation (Funamizu et al., 2013). Investigations using knock out MIF in tumour cells showed reduced proliferation via induction of growth related protein such as Bax, caspase-3, while anti-apoptotic proteins Bcl-2, pAkt, and p53 were decreased (Guo et al., 2015, Huang et al., 2014). Collectively these data point to the ability of MIF to induce proliferation of tumour cell in an autocrine manner. Interestingly, overexpression of MIF induces epithelial-to-mesenchymal transition (EMT) phenotype in pancreatic cancer cells. EMT is an aggressive feature characterized by decreased E-cadherin and increased vimentin expression in MIF expressing cancer cells and is associated with diminish responsiveness to chemotherapy (Funamizu et al., 2013). MIF has also been reported to induce migration of cancer cells *in vitro* (Ren et al., 2003, Shimizu et al., 1999).

One of the most important activities of MIF is its ability to act as a pro-angiogenic cytokine. Several published studies show that MIF can promote endothelial cell proliferation and motility (Chesney et al., 1999, Yang et al., 2000). Tumour-derived MIF has been reported to induce macrophages to upregulate angiogenic cytokines, such as CXCL8, CXCL1 and CXCL7 (White et al., 2001). In support of the role of tumour-derived MIF, deficiency of MIF in a B16 melanoma tumour model showed that isolated tumour-associated macrophages (TAMs) display an M2/pro-tumuoral phenotype. The level of pro-inflammatory cytokines, TNF-α, IL-12, cyclooxygenase-2 (COX-2) and inducible NOS (iNOS) were higher in TAM from tumour bearing MIF-deficient mice in compared to MIF wild-type mice (Yaddanapudi et al., 2016). Similarly, in an inflammatory model, the chemotactic response of neutrophils to CXCL1 (KC) was significantly impaired in MIF-deficient mice (Santos et al., 2011).

A recent study showed that the strong expression of MIF by tumours was associated with neutrophil infiltration that positively correlated with disease stage and negatively with disease outcome (Dumitru

et al., 2011, Trellakis et al., 2011a). The authors also showed that cross-talk between tumour cells and immune cells is necessary for cancer progression and altering the tumour microenvironment. For example, HNC cells were able to enhance the viability of neutrophils and induce the releases of inflammatory factor, such as CCL4, CXCL8 and MMP-9 *in vivo* (Dumitru et al., 2011, Trellakis et al., 2011a). These findings indicate the importance of the interaction between HNC and neutrophils in modulation of neutrophils biology and cancer progression. Interestingly, a distinct pattern of TAN infiltration as disease progress was observed in OSCC patients, as T3-T4 OSCC presented with higher neutrophil infiltration within the intratumoural region and higher neutrophil/lymphocyte ratio in the invasive front than T1-T2 OSCC tumours (Caldeira et al., 2015). Furthermore, expression of MIF has been found to be up-regulated by tumour hypoxia (Koong et al., 2000). Tumour hypoxia induces activation of hypoxia inducible factor α (HIF α), a transcription factor that controls expression of several key genes involves in tumour growth, invasiveness and angiogenesis, such as, vascular endothelial growth factor (VEGF) (Shweiki et al., 1992), lysyl oxidase (LOX) (Erler et al., 2006)and connective tissue growth factor (CTGF) (Higgins et al., 2004) . Deletion of MIF in pancreatic adenocarcinoma cells demonstrated that stabilization of HIF-α is MIF-dependant in hypoxia (Winner et al., 2007).

MIF knockdown murine models of ultraviolet B (UVB) showed a 45% reduction in epidermal tumorigenesis as a result of chronic exposure UVB irradiation. A further investigation showed that MIF-deficient mice not only had reduced neutrophil infiltration but they also show a diminished ability of the tumour to progress and grow mainly via stimulation of p53 and reduced levels of VEGF in the skin of these mice when compared to wild-type controls (Martin et al., 2009).

1.2.5.3.4. Targeting MIF in cancer

Thus far, three main approaches have been utilised in cancer studies to examine the role of MIF including the use of small molecules inhibitors, indirect stabilization of MIF and the use of monoclonal antibodies against MIF. Anti-MIF antibodies have been successfully generated

by Baxter and use of these showed a significant affect in reducing tumour growth in a prostate and colon xenograft model (Kerschbaumer et al., 2012, Hussain et al., 2013, He et al., 2009) Interestingly, the authors demonstrated that the binding region of anti-MIF was located within oxidoreductase motif. Today, the use of anti-MIF antibodies to treat patients with solid tumours is in Phase 1 trial (clinicaltrials.gov.NCT01765790).

The use of small molecular weight inhibitors that interfere with the enzymatic activity site of MIF is widely used in cancer biology. ISO-1, the gold standard MIF inhibitor, binds to the tautomerase active sit of MIF and restricts the pro-inflammatory activity of MIF (Al-Abed et al., 2005). The use of ISO-1 has been validated in multiple xenograft models, such as in lung (A549) (Rendon et al., 2007) prostate (DU145) (Meyer-Siegler et al., 2006) and glioblastoma (LN229) (Schrader et al., 2009) and has demonstrated significant results in controlling tumour growth. In a DU-145 xenograft prostate cancer model, treatment with 20 mg/kg of ISO-1 showed a significant reduction in tumour volume and blood vessel formation compared to control mice. Although, exogenous ISO-1 can inhibit the intracellular tautomerase activity of MIF (Al-Abed et al., 2005), tumour tissue showed no difference in total MIF protein content while MIF released in the serum of mice was significantly reduced in ISO-1 treated mice, suggesting that the MIF secreted form the tumour has been affected by ISO-1 treatment (Meyer-Siegler et al., 2006). Similarly, ISO-1 administration in colon carcinoma xenograft model showed the same suppresser effect on tumour growth via interfering with angiogenesis (He et al., 2009). Despite the interesting *in vivo* result, the use of ISO-1 in human clinical trial is limited, because of enzymatic kinetic and route of administration (interaperitoneal).

1.2.5.4. Neutrophil-derived molecules in cancer progression

As neutrophils play a well-established role in host defence and in killing invading microorganisms they produce secreted products, such as ROS, cytokines and proteinases, that are also capable of causing damage to host tissue and altering tumour cell behaviour in many aspects. The following section will describe the main neutrophil-derived molecules and their role in cancer progression and is summarised in figure 1.6.

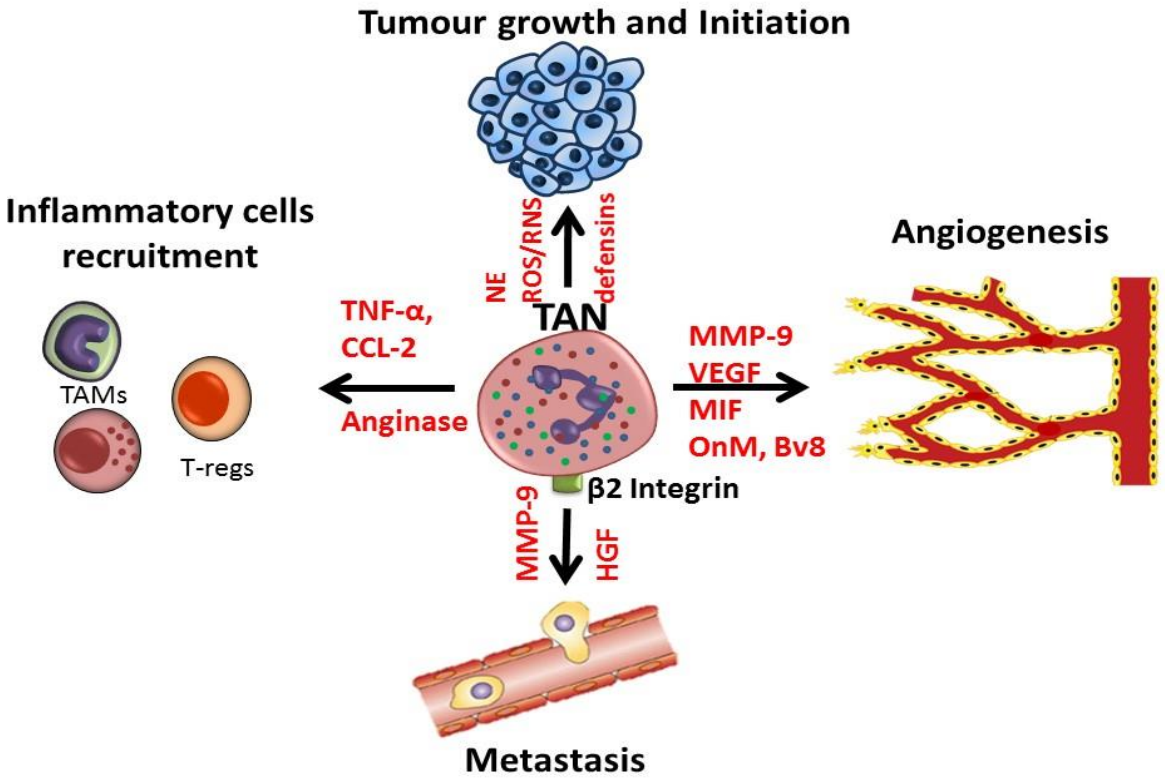

Figure 1.6 Schematic diagram summarising the role of TANs in tumour progression. Neutrophil-derived molecules play an essential role in tumour development from initiation to metastasis to distant sites.

1.2.5.5. Role of neutrophils in tumour initiation and carcinogenesis

As already mentioned, neutrophils are an abundant source of reactive oxygen (ROS) and nitrogen (RNS) species that are produced via the activity of an oxidant generating system within the phagososmes (Fialkow et al., 2007). In a mouse model, a strong link was observed between neutrophil infiltration and increased DNA mutation frequency in tumour cells. This

genotoxic capacity was proposed to be due to inducible nitric oxide synthase (iNOS) released from TANs and was measured using mutation at the hypoxanthine phosphoribosyltransferase (Hprt) locus (Sandhu et al., 2000). Other investigators point to the role that neutrophil accumulation in inflamed tissue may play toward cancer progression. Several colon cell lines were co-cultured with neutrophils in order to mimic chronic exposure within the tumour environment were tested *in vitro*. Activated neutrophils were able to induce DNA damage and replication error in colon epithelial cells via products other than ROS/RNS (Campregher et al., 2008).

1.2.5.6. Role of neutrophils in tumour growth, progression and metastasis

Several lines of evidence have shown that TANs can secrete factors that affect tumour cell proliferation. Neutrophil elastase (NE), the major component of neutrophil azurophilic granules, is a serine proteinase and was found to induce tumour cell proliferation in Lewis lung carcinoma cells by hyperactivity of the phosphoatidylinositol-3-kinase (PI3K) pathway and administration of NE inhibitors in mice reduced lung tumour growth by 69% (Houghton et al., 2010).

In addition, NE was found to be important in remodelling of the ECM, thus facilitating invasion and metastasis of tumour cells (Mainardi et al., 1980) as neutrophil-derived proteinases (elastase, cathepsin-G, protease-3) were reported to cause activation of MMP-2 and cooperating with membrane type-1 matrix metalloproteinase (MT1-MMP) to enhance cell invasiveness (Shamamian et al., 2000). In response to TNF-α or GM-CSF, neutrophils release protease and heparanase that degrade components of the extracellular matrix (ECM) as they transmigrate across endothelium (Mollinedo et al., 1997). The release of ECM degrading enzymes alters the expression of cell surface adhesion molecules and provides the neutrophil

with the ability to extravasate from the circulatory system, invade the surrounding solid tissue and play a crucial role in altering the tumour microenvironment. Of the proteases released by neutrophils, matrix metalloproteinases have been found to be a key player in promoting tumour progression. There are two types of MMPs within neutrophils, collagenase/MMP-8, and gelatinase B/MMP-9 located in secondary and tertiary granules, respectively. It was demonstrated that TAN, enhance invasion and metastasis of rat mammary adenocarcinoma cells through the secretion of elevated levels of MMP-9 and heparanase that remodel the ECM (Welch et al., 1989).

Other effectors exist within primary granules, antimicrobial peptides called human defensins have also been found to promote proliferation of a human lung epithelial cell line via the mitogen activated protein kinase (MAPK) signalling pathway (Aarbiou et al., 2002). Recent studies revealed that TANs induce a feedback effect on tumour cells. Dumitru and co-workers demonstrated that HNSCC supernatant stimulates p38-MAPK in neutrophils, which strongly increases the production of CCL4, CXCL8 and MMP-9 (Dumitru et al., 2012); factors that have been associated with tumour progression. For example, an association was found between CXCL8-induced neutrophil recruitment with increased tumour growth of a highly tumorigenic and metastatic melanoma cell line (Schaider et al., 2003).

Circulating tumour cells can use neutrophils as a vehicle to pass through the endothelial cell wall and this is another mechanism by which neutrophils facilitate tumour metastasis. Studies have shown that tumour cells (melanoma and lung) secreted CXCL8, causes neutrophil recruitment and increases the expression of adhesion molecules β_2–integrin (LFA-1, CD11a/CD18) on neutrophils that influence tumour cell binding by a “two-step adhesion” mechanism involving binding to the endothelial as well as the tumour cell via intracellular

adhesion molecules-1 (ICAM-1) (Huh et al., 2010, Slattery and Dong, 2003). Similarly, neutrophils were also found to promote liver metastasis by up-regulation of Mac-1 (Spicer et al., 2012). Alternatively, TNF-α-stimulated neutrophils up-regulated the expression of carbohydrate sialyl Lewis X (sLeX) on non-small cell lung cancer (NSCLC) and increased it is binding to selectin receptor (E-selectin) on the endothelial cell surface (St Hill et al., 2011).

Dumitru and colleagues notice that TAN infiltration was associated with increased expression of a cytoskeleton protein that is involved in cellular migration and invasion, cortical actin binding protein (CORTACTIN) in oropharyngeal cancer. The investigators provided evidence that neutrophils are required to induce migration of tumour cell via release of factors that phosphorylated CORTACTIN (Dumitru et al., 2013). Furthermore, neutrophils primed with HNC derived MIF have been shown to enhance the adhesion and migration properties of tumour cells in vivo (Dumitru et al., 2011).

A recent study demonstrated that tongue cancers containing high numbers of neutrophil infiltrate were associated with lymph node metastasis and predicted a poor clinical outcome (Wang et al., 2014). A very recent finding identified a new mechanism neutrophils use to mediate tumour cell seeding in the pre-metastatic niche. Coffelt and co-workers showed that tumour cells cooperate with gamma delta (γδ) T cells to promote a TAN phenotype via IL-17 expression. Moreover, neutrophil depletion by neutralizing IL-17 significantly reduced the metastatic spread to pulmonary and lymph node in a breast cancer mouse model (Coffelt et al., 2015). Increased expression of IL-17 from neutrophils of OSCC patients has been observed but no further investigation on the metastasis process was carried out in HNSCC (Garley et al., 2009).

In line with the observation that neutrophil numbers increase in the peripheral blood of patients with advanced stage of HNSCC (Trellakis et al., 2011a), gene and surface analysis of circulating neutrophils from patients with the advance malignancy demonstrated that these express a pro-tumorigenic TAN-like phenotype. Further studies using a tumour bearing mice model, showed that these neutrophils enhance tumour metastasis (Zhang et al., 2015).

1.2.5.7. Role of tumour-associated neutrophils in angiogenesis

Mounting evidence supports the association between TANs and the process of angiogenesis and neovascularization (Tazzyman et al., 2009). The mechanism by which neutrophils facilitate the formation of new blood vessels is believed to be mediated by the secretion of chemokines, protease and growth factors from internal pre-stored granules. These molecules can either stimulate angiogenesis directly or indirectly via remodelling of extracellular matrix or by promoting the release of angiogenic molecules. Neutrophils were found to be a plentiful source of the potent angiogenic vascular endothelial growth factor (VEGF) (Gaudry et al., 1997) and active recruitment of neutrophils containing VEGF has been observed in human endometrium during endometrial proliferation and angiogenesis through menstrual cycle (Mueller et al., 2000). An in vitro study showed that conditioned medium from neutrophils infiltrating A549 spheroid contains elevated level of VEGF and MMP-9 that were responsible for microvascular endothelial cell proliferation and tubule formation (Tazzyman et al., 2011). Furthermore, Bv8 has recently been identified as a neutrophil-derived mediator of tumour angiogenesis using rat insulin promoter (RIP)-T-antigen (Tag) transgenic mouse model of pancreatic cancer. This protein is structurally similarly to endocrine gland derived VEGF (EG-VEGF) both of which bind to receptors known as prokineticin (PKR) 1/EG-VEGF receptor 1 (PKR1/EG-VEGFR1) and PKR2/EG-VEGFR2 that are expressed on endothelial cells. Blocking

Bv8 using neutralizing antibodies at an early tumour stage resulted in a reduction in the number of pancreatic islets undergoing angiogenic switch and reduction in tumour infiltrating $CD11b^+$ $Gr1^+$ cells than controls (Shojaei et al., 2007).

Other neutrophil-derived molecules play a role in tumour vascularisation by degrading the ECM to facilitate endothelial cell and pericyte movement and stromal re-modeling that is crucial for angiogenesis. Of this, MMP-9 was identified as an essential indirect factor during the angiogenic switch. Immunohistochemical analysis showed that accumulated peritumoural neutrophils within HCC were the major source of MMP-9 in the tissue. An association was found between the high infiltration of neutrophils with angiogenesis and tumour progression at the tumour invading edge, and *in vivo* depletion of neutrophils significantly inhibited tumour angiogenesis and tumour growth (Kuang et al., 2011). In addition to its effect on the ECM, it has been shown that neutrophil-derived MMP-9 can promote the release of potent pro-angiogenic factors such as VEGF (Nozawa et al., 2006). Interestingly, neutrophils were found to release MMP-9 free of negative regulator, tissue inhibitors metalloproteinases (TIMP-1) and upon stimulation neutrophil TIMP-free proMMP-9 release in tumour microenvironment in a pro-enzyme form which is easily and rapidly converted to its biologically protolytic active form (Bekes et al., 2011). Furthermore, it has been reported that neutrophils secrete cytokines that can stimulate tumour cells to produce angiogenic factors. For instance, when neutrophils were co-cultured with human breast cancer cells, they released a large quantity of Oncostatin M (OSM), which is a pleiotropic cytokine belonging to the IL-6 family. Neutrophil-derived OSM enhanced the expression of VEGF from T47D and MDA-MB-231 breast cancer cell lines and increased the invasive and detachment capacity of the cells (Queen et al., 2005).

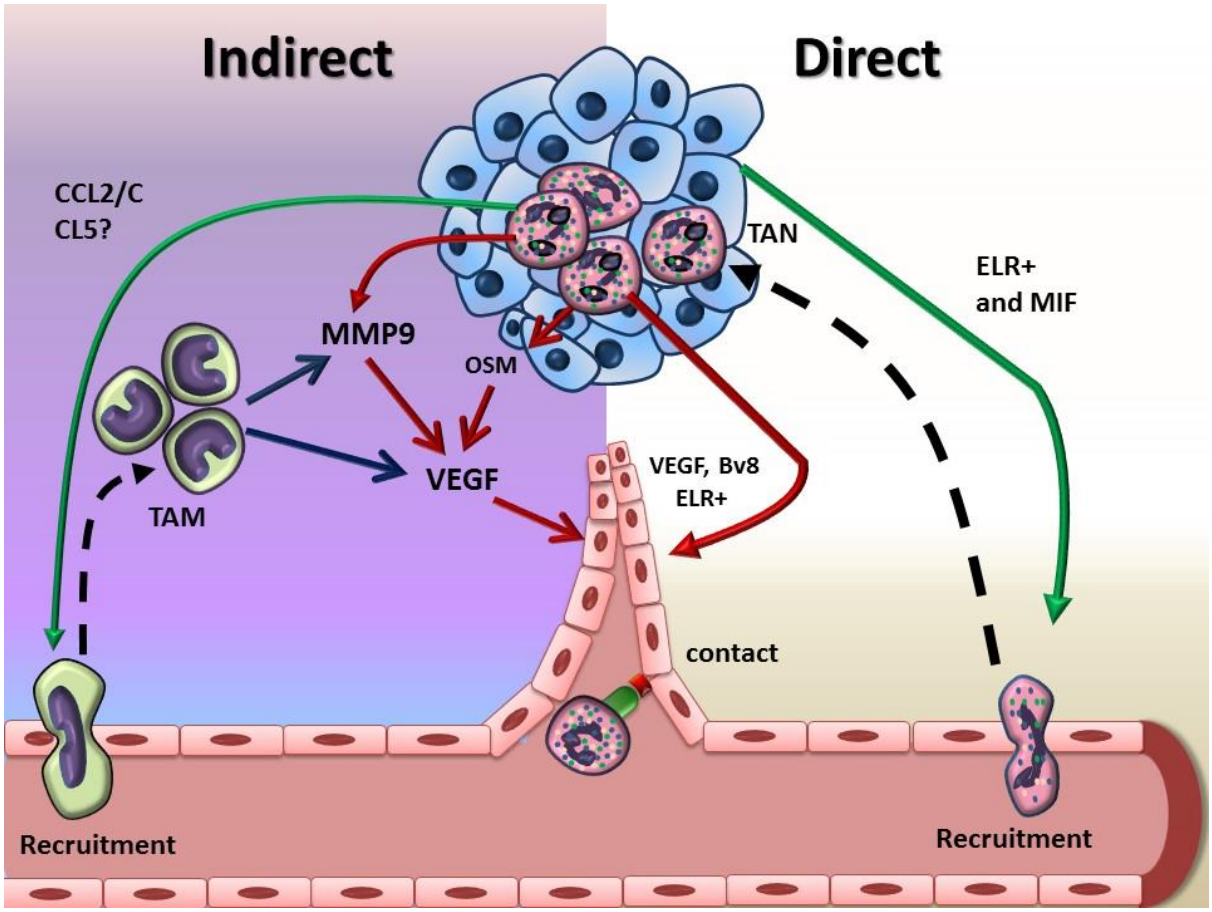

Figure 1.7 Mechanisms of neutrophil recruitment and neutrophil-mediated tumour angiogenesis. Neutrophils are recruited into the tumour from the circulation via the production of ELR+ chemokines or MIF that bind to CXCR2. Once inside the tumour, neutrophils can influence angiogenesis directly or indirectly. The direct mechanisms include release of such angiogenic factors as VEGF, ELR+ chemokines and Bv8 that promote endothelial cell migration and proliferation. The main indirect

mechanism appears to be the release of TIMP-1-free MMP-9 upon degranulation. TIMP-1-free MMP-9 has a dual role; it liberates the pro-angiogenic growth factors (VEGF & FGF-2) that are sequestered in the stromal matrix and also degrades components of the ECM. In addition, neutrophils can also secrete factors such as oncostatin M that stimulates tumour cells to increase their VEGF production and CCL2/CCL5 that may support the recruitment of TAM.

1.2.5.8. Role of Neutrophils in Immunomodulation

The possible mechanisms by which TAN can regulate innate and adaptive immune cell responses are less clear. However, evidence has shown that TAN are not only able to recruit more inflammatory cells to the tumour micro-environment but they can also induce suppressive effects on other immune cells. For example, neutrophils have been shown to inhibit T-cell effector functions. One explanation for the suppression of T-cell proliferation and activation is due to release of stored Arg-1from neutrophils that can cause degradation of extracellular arginine, an element required to activate T-cells (Rotondo et al., 2009). In addition, TAN mediated the recruitment of an immunosuppressive subset of T-cells, known as T-regulatory (T-regs) via the production of CCL17 (Mishalian et al., 2013). The same group showed previously that levels of CCL17 from N2 TAN was significantly higher compared to N1 TAN in this tissue (Fridlender et al., 2012). In agreement with this observation, Zhang et al reported that circulating neutrophils which exhibit an N2 TAN phenotype in the blood of patients with advanced cancer have an immunosuppressive function on peripheral leukocyte by increased expression of Arg-1(Zhang et al., 2015).

Traditionally, neutrophils can exert cytotoxic effect on tumour cells but there are several lines of evidence to suggest that tumour cells can escape the immune response directly or indirectly. For instance, when the direct contact between neutrophils and FaDu cells was prevented using antibodies against adhesion molecules, tumour cell-mediated lysis by neutrophils was significantly reduced (Bru et al., 2009).

1.3. Hypothesis

Tumour-derived factors drive neutrophil recruitment and induce polarisation by interacting with receptors on their cell surface. Interfering with this ligand-receptor interaction will reduce neutrophil recruitment to HNSCC that may disrupt tumour progression.

1.4. Aims

1. To examine distribution pattern and number of TAN in biopsies of HNC
2. To characterise a 3D *in vitro* model of HNSCC and use this to better understand the mechanism by which neutrophils are recruited into HNC tumour
3. Study the effect of neutrophil depletion and MIF inhibition on immune cell recruitment and tumour growth *in vivo*
4. To examine if MIF and HNSCC-derived factors affect human neutrophil phenotype.

Chapter 2: Material and Methods

2.1. Materials

2.1.1. Reagents

Reagents	Supplier
Agarose type V	Sigma-Aldrich
Bovine serum album (BSA)	Sigma-Aldrich
Cell Tracker ™ Green	Invitrogen, UK
CXCR2 antagonist (AZ10367797)	AstraZeneca, UK
CXCR2 antagonist (SB-265610)	GlaxoSmithKline
CXCR4 antagonist (AMD3100)	Sigma-Aldrich
Dimethylsulphoxide (DMSO)	Sigma-Aldrich
4',6-diamidino-2-phenylindole (DAPI)	Invitrogen, UK
FACS lysis buffer	
Foetal bovine serum (FBS)	Sigma-Aldrich
fMLP (f-Met_Leu-Phe)	Sigma-Aldrich
Ficoll-Paque ™ plus	GE Healthcare
HBSS medium without Ca^{+2}, Mg^{+2}or phenol red	Fisher Scientific
MIF antagonist (ISO-1)	Millipore
Penicillin/streptomycin	Sigma-Aldrich
Phosphate-buffered saline	Sigma
Recombinant human CXCL1	Peprotech, UK
Recombinant human CXCL5	Peprotech, UK
Recombinant human CXCL8	Peprotech, UK
Recombinant human MIF	Peprotech, UK
Recombinant human TGF-β	Peprotech, UK

Recombinant human TNF-α	Peprotech, UK
Recombinant human INF-γ	Peprotech, UK
RPMI-1640	Sigma-Aldrich
Sterile water	Baxter, UK
Thiazolyl Blue Tetrazolium Bromide (MTT) powder	Sigma, M5655
0.25%Trypsin/EDTA	Sigma
Non-enzymatic cell dissociation solution	

2.1.2. Equipment

Instrumentation	**Manufacturer**
Applied Biosystems 7900HT Fast Real-Time PCR System	Life technologies
Avanti J-26 XP Centrifuge	Beckman Coulte
Automated Cellular Imaging System III	Dako, Denmark
Attune Autosampler Flow Cytometry	Life technologies, USA
Axiovert 200M microscope	Zeiss, Germany
Class II Safety Cabinet	Walker, UK
Colorimetric (spectrophotometric) plate reader	Infinite® M200, TECAN, USA
Cytospin	CytoFuge 2
Cryostat	Leica, Germeny
FACS Calibur	Becton-Dicknson, USA
FACS LSRII	Becton-Dicknson, USA
Galaxy CO_2 incubators	Eppendorf
High-Speed Centrifuge	Sigma-Aldrich
MACSmix tube rotator	Miltenyi Biotec
MACSexpress Separator	Miltenyi Biotec
Microtome	Leica, Germeny
NanoDrop 1000	ThermoFisher, UK
Spanning disc confocal system	PerkinElmer UltraView

Slide Stainer	Leica, Germeny
TissueFAXS plus 200 system	TissueGnostics GmbH, Austria

2.1.3. Commercial kits

Commercial Kits	**Supplier**
ABC Vectastain kit alkaline phosphates mouse IgG	Vector Labs
ABC Vectastain Elite kit peroxidase rabbit IgG	Vector Labs
Alkaline phosphate substrate kit	Vector Labs
ArC™ Amine Reactive Compensation Beads	ThermoFisher
BD™ CompBeads (anti-mouse IgK/negative control compensation particle set)	BD biosciences
Bioline Isolate RNA mini kit	Bioline
BrdU (B5002)	Sigma
CCL4 ELISA kit	R & D system
CXCL8 ELISA kit	Peprotech
DAB substrate Kit	Vector Labs
FACS lysis buffer	BD biosciences
Human cytokine array panel A	R & D system
High Capacity cDNA Reverse Transcription kit	Life Technologies
MIF ELISA kit	R & D system
LIVE/DEAD™ Fixable Blue Dead Cell Stain Kit	Invitrogen
Vectastain Elite ABC Kit Rat IgG	Vector Labs
Vector Red substrate (SK-5100)	Vector Labs
VEGF ELISA kit	R & D system
TACS Annexin V apoptois kit (4830-01-K)	Trevigen
TMB substrate	BD biosciences

2.1.4. Buffers

Solution	Preparation
Acidified Isopropanol	1 µl Hydrochloric acid to 1 ml isopropanol
FACS buffer	PBS + 0.1% BSA + 0.1% sodium azide
Cryopreservation media	90% FCS and 10% DMSO
Formalin agarose	2 g of Agarose dissolved in 90 ml of distilled water and mixed with 10 ml of 40% formaldhyde

2.1.5. Antibodies

Antibody (Clone)	Working concentration	Labelled	Supplier	Application
Goat Anti-Mouse IgG	As required	AlexaFluor® 488	Invitrogen, UK	IC
Anti-Mouse IgG	As required	R-phycoerthrin(PE)	Sigma	IC
Rat anti-mouse Ly6G (1A8)	1:50	R-phycoerthyrin (PE)	BD Bioscience	IMF
Rat anti-mouse F4/80 (Cl: A3-1)	1:50	Alex flour-488	AbD Serotec	IMF
Anti-mouse CD31 (Clone 390)	1:50	Allophycocyanin(APC)	eBioscience,	IMF
Rat IgG_{2a}	1:50	AlexaFlour488	Santa Cruz (sc-3896)	IMF
Rat IgG2a	1:50	APC	eBioscience	IMF
Anti-mouse IgG F(ab) fragment R-PE	1:50	PE		IMF
Mouse anti-human CD66b (80H3)	1/50 (IHC)	UL	Beckman Coulter	IHC/Flow
Mouse anti-human MIF antibody(10C3)	25 µg/ml	Biotin	Biolegend	IHC (Human section)
Mouse anti-human ICAM-1			Abcam	Flow
Rat anti-human CD31 /DIA-310 (SZ31)	1:20	UL	Dianova	IHC

Rabbit anti-PIMO antisera	1:20	UL	Hypoxyprobe	IMF
Rabbit anti-human MIF antiserum (FL-115)	1:50	UL	Santa Cruz	IHC (mouse section)
rabbit serum IgG Isotype control	As required	UL	Abcam	IHC
Sheep anti-BrdU (ab2285)	1:20	HRP	Abcam	IHC
Mouse anti-human MIF (10C3)	1:20	Biotin	Biolegend	IHC

2.1.6. Cells

Adherent Cells			
Cell line	**Source Tissue**	**Culture Medium**	**Supplier**
FNB6	Immortalized normal keratinocyte (Buccal)	*Green's Medium* 330 ml DMEM, 108 ml F-12, 50 ml FCS, 5 ml P/S, 1.25 ml Amphotericin B, 2 ml Adenine, 0.5 ml T3, 25 µl EGF, 80µl Hydrocortisone, 2.5 ml Insulin, 500µl Cholera Toxin	Beatson Cancer Institute, Glasgow, UK
OKF6	Immortalized normal keratinocyte (floor of the mouth)	Defined keratinocyte serum-free medium (GIBCO) + 1 ml growth supplement	James Rheinwald, Brigham and Women's Hospital, Harvard Institutes of Medicine, Boston, USA
SCC-4	OSCC (tongue)	250 ml DMEM, 250 ml Ham's nutrition mixture F12, 10% FCS, 1% P/S + 50 µl Hydrocortisone	ATCC
SCC-9	OSCC (tongue, HPV-ve)	DMEM (low glucose),10% FCS, 1% P/, 2mM L-glutamine	ATCC

SCC2	Hypopharynx carcinoma (HPV+)	DMEM (low glucose), 10% FCS, 1% P/S, 2mM L-glutamine	Prof. S. Gollin, University of Pittsburgh School of Public Health, Pittsburgh, USA
SCC89	Tonsil carcinoma (HPV-)	DMEM (low glucose), 10% FCS, 1% P/S, 2mM L-glutamine	Prof. S. Gollin, University of Pittsburgh School of Public Health, Pittsburgh, USA
SCC72	Tonsil carcinoma (HPV-)	DMEM (low glucose), 10% FCS, 1% P/S, 2mM L-glutamine	Prof. S. Gollin, University of Pittsburgh School of Public Health, Pittsburgh, USA
H357	OSCC (tongue)	Green's medium (see FNB6)	Prof. Steven Prime, University of Bristol, UK
T5	OSCC (buccal)	Green's medium (see FNB6)	Beatson Cancer Institute, Glasgow, UK
FaDu	Hypopharygeal carcinoma (HPV-)	RPMI-1640, 10% FCS, 1% P/S, 2mM L-glutamine	ATCC
Cells cultured in suspension			
Cell line	**Source Tissue**	**Medium**	**Origin**
THP-1	Acute Monocytic leukemia	RPMI-1640, 10% FCS, 1% P/S, 2mM L-glutamine	ATCC
Primary human cells			
Cell number	**Source Tissue**	**Medium**	**Origin**
OK334	Buccal mucosa	Green's medium (see FNB6)	Healthy volunteer
NOK340	Buccal mucosa	Green's medium (see FNB6)	Healthy volunteer

NOF316	Wisdom tooth extraction	DMEM+10% FCS+ 1% P/S +L-glutamine	Healthy volunteer
NOF320	Wisdom tooth extraction	DMEM+10% FCS+ 1% P/S +L-glutamine	Healthy volunteer
NOF343	Wisdom tooth extraction	DMEM+10% FCS+ 1% P/S +L-glutamine	Healthy volunteer

All normal oral keratinocytes (NOKs) and fibroblasts (NOFs) were isolated from biopsies obtained from patients during routine dental procedures with written, informed consent (ethical approval number 09/H1308/66; cells were used with permission from Dr Helen Colley).

2.2. Methods

2.2.1. Cell Culture

2.2.1.1. Routine cell culture procedure

Using aseptic technique in all procedures; FaDu cells were cultured in tissue culture flaks with their specific media (See tables 2.1.6) and incubated at 37˚C with 5% CO_2 in a humidified incubator. The morphology and cell growth was monitored by microscopy. Cells were allowed to grow until they reached 80% confluence whereupon they were either sub-cultured for use in experiments or maintained as stock cultures. Growth medium was replenished every 2-3 days by aspirating half of the medium and replacing it with fresh medium. Cells were tested on regular basis for the presence of mycoplasma.

2.2.1.2. Hypoxic cell culture

Normal or cancer cell lines were seeded in triplicate at 1×10^5 cells per well in 6-well plates. Cells were incubated with 2 ml of specific media and were allowed to attach for the next 24 hours at 37°C, 5% CO_2 in a humidified incubator under normoxic (21% O_2) conditions. Non-

adherent cells were removed, fresh 1.5 ml serum-free medium added and cells cultured under hypoxic (0.5% O_2) or normoxic (21% O_2) conditions for 24 hours. Following incubation, cell culture conditioned medium was collected, centrifuged at 5000 rpm for 5 minutes to remove cell debris and stored at -70 ˚C for further analysis. Cells were harvested from the wells using trypsin/EDTA, centrifuged at 1000 rpm for 5 minutes and the cell pellet stored at -70˚C for total RNA extraction.

2.2.1.3. Sub-culturing adherent cells

Cell culture medium was removed and cells were washed twice with sterile phosphate buffer saline (PBS) without calcium and magnesium. Pre-warmed Trypsin/EDTA solution was added and cells incubated for 3-5 minutes at 37 °C, 5% CO_2 to detach the monolayer from the flask surface. Upon cell detachment an equal volume of serum containing growth medium was added to neutralise the trypsin activity, and the cell suspension was centrifuged at 1000 rpm for 5 minutes. The cell pellet was then re-suspended in the required volume of medium and the number of cells determined using a haemocytometer. For general passaging, cells were seeded at 1×10^6 in pre-warmed fresh culture medium in 75 cm^2 tissue culture flasks.

2.2.1.4. Sub-culturing suspension cells

THP-1 cell cells were seeded between 2-4× 10^5 cells/ml in their specific medium (Table 2.1.6) and maintained by renewing the medium every 2 to 3 days. Expansion of cells was continued until they reached approximately 8×10^5 cell/ml; whereupon cells were collected by centrifugation at 1000 rpm for 5 minutes then cells resuspended with fresh pre-warmed media to 2-4× 10^5 cells/ml. Cells were incubated at 37 °C, 5 % CO_2 in a humidified incubator in flasks in an upright position. Although, THP-1 can be cultured in vitro up to 25 passages, but for the propos of our study, cells were used within 10 passages after thawing to prevent

unwanted phenotypic drift, as it has been reported that THP-1 are sensitive for culture condition and it could alter their response (Aldo et al., 2013).

2.2.1.5. Cell counting

Routine cell counting was performed using a haemocytomer. After harvesting cells, 10 µl of a cell suspension was added to a clean chamber and the number of cells counted using an inverted microscope with a 10 x objective. The number of cells were counted in four of the 1 mm corner square, as shown in the figure 2.1 below, and then the average number of cells was multiplied by 10^4 to calculate the number of cells in 1 ml. If the sample was diluted before counting, then the number of cell/ml was multiplied by the dilution factor to calculate the final concentration of cells.

The viability stain Trypan Blue was used to determine cell viability. Live cells can exclude the dye from the inside of cells and so only dead are stained blue under light microscopy. The number of cells within the haemocytometer was counted as before and cell viability was determined according to following formula:

$$\% \text{ Cell Viability } = \frac{\text{number of blue (dead) cells}}{\text{number of total cells}} \times 100$$

Greater than 90% viable cells were used in each experiment.

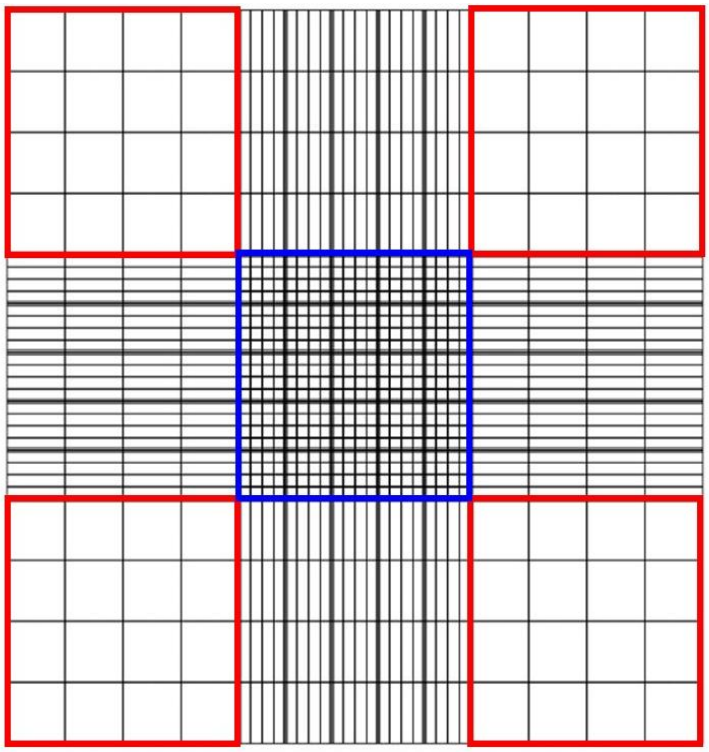

Figure 2.1 Counting chamber haemocytometer. Cells were counted in larger squares (Red).

2.2.1.6. Cryogenic preservation and recovery

For long-term storage, cells were re-suspended at a density of 1× 10^6 cells/ml in freezing medium (90% FBS, 10% DMSO), aliquoted into cryovials, and then placed into a cooling box (Mr.Frosty) at -80°C for overnight; this allows the temperature to be lowered slowly by 1°C /min prior to the cells being transferred to liquid nitrogen.

To resurrect cells, cryovials containing cells were thawed rapidly in a 37˚C water bath. The cells were slowly re-suspended in 9 ml pre-warmed medium and centrifuged at 1000 rpm for 5 minutes to remove any remaining DMSO. Pelleted cells were re-suspended in 5 ml specific medium, placed in a T25 cm^2 tissue culture flask and incubated at 37°C, 5 % CO_2 in a humidified incubator as previously described. After 24 hours, non-adherent cells were removed and fresh medium was added.

2.2.2. Neutrophils isolation and culture

2.2.2.1. Isolation of human neutrophils from peripheral blood using density centrifugation

Density gradient centrifugation was used to isolate human neutrophils from whole blood according to the modified method by Ferrante and Thong (Ferrante and Thong, 1978). Periperhal blood was collected by venipuncture from healthy volunteers with written, informed consent (University of Sheffield Ethical Approval). Blood was anticoagulated with 3.8% sodium citrate (1 part to 9 parts blood) and centrifuged at 400 x g for 20 minutes to separate the serum from cells. The upper serum layer was removed and the remaining blood cells were diluted 1:1 with HPSS without Ca^{+2} or Mg^{+2}. The blood mixture was layered slowly over 20 ml of Ficoll-Paque and centrifuged at 400 x g for 40 minutes at room temperature with the break set to 0 to separate cells. Following centrifugation, the blood was separated

into four distinct layers (Fig. 2.2), the top three layers were carefully removed and discarded. Neutrophils are present within the lower polymorphonuclear granulocyte/erythrocyte layer at the bottom of the tube. Erythrocytes were lysed by hypertonic lysis using ice cold sterile water for 30 seconds followed by the addition of an equal volume of 1.8% NaCl to bring the suspension to an isotonic state. Cells were centrifuged at 400 g for 15 minutes and the process repeated 3-4 times until all erythrocytes had been lysed. Neutrophils were then washed in HPSS without Ca^{+2} or Mg^{+2} and counted before being resuspended to the required cell density. Cell viability was assed using Trypan blue (2.2.1.5) and neutrophil viability was greater than 90% in all experiments. Neutrophil purity was evaluated by flow cytometry using the neutrophil-specific marker CD66b. The neutrophil sample was discarded if signs of neutrophil activation was observed at any step during the isolation process.

2.2.2.2. MACSexpress separation for neutrophil isolation

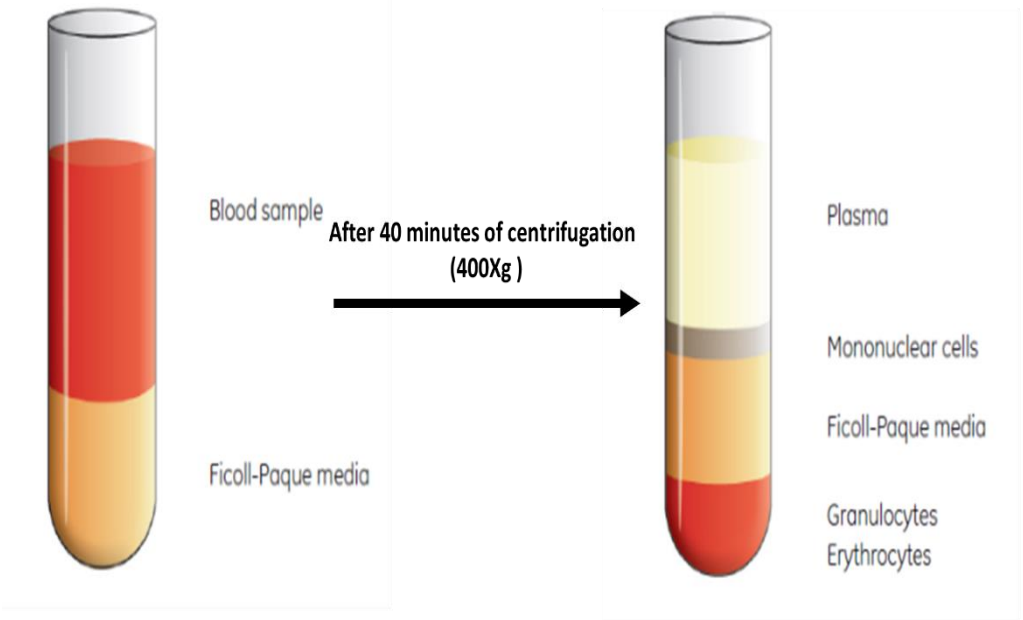

Figure 2.2 Schematic diagram for layers obtained after Density gradient centrifugation

This method allows for the fast isolation of neutrophils from whole blood without the need for density centrifugation or erythrocyte lysis. The procedure uses a cocktail of antibody-conjugated beads that are specifically designed to bind to erythrocytes and other leukocyte populations besides neutrophils. The neutrophils are then purified by immunomagnetic negative selection. Venous blood was collected from healthy volunteers into EDTA anticoagulant tubes. The lyophilized antibody cocktail was prepared freshly before each cell separation according to manufacture instructions and the final cocktail mixture used in the recommended volume of whole blood. For example, for 8ml of blood, one vial of antibody cocktail was reconstituted in 2 ml buffer A by pipetting up and down 3 to 4 times. Then 2 ml of buffer B was added to the cocktail mixture and mixed gently for 3 to 4 times. Eight ml of blood was transferred into a 15 ml universal tube and mixed with 4 ml of the prepared antibody cocktail and incubated in a MACSmix tube rotator at approximately 12 rpm for 15 minute. Following this incubation, the mixture removed from the rotator and placed in a magnetic field using a MACSexpress Separator without the lid for 15 minutes. The cell fraction was collected from the supernatant from the front wall of the tube and the supernatant containing the neutrophils was suspended in sterile HBSS without calcium and magnesium and the number of cells determined using a haemocytometer. Cell purity of the isolated neutrophils was evaluated by flow cytometry using the neutrophil-specific marker CD66b and a yield of >95% neutrophils with >95% viability was used in downstream applications.

2.2.2.3. In vitro differentiation of neutrophils into an N1 or N2 phenotype

Directly after isolation, neutrophils were suspended at a concentration of 1×10^6 cells/ml; a portion of the suspension was removed for flow cytometric staining on naive (untreated) neutrophils. Neutrophils were stimulated with 25 ng/ml human recombinant TGF-β for N2 polarisation (Fridlender et al., 2009), 100 ng/ml human recombinant INFγ for N1 polarization (van Egmond et al., 2001), 100 ng/ml human recombinant MIF or incubated with serum free-conditioned medium collected from FaDu spheroids for 8 or 24 hours at 37°C, 5% CO_2 under humidified conditions. Untreated cells were incubated under the same conditions and used as a negative control. At the end of incubation period, the neutrophil condition medium was collected and centrifuged at 1000 rpm for 10 minutes to remove cell debris. The supernatant was then filtered through a 0.2 µm filter, aliquoted and then frozen at -70^oC for later analysis. Cell pellets were collected and resuspended in FACS buffer analysed by flow cytometry to measure the expression of N1 or N2 markers as described in section 2.2.9.7.

2.2.2.4. Cytospin preparation and staining

The morphological properties of treated neutrophils were studied using light microscopy. Cells were resuspended in HBSS with 1% BSA to aid cell adherence to microscope slides. One hundred µl of a 2.5×10^5 cell suspension was loaded into a cytospin funnel and centrifuged onto Superfrost slides. The slides were left to air-dry overnight and then stained with haematoxylin and eosin (H&E).

2.2.3. Culture of multi-cellular tumour spheroids (MCTS)

2.2.3.1. Tumour spheroid culture

FaDu MCTS were generated from single cell suspensions using the liquid overlay technique (Carlsson and Yuhas, 1984). Tumour cells were prevented from adhering to the tissue culture plastic by covering each well of a 96-well plate with a layer (100 µl/well) of 1.5% agarose in serum-free media and allowed to dry at room temperature for 1 hour. Pre-coated agarose plates stored inverted at 4 °C for use for up to 8 weeks. FaDu cells were cultured as monolayers, harvested as described in 2.2.1.4 and re-suspended at 1×10^5 cells/ml in culture medium, then 100 µl of the cell suspension was added to each well of a pre-warmed agarose-coated plate and incubated at 37˚C, 5% CO_2 for 6-7 days (unless otherwise stated). Tissue culture medium was replaced every 2 days by adding 100 µl of fresh medium to each well and then removing 100 µl medium. The size of the resulting spheroids was measured using Axiovision software (Zeiss) to obtain a growth curve.

2.2.3.2. Generation of MCTS conditioned medium

Media conditioned by FaDu MCTS was generated for the analysis of secreted cytokines, chemokines and growth factors and to stimulate neutrophils. To generate FaDu MCTS conditioned medium day-6 MCTS were washed three times with serum-free RPMI and incubated with or without TNF-α (50 ng/spheroid) at 37˚C in a 5% CO_2 incubator for 5 hours. Condition media was collected, centrifuged at at 1000rpm for 10 minutes to remove cell debris, filtered through a 0.2 µm, aliquoted and then stored at -70^{o}C for later analysis.

2.2.3.3. Neutrophil and monocyte Infiltration into FaDu MCTS

Day-6 FaDu MCTS were stimulated with 50 µl TNF-α (final concentration 50 ng/spheroid) in serum-free media and spheroids incubated overnight. The following day MCTS were washed with serum-free RPMI media three times. Freshly isolated neutrophils or THP-1 cells were re-suspended in 10 ml pre-warmed serum-free RPMI containing a final concentration of 2 µM CellTracker Green$_{TM}$ and incubated for 45 minutes at 37˚C, 5% CO_2, after which a 500µl of FBS was added and the cells centrifuged at 1000 rpm for 5 minutes. The cell pellet was re-suspended in serum-free RPMI and incubated for another 15 minutes at 37˚C, 5% CO_2. Cell-tracker-labelled neutrophils were counted and re-suspended at 6×10^5 cells/ml; 50 µl of cell suspension were added to each well containing a single FaDu MCTS and incubated for increasing lengths of time at 37˚C in a 5% CO_2 incubator to allow neutrophil infiltration. In some experiments, neutrophils were pre-exposed to synthetic CXCR2 antagonist AZ-10397767 (25 nM) or SB-265610 (100 nM) and/or CXCR4 antagonists AMD3100 (500 ng/ml) or FaDu spheroids were pre-incubated with MIF antagonist ISO-1 (4,5-Dihydro-3-(4-hydroxyphenyl)-5-isoxazoleacetic acid methyl ester) at concentration of 500 µM for 1 hour prior to being added to the assay. DMSO was added as a vehicle control and incubated for the same length of time.

At the end of assay, MCTS were collected in a 25 ml universal tube and culture media collected, filtered and stored for further analysis (see section 2.2.3.1). FaDu MCTS were then washed three times in PBS to remove non-infiltrated neutrophils and individual spheroids were placed in microtubes in the presence of 300 µl of 0.25% trypsin/EDTA solution for 10 minutes. MCTS were disaggregated by flicking the microtube, then 700 µl of media was added to neutralize the effect of the trypsin/EDTA. Disaggregated MCTS were centrifuged at 5,000

rpm for 2 minutes, after which the cells were re-suspend in 300 µl 1% paraformaldehyde and stored in the dark at 4˚C until analysis by flow cytometry.

2.2.3.4. Collecting, fixing and processing MCTS for immunostaining

MCTS were collected in 25ml universal tubes, then, after the MCTS had settled to the bottom of the tube, excess media was removed and the spheroids were washed with PBS 3-4 times. After final wash MCTS were fixed with 10% PBS-buffered formalin overnight; then after transferring to a flat bottomed plastic embedding tray, the excess fixative was removed and the MCTS were embedded using a solution of 2% agarose and 4% formaldehyde (the solution was slowly added so as not to disturb the MCTS). The agarose was allowed to set before placing in a cassette and then paraffin-wax embedding. Using a microtome, 5 µm sections of embedded MCTS were cut, placed onto Superfrost glass slides and dried for later analysis.

For frozen sections, spheroids were embedded in optimum cutting temperature (OCT) medium and rapidly frozen using dry ice or liquid nitrogen. Ten µm sections were cut, placed onto Superfrost glass slides and dried prior to store at -80˚C for later analysis.

2.2.4. Functional assays

2.2.4.1. Migration assay

Neutrophils migration towards chemoattractants or CM was tested using a 48-well micro-chemotaxis chamber and the number of cells migrated through a porous membrane during a specified period of time was assessed by flow cytometry. Chemokines or control were diluted in serum-free RPMI supplemented with 0.1% BSA (filter- sterile) with 1% antibiotics and 28 µl added to the lower wells of the chamber and overlaid with a nitrocellulose membrane filter (3 µM pore size). After the upper part of chamber was assembled, 50 µl of neutrophil cell

suspension (1×10^6 cells/ml) was added to the upper wells and chamber incubated for 3 hours at 37˚C in a 5% CO_2 incubator. At the end of incubation period, non-migrated neutrophils were removed from the upper wells by tapping the chamber on clean tissue and the content of the lower wells were transferred to micro-tubes containing 300 µl of 1% paraformaldehyde for further analysis by flow cytometry (see section 2.2.9.2). Chemoattractant used were: CXCL1, CXCL5, CXCL8, MIF and fMLP at varying concentrations or buffer alone as a control.

2.2.4.2. Cell viability assay (MTT)

This assay was applied to test the cytotoxicity of ISO-1 on FaDu cells by measuring the metabolic activity of these cells as a surrogate marker for viability. Briefly, cells were harvested as described in section 2.2.1.3 and seeded at 4,000 cells per well in a 96-well plate. Then 10 µl of a solution of ISO-1 or vehicle control (DMSO) at double the desired final concentration was added to the cells and incubated for 2, 24, 48, and 72 hours. At the end of incubation time, cells were washed with PBS and 100 µl fresh medium added. MTT solution was prepared by dissolving 0.5 mg/ml Thiazolyl Blue Tetrazolium Bromide (MTT) powder, in PBS and 100 µl of the MTT solution was incubated with the cells for 2 hours. The mitochondrial dehydrogenases of living cells can reduce the yellowish MTT dye to an insoluble formazan (dark blue). The blue crystals formed were solubilized by the addition of 50 µl acidified isopropanol and the intensity of the colorimetric reaction measured using a plate reader at 540 nm with correction readings taken at 630nm. Reading were normalized to a control sample of untreated (100% viable) cells.

2.2.5. Molecular assays

2.2.5.1. RNA extraction

Total RNA from cell pellets was isolated using Bioline Isolate RNA mini kit, according to the manufacturer's instructions. Briefly, cell pellets were lysed and filtered by centrifugation for 1 minute at 11,000g. Then an appropriate amount of 70% ethanol was added to the homogenized lysate to improve binding of the RNA to the silica-based membrane of the spin column during centrifugation. Complete removal of genomic DNA was achieved by incubation with DNase I for 15 minutes. Column-bound RNA was washed three times and eluted in RNase/nuclease-free water. The concentration and purity of the isolated RNA was measured using a NanoDrop spectrophotometer and only RNA samples with high-purity (A_{260}/A_{280} ratio) more than or equal to 2.0 were used for complementary DNA preparation and qPCR analysis.

2.2.5.2. Complementary DNA (cDNA) preparation

Single stranded cDNA synthesized from total RNA was achieved using High Capacity cDNA Reverse Transcription kit, according to manufacturer's instructions. In this protocol, 300 ng of total RNA was reverse transcribed per reaction containing the following reagents:

Component	**Volume/Reaction(µl)**
10 × RT Buffer	2
25 × dNTP Mix (100 mM)	0.8
10 × RT Random Primers	2
MultiScribe™Reverse Transcriptase	1
Nuclease-free water	5.2
Sample RNA (300 ng)	9
Total per Reaction	20

Samples were then loaded in a thermal cycler and recommended protocol was followed as instructed below. At the end of the run, reverse transcription reactions were stored at -20 ˚C for qPCR.

	Step 1	Step 2	Step 3	Step 4
Temperature	16 °C	42 °C	85 °C	4 °C
Time	10 min	120 min	5 min	∞

2.2.5.3. Quantitative polymerase chain reaction (qPCR)

Quantitative detection of target genes (MIF, VEGF) was achieved using pre-designed TaqMan® primers. In each of 96-well plate, a mixture of target gene (labelled with FAM reporter) and suitable reference control (labelled with VIC reporter) were added to the following mixture of reagents:

Reagents	**µl/well**
Master Mix (life Technology)	5
TaqMan®gene's primers	0.5
Endogenous control primers	0.5
cDNA	0.5
Nuclease-free water	3.5
Total volume	10

Each sample was run in triplicate in the 96-well plate and negative control (no cDNA) sample was run for quality control. PCR plates were centrifuged briefly before loading into the ABI 7900HT Fast Real-Time PCR machine with the following thermocycle settings:

Initial hold at 50˚C for 2 minutes, DNA Polymerase Activation at 95˚C for 10 minutes, followed by 40 cycles of Annealing and Extension at 95˚C for 15 second, 1 minute at 60˚C, respectively.

The relative quantification comparative delta threshold cycle (ΔCT) value was used to calculate fold change gene expression using the $2^{\Delta Ct}$ equation.

2.2.6. Immunoassays

2.2.6.1. Chemokine/cytokine protein arrays

Human cytokine array panel A (ARY005, R&D system) was used to screen conditioned medium generated from FaDu MCTS, according to manufacturer's instruction. In this assay, different antibodies have been spotted in duplicate on nitrocellulose membranes. Conditioned medium was mixed with biotinylated detection antibodies prior to loading to the BSA-blocked membrane. At the end of incubation period, captured proteins were visualized using chemiluminescent detection using hyper-film. The relative expression levels of each cytokine were determined by densitometry using Quantity One software (Biorad, CA, USA). Here, the intensity of each dot was measured by drawing a circle around its circumference and comparing its intensity to the negative control.

2.2.6.2. Enzyme-Linked Immunosorbent Assay (ELISA)

ELISA was used to measure the levels of MIF, VEGF, CXCL8 in the conditioned medium collected from various experiment according to the manufacturer's instructions. Wells of a 96-well plate was coated with the recommended concentration of capture antibody and incubated at room temperature overnight. The following day, unbound antibody was removed and nonspecific binding sites blocked with a BSA-containing solution before samples/standards were incubated for 2 hours at room temperature. Unbound protein was removed by washing with wash buffer and the recommended concentration of biotinylated-detection antibody was incubated for 2 hours. Finally, horseradish peroxidase (HRP)-conjugated streptavidin was added to each well for 30 min at room temperature followed by TMB substrate and the colorimetric reaction was measured using micro-plate reader set to 450nm and 540nm for correction. The reading at 540nm was subtracted from the reading at 450nm before averaging the reading of each samples/standards. A standard curve was

created using Deltasfot software by generating four parameter logistic (4-PL) curve fit and the concentration of target protein was obtained from standard curve.

2.2.7. Immunohistochemistry

2.2.7.1. De-waxing of tissue

IHC was used to detect the presence of a cell specific marker in tissue sections. Paraffin-embedded tissue was sectioned (5 µm) and mounted onto adhesive SuperFroset slides. Complete removal of paraffin was achieved by treating the slides with two changes of Xylene. Then the tissue was rehydrated through descending concentrations of ethanol (100%, 95%, 75%) before endogenous peroxidase sites were blocked using 3% H_2O_2 diluted in methanol for 15 minutes. The sections were washed in water in preparation for antigen retrieval.

2.2.7.2. Antigen (Epitope) retrieval methods

Methylene bridges formed during the tissue fixation process can mask the antigen binding site. These antigen sites can be 'un-masked' using a variety of treatments; each treatment being dependent on the primary antibody used. For many antibodies heat-induced epitope retrieval (HIER) is the method of choice but different buffers may be used in this process. For the anti-BrdU antibody used in this study acidic antigen retrieval (AAR) using 10 mM anhydrous citric acid (pH 6) buffer was used to denature DNA and permit the access of anti-BrdU antibodies to the previously incorporated BrdU label. In contrast, a basic sodium citrate buffer (pH 6) was used for other antigen retrieval methods. For both buffers, 0.5% Tween-20 was added to enhance antigen un-masking. The antigen retrieval solution was pre-heated to 95°C and slides were immersed in buffer for 15 minutes. The buffer was then removed from

the steamer and slides allowed to cool to ambient temperature for approximately 15 minutes before being transferred to PBS with 0.05% Tween 20 (TBS).

2.2.7.3. Detection of neutrophils in MCTS

Neutrophils within MCTS were identified using the neutrophil-specific marker, CD66b (also known as carcinoembryonic antigen-related cell adhesion molecule 8) . Following fixation and antigen retrieval using sodium citrate buffer (see section 2.2.7.2), tissue sections were incubated overnight at 4°C with normal horse serum to block non-specific binding sites. The following day, serum was removed and 4 µg/ml mouse monoclonal anti-human CD66b or Isotype control diluted in TBS buffer was added to each slide and incubated for 60 minutes at room temperature. After washing the unbound antibody three times with TBS, biotinylated anti-mouse secondary IgG antibody from vector kit (VECTOR Ltd, Peterborough, UK) was added for 30 minutes at room temperature. The advantage of using a biotinylated antibody is to amplify the staining signal by formation of an avidin-biotin complex. After washing with TBS a solution of streptavidin-conjugated HRP was added and incubated for 30 minutes at room temperature. Colour was developed using the DAB chromogen from Vectorstain and the reaction was stopped by washing in distilled water. Slides were counter-stained with Haematoxylin, 0.1% acid alcohol, Scott's tap water, dehydrated in ethanol (95% then 100%) and then dipped in xylene, prior to mounting in DPX and coversliping.

2.2.7.4. Immunolocalization of CD66b and MIF in OSCC tissue sections

The detection of neutrophils in human biopsy tissue sections using CD66b was carried out as described in section 2.2.7.3. However, in this protocol, an alkaline phosphatase detection system was used according to manufacturer's instructions and Vector Red substrate was used

to localize the neutrophils in tissue sections by incubating in substrate for 30 minutes to allow red/magenta colour development. The reaction was stopped by washing the slides in TBS buffer followed by rinsing in water. For dual staining the sections were incubated for 60 minutes at room temperature with normal horse serum before the addition of biotin-conjugated monoclonal mouse anti-human MIF antibody (Biotin anti-Human MIF) at a concertation of 25 µg/ml. Mouse IgG at the same concentration was used as a control. Sections were incubated overnight at 4°C and washed three times with TBS. Next, the sections were incubated with streptavidin-conjugated HRP for 30 minutes at room temperature, followed by TBS washes and then colour development with DAB chromogen for 10 minutes. The reaction stopped by washing the slides in distilled water before slides were counter-stained with haematoxylin and mounted as described previously.

2.2.7.5. MIF staining of FaDu Tumour Xenografts

The expression level of MIF in both treated (Ly6G & ISO-1) and control (PBS) groups of FaDu xenograft murine models were examined in tissue sections using a polyclonal rabbit anti-human MIF antiserum. Slides were de-waxed and treated with sodium citrate buffer for antigen retrieval (see section 2.2.7.1 and 2.2.7.2). Tissue sections were blocked with normal goat serum for 60 minutes at room temperature before the addition of 1:50 diluted anti-MIF antiserum diluted in neat goat serum or a rabbit serum IgG Isotype control and the slides incubated overnight at 4 °C. The following day, the slides were washed in TBS and then incubated with secondary biotinylated goat anti-Rabbit antiserum from Vectastin Elite kit as per the manufacture guidelines, followed by colour development using DAB chromogen. The remaining procedure was carried out as in section 2.2.7.3.

For this study, a semi-quantitative approach was applied using a modified 'quickscore' method (Detre et al., 1995). The main factors considered in this method is the staining intensity of the tumour cells within sections corresponding to 0 = no staining, 1 = week staining, 2 = moderate staining and 3 = intense staining. The second factor is the proportion of positive (brown) cells in each field of view that is scored from 0 to 4 (0 = no cells positive, 1 = 1-25% of cells, 2 = 26-50% of cells, 3 = 51-75% of cells and 4 = 76-100% of cells). All the slides were examined under low power (10 x magnification) and scored by an oral pathologist (Dr Keith Hunter). The intensity score was multiplied by the proportion of positive stained cells to give an overall score for each section.

2.2.7.6. Bromodeoxyuridine and CD31 dual labelling to identify proliferating cells and the endothelium in sections of FaDu tumour xenografts

Actively proliferating cells in each of the treated (ISO-1, anti-Ly6G) and control group was detected using anti-BrdU antibody (sheep polyclonal anti-BrdU HRP). Mice were injected with 100 mg**/**kg of the thymidine analog, BrdU, (see section 2.2.2.10) that is incorporated into newly synthesised DNA, while the endothelial marker CD31 was used to evaluate the presence and number of blood vessels in the same section. Following sample preparation (section 2.2.7.1), antigen retrieval was by HIER in 10 mM citric acid (section 2.2.7.2), then tissue sections were incubated with normal rabbit serum to block non-specific sites for 1 hours at room temperature. Samples were then incubated with rat anti-human CD31 or rat IgG isotype for 24 hours at 4°C. Slides were washed in TBS and the ABC alkaline phosphatase detection system was used as per the manufacture instructions. Vector Red substrate was used to visualise the immunoreactive areas by incubating with substrate for 30 minutes before the reaction was stopped by incubating slides in TBS buffer then water. Sections were

blocked again with normal rabbit serum for 30 minutes and then directly labelled with HRP-conjugated anti-BrdU antibody diluted at 1:20 in TBS or Sheep IgG isotype control overnight at 4°C. Sections were then incubated with Streptavidin-HRP for 30 minutes, followed by incubation with DAB chromogen substrate for 10 minutes. The reaction was stopped by washing in water and the samples counterstained with haematoxylin prior to mounting in DPX and coversliping as described previously.

2.2.7.7. Image analysis of MPO immunostained HNSCC tissue section

MPO-immunostained whole sections were scanned automatically using an ACIS® inverted research microscope at 40 x magnification. These images of can be digitally visualised using the associated software. In the image analysis, MPO+ neutrophils were defined as cells with dark brown staining and this colour selection was maintained for analysis of all images. For analysis of tumour sections, a circle representing 40 x in diameter (0.53mm) were randomly placed in each area of interest. Eight individual fields of view were found to be the minimum number required to minimize data variation (see section3.4.3). The number of neutrophils in each of the following areas within the sections were measured automatically using image analysis software: (1) invasive front of the tumour (2) tumour stroma (3) tumour body and (4) areas of necrosis (Fig. 2.3)

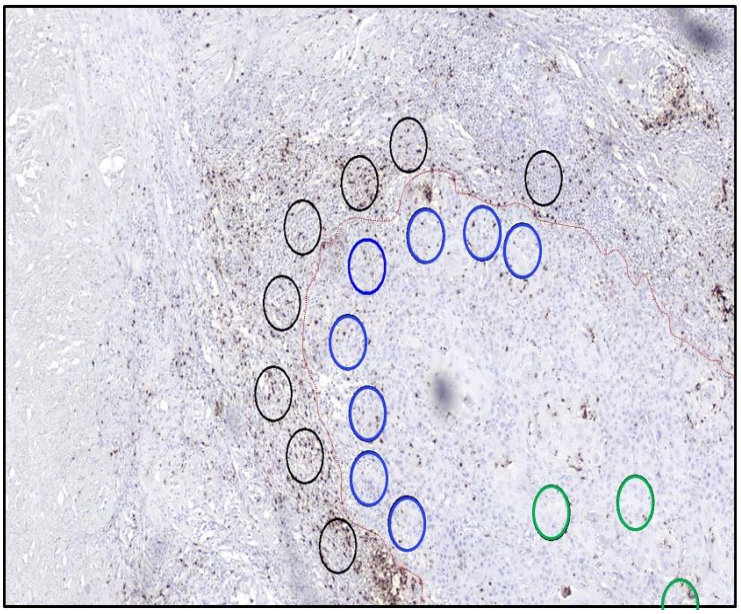

Figure 2.3 Representative example for evaluation of MPO+ immunostaining in paraffine-embedded HNSCC section. Distribution of MPO+ cells was evaluated in four tumour compartments; tumour invasive (blue circle), tumour invasive (black circle) and tumour body (Green circle) by selecting eight random filed per area

2.2.8. Immunofluorescence staining

2.2.8.1. Staining of hypoxic areas in MCTS

The presence of hypoxia (low oxygen concentration) in MCTS was determined using the hypoxic marker, Pimonidazole hydrochloride (PIMO). PIMO was diluted 1:200 in pre-warmed serum free medium and 10 µl added to each well containing an MCTS and incubated for 2-3 hours at 37°C. At the end of the incubation period, MCTS were collected, washed in PBS and snap-frozen as describe in section 2.2.3.4. MCTS were then cyrosectioned into 6 µm sections onto Superfrost slides and fixed in cold acetone (4°C) for 10 minutes. Sections were washed in PBS before the addition of rabbit anti-PIMO antisera, diluted at 1:20 in TBS with 0.1% bovine serum albumin (BSA), and incubated for 1 hour at room temperature. The sections were further washed before incubation with Texas red-conjugated secondary antibody for 30-45 minutes at room temperature. Slides were washed twice in cold TBS and nuclei

counterstained with DAPI for 2 minutes. Finally, slides were washed with TBS and mounted with ProLong Gold anti-fade, coverslipped and left to cure for 24 hours in dark before being analysed by fluorescent microscopy.

2.2.8.2. Immunolocalization of monocyte/macrophage, neutrophils and endothelium in FaDu tumour xenografts

OCT-embedded frozen tumours were cut into 6µm thick sections and placed on super-adhesive slides. Sections were warmed to room temperature and washed for 5 minutes with PBS prior to blocking with normal rabbit serum for 30 minutes at room temperature. Serum was removed and 100 µl of antibody cocktail (see table of antibodies in section 2.1.5) or isotype control were applied and incubated for 30 minutes at room temperature in the dark. Slides were then washed three times in TBS, 5 minutes each in duration. After the final wash, sections were counterstained with 5µg/ml DAPI diluted TBS for 2 minutes, then rinsed in excess TBS. ProLong Gold Anti-fade mountant was applied to slide to avoid loss of fluorescence signal during analysis performed with a PerkinElmer UltraView spinning disc confocal microscope at 488 nm excitation (F4/80-Alexflour 488; green), or mixed gas argon-krypton laser at 568 nm (Ly6G-PE; yellow green) and 647 nm (CD31-APC; red) excitation and UV laser, at 355 nm (DAPI, deep blue) with the appropriate emission filters.

2.2.8.3. Image analysis of immunofluorescence-stained tumour xenografts sections

To quantify the number of infiltrated neutrophils, macrophage and blood vessel density in the fluorescently stained xenograft sections, 10 random fields for each tumour section were captured using a PerkinElmer confocal system with a 10 x objective. The images were acquired as Z-stacks and captured using Volocity software (version 6.3). Images were analysed by

thresholding the images and measuring intensity and area of fluorescence in mm^3 per microscopic field that was then converted to pixel density for each wavelength.

2.2.9. Flow Cytometry

2.2.9.1. Analysis neutrophil viability and purity

The purity of neutrophils isolated from whole blood was determined by flow cytometry based on expression of the neutrophil-specific cell surface marker, CD66b. Cells washed in FACS buffer twice, and re-suspended in 100 µl of ice-cold FACS buffer containing 2.5×10^5 cells. Neutrophils were incubated with appropriate concentration (1:50) of APC-conjugated CD66b and incubated for 30 minutes on ice in the dark. Cells were washed with cold FACS buffer and the viability of purified blood neutrophils assessed using LIVE/DEAD™ Fixable Blue Dead Cell Stain Kit. This dye reacts with intracellular amines in cells with compromised cell membranes resulting in a strongly fluorescent intensity in dead cells compared to live cell populations. Cells were washed with protein/azide free-PBS and re-suspended in 1 ml of PBS. Then 0.25 µl of freshly reconstituted dye was added to the cell suspension and incubated at room temperature for 30 minutes. Cells were then centrifuged, washed with 1 ml PBS, fixed with 300 µl of 1% paraformaldehyde and kept in 4˚C until flow cytometry was performed. To achieve gating based on viable cells only, cells were killed by heat-shock where cells were incubated for 5 minutes in a water bath at 70 °C and then transferred to ice for 5 minutes. Then untreated cells were mixed with the heat-shock treated cells at a 1:1 ratio and the viability dye added as described above.

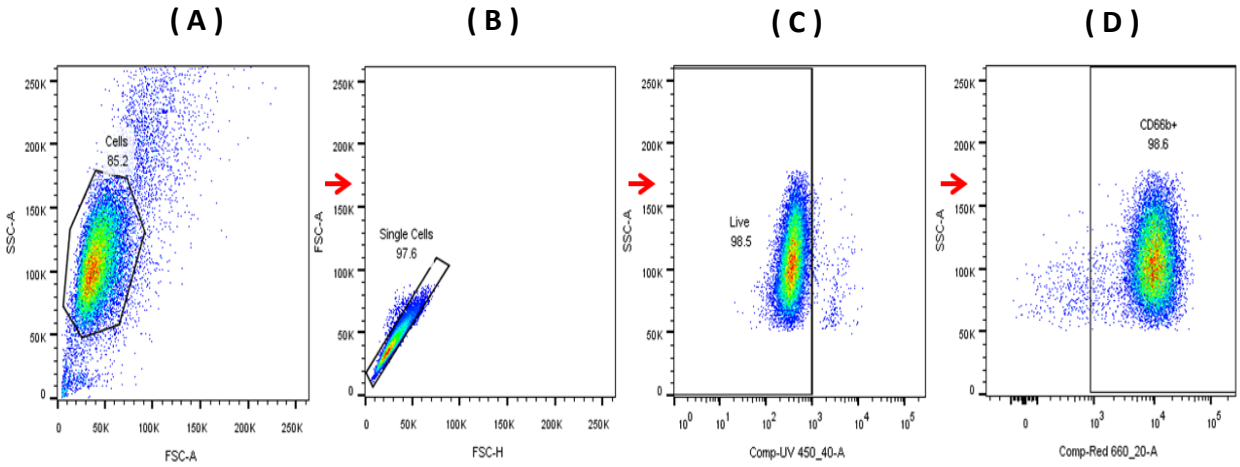

Figure 2.4 Dot plot show gating strategy applied after neutrophils isolation. Other leukocyte populations were removed by negative selection (A), followed by single cell gating (B) and exclusion of dead cell (C) and neutrophils were selected using CD66b+ marker (D).

2.2.9.2. Flow cytometric analysis of neutrophil chemotaxis using celltracker

A FACS Calibur or ATTUNE was used to analyse migration of neutrophils toward control media or media containing various chemoattractants. The contents of the lower wells of a 48-well Boyden chamber were collected and fixed in 300 µl 1% paraformaldehyde (as described in section 2.2.2.4). The forward incidental light scatter (Fsc) and side incidental light scatter (Ssc) detectors were set to values that optimised visualisation of granulocytes. A threshold was set on the Fsc detector to exclude small sub-cellular particles from data acquisition. Samples were then acquired for a set time of 30 seconds. The number of events registered by the flow cytometer during this time was used as a measure of relative chemotaxis rate of neutrophils from the upper wells across the membrane to the lower wells of the Boyden chamber (Tazzyman et al., 2011).

2.2.9.3. ICAM-1 expression by FaDu cell

FaDu cells were seeded at 5×10^5 cells/well in 6 well plates and allowed to adhere at 37˚C in a 5% CO_2 incubator. After 24 hours incubation, the medium was removed and 2 ml of TNF-α containing medium (50 ng/ml), a pro-inflammatory cytokine known to induce the expression of ICAM-1 (Chiu et al., 2004), was added and the cells incubated overnight. The following day, media was removed and replaced with fresh media with or without TNF-α for 5 hours and incubated at 37˚C in a 5% CO_2 incubator after which conditioned media was collected and stored at -20˚C for analysis by ELISA. Cells were washed twice with PBS prior to removal from tissue culture plates by addition of 750 µl non-enzymatic cell dissociation solution for 15 minutes at 37˚C. The effect of cell dissociation solution was neutralized by the addition of an equal volume of medium to each well and the cell suspension centrifuged at 5000 rpm for 2 minutes to the pellet cells. Each sample was then re-suspended in 50 µl of mouse anti-human ICAM-1 or mouse IgG1 control antibody (10ug/ml) in FACS buffer (PBS + 0.1% BSA + 0.1% sodium azide) and incubated on ice for 45 minutes. Excess antibody was then removed by washing with 1 ml FACS buffer followed by centrifugation at 5000 rpm for 2 minutes. The supernatant was discarded and the cell pellets re-suspended in 50 µl of anti-mouse IgG Fab_2 fragment R-PE antibody diluted 1:50 in FACS buffer and incubated on ice for 30 minute in the dark. Finally, cells were washed as before and cell pellets re-suspend in 300 µl, 1% paraformaldehyde and kept at 4˚C until flow cytometry was performed.

Expression of ICAM-1 on day 6 FaDu spheroids was detected by disaggregating 3 spheroids from each treatment with 300 µl of non-enzymatic cell dissociation solution for 15 minutes at 37˚C; then 700µl of media was added and cells centrifuged at 5000 rpm for 2 minutes to pellet cells. The cells were re-suspended in 50 µl FACS buffer and 50µl of mouse anti-human

ICAM-1 or mouse IgG1 control, as described previously. Excess antibody was removed by addition of 1 ml FACS and then centrifuged at 5000 rpm for 2 minutes. The supernatant was discarded and the cell pellets re-suspended in 50µl of Alexa Fluor® 488 goat anti-mouse IgG followed by incubation on ice for 30 minutes in the dark. Finally, cells were washed as before and cell pellets re-suspended in 300 µl, 1% paraformaldehyde and kept in 4˚C until flow cytometry was performed.

2.2.9.4. Flow cytometric analysis of neutrophil/monocyte infiltration to MCTS

Dissociated spheroids (as described in section 2.2.3.3) containing neutrophils or monocytes were analysed by flow cytometry. The cell population was sorted according to forward scatter (Fsc) and fluorescence to allow differentiation between immune cells (neutrophils or THP-1 cells) and tumour cells (Fig. 2.5 -A&B). Each sample was collected until the flow cytometer had registered 10,000 events and then the data stored and analysed using CellQuest™ (Becton Dickinson) software. For analytical purposes, and after making sure the detector was optimised to visualise both cell populations, a mixture of labelled neutrophils or THP-1 cells and tumour cells were plotted as Fsc against fluorescence and a gate was placed around green fluorescent neutrophils only. This gate was applied to all of experiential test groups and the number of events represented as % infiltration.

2.2.9.5. CXC receptor expression on whole blood

Expression of CXCR receptors (CXCR1, 2 and 4) were stained on neutrophils, monocyte and T cells from isolated whole blood anti-coagulated with a 1 in 10 dilution of 3.8% sodium citrate. 200 µl of whole blood was added to Eppendorf tubes and mixed with 100 µl of FACS buffer containing CXCR1, CXCR2, CXCR4, CD66b, CD14 or IgG mouse control antibody (final

concentration 10 µg/ml), and the cells incubated at room temperature for 30 minutes. Cells were washed twice with 1 ml FACS buffer and centrifuged at 5000rpm for 2 minutes. After removal of supernatant 50 µl of R-phycoertherin-conjugated anti-mouse antibody was added to each tube or directly R-phycoertherin-conjugated CD3 antibodies and cells incubated for 30 minutes on ice in the dark. Cells were washed and RBC lysed by the addition of 1 ml FACS lysis buffer and incubated for 10 minutes at room temperature in the dark. Cells were centrifuged as before and the lysis step repeated until the removal of all erythrocytes. Finally, cells were re-suspended in 300 µl 1% paraformaldehyde and kept on ice until flow cytometry was performed. For each sample 10,000 events were collected. Three populations corresponding to granulocyte, monocyte and lymphocyte sub-populations were distinguished by flow cytometry based on their forward (Fsc) and side scatter (Ssc) characteristics. During analysis of each of the receptor a gate was set around the required cell population based on expression of a cell specific marker (CD66b = neutrophils, CD14 = monocytes, CD3 = T cells) (Fig. 2.6); then the relative median fluorescence intensity was obtained after subtracting IgG background fluorescence.

2.2.9.6. Analysis of necrosis and apoptosis

Neutrophil cell death by apoptosis and necrosis after exposure to ISO-1 were determined using flow cytometry. Neutrophils were isolated (section 2.2.2.1) and reconstituted at 1×10^6 cells in media containing 10 nM recombinant MIF. Cells were then treated with ISO-1 or vehicle control (DMSO) at equivalent concentrations of 0.05 µM 0.5 µM, 5 µM, 50 µM, 500 µM or 5000 µM for 24 hours at 37˚C. After incubation, cells were pelleted by centrifugation at 6000 rpm for 2 minutes, washed with ice cold PBS and labelled with Annexin V-FITC that binds to phosphatidylserine (PS) of cells undergoing apoptosis while propidium iodide (PI)

enters permeabilised cells and binds to the DNA of necrotic cells according to manufacturer's instructions. Cells were analyzed using a LSRII cytometry (BD Biosciences) equipped with Cell Quest software for cells acquisition and data analysis.

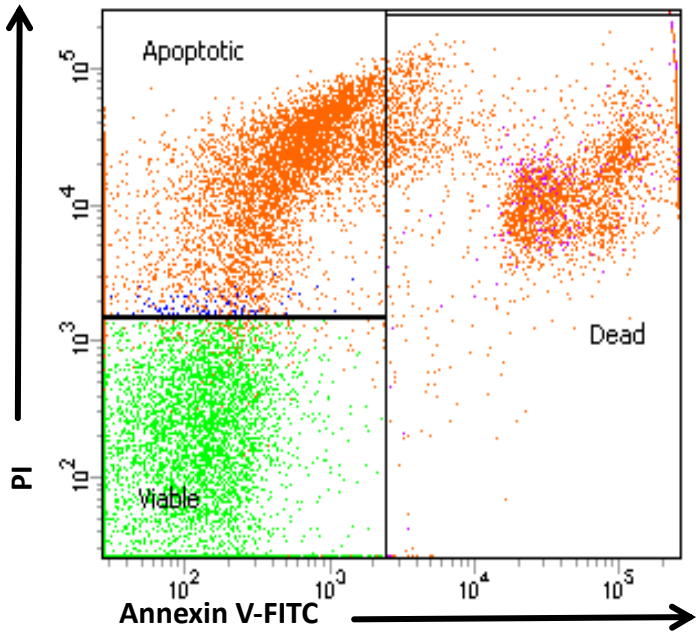

Figure 2.5 Analysis of ISO-1 traeted neutrophils using Annexin V and Propidium Iodide (PI).

2.2.9.7. Multicolour phenotypic characterization of polarized neutrophils

Immediately after incubation with polarising agents (see section 2.2.2.3) cells were washed once with ice cold FACS buffer and resuspended in 100 µl FACS buffer at final concentration of 2.5×10^5 cells/test. Cell markers were classified into four groups based on antibody fluorochrome availability and expression levels; CXCR receptor (CXCR1, CXCR2, CXCR4), adhesion molecules (CD62-L, ICAM-1), CC receptor (CCR5) and Fcγ receptor (CD64). A cocktail of antibodies at optimized concentrations (table below) was added to neutrophils to a final volume of 100 µl, in addition to 2.5 µl neutrophil specific marker CD66b-APC for each tube.

Unstained cells were used as negative control and stained cells were used as florescence minus one (FMO) controls for each of the four groups for cell gating and to exclude any spectral overlap due to use of multiple fluorochromes. Cells were incubated at 37 ˚C for 1 hour for CCR5, while all other antibodies included in the panel were incubated on ice for 30 minutes. At the end of incubation period, cells were washed once with 1 ml FACS buffer and then with protein/Azide free-PBS before being re-suspended in 1 ml of PBS. Then, 0.25 µl of freshly reconstituted LIVE/DEAD™ Fixable Blue Dead Cell dye was added to cell suspensions and incubated with cells for 30 minutes on ice. Cells were then pelleted by centrifugation and washed with 1 ml PBS before fixation with 300 µl of 1% paraformaldehyde. Cells were kept at 4˚C until flow cytometry was performed.

Specificity	Fluorochrome	Ab clone	Dilution/ 100 µl	Staining condition	Expression on Blood neutrophils
CXCR1(CD181)	FITC	eBio8F1-1-4	2.5 µl	4 ˚C	+++
CXCR2 (CD182)	PE	eBio5E8-C7-F10	2.5 µl	4 ˚C	+++
CXCR4 (CD184)	PE-Cyanine7	12G5	2.5 µl	4 ˚C	+
ICAM-1 (CD54)	PE	YN1/1.7.4	2.5 µl	4 ˚C	+/-
L-Selectin (CD62L)	FITC		2.5 µl	4 ˚C	+++
CCR5 (CD195)	PE	NP-6G4	1.5µl	37˚C	+/-
Fc γ receptor 1 (CD64)	FITC	10.1	2.5 µl	4 ˚C	-
CD66b	APC	G10F5	2.5 µl	4 ˚C	++

Table 2.1. Reagents used to identify N1 and N2 polarised neutrophils. All antibodies were purchased from eBioscience, **+++** = strong expression, **++** = moderate expression, **+/-** = weak expression, **-** = no expression

2.2.9.8. Compensation for multicolour flow cytometric experiments

Compensation controls were used to determine the extent of fluorochrome spectral overlap in all detectors using two types of beads; BD™ CompBeads for each of the fluorochrome labelled antibodies used in the study or ArC™ Amine Reactive Compensation Beads for LIVE/DEAD™ staining according to manufacture instructions. Firstly, the unstained cell sample was run through LSRII Cytometer (BD Biosciences) with a three-laser (blue/red/violet) configuration, to set up the voltages for each of the fluorescence channels used. Then, tubes containing the BD™ CompBeads with attached fluorochrome-conjugated antibodies were run on the flow cytometry and the gate was adjusted on a single bead population. Then, using a histogram plot, a gate was placed around the negative and positive bead population for each of the fluorochromes used. Finally, spectral overlap values were converted by mathematical algorithms within the instrument software (DB FACSDiva software) to yield accurate compensation values.

2.2.9.9. Gating and analysis of multicolour flow cytometry

Cells were firstly gated using FSC and SSC, followed by single cell gating and then positive selection of live cells (Fig. 2.5). Neutrophils were gated using the neutrophil-specific marker CD66b (APC) and then expression of target cell surface markers on the neutrophil population was examined after adjusting the gating using the FMO control. The median fluorescence intensity (MFI) of the target population was compared to controls and normalized as follows:

$$\text{Normalized MFI} = \frac{\text{Median fluorescence intensity (MFI) of positive staining}}{\text{Median fluorescence intensity (MFI) of unstained sample}}$$

2.2.10. Murine tumour xenografts model

Male CD1 nude mice aged 8-weeks, were purchased from Charles River, UK. All mice were

kept in ventilated cages with food and water provided and maintained in pathogen-free conditions in the Field Laboratories, Veterinary Services Unit, Medical school, University of Sheffield. FaDu cells, were suspended in PBS (pH 7.4) at a density of 5×10^7 cells/ml and each animal received a subcutaneous (S.C) injection of 5×10^6 cells (100 µl). Once xenografts were established, tumours were measured every third day using measuring callipers and tumour volume calculated based on modified ellipsoidal formula = (length × width^2)

Tumours were allowed to grow for 3 days and mice were assigned randomly into groups (n = 5 per group) before beginning the treatment schedule (Fig. 2.8). The control group received Intraperitoneal (i.p.) injections of 100 µl PBS three times a week over a 3 week period, with the treatment groups receiving either 200 µg anti-Ly6G in PBS or 100 µl ISO-1 twice weekly at 20 mg/kg by the same route. For all groups, tumour volumes were monitored regularly, and the experiment ended 3 weeks after treatment or when tumours reached the maximum permitted size (15 mm diameter). To assess FaDu tumour cell proliferation, mice were injected i.p with 100 mg**/**kg BrdU for 1 hour before being Schedule 1 culled.

Blood sample was collected from cardiac puncture and stored at -80°C for further analysis. Tumours were removed and divided into two; one section was placed into labelled microfuge tubes and snap-frozen in OCT, then transferred to -80°C for further analysis. The other half of the tumour was fixed in 10% PBS-buffered formalin and paraffin-wax embedded for immunohistochemical analysis (section 2.2.7.5 & 2.2.7.6).

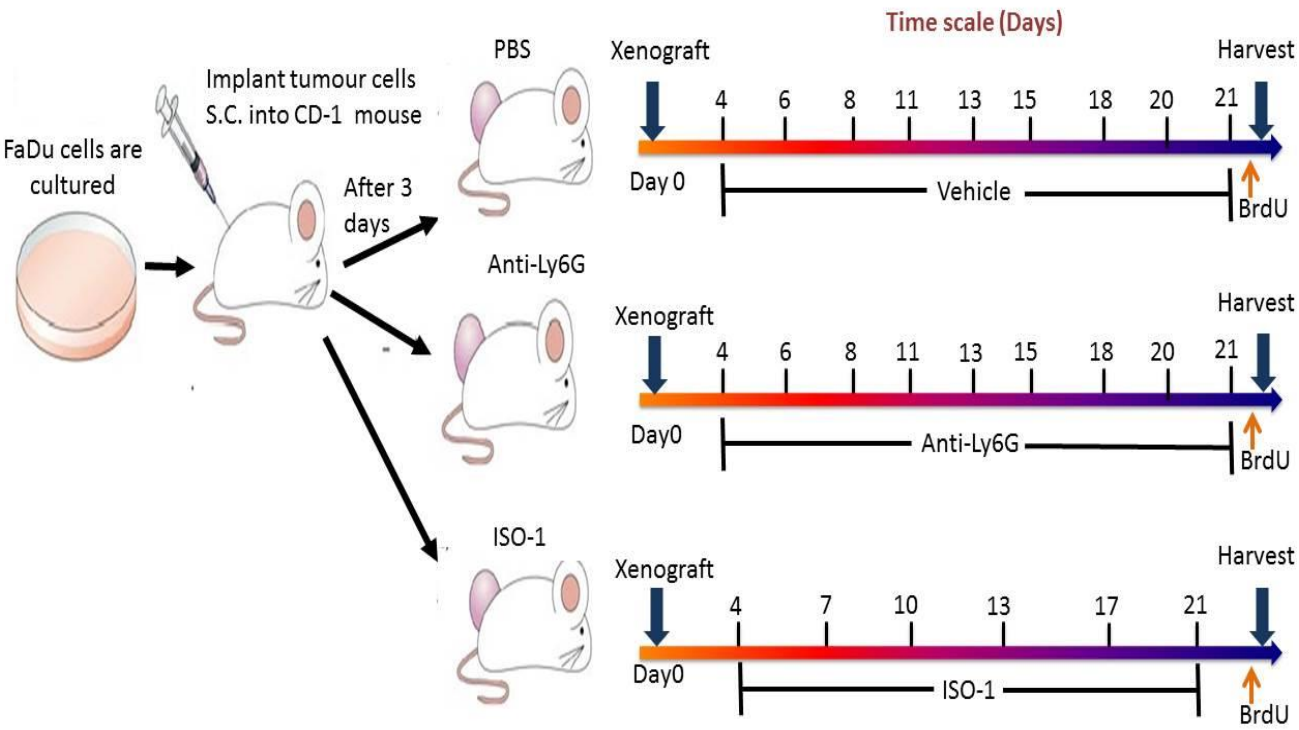

Figure 2.6 Experimental design of xenograft murine model. CD-1 nude mice subcutaneously with FaDu cells and tumours allowed to grow before treatment start. Mice received Intraperitoneal dose of vehicle (PBS), anti-Ly6G (200 µg) and ISO-1 (20 mg/kg) for period of three weeks. BrdU were injected one hour prior to culled schedule.

2.2.11. Statistical analysis

All experiments were repeated a minimum of three times and results are expressed as mean ± standard deviation (SD) or median ± 25-75% quartile ranges (min and max) unless otherwise stated. Data was subjected to normality testing and statistical significance was evaluated using an unpaired Student's t-test (parametric) or Mann-Whitney U test (non-parametric) to test the difference between two variables and one-way ANOVA (parametric) of Kruskal–Wallis test (non-parametric) for multiple variables. p-values of ≤ 0.05 were considered statistically

significant. All statistical evaluation was performed using GraphPad Prism software (GraphPad Prism software, CA, USA).

2.2.12. Ethics

Ethical approval for the use of volunteer's peripheral blood in this study was approved by The University of Sheffield Ethics Committee. All volunteers participated in the study with written, informed consent. Use of archival tumour tissue was permitted with National Ethical Approval (08/S0709/70) and the isolation and use of normal oral keratinocytes was permitted with National Ethical Approval (09/H1308/66). All animal experiments were conducted in accordance with the UK Home Office Regulations under the Animals (Scientific Procedures) Act 1986 and the awarded project licence number under which these protocols were performed is PPL:40/3424 (Dr Munitta Muthana). In addition, the University of Sheffield Animal Welfare & Ethical Review Body approved all the *in vivo* experiments performed in this study.

Chapter 3: Histological localization of Tumour-Associated Neutrophils in a cohort of patients with head and neck squamous cell carcinoma

3.1. Introduction

Several clinical studies have shown that TAN are associated with poor patient prognosis in a variety of human tumours including renal cell carcinoma (Jensen et al., 2009b), hepatocellular carcinoma (HCC) (Kuang et al., 2011), non-small cell lung cancer (Ilie et al., 2012), gastric adenocarcinoma (Zhao et al., 2012), colorectal carcinoma (Rao et al., 2012) and melanoma (Jensen et al., 2012). To date, few studies have examined the presence of TAN in HNSCC. Wan *et al* (2014) observed high levels of TAN in squamous cell carcinoma of the tongue whilst Trellakis and colleagues demonstrated that patients with advanced stage HNSCC tumours (T4) displayed higher levels of neutrophil infiltration compared to early stage T1 and T2 tumours and that levels of TAN related to poor patient prognosis (Trellakis et al., 2011). These studies examined TAN enrichment within the body of the cancerous epithelium, often termed tumour nests. However, tumours do not solely consist of tumour nests but also contain large areas of stromal tissue that is comprised of fibroblasts and blood vessels that surrounds the tumour epithelium. Moreover, the tumour epithelium itself can be sub-divided into the invasive front (the region of the tumour that invades into the stromal tissue) and the tumour body. In oral cancer, tumour cells at the invasive front of the tumour (IFT) have been found to behave differently from those within the tumour body. For example, cells located at the IFT have been shown to have a high proliferative activity (Piffko et al., 1997) and display more aggressive characteristics that are important for tumour spread and metastasis (Bànkfalvi and

Piffkò, 2000). The different areas within a tumour create distinct tumour microenvironments that may have different capacities to recruit leukocytes and so it is possible that neutrophil recruitment is not evenly distributed within tumour tissue. For example, Kuang *et al* showed that 72 cells/field were detected in the peri-tumoural stroma and only 8.7 cells/field were present in the cancer nests in HCC (Kuang et al., 2011). Moreover, these peri-tumoural neutrophils were exclusively found to express MMP-9, a known inducer of angiogenic regulatory molecules, which stimulate the angiogenesis of adjacent tumour cell. These data suggest that TAN within different tumour locations may experience different stimuli leading to the generation of different phenotypes or alerted responses that may have profound effects on tumour invasion or progression. However, to date, little is known about the spatial distribution of TAN in HNSCC. Based on this it was hypothesised that the microenvironment within different tumour sites will cause TAN to be preferentially recruited to some sites more than others and that neutrophil-tumour cell interactions at these sites could influence tumour behaviour and as a result clinical outcome.

3.2. Aims

To evaluate the number and location of TAN within biopsies of HNSCC tumour tissue using immunohistochemical staining for TAN to enable an investigation of their distribution pattern in each of the following areas: invading front of tumour, tumour stroma, tumour nest and necrotic tumour areas.

3.3. Methods

The presence of neutrophils in normal healthy oral mucosa compared to tumour tissue was evaluated in biopsies from 9 normal healthy volunteers and 9 patients with clinically diagnosed HNSCC. Sections were stained with neutrophil-specific anti-CD66b antibody (as described in section 2.2.7.4) and the number of neutrophils per high power field (HPF = x40 magnification) were counted in five random field. Cells within blood vessels were exclude form the analysis.

To examine TAN within specific tumour areas, neutrophils within paraffin-wax embedded histological tissue sections from 30 HNSCC patients were stained using an anti-MPO antibody followed by visualization using DAB chromagen. Tissue sections were digitally scanned using a 40x objective attached to an ACIS inverted research microscope. The images of section were visualised on screen and tumour areas were selected manually by placing circles of 40 x in diameter (0.53mm) in different regions of the tumour tissue. Cumulative means were calculated from eight individual fields of view to minimize data variation. Images were analysed digitally using ACIS III image analysis software (see section 2.2.7.7 for detailed method).

3.4. Results

3.4.1. The presence of neutrophils in normal and cancer tissues

In general, CD66b cells were not detected in the epithelium or stroma of normal healthy tissue (Fig. 3.1) (for patients demographic see appendix I, table 1). In contrast, in the HNSCC tissue sections the presence of CD66b cells were detected mainly in tumour stroma tissue with a median number of 3.6 TAN/HPF. In contrast, fewer CD66b neutrophils were detected within the tumour epithelium (median number 0.4 TAN/HPF). There was a statistical significant difference between the number of CD66b neutrophils in the tumour epithelium compared to normal epithelium ($p=0.0294$) and also the number of CD66b cells in the tumour stroma compared to the normal stroma ($p <0.0001$) (Fig. 3.2)

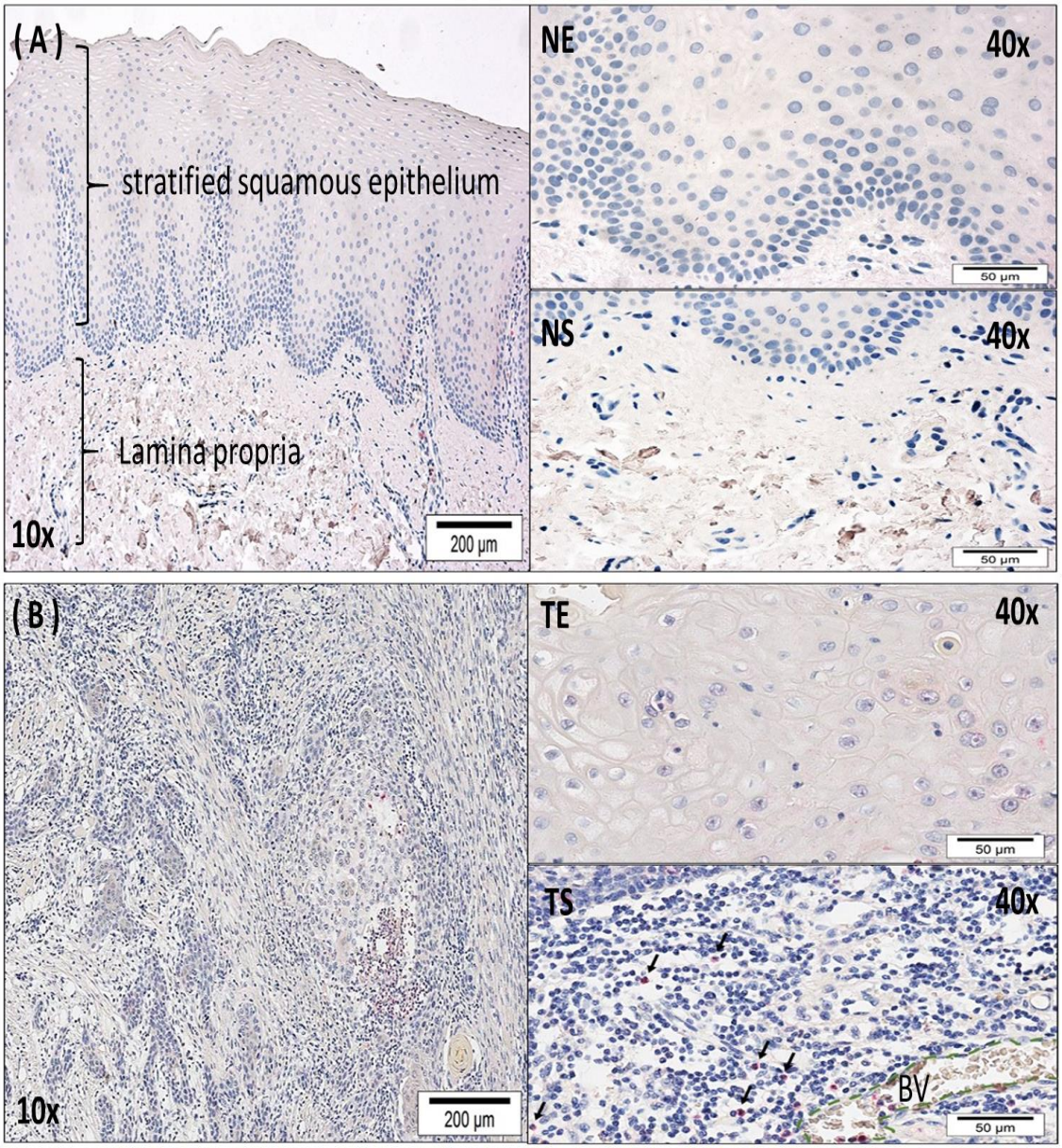

Figure 3.1 Detection of CD66b^{+} neutrophils in healthy and cancer tissue. A panel of nine normal and nine HNSCC tumour tissue sections were screened for the presence of neutrophils using the neutrophil-specific marker CD66b **(A)** Healthy tissue form buccal mucosa shows stratified squamous epithelium (NE) with underlying lamina propria or connective tissue (NS) **(B)** moderately differentiated OSCC of the tongue with tumour epithelium (TE) cells, containing large nuclei and increased nuclear-to-cytoplasmic ratio (left top). Dense Lymphocytic infiltration was observed in tumour stroma (TS) with neutrophils infiltration (bottom left, arrows).

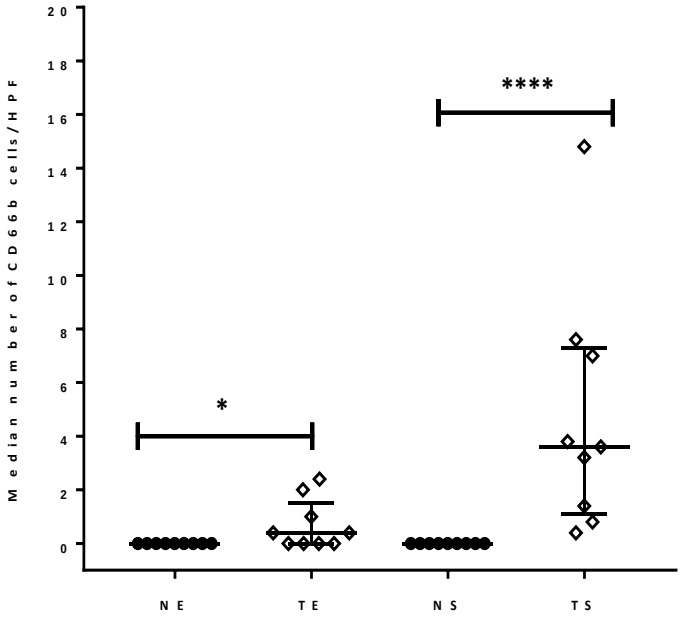

Figure 3.2 Detection of CD66b neutrophils in healthy and cancer tissue. A panel of nine normal and nine HNSCC tumour tissue sections were screened for the presence of neutrophils using the neutrophil-specific marker CD66b**.** The number of neutrophils was counted per high power filed (HPF)(40x). Non-parametric Mann Whitney test was used to show a statistically significant difference between the number of CD66b neutrophils in TE compared to NE (*p=0.0294) and number of CD66b cells in the tumour stroma compared to the normal stroma (****p <0.0001)

3.4.2. Study of MPO localization patient demographics

In this study, pathological specimens from 30 patients with HNSCC were examined. These patients comprised of 10 (30%) women and 20 (70%) men with an average follow up time of 47.03 months (range 6-144 months). The average age of the patients was 60 (ranging between 37-83). The HNSCC lesions were located in retromolar trigone (RMT) (n=5, 16%), floor of mouth (FOM) (n=15, 50%), anterior tongue (AT) (n=6, 20%), posterior tongue (PT) (n=2, 6.6%), hard palate (HP) (n=1, 3.3%) and soft palate (SP) (n=1, 3.3%). Lymph node involvement was observed in all the cases. Thirteen (42.3%) cases had a single lymph node metastasis (N1), 8 (26.6%) with metastasis in multiple lymph nodes (N2b), 3 (10%) with metastasis in the bilateral or contralateral lymph nodes (N2c) and 5 (16.6%) with distant metastasis. Five (16.6 %) patients had recurrence, 3 (10%) patients had a secondary primary tumour, and 6 (20%) of the patients the data were not available. During the follow-up, 1 (3%) patient died of disease (DOD), 6 (20%) died of an unrelated cause (DUR), 14 patients (46.6 %) were disease free (DF) and 2 (6.6%) patient was alive with disease (AWD).

Patient characteristics are summarized in appendix I (Table 2), while the full details about the patients that participated in this study have been published previously (Alkureishi et al., 2010).

3.4.3. Selection of observation field

In order to obtain the number of areas of assessment for each parameter required to minimise variation, cumulative means plots were constructed. Presence of MPO+ neutrophils was evaluated in four tumour compartments; (a) invasive front of tumour, (b) tumour stroma, (c) tumour body, (d) necrosis centre of tumour, if present. These areas were defined accordingly:

The invasive front (IF) is the periphery or the leading edge of the tumour as it progress. It comprises tumour tissue and breaks through the sub-epithelial connective tissue. *Tumour Stroma (TS)* is the connective tissue separating the solid tumour nest and is often accompanied by a desmoplastic stromal reaction and a dense inflammatory infiltrate (Fig. 3.3-A). *The tumour body (TB)* is located in central tumour areas where the characteristic of squamous carcinoma is well represented by irregular cell shape (Polygonal), enlarged cytoplasmic membrane and large nucleus with multiple prominent nucleoli (Fig. 3.3-B). Area of necrosis were identified by fragmented cells, nuclear shrinkage and cellular debris surrounded by tumour epithelium. *The necrotic centre (NC)* was associated with dense infiltration of leukocytes (fig. 3.3-C)

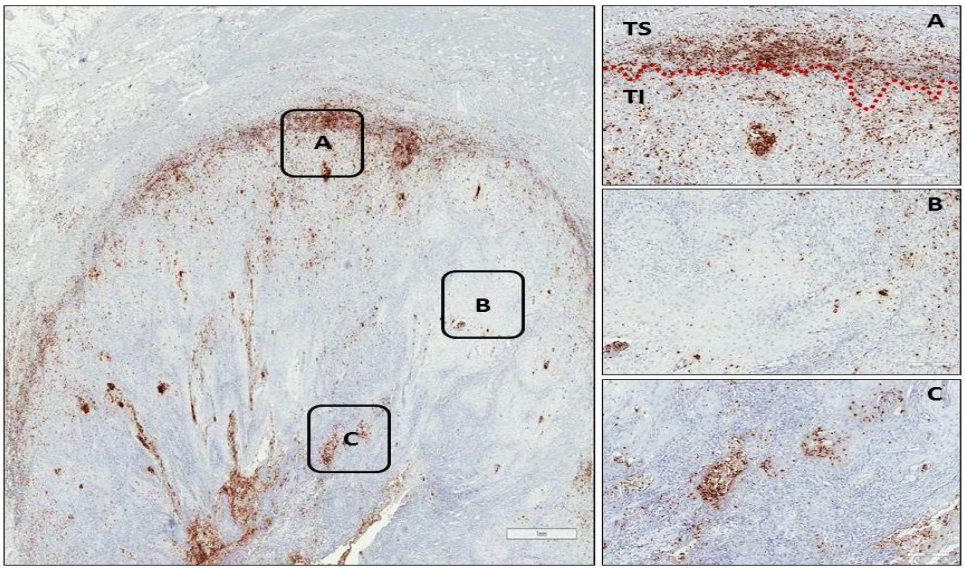

Figure 3.3. Photomicrographs of HNSCC tumour section shows the distribution of MPO+ cells within tumour. The presence of MPO+ neutrophils was observed throughout the tissue (left, Scale bar=1mm) and the localization of MPO+ neutrophils was evaluated in four tumour compartments; **(A)** Red dots line separated tumour invasive (TI) area from tumour stroma (TS) **(B)**Tumour body **(C)** and necrotic centre. The numbers of MPO+ was quantified in each of the patient in the cohort (right,Scale bar=200µm).

Cumulative means plot analysis showed that the variability in most assessments was minimised upon assessing eight individual HPF, selected at random in the area of interest (Fig. 3.4) and so in subsequent analysis each area within a histological section was evaluated with 8 HPF per area of interest for each patient tumour section in order to obtain representative data.

3.4.4. Spatial Distribution of MPO+ Neutrophils in Histological Sections of HNSCC

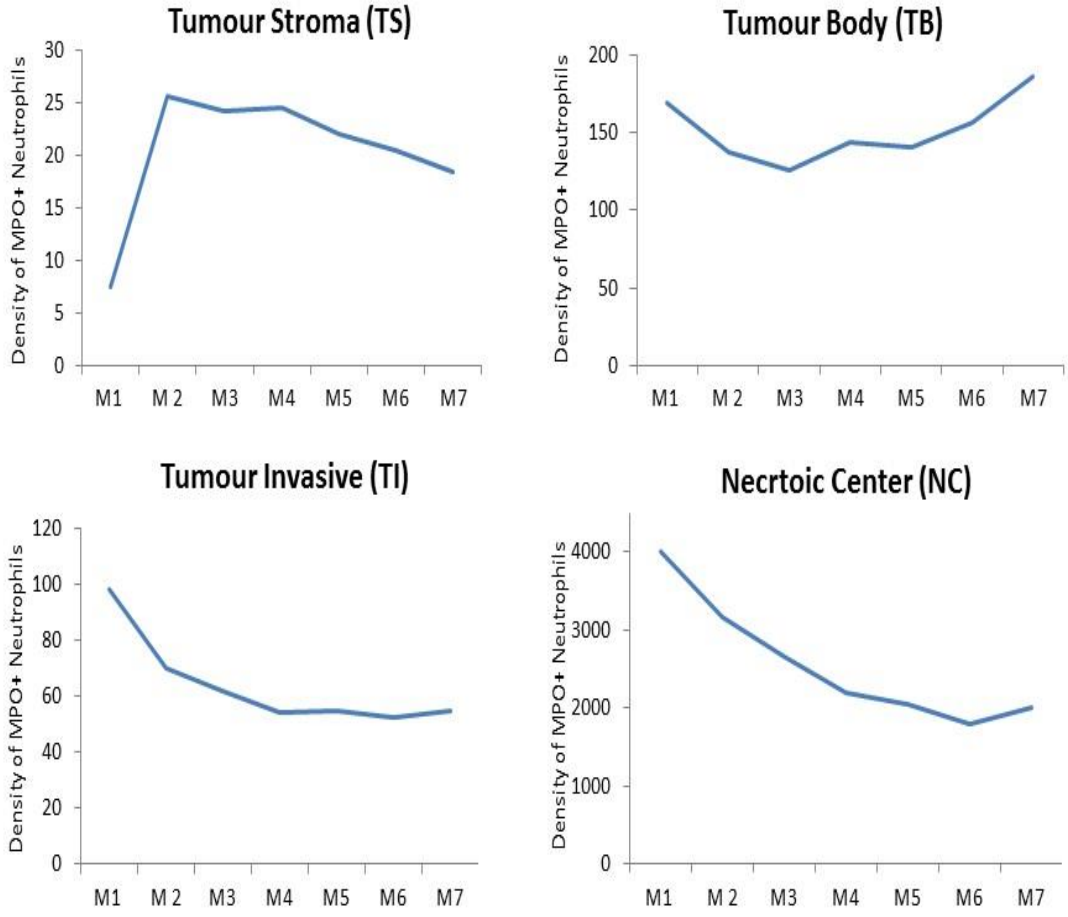

Figure 3.4 Cumulative means required for adjusting the variability for the image analysis to quantify the intensity of MPO immunostaining. Cumulative means calculated by adding up the mean of each view field to the sum of its predecessors as you go along, for the eight fileds to determine the value that lie above or below, for example, M1= number of cells in field 1 + number of cells in field 2.

The distribution of neutrophils in HNSCC was investigated in paraffin-embedded tissues sections from 30 HNSCC patients. The presence of neutrophils was visualized by immunostaining and the number of MPO-positive cells was quantified by digital image analysis and in each of the selected area and presented as mean number of cells ± SEM/HPF. The presence of MPO+ cells was detected in all cases, except one, throughout the tissue. Figure 3.5 shows that there was much variation in the number of neutrophils in each tumour site analysed in each patient. The tumours of some patients contained numerous neutrophils at some or all of the tumour sites analysed whilst others contained very few. When the median values of all the patients were calculated and compared the presence of MPO+ neutrophils in the different tumour compartments showed that the number of MPO+ cells in the tumour stroma (TS) was 366±109 cells/HPF and 172±62 cells/HPF was detected in the tumour invasive front (TI). The number of MPO+ cells in tumour body (TB) was only 37±10 cells/HPF. In contrast, the number of MPO+ cells observed in the centre of the necrotic tissue was 3059±602 cells/HPF (Figure 3.6). Thus, the density of MPO+ cells in necrotic tissue (NC) was significantly higher in comparison to TI, TS and TB ($P<0.0001$) (Fig. 3.6-C). To evaluate the prognostic importance of MPO+ cells in each of the tumour compartments, the data was analysed according to patient survival status (Fig.3.7). No correlation was found between overall survival and number of MPO+ cells in any of the tumour areas analysed. This result was expected as this pilot cohort was too small to allow robust survival analysis.

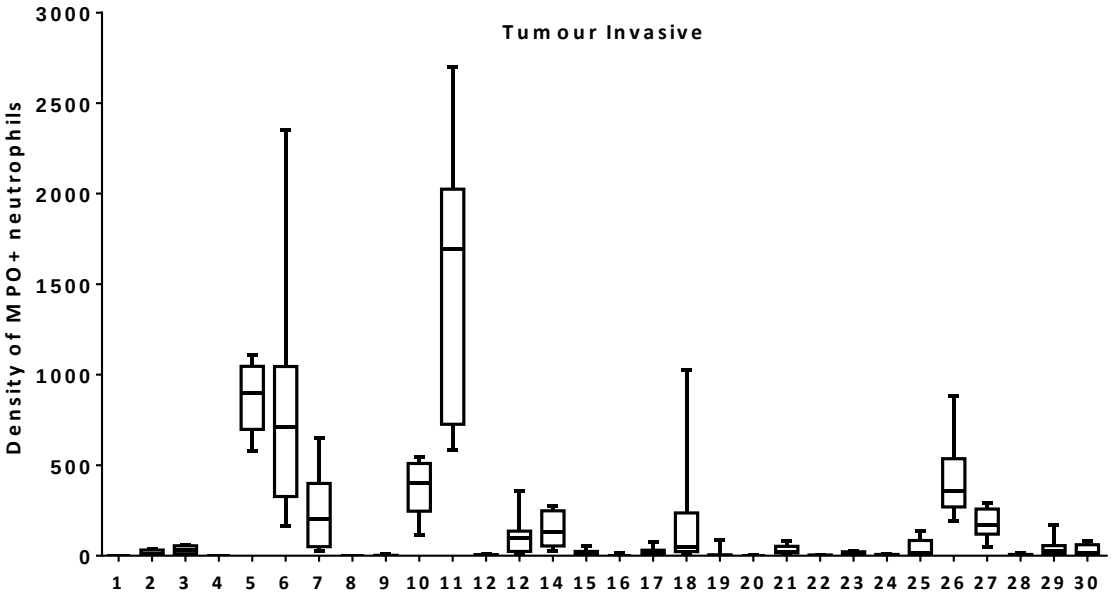
Tumour Invasive
Density of MPO+ neutrophils
3000
2500
2000
1500
1000
500
0
1 2 3 4 5 6 7 8 9 10 11 12 12 14 15 16 17 18 19 20 21 22 23 24 25 26 27 28 29 30

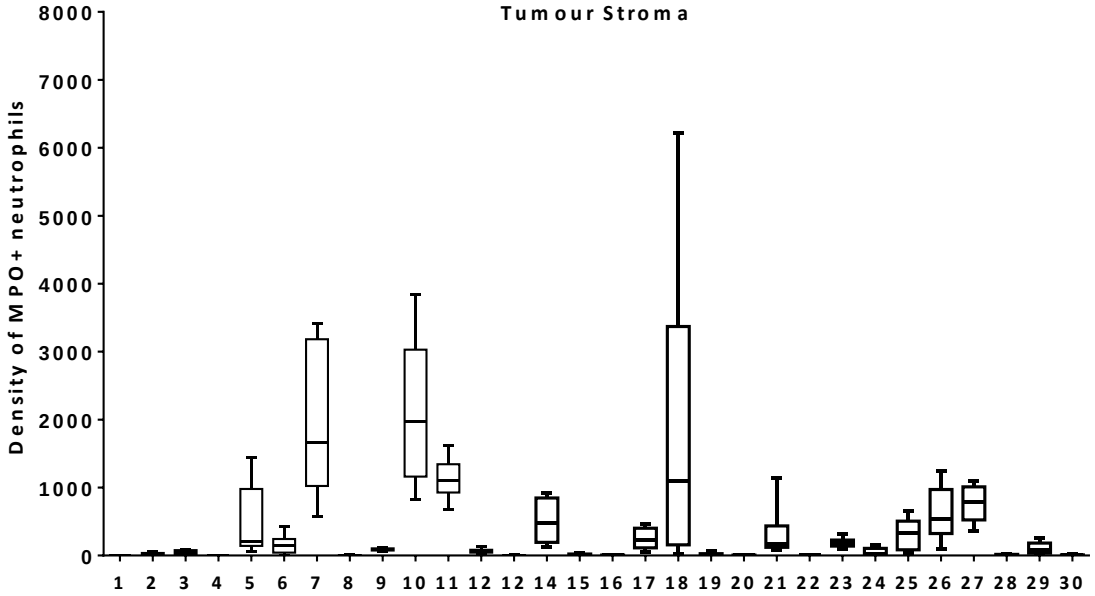
Tumour Stroma
Density of MPO+ neutrophils
8000
7000
6000
5000
4000
3000
2000
1000
0
1 2 3 4 5 6 7 8 9 10 11 12 12 14 15 16 17 18 19 20 21 22 23 24 25 26 27 28 29 30

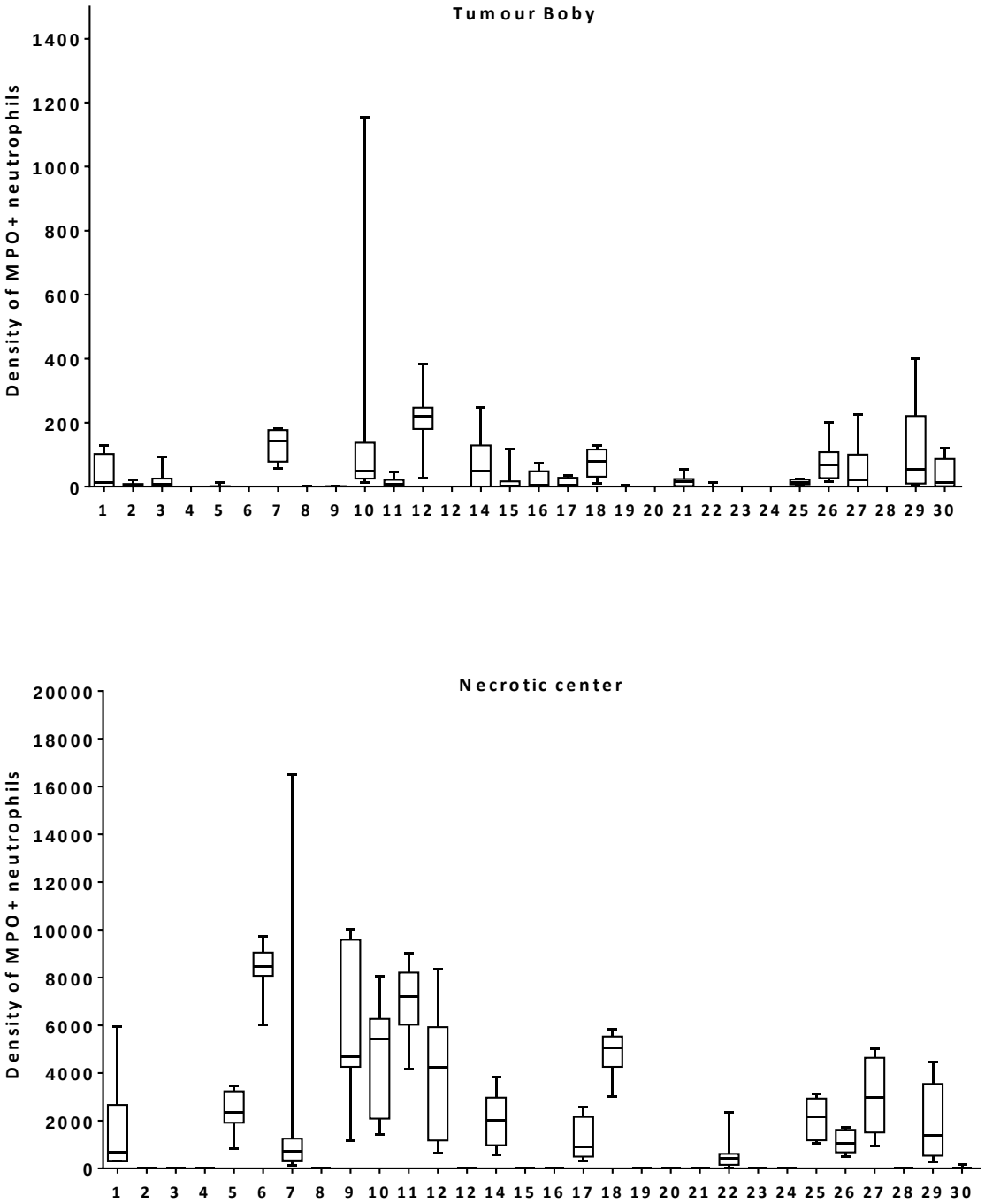

Figure 3.5 Individual patient analysis for MPO+ neutrophil infiltration in different tumour compartments showing variation between the cases. Number of MPO+ neutrophils calculated in eight fields in each of selected area presented as box and whisker blot with minimum and maximum number of MPO+ cells detected. X-axis represent the 30 individuals included in this study. The band inside the box represent the median.

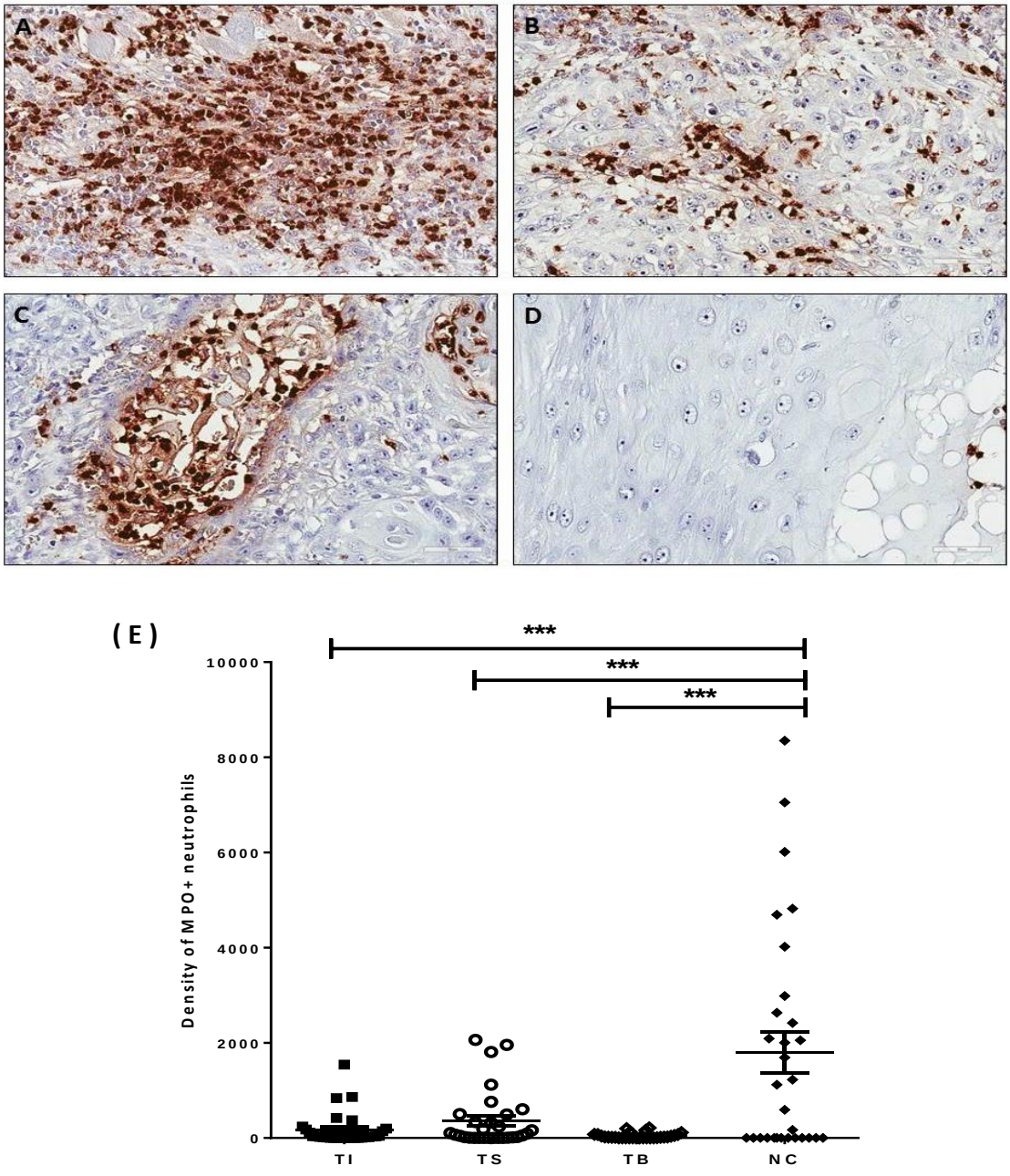

Figure 3.6 A screen for distribution of MPO+ neutrophils in HNSCC tissue. High MPO+ neutrophils was observed in tumour stroma **(A)** and invasive front of the tumour tissue **(B)**, whereas the presence of MPO+ neutrophils toward in the tumour body was scarce **(D).** The accumulation of MPO+ neutrophils was predominant within the necrotic tissue **(C)**. Scatter plot of the thirty patients involved in the study showing the median differential localization of MPO+ neutrophils in selected areas of tumour, the intensity of MPO+ cells was significantly different in the necrotic centre compared to TI, TS, TB using one way ANOVA ($p < 0.0001$). Scale bar = 50 uM

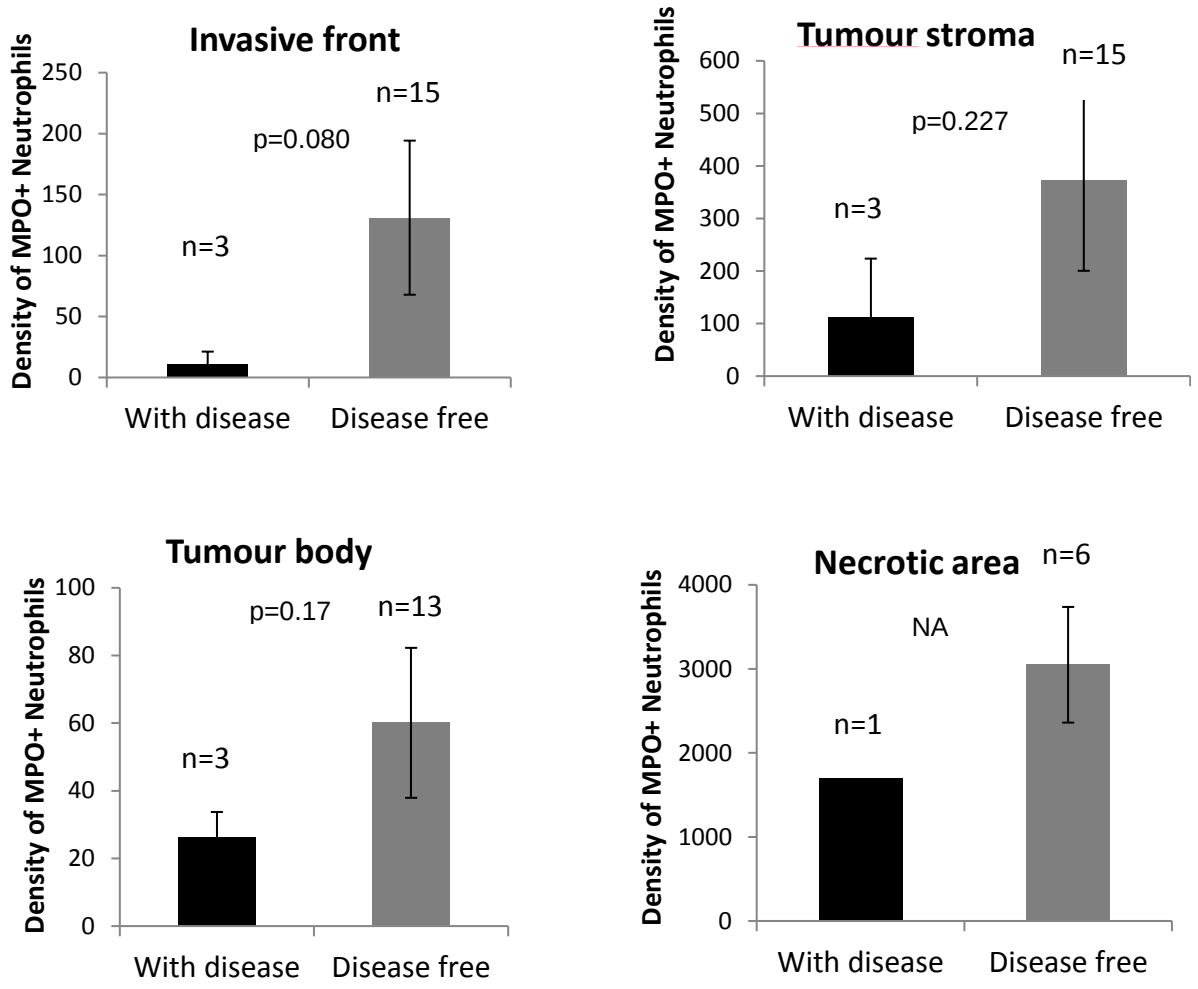

Figure 3.7 Analysis of infiltrated neutrophils in HNSCC tissue. Paraffin-embedded OSCC samples were stained with MPO and distribution of MPO^+ neutrophils were evaluated in each of invading front of tumour (TI) and tumour stroma (TS), tumour nest and necrotic areas according to patient's survival show no significant difference (Students t-test)

3.4.5. Presence of necrosis associated with influx of high number of neutrophils

Based on the above data, we predicted a correlation between presence of necrosis and number of neutrophils in tumour tissue. Large areas of necrosis were observed in 17 patients (57%) and this was associated with the influx of large number of neutrophils to the tissue (median number of neutrophils 944 cells/tumour) when compared to the 13 patients (43%) with no apparent necrosis where the number of neutrophils were significantly lower (median number of neutrophils 14 cells/tumour, $P<0.01$) (Fig. 3.8). The reduction in number of neutrophils in the absence of necrosis was associated with better outcome, since 61.5% (n=8) of patients were free of disease, and 15% (n=2) were alive with disease and one patient died of an unrelated disease. On the other hand, the presence of neutrophils in patients with necrosis were associated with death in 35.5% (n=6), 35.5% (n=6) were free of disease while the survival for 5 (30%) patients were unknown.

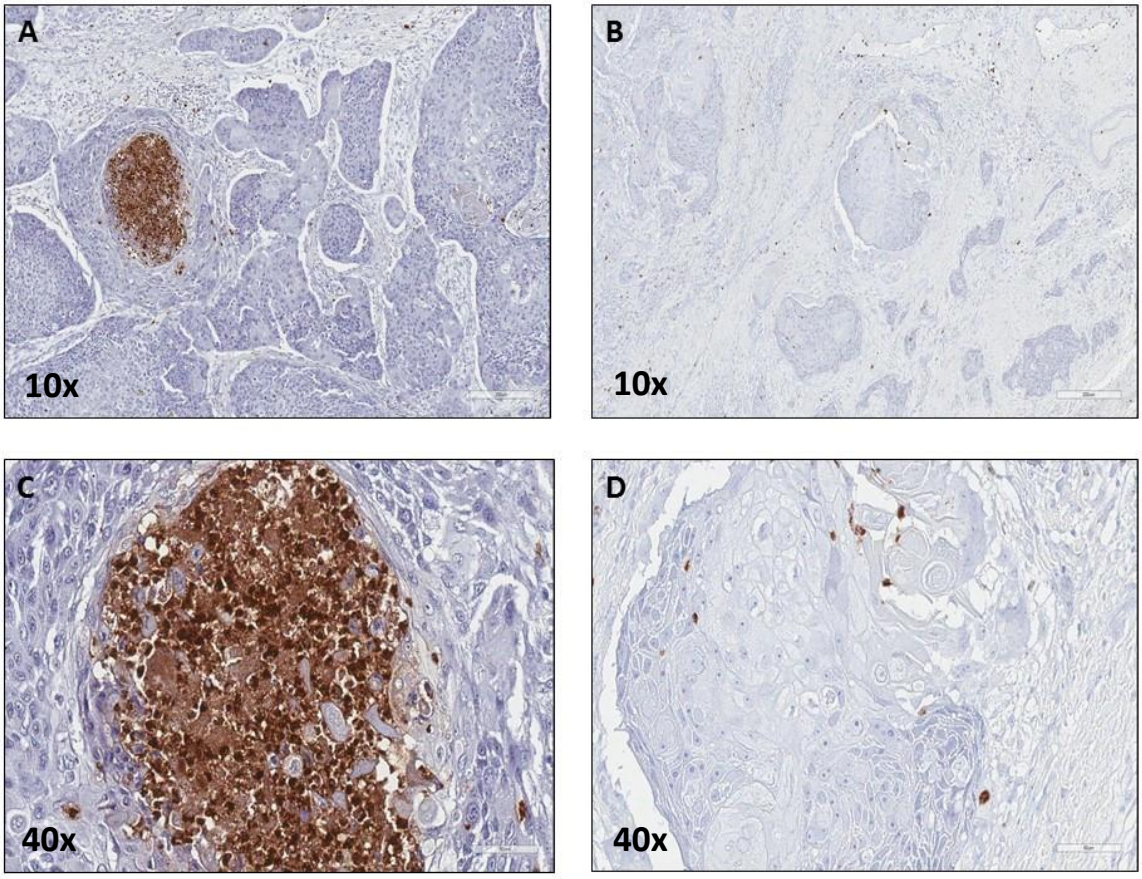

(E)

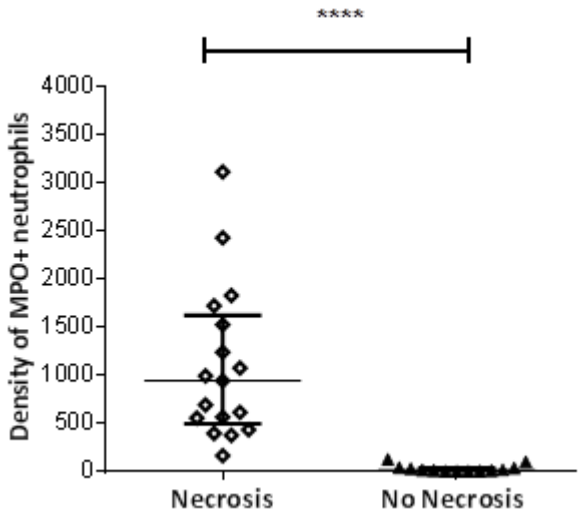

Figure 3.8 MPO+ neutrophils level in necrotic areas in a cohort of biopsy tissue from HNSCC patients. Patients were grouped according to the presence (**A** and **C**) or absent (**B** and **D**) of necrotic tissue. Mann-Whitney U test was used to compare the statistical significance of intensity of the stain between the two groups **(E).**The infiltration index of MPO+ neutrophils in tissue with necrosis was significantly higher (median number of neutrophils 944 cells/tumour) when compared to tissue with no necrosis (median number of neutrophils 14 cells/tumour; $p<0.001$).

3.4.6. Association of MPO+ neutrophils with T stage

Cases were classified into two groups according to T stage. Among the 30 patients studied 70% (n=21) had T1-T2 tumours and 30% (n=9) had T3-T4 tumours. Statistical comparison using *Mann-Whitney U test* was applied to evaluate the impact of T status on the distribution of neutrophils in tumour tissue. In general, the number of MPO+ cells present in the T1-T2 tumour was slightly higher than T3-T4 lesion, although there was a no statistically significant difference in the MPO+ index in the tumour with median number of 16 cells/tumour versus 9.5 cells/tumour, for T1-T2 and T3-T4 respectively (Fig. 3.9). In addition, no significant difference was observed between late and early stage of MPO+ cells detected in the tumour stroma with median of 67 cells/tumour for T1-T2 group versus 54 cells/tumour for T3-T4 tumours (Fig. 3.9-B). The lowest number of MPO+ infiltration was detected in tumour body with median number of 5.7 cells/tumour and 3 cells/tumour for T1-T2 and T3-T4, respectively (Fig. 3.10). The data also showed an increased number of neutrophils MPO+ accumulated in the necrotic tissue of T1-T2 patients with median number of cells 677 when compared to late stage tumours (T3-T4) but once again this was not statistically significant (Fig. 3.9). In conclusion, patients with T1-T2 tumour had abundant accumulation of neutrophils at the NC (2016 cells), which was significantly higher than neutrophils detected at TS (344 cells), TI (204 cells) and TB (29 cells) (Fig. 3.10-A). On the other hand, patients with advanced stage (T3-T4) had fewer numbers of MPO+ cells detected in the tissue with similar pattern of distribution. The highest accumulation was observed in NC with mean value of 894 cells, followed by TS 199.8 cells, very few in TI (65 cells) and almost no cells was detected at TB (18 cells) (Fig. 3.10-B)

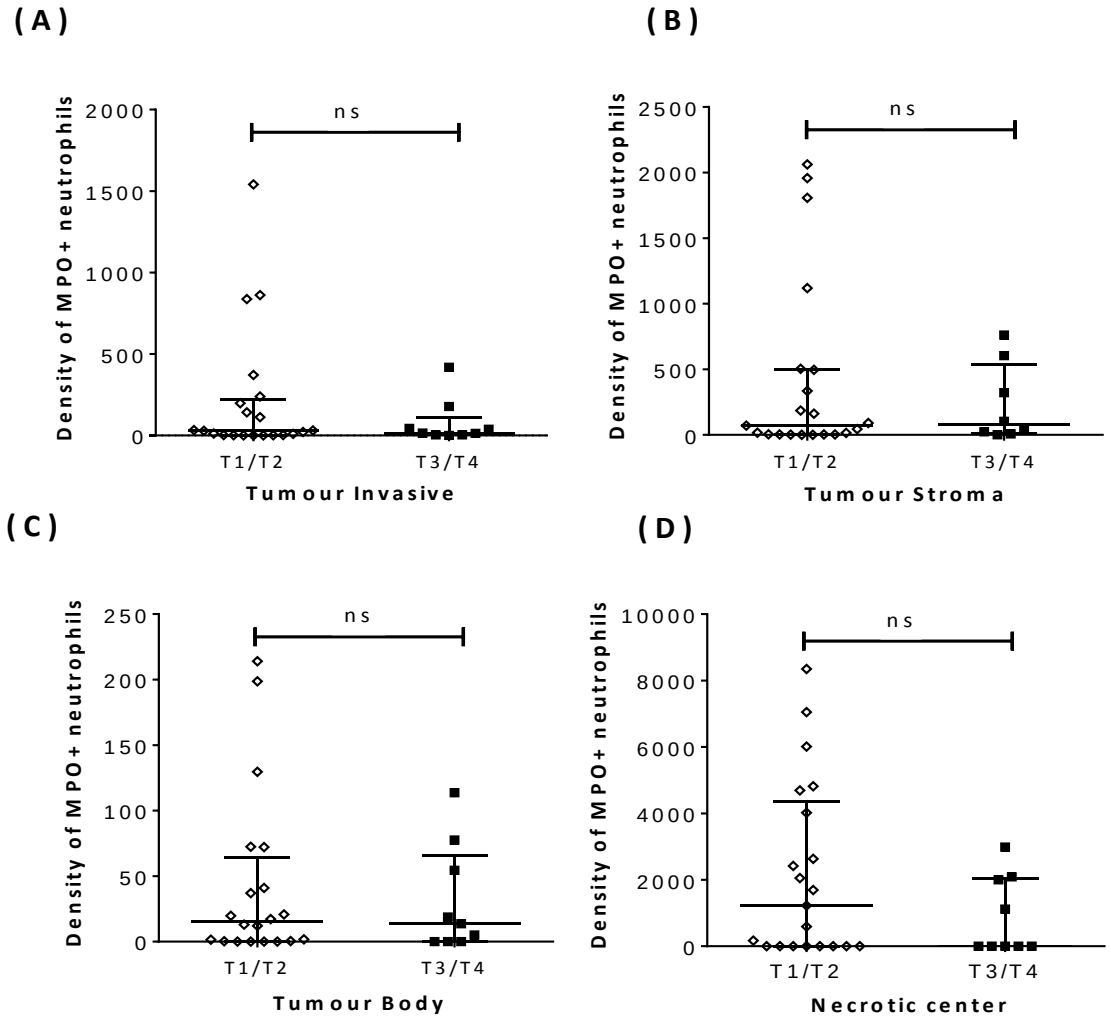

Figure 3.9 Analysis of MPO+ distribution according to T stage of disease. There was a high infiltration index of MPO+ neutrophils observed in T1-T2 (n=21) patients in compared to T3-T4 (n=9) and there was no significant difference in the number of MPO+ neutrophil infiltration between T1-T2 and T3-T4 lesions. Data are displayed as median +/- interquartile range. Mann-Whitney U test was used to calculate significant differences.

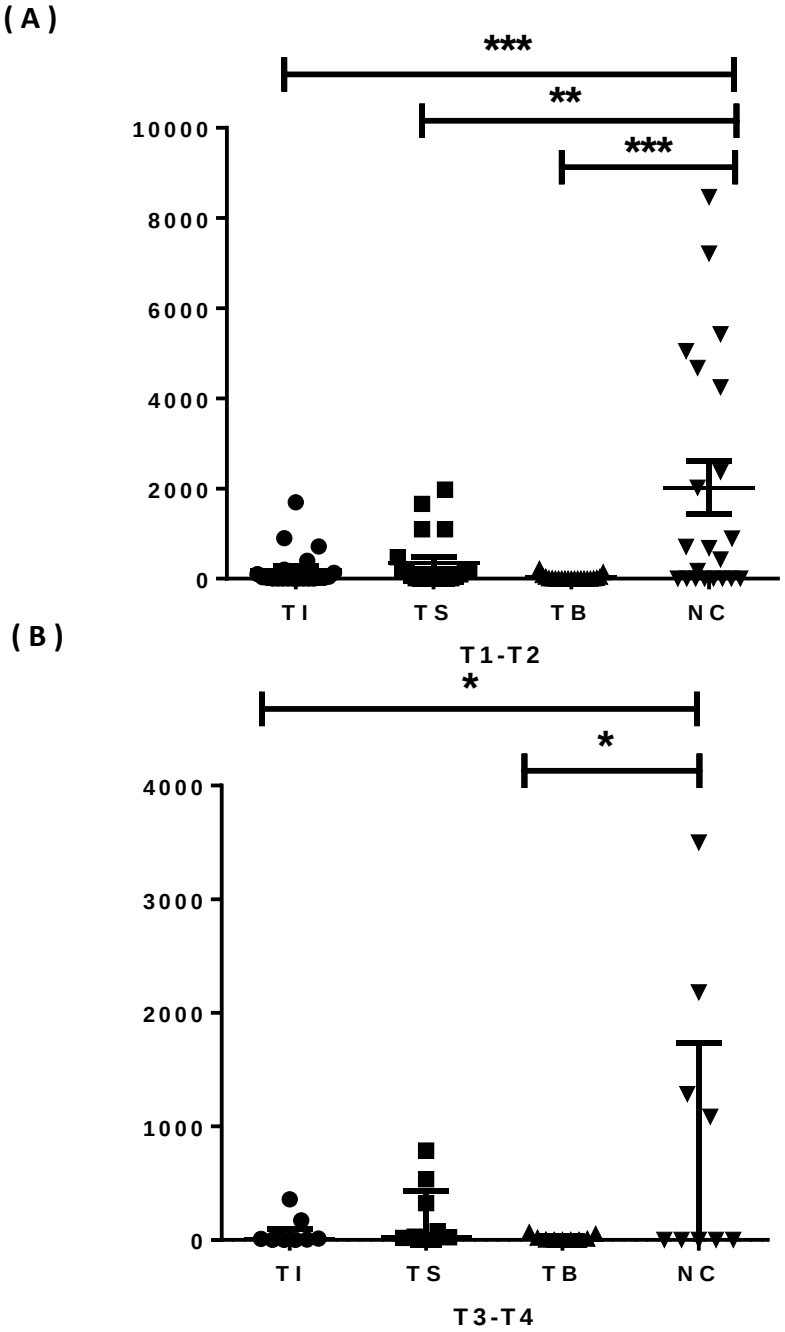

Figure 3.10 Frequency of MPO+ cells in each tumour compartment according to disease stage. Multiple comparisons using one way ANOVA test was used to compute distribution of MPO+ cells at different stage of disease. Patients at early stage T1-T2 had more neutrophils accumulation at TI, TS, NC while patients with advance stage T3-T4 show no evidence of MPO+ cells in TB and very few in TI. However, the predominate accumulation of MPO+ cells was presented at NC of T3-T4, then in TS. Data are displayed as Median ± interqurtile range. *** $p<0.0001$, ** $p<0.005$, * $p<0.05$.

3.5. Discussion

The concept of cancer related inflammation was raised as a new hallmark of cancer by (Hanahan and Weinberg, 2011) and emerging evidence has demonstrated the presence of large populations of inflammatory cells within the tumour microenvironment, including tumor-associated neutrophils (TAN).

As a tumour grows its complexity increases and it invades the surrounding connective tissue, often termed the tumour stroma, in which tumour cells are involved in cross-talk with the stromal cells. The tumour neighbourhood includes a multitude of cells such as fibroblasts, pericytes, endothelial and immune cells. The communication between all these cell types has been shown to influence the tumour microenvironment such as oxygen tension, tissue necrosis, local inflammation and degradation and remodelling of extracellular matrix (ECM) leading to tumour angiogenesis (Curry et al., 2014). For this purpose, the distribution of infiltrated neutrophils in different HNSCC tumour compartments including invading front, stroma, tumour body and necrotic areas was examined.

Despite the small study sample size, and the inability to perform Kaplan-Meier survival plots due to lack of clinical information, several important observations were noted. MPO+ neutrophils were present throughout cancer tissue samples with most of neutrophils accumulating in the stromal tissue and necrotic areas rather than in the tumour body. The number of neutrophils infiltrating into the necrotic foci was significantly higher than other areas, suggestes that neutrophils might be recruited to areas of necrosis under the influence of specific molecules. This feature was also evident at all stages of cancer progression, suggesting its prolonged importance over the life-span of a tumour. Like macrophages, neutrophils are innate immune phagocytes that are pre-programmed to engulf cellular necrotic debris in order to clear areas of cellular material during wound healing so it is reasonable that neutrophils are recruited to sites of necrosis to clear debris and so neutrophils could be directed to these necrotic sites under the influence of chemoattractants.

Evidence that necrotic cells can cause neutrophil accumulation has been observed *in vivo*. Injection of P388 necrotic leukemic cells in the peritoneal cavity in mice induced neutrophil infiltration into the site of injection via the production of chemokines KC and MIP-2, suggesting that neutrophils are attracted to tumours by necrotic cues (Tanimoto et al., 2007). Another study showed that necrotic but not apoptotic cells release both nuclear factor and secreted protein HMGB1, which has the ability to trigger inflammation and enable neutrophil recruitment to sites of tissue injury (Scaffidi et al., 2002). In fact, HMGB1 protein is responsible for the Mac-1-dependent neutrophil recruitment via the receptor for advanced glycation end products (RAGE) present on neutrophils (Scaffidi et al., 2002). Further investigation showed that deletion of HMGB-1 diminished the ability of necrotic tissue lysates to induce neutrophil migration but did not affect macrophage ability to migrate to HMGB-1 null tissue lysates. The HMGB-1 mediated neutrophils recruitment of was not dependent on CXCR4, as the use of small molecule inhibitors AMD3100 or neutralizing antibody did not inhibit the recruitment, whereas, deletion of RAGE on neutrophils, significantly reduced migration toward necrotic tissue lysate (Huebener et al., 2015).

However, it has been demonstrated recently that recruitment of neutrophils to tissue leads to what called as 'inflammatory hypoxia', where neutrophils can themselves evoke hypoxia by depleting sites of molecular O_2 as result of reactive oxygen or nitrogen species generation (Campbell et al., 2014). Like other solid tumours, HNSCC usually develop a hypoxic microenvironment along with necrosis and this also imparts a negative prognostic factor and induces a more aggressive cancer phenotype (Swartz et al., 2015). Tumour hypoxia is developed as a result of the low oxygen tension in tissue, caused by high cellular demand and an inadequate supply of oxygen. Clinical studies have shown that the 'hypoxic tumour volume'

is now is an important prognostic factor in HNSCC (Dunst et al., 2003). Although there are no direct evidence that links the presence of neutrophils in hypoxic tissue in HNSCC but a very elegant study using a uterine cancer mouse model, showed that neutrophil recruitment occurred at early stages of tumour was associated with development of tumour hypoxia (Blaisdell et al., 2015). Other studies have shed light into the underlying mechanism of neutrophils homing to sites of localized hypoxia and necrosis. Hypoxic tissue up-regulates the expression of vascular endothelial growth factor A (VEGF-A) which induces the trafficking of a specific subpopulation of circulating neutrophils that co-express VEGF receptor1 (VEGFR1), CXCR4 and Integrin Subunit Alpha 4 (CD49d). Their recruitment to VEGF-A foci was found to be dependent upon activation of VEGFR1 on neutrophils. However, when recruitment of the newly identified neutrophil population was inhibited by targeting CD49d in an *in vivo* model, not only was the number of neutrophils migrating to site of hypoxia affected significantly but also tumour angiogenesis was impaired (Massena et al., 2015). Of note, in response to hypoxia human neutrophils can survive longer *in vitro* and produce anti-apoptotic effect that is associated with up-regulation of hypoxia inducible factor HIF-1α (Walmsley et al., 2005). This evidence supports the notion that neutrophils recruited to low oxygen tension area of tumours such as hypoxic and necrotic sites are able to live longer and be more likely detected than in other areas and potentially are likely to play a crucial role in disease pathogenesis.

To date, among all studies evaluating the role of TANs from the standpoint of their histological localization in cancer tissue it has been shown that the presence of neutrophils either in intratumoural or peri-tumoural stromal was associated with poor outcome in various malignancies. To the best our knowledge, this is the first study identifying the presence of

increased number of neutrophils in necrotic areas compared to other tumour sites and demonstrates that patients without necrosis that have significantly lower number of neutrophils may have a better prognosis.

When the distribution of TAN in relation to disease stage was assessed, results showed that most of the T1-T2 tumours displayed high numbers of neutrophils in most areas, except the tumour nest, whereas tumours at T3-T4 exhibited a lower degree of infiltration. These findings contradicted those of Trellakis et al, (2011), Caldeira et al, (2015) who showed that patients with advance stage disease displayed a strong neutrophil infiltration (mean of 71) when compared to less advanced tumours (mean of 63) (Caldeira et al., 2015, Trellakis et al., 2011a). Mouse models have been used to evaluate the localization of TAN at early and late stage of tumour growth. There was no difference in the percentage of TAN in early compared to later stage tumours of Lewis lung xenograft models, whereas a minor increase at later stage was observed in AB12 mesothelioma tumours. The distribution of TAN at the early stage was found mainly at the periphery of the tumour, while in more advance stage tumours TAN was seen in the tumour periphery and the central parts of tumour (Mishalian et al., 2013).

In summary, this chapter has shown that neutrophils are recruited to HNSCC in large numbers and this occurs in both early and late stage tumours. More specifically, they are preferentially recruited to certain sites within tumours such as necrotic areas and this is undoubtedly in response to specific chemoattractant cues. There is now increasing evidence that TAN play a major role in tumour progression (Tazzyman et al., 2011) in many tumours including HNSCC by releasing tumour promoting factors or molecules that stimulate tumour angiogenesis. However, little is known about the specific molecules that recruit neutrophils form the peripheral blood to HNSCC. These are crucial molecules in directing the fate of neutrophils

and their discovery could pave the way for the generation of novel therapeutics. The following chapter will investigate the likely neutrophil chemoattractants that HNSCC cells generate and which of these are the most important for mediating TAN recruitment in HNSCC.

Chapter 4: Mechanisms driving neutrophil recruitment into head and neck tumours: in vitro analysis using a multi-cellular tumour spheroid model

4.1. Introduction

Data from the immunohistochemical analysis of HNSCC patient biopsies (Chapter 3) showed accumulation of neutrophils (TAN) in HNSCC tissues. This raises the question of precisely how neutrophils are recruited to these tumour sites. Two-dimensional (2D) cell culture models lack essential components of the complex tumour microenvironment such as tumour hypoxia, necrosis, gradients of nutrients and metabolites, and are therefore an undesirable option to represent tumours *in vivo*. The growth of cancer cells in a three-dimensional (3D) context that recapitulate the characteristic features of solid a tumour was made by Sutherland *et al* in 1970s (Sutherland et al., 1971), and today these models are known as multi-cellular tumour spheroids (MCTS). In these models, aggregates of cells have been shown to mimic common properties seen in avascular tumours or intervascular micro-regions of solid tumours *in situ*. As MCTS grow to 200-500µm in diameter, they develop a central area of hypoxia as a result of insufficient supply of oxygen, nutrients and accumulation of waste products, and this further develops into necrosis when MCTS grow beyond 500 µm. In contrast, the well-oxygenated rim of the MCTS typically contains large numbers of proliferative tumour cells similar to that seen *in vivo* (Sutherland and Durand, 1984, Groebe and Mueller-Klieser, 1991).

Many research groups have employed the MCTS model in different tumour biology fields and there is overwhelming evidence that cells grown in 3D behave differently to those cultured in conventional 2D culture. For example, gene expression and protein profiling of cells cultured

in 3D was similar to that observed in a clinical sample than the same cells grown in 2D (Kumar et al., 2008b). Moreover, generation of a 3D placental vascular model by co-culturing three cells components, (cytotrophoblasts, villous stromal cells and endothelial precursor cells) showed that cells cultured in a 3D system had structurally and morphologically similar phenotype to tissues from early placenta (Baal et al., 2009). For these reasons MCTS are now frequently used as pre-clinical screening systems in drug evaluation for many new anticancer therapies. For example, Hirschhaeuser et al used the MCTS system to test Catumaxomab, a trifunctional hybrid monoclonal antibody that binds to tumour cells via epithelial cell adhesion molecule (EpCAM), CD3 on T cells and antigen-presenting cells via the Fc receptor, thereby linking the three cell types together. Addition of Catumaxomab and peripheral blood mononuclear cells to an EpCAM-positive MCTS tumour model showed active tumour killing in a realistic 3D *in vitro* model compared to 2D models (Hirschhaeuser et al., 2009). This model also demonstrates the usefulness of MCTS when combined with leukocytes and provides an opportunity for the use of 3D methodologies to analyse the interaction of leukocytes with tumour cells in a realistic tumour microenvironment *in vitro*. Such models have been used previously to analyse the role of neutrophils in lung cancer (Tazzyman et al., 2011) but none have yet been established for use in HNSCC research.

4.2. Aims

The aim of the experiments outlined in this chapter were to firstly characterise the features of a HNSCC cell line grown as an MCTS (growth, morphology, expression of inflammatory molecules etc.) and then to use this model to identify specific factors responsible for the recruitment of TAN into HNSCC.

4.3. Methods

MCTS were generated by an agarose over-lay technique **(2.2.3.1)** using a hypopharyngeal HNSCC cell line (FaDu). MCTS were grown in culture until day 6 and then analysed for features characteristically observed in avascular tumours *in vivo* (hypoxia, necrosis and proliferation). The release of factors by FaDu MCTS into the culture media was identified using a cytokine array **(2.2.6.1)**. The optimum conditions for neutrophils isolated **(2.2.2.1)** from the peripheral blood of healthy volunteers and added to the MCTS either with or without stimulation with TNF-α **(2.2.3.3)** for different time points were assessed. The infiltration of fluorescent-labelled neutrophils into FaDu MCTS in presence or absence of receptor antagonists or small molecular inhibitors was quantified by flow cytometry **(2.2.9.4)**.

4.4. Results

4.4.1. Culture of the head and neck cancer cell line FaDu as MCTS

The use of *in vitro* 3D culture systems has been proposed as a valuable tool in cancer research that holds several advantages in comparison to monolayer cultures. Although tumour spheroids have been made from cancer cells of several tumour types, MCTS made from head and neck cancer cells have not been fully characterised. MCTS were generated from FaDu cells using the agarose overlay technique. A few hours after initial seeding the FaDu cells started to aggregate into small clumps in the centre of each well of the 96-well plate and began to adhere to one another. The cells formed a characteristic spherical shape over the first 24 hours with an average diameter of 694 µm (Fig. 4.1A). Over the next three days in culture the MCTS developed a uniform appearance and increased in size reaching an average of 731 µm in diameter at day 3 with very few cells seen unattached to the spheroid border. When observed using light microscopy, necrosis could be seen at day 3 (Fig. 4.1-A) as a darker area at centre of the growing spheroid and this continued to enlarge as the size of MCTS

increased in subsequent days of culture (Figure 4.1A). By day 6 the FaDu MCTS had reached a mean diameter of 937 µm and the size gradually increased to reach an average diameter of 1482 µm by day 13. MCTS growth slowed by day 14 (1457 µm) to reach a maximum diameter of 1533 µm at day 15 (Fig. 4.1B). As the MCTS further enlarges the necrotic centre increases and the viable rim becomes smaller.

Upon histological analysis, the darker area at the centre of FaDu MCTS observed from day 3 was confirmed as necrosis surrounded by a viable rim of tumour cells. Haematoxylin and eosin stained sections showed an expands area of necrosis over time to reach up to 90% of the diameter of the whole spheroid by day 15 with a corresponding shrinkage of the outer viable rim. As a result of the larger necrotic core, the spheroids become more fragile during the histological processing (Fig. 4.2)

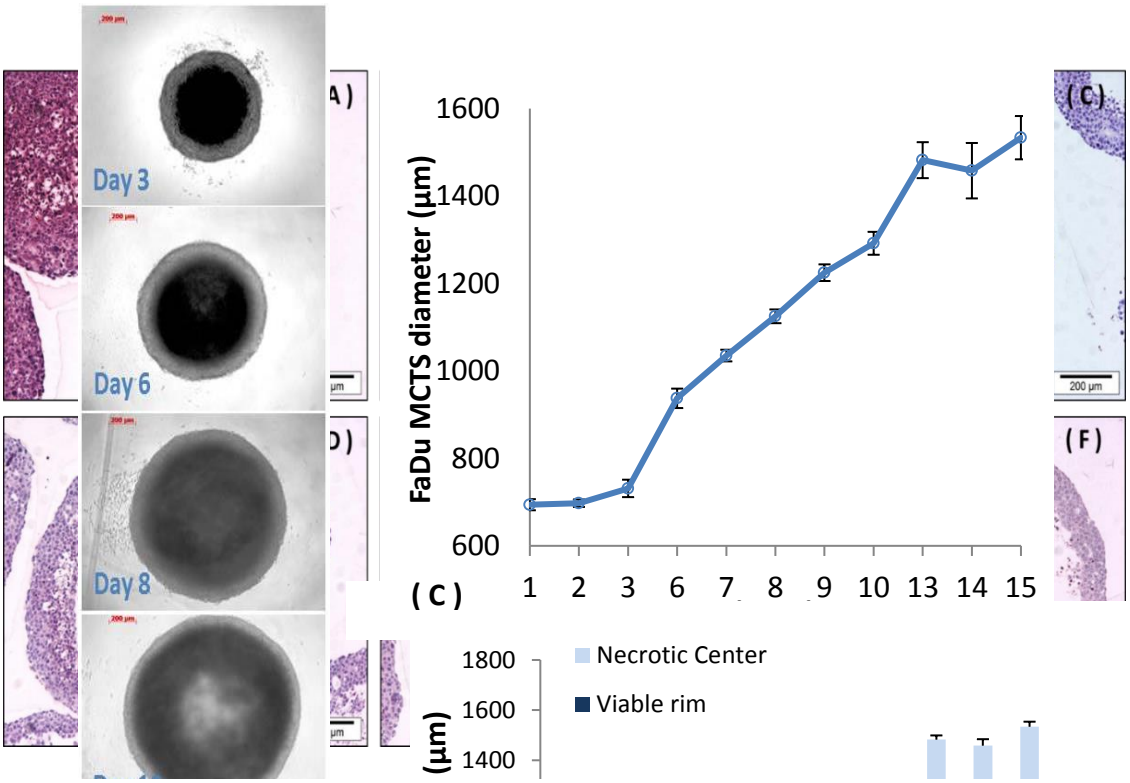

Figure 4.2 Representative images of haematoxylin and eosin-stained sections of FaDu MCTS showing necrotic centre and viable tumour cell rim at day 3 (A), day 6 **(B)** day 8 **(C)**, day 10 **(D)** day 13 **(E)** and day 15 **(F)**. Scale bar = 200µm

Figure 4.1 Pharynx SCC cancer cell grows as MCTS in culture (A) Light microscopy images of FaDu MCTS in culture over a 15-day period (10x magnification), **(B)** growth curve of FaDu spheroids shows the mean diameter measurements from six spheroids ± SD. Scale bar =200µm **(C)** The diameter of the necrotic core (light blue) and the viable rim (dark blue) from FaDu MCTS were measured under light microscopy using Axiovision software.

4.4.2. FaDu MCTS as a model of avascular HNSCC tumours

Tissue necrosis and hypoxia are characteristic features seen in most of solid tumours. The oxygen tension expressed as partial pressure of oxygen (pO_2) within primary HNSCC tumour was measured 8.6 mmHg (Becker et al., 2002), whereas advance stage SCC was found to have even lower oxygen tension as low as ≤ 2.5mmHg which associated with poor prognosis (Nordsmark and Overgaard, 2000). Light microscopy suggests the presence of necrosis at the central area of FaDu MTCS from day 3. This was confirmed by histological analysis, which showed a necrotic focus at the centre of spheroid and tissue architecture breakdown that was the same as observed clinically (Fig. 4.3-A&B). The presence of hypoxia within MCTS was measured using the hypoxia-sensitive dye PIMO (Raleigh et al., 1991). MCTS at day 6 were selected as these developed a necrotic core but still contain a large viable rim (295 µm) (Figure 4.2-B). Fluorescence microscopy of PIMO-stained FaDu MCTS showed strong red fluorescence staining in the centre of the spheroid that then slightly decreased within the viable rim towards the periphery (Fig. 4.3-C). The presence of hypoxia around a necrotic area observed

in the MCTS was similar to that observed in HNSCC (Fig. 4.3-D). Figure 4.3 shows proliferating cancer cells (Ki-67 positive cells) that were located in outermost part of the spheroid (Fig. 4.3-E); an observation that was in line with the distribution of Ki-67 staining observed in a patient biopsy of HNSCC (Fig. 4.3-F).

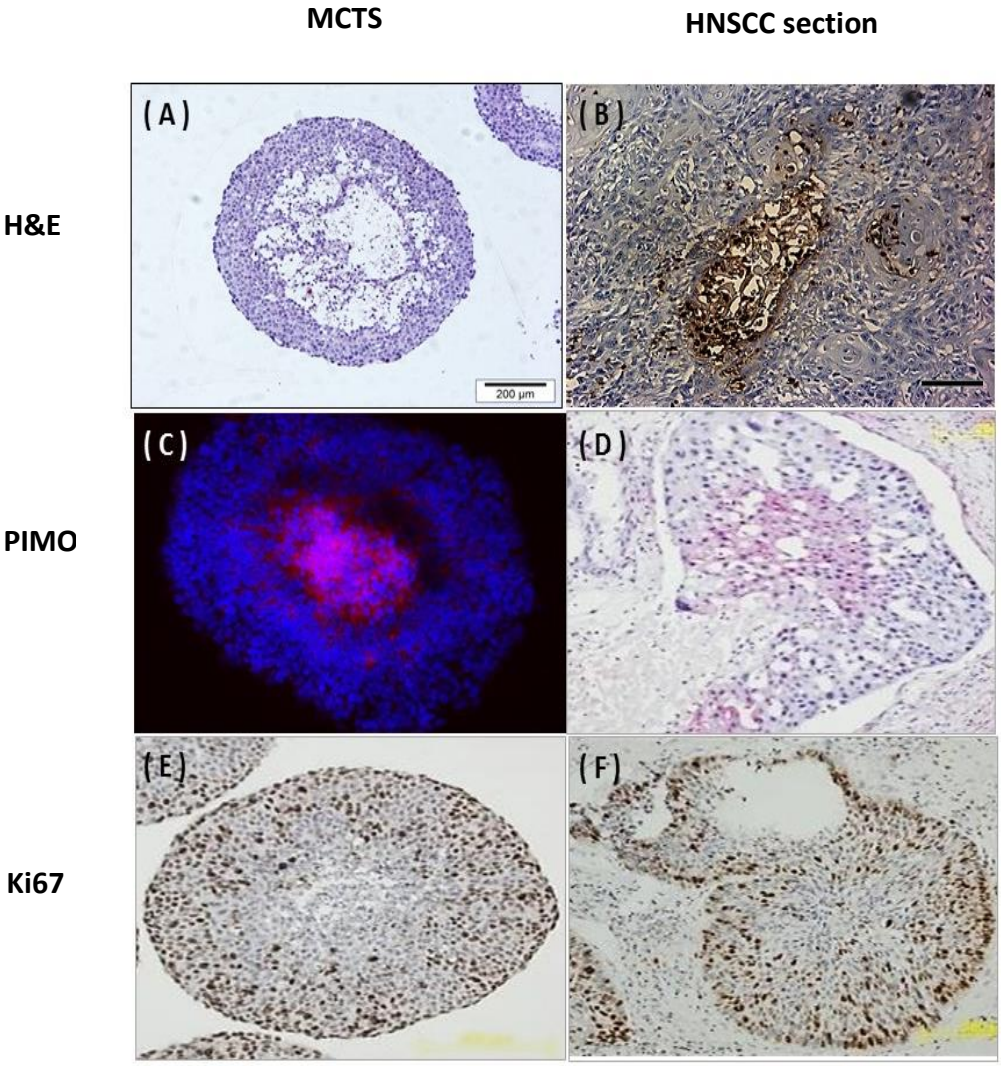

Figure 4.3 Characterisation of *in vitro* MCTS as a model of avascular HNSCC tumours. FaDu MCTS **(A)** and HNSCC tumour island **(B)** showing necrotic centres. FaDu MCTS stained with pimonidazole **(C)** to demonstrate hypoxia as is commonly observed in HNSCC in vivo **(D).** Ki67-positively stained proliferating cancer cells (Brown) at the well-oxygenated periphery of FaDu MCTS **(E)** and a human biopsy tumour island **(F).** Scale bar = 200. Patient biopsy slides were kindly provided by Dr Helen Colley.

4.4.3. Neutrophil infiltration into FaDu MCTS

To assess the ability of neutrophils isolated from peripheral blood to infiltrate HNSCC *in vitro* fluorescently-labelled neutrophils were co-cultured with FaDu MCTS (for 2, 5 and 20 h) in the absence or presence of 50 ng/ml recombinant human TNF-α (for 5 or 18 h) and infiltration measured by flow cytometric analysis of dispersed MCTS (as described in Fig. 4.19-A). TNF-α was used as a stimulant because HNSCC are known to be within a pro-inflammatory micro-environment (Soylu et al., 1994) and this cytokine also regulates expression of adhesion molecule intercellular adhesion molecule-1 (ICAM-1) on epithelial cells (Burke-Gaffney and Hellewell, 1996). Flow cytometric analysis showed that neutrophils infiltrated tumours in the absence of a pro-inflammatory stimuli but this was significantly ($p<0.05$) increased by addition of TNF-α (Fig. 4.4-B). In fact, neutrophil infiltration for 2 h was markedly increased upon stimulation of FaDu MCTS with TNF-α for 5 h (10.8%) and 18 h (14.5%) compared to un-stimulated FaDu spheroids (1.3%). Neutrophil infiltration after 5 h co-culture with FaDu MCTS was significantly increased after 5 h prior stimulation with TNF-α, reaching a peak of 15% compared to un-stimulated FaDu spheroids (2.1%). However, stimulation of MCTS with TNF-α for 18 h resulted in a reduction in the number of infiltrated neutrophils (11.9%) after 5 h. Eighteen hours incubation of neutrophils with FaDu MCTS stimulated for either 5 or 18 h showed a reduced level of neutrophil infiltration reaching 10.4% and 11.1% respectively, compared to un-stimulated FaDu MCTS (2.6%). A similar trend was observed in all experiments (n= 4) although the infiltration rate varied slightly from donor to donor (Fig. 4.4-B).

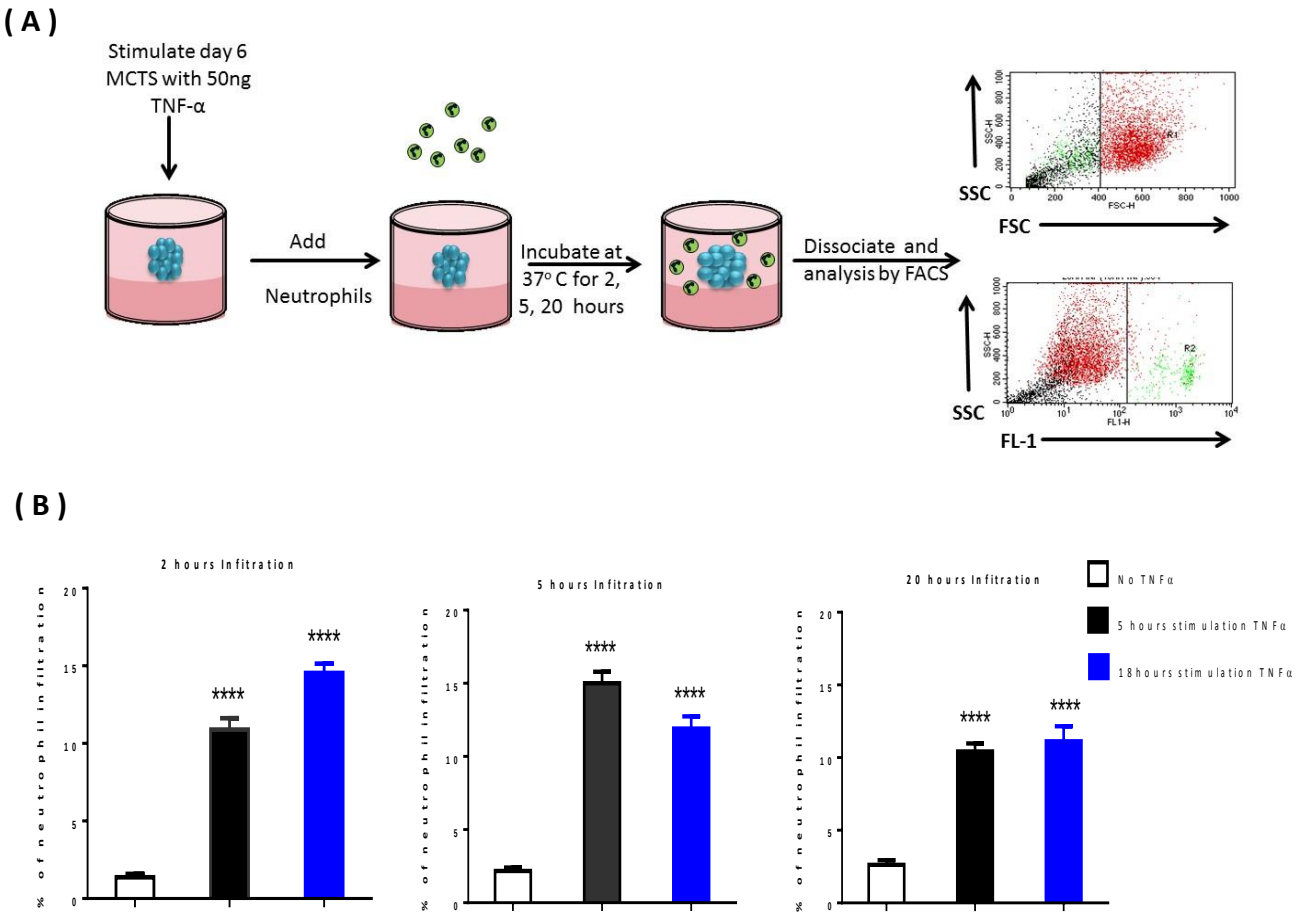

Figure 4.4 Neutrophil infiltration into TNF-α-stimulated FaDu MCTS. (A) FaDu MCTS were incubated with fluorescently labelled neutrophils and number of infiltrated neutrophils was assessed by flow cytometric analysis. Dot plot shows the gating around the fluorescently labelled neutrophils (FL-1) and the number of neutrophils in FaDu MCTS measured as % infiltration. **(B)** Bar chart of flow cytometric analysis shows stimulation of MCTS with TNF-α leads to significant increase of neutrophil infiltration into MCTS over time. One-way ANOVA was used to compute the difference in neutrophils filtration after with or without TNF-α stimulation. **** P< 0.0001. Data are mean of 3 FaDu MCTS per time point ± SD, and are representative of n=4 independent experiment.

Neutrophil infiltration into FaDu MCTS at selected time points was confirmed by analysing frozen (Fig. 4.5A&B) and formalin-fixed, paraffin wax-embedded sections by immunohistochemistry (Fig. 4.5-C & D). These data show that neutrophil infiltration into MCTS is maximal under pro-inflammatory conditions upon treatment with TNF-α for 5 h followed by neutrophil infiltration for 5 h. Since neutrophils are recruited to tumours *in vivo* and MCTS *in vitro*, it was reasoned that this was due to increased expression of neutrophil specific chemotactic factors. Thus, the presence of chemo-attractants in the conditioned medium of MCTS was investigated.

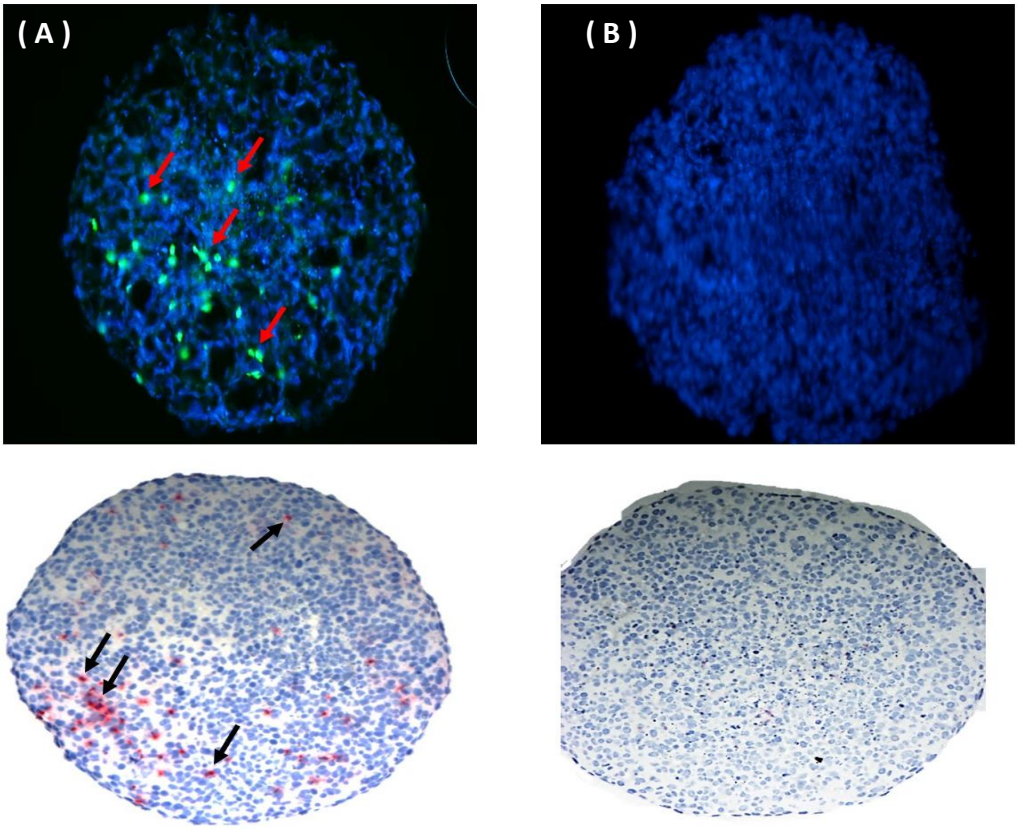

Figure 4.5 Neutrophil infiltration into FaDu MCTS. (A) Image of 6µM frozen section of day 6 FaDu MCTS showing infiltrated of MCTS with green fluorescently labelled (red arrows) neutrophils for 5 h **(B)** or FaDu MCTS alone. FaDu MCTS were immuno-stained for the neutrophil marker CD66b (Red, black arrows; **(C)** compared to control MCTS **(D).**

4.4.4. FaDu MCTS secrete neutrophil chemoattractants

To identify factors present in FaDu MCTS responsible for neutrophil infiltration, FaDu MCTS were grown until day 6, and were either unstimulated or stimulated with TNF-α in the absence of presence of neutrophils and their conditioned medium collected after 5 h and analysed by multiplex cytokine array followed by densitometry (section 2.2.6.1). Among 36 cytokines tested, data shows that unstimulated FaDu MCTS released several well-known neutrophil chemokines including CXCL-1 (Gro-α), CXCL-8 (IL-8) and CCL5 (RANTES) and these chemokines, particularly CXCL8, were increased by treatment with TNF-α with no further increase upon the addition of neutrophils. However, in both unstimulated and stimulated MCTS the most abundant protein released was Macrophage migration inhibitory factor (MIF). Other molecules released include IL-6, IL-23, IL-1 receptor antagonist (IL-1ra), INFγ and SerpinE1 also known as plasminogen activator inhibitor type-1 (PAI-1) (Fig. 4.6 and 4.7).

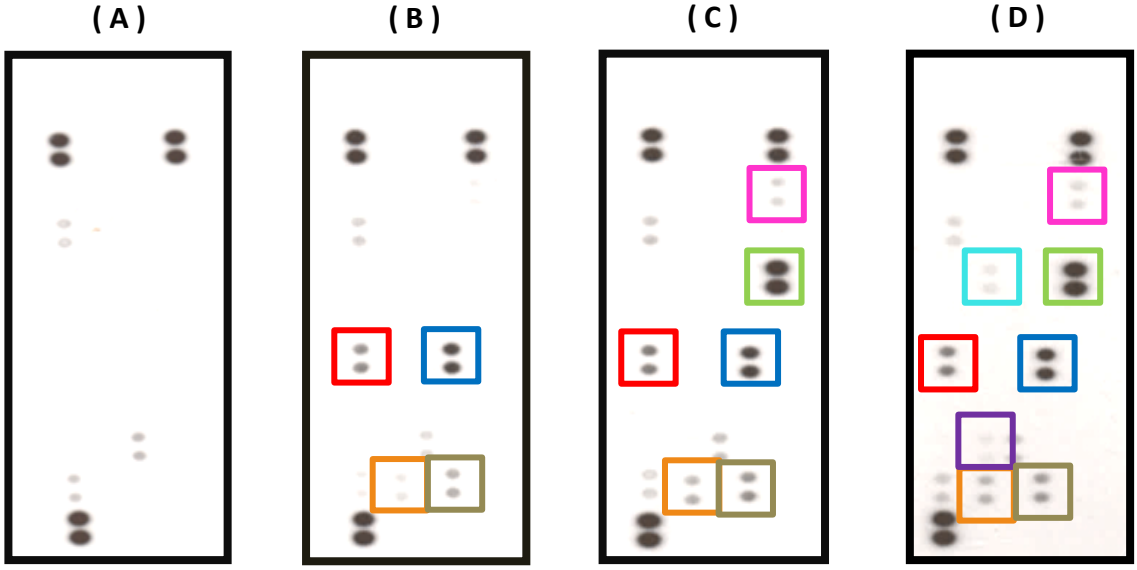

Figure 4.6 Cytokine array analysis of FaDu MCTS conditioned media at day 6 (A) Control media alone (RPMI), **(B)** conditioned media from FaDu MCTS, **(C)** conditioned media from FaDu MCTS stimulated with TNF-α, **(D)** conditioned media from FaDu MCTS stimulated with TNF-α and infiltrated with neutrophils for 5 h. Each cytokine is duplicated with the one dot directly above the other and six positive controls can be seen, two at each upper corner of the membrane and two in the lower left corner. Each colured box highlights detected chemoattractant, from top left to bottom right are: RANTES (CCL5), IL-1ra (IL-1F3), TNF- α, GRO-α (CXCL1), MIF, IL-6, IL-8 (CXCL8), SerpinE1 (PAI-1). A list of the cytokines detected by the arrays is provided in appendix II.

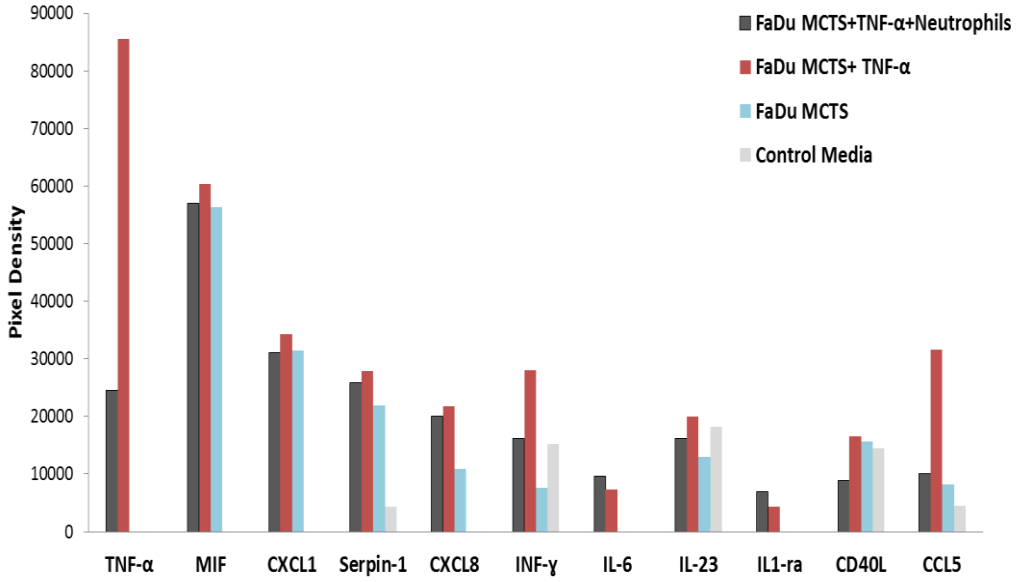

Figure 4.7 Densitometry analysis of cytokine array data showing the difference in the level of molecules in conditioned media from FaDu MCTS, conditioned media from FaDu MCTS stimulated with TNF-α, conditioned media from FaDu MCTS stimulated with TNF-α and infiltrated with neutrophils for 5 hours compared to control media alone.

Immunohistochemical analysis was then performed to confirm the presence of the most abundant cytokines detected from the cytokine array; MIF and CXCL1 in sections of FaDu MCTS. Formalin fixed paraffin-wax embedded (FFPE) sections of day 6 spheroid were stained for MIF and CXCL1 according to the methods described in section 2.2.7.4. Microscopic analysis demonstrated expression of MIF protein throughout the spheroid with slightly increased expression around the necrotic centre (Fig. 4.8). Similarly, expression of CXCL1 was observed throughout the spheroid confirming the array data (Fig. 4.8)

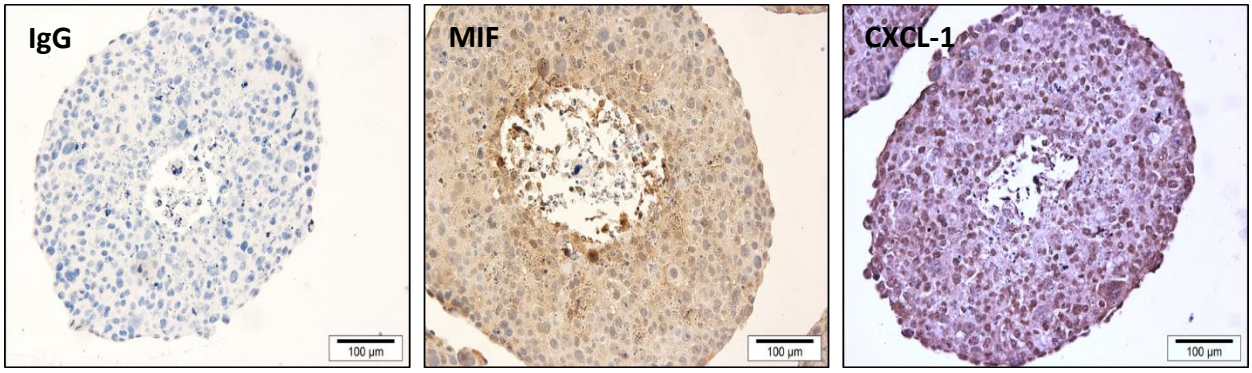

Figure 4.8 Immunohistochemical identification of MIF and CXCL1 expression in FaDu MCTS. 6µM FFPE FaDu MCTS were immunostained using IgG control, biotin-conjugated monoclonal anti-human MIF antibody or anti-human CXCL1 antibody. Scale bar = 100 µm.

4.4.5. Expression of ICAM-1 on FaDu cells

To be recruited to the tumour site, neutrophils must first leave the general circulation by extravasation up a chemoattractant gradient into tumour tissue. Once across the endothelium, neutrophils enter the tumour using the adhesion molecule ICAM-1 expressed on the epithelial cell surface and the integrin CD11a/CD18 on the neutrophil surface (Wu et al, 2001). As well as increased chemoattractants, the migration of neutrophils into MCTS may also require increased ICAM-1 expression. Therefore, the level of ICAM -1 expressed on the cell surface of FaDu cells cultured as monolayers or MCTS was tested using flow cytometry in the absence or presence of 50 ng/ml recombinant human TNF-α for 5 and 18 h. There was not a significant difference in ICAM-1 expression on the cell surface of FaDu cell monolayer after 5 h stimulation with TNF-α (median fluorescence 9.22) compared to un-stimulated controls (median fluorescence 6.3). However, the level of ICAM-1 was markedly up-regulated upon 18 h TNF-α stimulation (median fluorescence 36.85) (Fig. 4.9-A). Day 6 FaDu MCTS were disaggregated, labelled with antibodies raised against ICAM-1 or an isotype-matched IgG antibody (negative control) and then analysed by flow cytometry. After 5 h stimulation with

TNF-α, the expression level of ICAM-1 was not significantly different (median fluorescence of 62) when compared to un-stimulated FaDu MCTS (median fluorescence of 78). However, the histogram plot for 18 h TNF-α stimulated FaDu MCTS showed a significantly ($p<0.05$) high level of ICAM-1 expression (median fluorescence of 97) and the presence of another population of cells expressing low levels of ICAM-1 (Fig. 4.9-B). This could be due cells at the outer surface of the spheroid encountering high levels of TNF-α and therefore expressing high levels of ICAM-1, whilst those on the inside of spheroid may not directly experience contact with TNF-α and express low levels of ICAM-1. Taken together these data suggest that when experiencing pro-inflammatory conditions FaDu MCTS increase expression of chemokines and adhesion molecules that are likely to be the reason for the increased neutrophil infiltration.

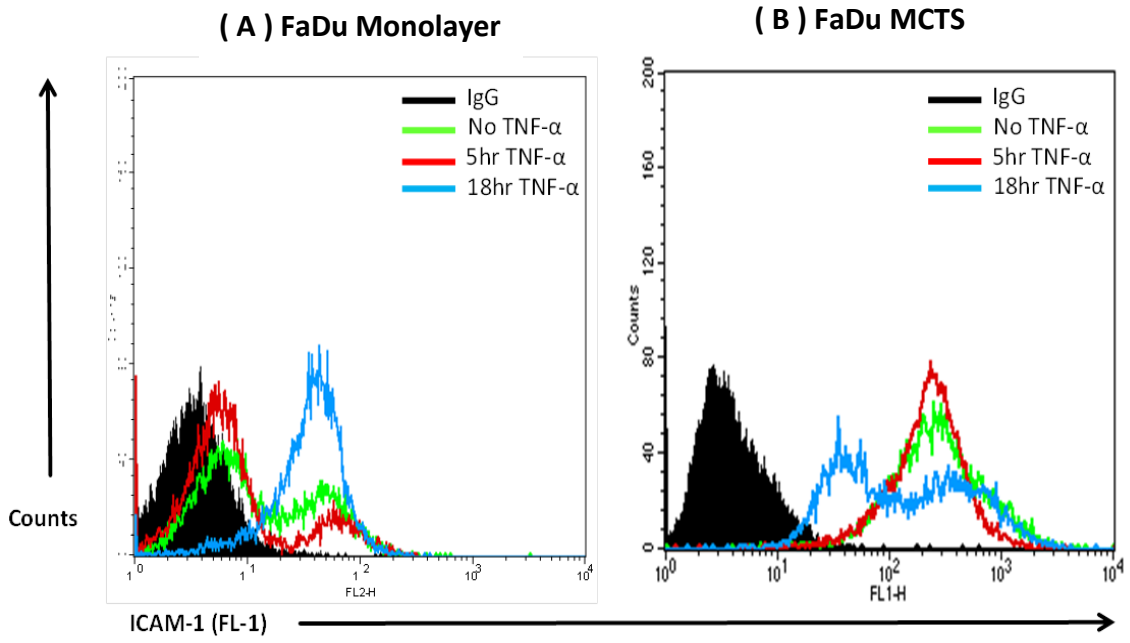

Figure 4.9 Flow cytometric analysis of ICAM-1 expression on FaDu monolayers and MCTS. Histogram overlay showing IgG negative control (black filled histogram), and ICAM-1 of un-stimulated FaDu (green), TNF-α stimulated 5 h FaDu monolayers and MCTS for 5 (red) and 18 h (blue) significantly increased the expression of ICAM-1 in FaDu monolayers (A) and FaDu MCTS (B).

The data from the cytokine array showed that FaDu MCTS express known neutrophil chemoattractants and MIF at high levels. Neutrophil migration towards recombinant forms of these proteins was performed (as described in section 2.2.4.1) to ensure their chemoattractant abilities and to test if MIF was able to act as a chemoattractant. In these experiments the bacterial-derived peptide, N-formyl-methionine-leucine-phenylalanine (fMLP) (which binds to the G-protein coupled seven-transmembrane formyl peptide receptor on neutrophils). Migration towards fMLP and CXCL8 yielded a typical bell-shaped curve with a peak of migration at 1 nM for both fMLP and CXCL8 (Fig. 4.10). Migration toward CXCL1 was dose-dependent up to 1000 nM, while migration towards CXCL5 peaked at 100 nM (Fig. 4.10). Interestingly, neutrophils migrated towards MIF with a classical bell-shaped response with peak migration at 10 nM. These data show that human neutrophils migrate towards classical neutrophil chemokines (CXCL8, CXCL1, CXCL5) as expected but also specifically migrate towards MIF.

4.4.7. Chemokine receptor expression on neutrophils form whole blood

Next the cell surface expression of chemokine receptors on neutrophils (CXCR1 and CXCR2) was examined by flow cytometry. Although MIF was first described in the mid-1960s, the first identified cell surface receptor for MIF (CD74) was only discovered in 2003 (Leng et al., 2003). However, Dumitru et al (2011) showed that neutrophils do not express CD74, suggesting that MIF acts and functions through a different receptor. Molecular and cell transfection studies have suggested that MIF may bind to CXCR2, CXCR4 and/or CD44 (Bernhagen et al., 2007). Therefore, in addition to CXCR1 and CXCR2, expression of CXCR4 and CD44 was also measured on CD14-positive monocytes (Griffin et al., 1981), CD3-positive T cells (van Dongen et al., 1987), as well as CD66b-positive neutrophils (Torsteinsdóttir et al., 1999).

Three distinct leukocyte populations were detected by flow cytometry based on size (forward scatter FSC) and granularity (side scatter SSC) from whole blood samples from healthy volunteers (Fig. 4.11). The most abundant cell population (high cell granularity, gated green, CD66b-positive) represents neutrophils, while the red CD14-positive region represents monocytes and yellow CD3-positive region represents lymphocytes. The expression of CXCR1, CXCR2, CXCR4 and CD44 in each of the three populations is represented in figure 4-12. Data were normalised to isotype control and are presented as median fluorescent intensity (Fig.4.12). As expected, the expression of CD66b was highest on neutrophils (17036), when compared to monocytes and lymphocytes (7246 and 2208, respectively). CD14 was highly expressed on monocytes (44329) in comparison to neutrophils (8009) and lymphocytes (3369). Neutrophils were found to express abundant cell surface levels of CXCR1 (30289), and slightly less but still marked amounts of CXCR2 (11157), CXCR4 (6752) and CD44 (11617). On the other hand, monocytes were found to express high levels of CD44 (39834) and abundant CXCR4 (11985), followed by CXCR2 (9443) with lower expression of CXCR1 (3215). CD3-

positive T cells expressed low levels of CXCR1 (2793) but moderate levels of both CXCR2 and CXCR4 (3673 and 4871 respectively) as well as high levels of CD44 (33077). These data show that neutrophils (and monocytes) express receptors for not only classical neutrophil chemokine but also MIF and these data provide an explanation as to why MIF caused neutrophil chemotaxis *in vitro* previously.

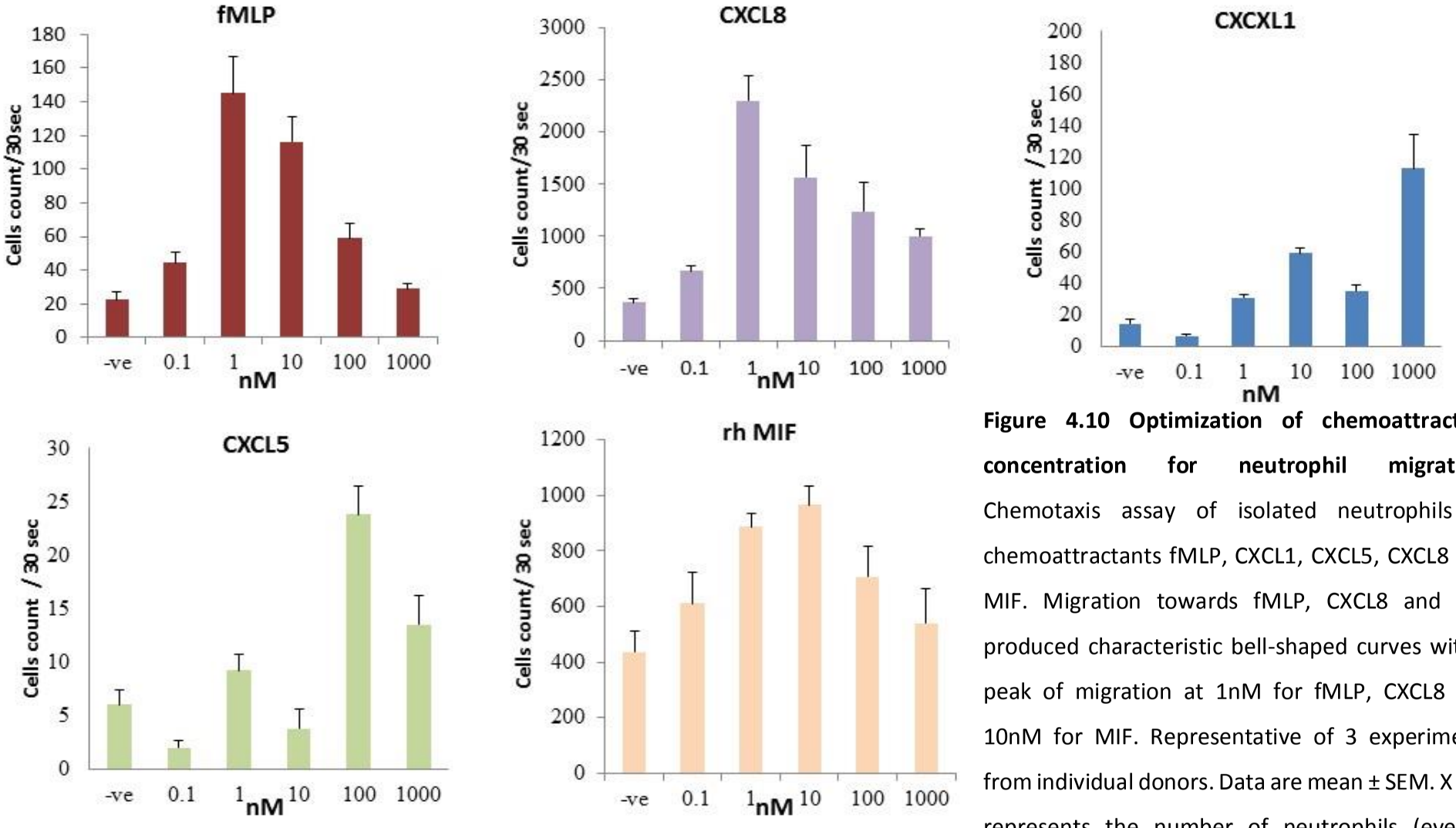

Figure 4.10 Optimization of chemoattractant concentration for neutrophil migration. Chemotaxis assay of isolated neutrophils to chemoattractants fMLP, CXCL1, CXCL5, CXCL8 and MIF. Migration towards fMLP, CXCL8 and MIF produced characteristic bell-shaped curves with a peak of migration at 1nM for fMLP, CXCL8 and 10nM for MIF. Representative of 3 experiments from individual donors. Data are mean ± SEM. X axis represents the number of neutrophils (events) counted in 30 seconds by the flow cytometer. rh=

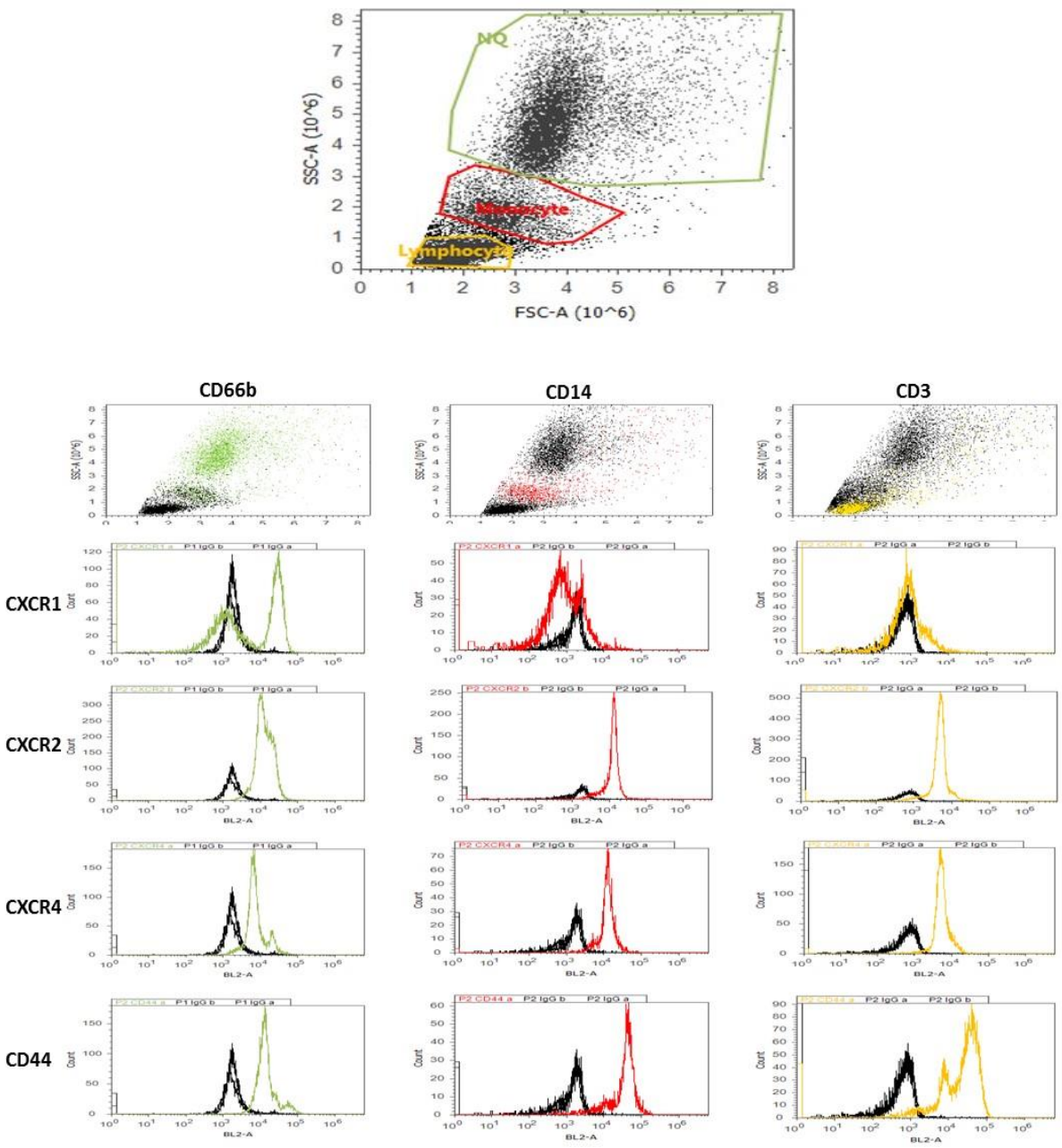

Figure 4.11 Flow cytometric analysis of receptor expression on human whole blood leukocyte. Dot plots show three populations (neutrophils, monocytes, lymphocytes) based on forward scatter (FSC) and side scatter (SSC) for size and granularity respectively from whole blood sample stained as describe in 2.2.9.5. CD66b/Neutrophils, CD14/Monocyte, CD3/T-Lymphocyte were used as specific cell markers for gating and histograms of CXCR1, CXCR2, CXCR4, CD44 surface expression for each of the three were compared to isotype control (black line).

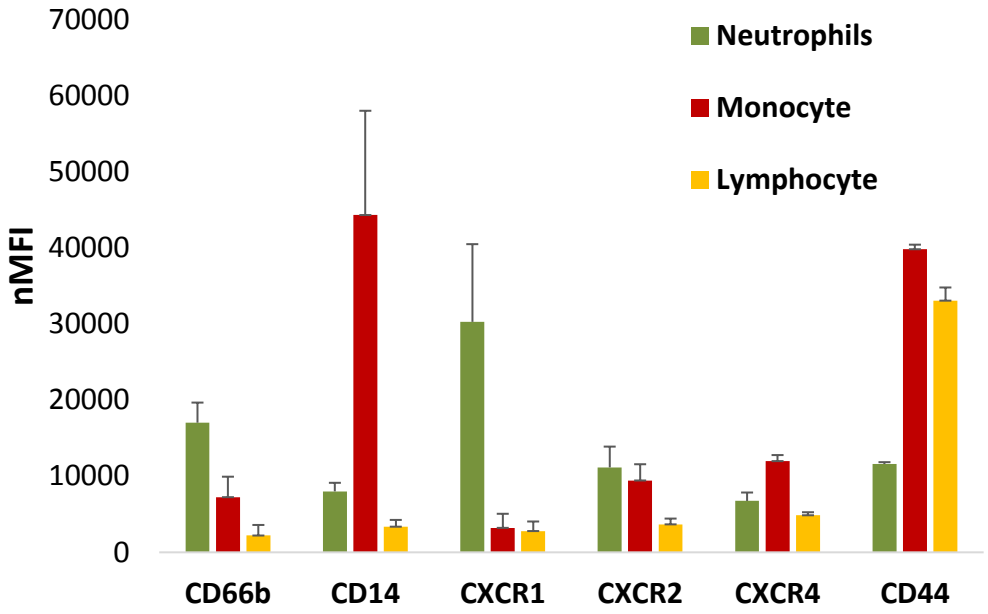

Figure 4.12 Expression of cell surface receptors on whole blood leukocyte populations by flow cytometry. Bar chart summarising the expression of CD66b, CD14 CXCR1, CXCR2, CXCR4 and CD44 on neutrophils, monocytes and T lymphocytes. Data are normalised median fluorescence intensity (nMFI) ± SEM and are representative of 3 patient samples (n=3).

4.4.8. MIF is expressed at higher levels by FaDu MCTS than monolayer cultures

Previous cytokine array densitometry and IHC data showed that MIF is highly expressed by FaDu MCTS but these methods are not fully quantitative. Therefore, MIF levels were assessed in conditioned medium from 2D and 3D FaDu culture by ELISA. FaDu were seeded at 1×10^6cell/ml into T25 flask and allowed to adhere for overnight, then un-attached cell were removed and replaced media with serum free media and incubated for 24hours before collecting the CM for analysis. FaDu MCTS CM were generated as previously describe at 2.2.3.2 and collected after 24hours incubation. Strikingly, ELISA analysis revealed that levels of MIF was significantly ($p<0.0001$) elevated when FaDu were cultured as MCTS compared to 2D monolayer cultures (576 pg/ml to 89 pg/ml). A slight but not significant increase in expression of MIF was detected upon TNF-α-stimulation (637pg/ml) and MCTS infiltration with neutrophils (716pg/ml). Neutrophils secrete very low levels of MIF (56pg/ml) (Fig. 4.13-B).

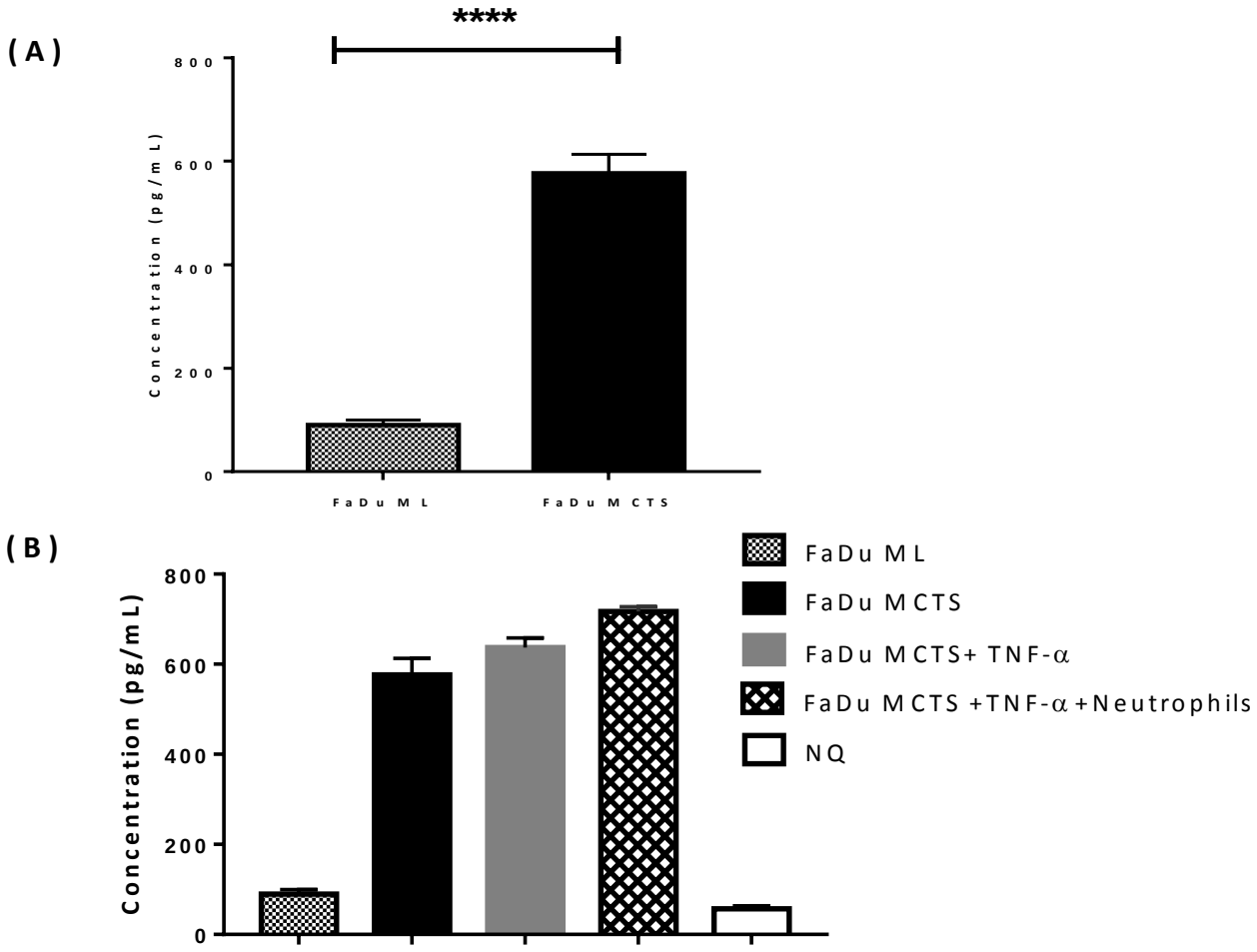

Figure 4.13 Quantitative measurement of MIF from conditioned media collected from FaDu cultured as monolayers or MCTS. (A) t test was used to compare the statistical significance of MIF protein level in serum free CM collected from FaDu grown in monolayer and Day 6 FaDu MCTS showed a significant increase in level of MIF protein ($p<0.0001$) in MCTS model **(B)** Stimulation with TNF-α or co-culture with neutrophils dose not stimulate the production of MIF from MCTS, while CM collected from NQ detected very low amounts of MIF release into media

4.4.9. MIF mRNA level in a panel of HNSCC cell line

Thus far, this study has focussed on the FaDu cell line. However, to ascertain whether the MIF high expression observed in the FaDu ELISA data is a global head and neck cancer cell response, a panel of normal oral keratinocyte (NOK) and different types of HNSCC (tongue, HPV-, HPV+) were screened for gene expression of MIF. All the cells used in this analysis were cultured as monolayers as not all cell types can form MCTS. Quantitative PCR demonstrated that although MIF expression was observed in NOK, MIF overexpression was detected in a panel of HNSCC. Of note, the expression level of MIF differed between the tested cell lines, with the highest level detected in SCC89 (3), SSC72 (2.2), T5 (1.8), SCC2 (1.7), SCC4 (1.4) with fold increases compared to NOK. Surprisingly, the mRNA level of MIF detected from FaDu (0.9), SCC90 (0.7) and H357 (0.45) was low and almost the same as NOK (Fig. 4.14-A) showing that other cancer cells lines express more MIF than FaDu and that high MIF expression is a widespread response. HPV-negative cells generally displayed higher MIF expression levels than HPV-positive cells (Fig. 4.14-B) and expression in tongue cancer cells was varied with 2 out of 3 cell lines showing high expression.

4.4.10. Hypoxia upregulates the expression of MIF in vitro

The data provided previously shows that MIF mRNA is highly expressed by HNSCC. In addition, IHC studies showed higher MIF expression around the necrotic centre of the MCTS and the results in Chapter 3 show that neutrophils are more abundant in the hypoxic/necrotic centres of tumours. Taken together these data suggest that expression of MIF may be regulated by hypoxia. Indeed, increased expression of MIF in response to hypoxia has been demonstrated in other cancers (Larsen et al., 2008). Therefore, a panel of HNSCC cells were subjected to low oxygen concentration (0.5% O_2) and gene expression of MIF analysed by qPCR. VEGF, a cytokine known to be upregulated by hypoxia, was used as a positive control and β2 microglobulin (B2M) was selected as a housekeeping gene for normalisation of gene expression as this gene has been found to be unaffected by hypoxia (Baddela et al., 2014). The gene expression for MIF mRNA was generally up-regulated in cancer cells subjected to hypoxia when compared to cells cultured in normoxic conditions, but no significant affect was observed in normal OK or immortalize NOK. In contrast, a significant increase of MIF mRNA expression was observed in H357 (P=0.0147) SCC2 (P= 0.0228) in compare to normoxic condition. Even more upregulation of MIF was observed in SCC4, SCC72 and SCC90 (P <0.0001) by hypoxia, while no significant difference was detected in FaDu (Fig. 4.15-A). Hypoxia is the main regulator of VEGF production in many cells (Buchler et al., 2003) and this was the case for all head and neck cells tested in the panel. As expected, the upregulation of mRNA for VEGF was detected in most of cancer cells, except H357, when culture under low oxygen tension. Highest level of hypoxic-induced VEGF detected in SCC4, SCC90 (P <0.0001), T5 (P= 0.0140) FaDu (P=0.0045), SCC72 (P=0.0216), SCC89 (P=0.0061) and SCC2 (P= 0.0054) compared to cells cultured under normoxic conditions. Unlike MIF, the levels of VEGF detected from FaDu cells cultured under hypoxic conditions was significantly increase (Fig.

4.15-B), suggesting that MIF upregulation in FaDu may not be as responsive to hypoxia as other cancer cells.

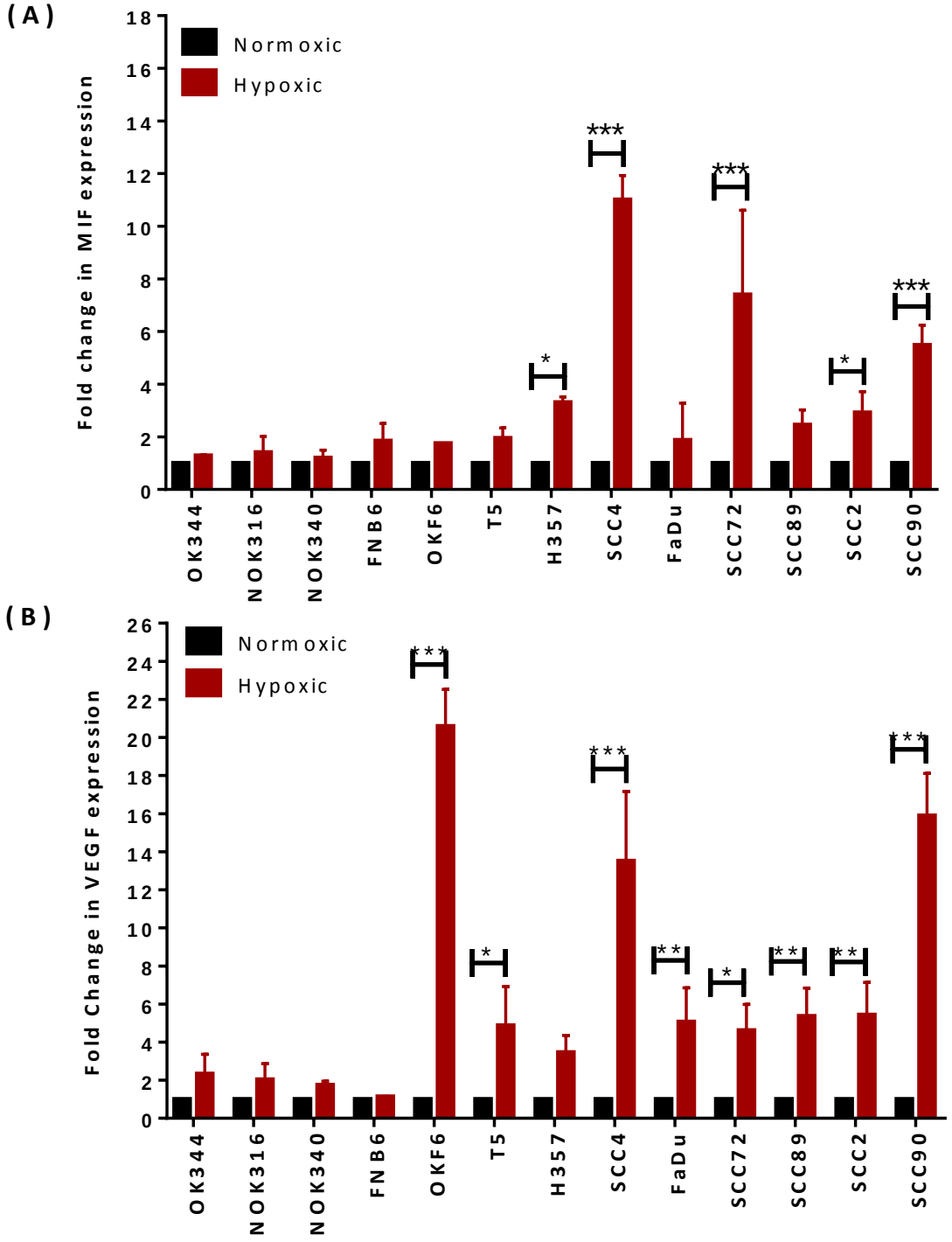

Figure 4.15 Effect of hypoxia on expression of MIF on a panel of HNSCC. Cells were subjected to hypoxic (0.5% O_2) or normoxic conditions (21% O_2) overnight. The gene expression change in each of the tested cell were compared to normoxic cultured cells and expressed as fold change in gene expression. Multiple comparison using two-way ANOVA test was used to calculate the significant differences. Data are mean ± SEM from three independent experiments. * P<0.05, ** P<0.005, ***P<0.0001

4.4.11. FaDu cells secrete more chemoattractants when cultured under hypoxic conditions.

Results from the cytokine array showed that FaDu cells produce classical neutrophil chemokines (CXCL1 and CXCL8) and MIF. Moreover, MIF gene expression is increased by hypoxia and more neutrophils were observed in hypoxic/necrotic areas of HNSCC tumours. Therefore, it was reasoned that hypoxic HNSCC cells would produce more chemotactic factors and so have increased neutrophil chemotactic capacity. This was assessed by measuring the migration of freshly isolated human neutrophils towards serum-free conditioned medium generated from FaDu monolayers cultured under normoxic or hypoxic conditions for 24 h. The results shown in figure 4.16 indicate that conditioned medium from FaDu cultured in normoxic conditioned is chemotactic for neutrophils. However, a significant increase in level of neutrophil migration was observed with the conditioned medium from FaDu cultured under hypoxic conditions (0.5% O_2), showing approximately 2.6 fold increase in neutrophil chemotaxis.

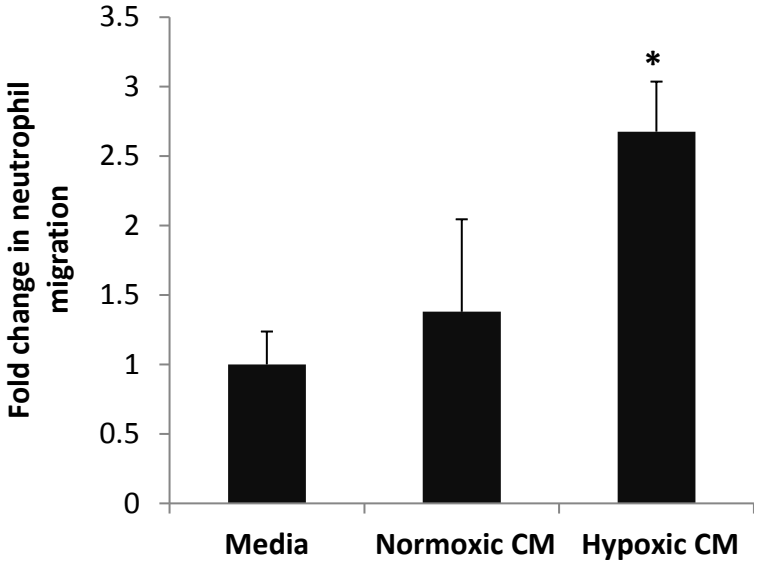

Figure 4.16 Migration of neutrophils toward FaDu condition media. Flow cytometric analysis of neutrophils migrated towards FaDu conditioned medium collected under normoxic (21% O_2) or hypoxic (0.5% O_2) conditions. The data is expressed as fold change in neutrophil migration compared to control media. One –way ANOVA show significant (*$p<0.05$) increase in migration towards hypoxic condition media was observed compared to normoxic conditioned medium or medium alone. Data are mean ± SD, n=3 independent experiments.

4.4.12. MIF protein level of in HNSCC tissue sections

The data presented in this chapter so far has focussed on expression of MIF by HNSCC cell lines, in particular FaDu cells. To examine whether MIF over-expression occurs in HNSCC cancer, a screen of MIF expression in human HNSCC cancer tissue specimens was conducted by immunohistochemically analysis and compared to expression in healthy oral mucosa. The intensity of MIF stain was evaluated using a semi-quantitative quick scoring method (described in section 2.2.7.5). Low expression of MIF was detected in the basal layer of the stratified squamous epithelium in normal tissue (Fig. 4.17- A & B). The staining intensity was significantly ($p<0.05$) increased in HNSCC epithelium, with abundant expression predominantly localized at the surface of tumour (Fig. 4.17- C & D). In some of the cases

expression of MIF was variable between surface and deeper SCC although statistical analysis showed that that there were no significant differences.

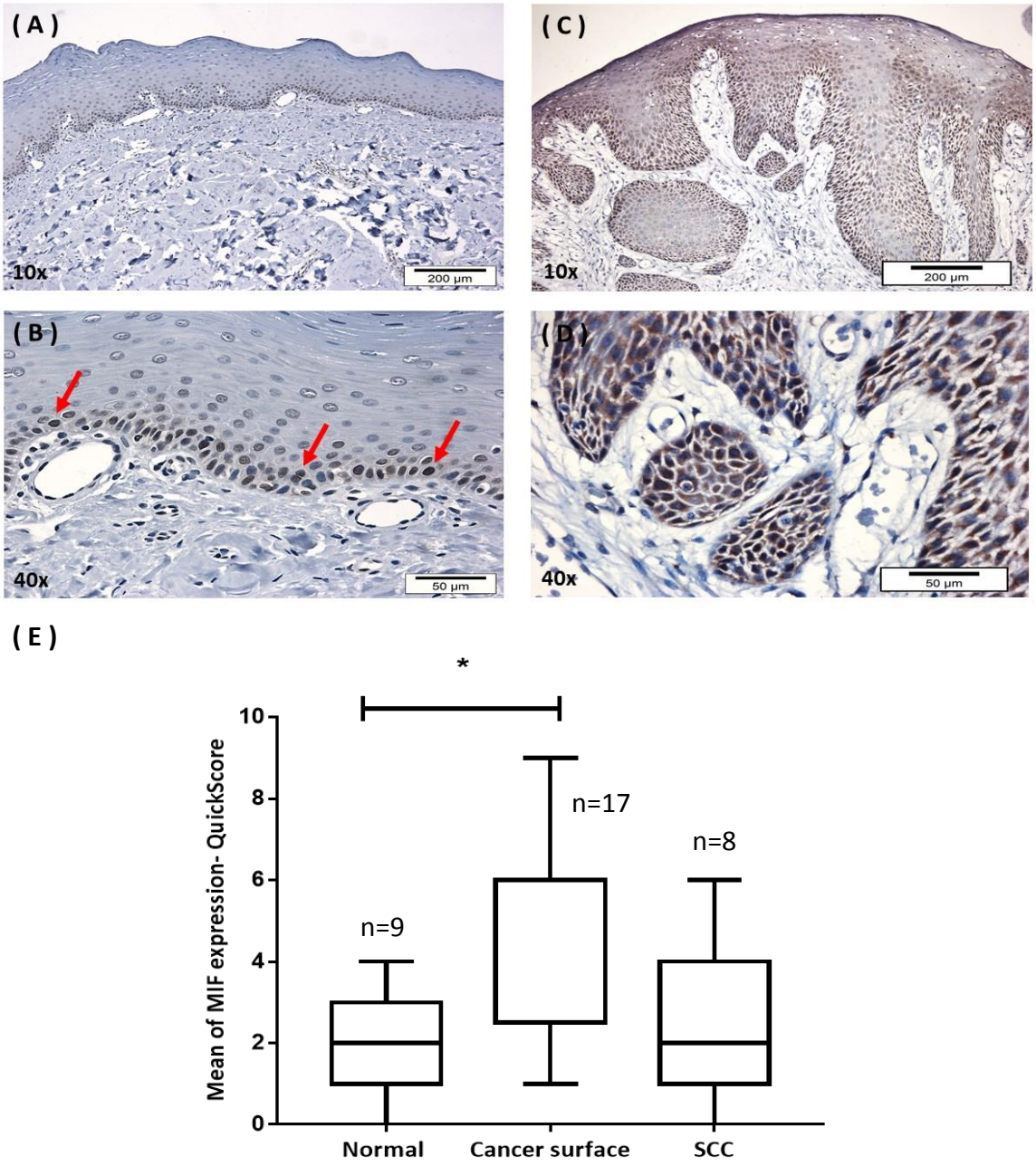

Figure 4.17 MIF protein expression in a cohort of HNSCC tissue biopsies. Paraffin-embedded samples from normal and HNSCC were stained with anti-MIF antibody and stain intensity evaluated using a quick-score method. Normal tissue displayed low expression of MIF in the basal layer (**A** and **B**), while in HNSCC epithelium the level of MIF protein was found to be significantly higher in surface epithelium (**C** and **D**) and moderate to low expression was detected in the deeper cancer cells (SCC). One-way ANOVA test was used to compare the statistical significance of the scores of normal and cancer tissue (E). The number of cases in each category is shown in E.

4.4.13. Effect of MIF small molecules inhibitor ISO-1 on viability of FaDu

Neutrophils migrate toward the conditioned medium from FaDu and recombinant chemoattractants in Boyden chamber chemotaxis assays. In addition, it was found that FaDu MCTS secrete chemoattractants and recruit neutrophils but it is not known which chemoattractants or neutrophil receptors are the most important in this process. One way to determine this is to block chemoattractant receptors expressed by neutrophils or inhibit chemoattractant activity. Small molecule inhibitors of CXCR2 (AZ-767, SB265610) and CXCR4 (AMD3100) are well-characterised in terms of toxicity and potency (Tazzyman et al., 2011), whereas the toxicity of (S,R)-3-(4-hydroxyphenyl)-4,5-dihydro-5-isoxasole acetic acid methyl ester (ISO-1), a specific MIF inhibitor, have not previously been determined. The cytotoxic effect of ISO-1 on FaDu cells was assessed using MTT viability assay and compared to vehicle control (DMSO). The concentration of ISO-1 that was toxic to 50% FaDu cells (IC_{50}=250 µM) was calculated, by plotting the percentage of viable cells against log (concentration, µM) of ISO-1. Among the tested concentrations, 500 and 100 µM were found to be the most cytotoxic concentration at 24, 48, and particularly 72 h compared to the DMSO control (Fig. 4.18). Therefore, a treatment of 50 µM and was selected for the infiltration experiment as it did not show toxicity to cells at 24, 48, 72 hours.

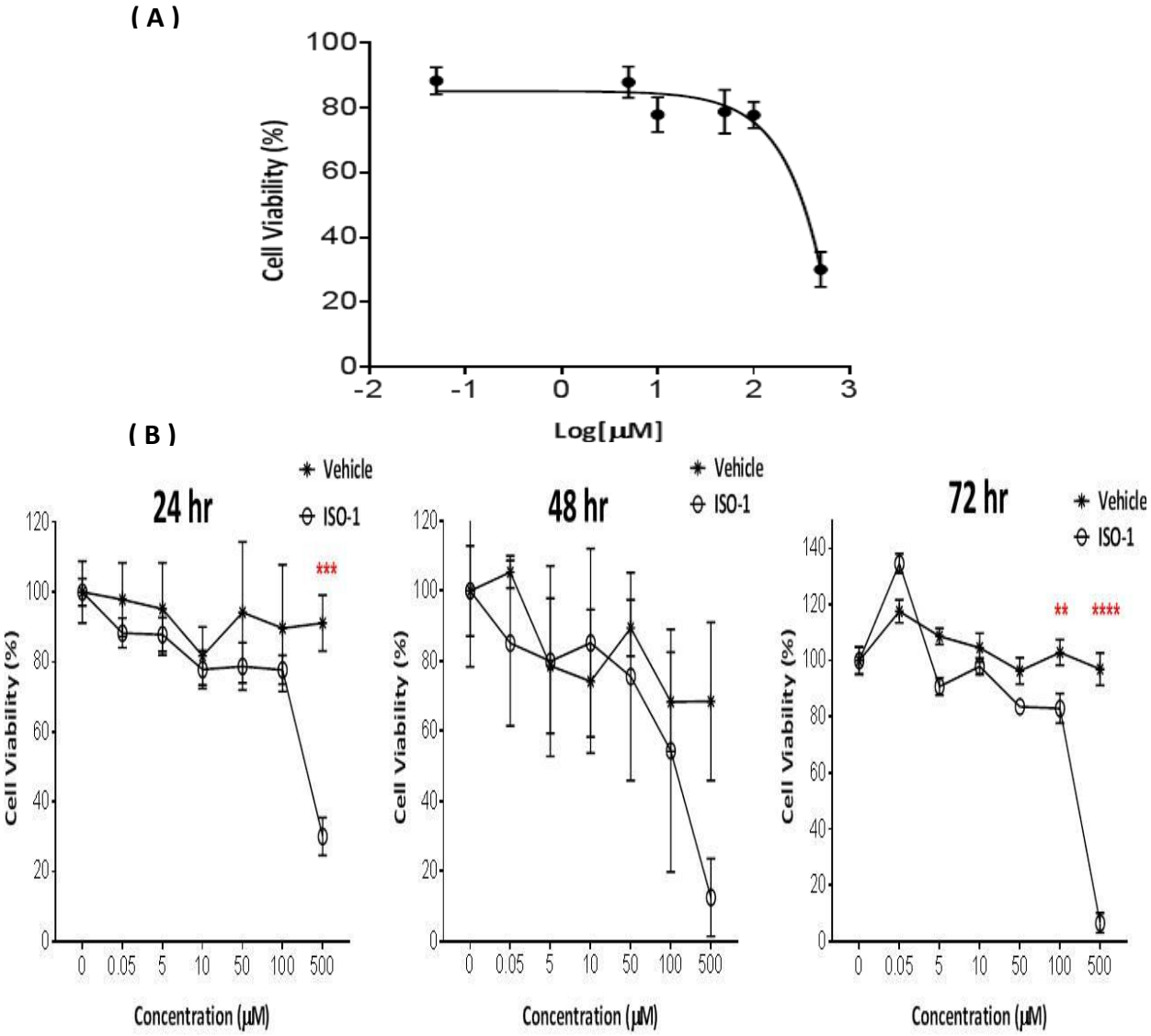

Figure 4.18 Assessment of cell viability of FaDu in response exposure to increasing concentrations of ISO-1. FaDu monolayer were treated with ISO-1 (0.05, 0.5, 5, 50, 500 or 5000 µM) or it vehicle control DMSO for 24 h. **(A)** The IC_{50} of ISO-1 on FaDu was calculated by plotting the percentage of viable cells against log (µM) after 24hr ISO-1 treatment. Data are representative of 3 independent experiments. **(B)** ISO-1 was observed to be cytotoxic at higher concentrations at 24, 48 and 72 h. Data are mean ± SEM, n = 3. ** P<0.005, ***P<0.0001

4.4.14. Effect of ISO-1 on neutrophil viability and apoptosis

To determine whether ISO-1 was cytotoxic to neutrophils, freshly isolated neutrophils were treated with increasing concentrations of ISO-1 or DMSO for 24 h. The cells were then analysed for markers of apoptosis and necrosis using Annexin-V and propidium iodide (PI) by flow cytometric analysis (described in section 2.2.9.6). After 24 h 75.1% of untreated neutrophils were viable, less than 20% undergo natural apoptosis and 6.3% of the cell population was necrotic. The use of 5000 μM ISO-1 was very cytotoxic and ISO-1 treated cells displayed 73% necrosis, 11% apoptosis and only 14% viability. However, similar findings were observed with the DMSO vehicle control where 87% of cells were necrotic, 7% apoptotic and only 1% viable cells were detected, suggesting that the high concentration of vehicle could be responsible for the loss of viability. Treatment with 500 μM ISO-1 had negligible effect on necrosis (5%) but induced around 25% of apoptosis in cells with 68% of cells being viable. Use of drug concentrations ranging between (0.05 to 50 μM) had little effect on neutrophils, with almost 70% of cells being viable, approximately 25% apoptotic (not significantly different from untreated cells) and less than 5% of population was necrotic (Fig. 4.19). These data showed that use of ISO-1 at 50 μM is not significantly toxic and so was used in future experiments.

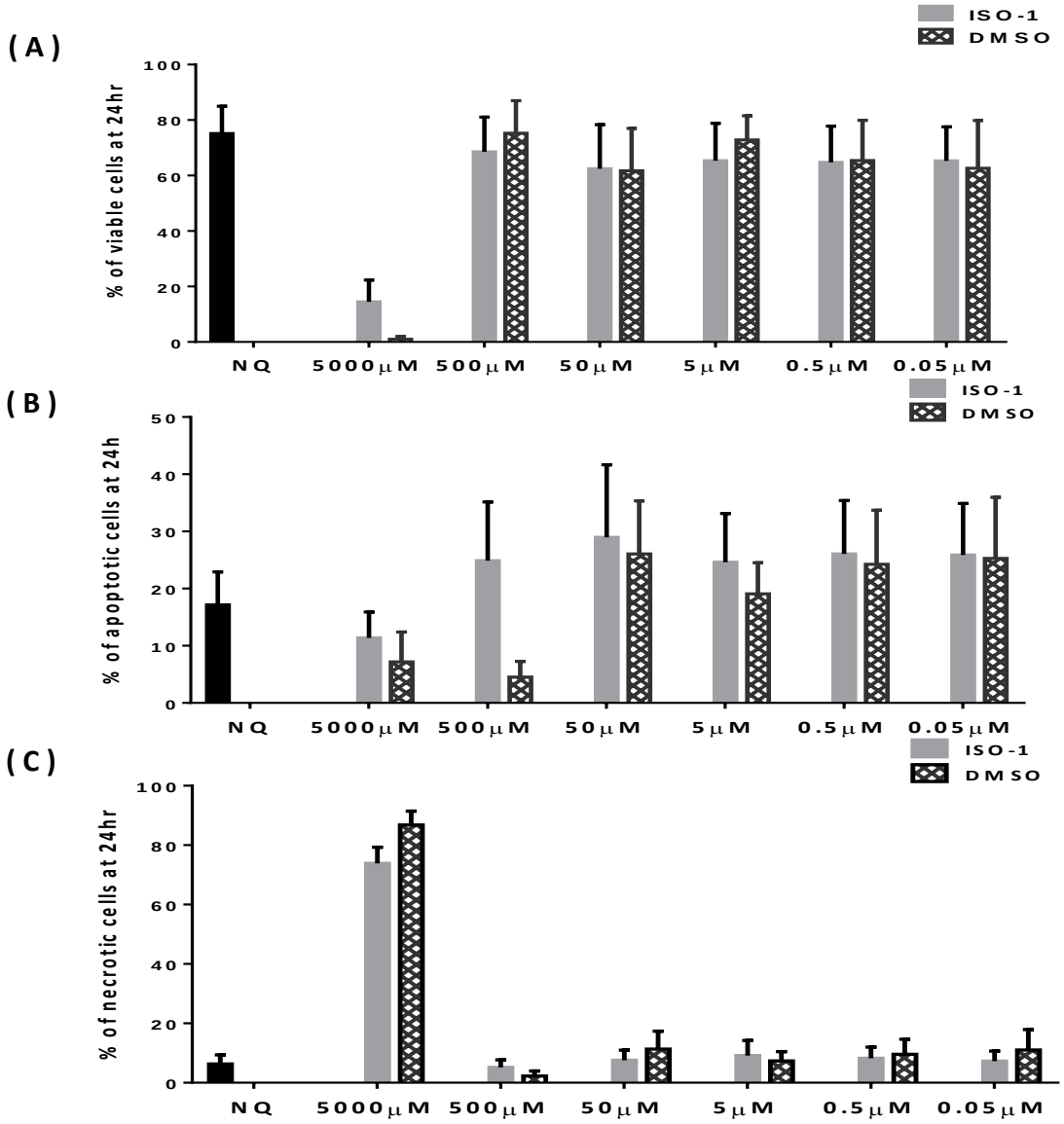

Figure 4.19 Flow cytometric analysis of apoptosis and necrosis induced in neutrophils by exposure to increasing concentrations of ISO-1. Freshly isolated neutrophils were treated with ISO-1 (0.05, 0.5, 5, 50, 500 or 5000 μM) or it vehicle control DMSO for 24 hours. Cells were stained with Annexin V-FITC and PI to determine the level of viability **(A)**, apoptosis **(B)** and necrosis **(C)**. Data are representative of 3 pooled experiments from individual donors. Data are mean ± SEM.

4.4.15. Infiltration of neutrophils into FaDu MCTS is blocked using specific inhibitors.

Small molecule inhibitors for CXCR2 (AZ767 and SB265610), CXCR4 (AMD3100) and MIF (ISO-1) were used to determine the importance of these molecules in directing neutrophil migration into FaDu MCTS. Neutrophils from healthy volunteers were pre-incubated with saturating concentrations of AZ767 25nM, (Tazzyman et al., 2011), SB265610 100nM, (Bradley et al., 2009) or 500ng/ml AMD3100 (Bot et al., 2014) for 1 h to block their respective receptors, or FaDu MCTS cultures were incubated with 50 µM ISO-1 for 1 h. DMSO was used as a vehicle control. Untreated FaDu spheroids were then incubated with receptor-blocked neutrophils for 5 h, whilst ISO-1 treated FaDu were incubated with untreated neutrophils for 5 h. Flow cytometric analysis of disaggregated FaDu MCTS was carried out as described in section 2.2.4.3 to determine the number of infiltrated neutrophils in treated and control MCTS. Neutrophil infiltration into the vehicle control group was an average 19%, whereas in the AMD3100 (CXCR4 antagonist)-treated group, neutrophil infiltration was significantly reduced to an average 6% infiltration. Treatment with either CXCR2 antagonist (AZ-767 and SB265610) caused a significant reduction in neutrophil infiltration up to approximately 5%. Moreover, inhibition of neutrophil infiltration using the MIF specific inhibitor (ISO-1) was most pronounced at 2.5% (Fig. 4.20).

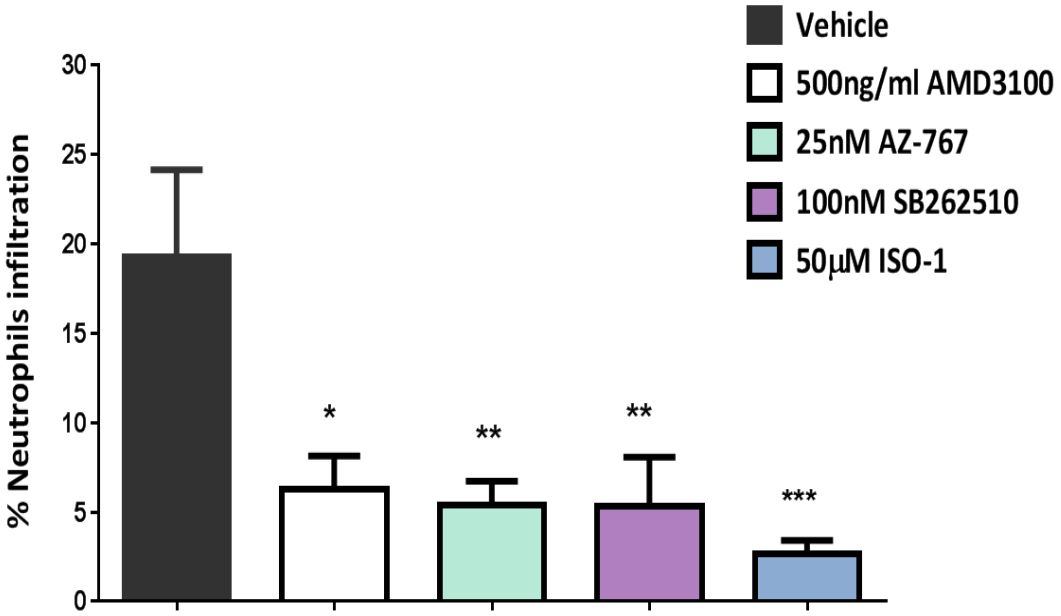

Figure 4.20 Flow cytometric analysis of neutrophil infiltration into FaDu MCTS. Neutrophils pre-incubated with CXCR2 antagonist (AZ-10397767 or SB-265610) CXCR4 antagonist (AMD3100) and the MIF inhibitor (ISO-1) reduced neutrophil migration into FaDu MCTS compared to vehicle control. One-way ANOVA test was used to compare the statistical significance of neutrophils infiltration (*P<0.05, **0.01, ***0.001). Data is pooled from six individual experiments as mean % of Infiltration ± SEM.

4.4.16. Infiltration of THP-1 monocytes into FaDu MCTS is blocked using specific inhibitors.

Previous data showed that human monocytes also express receptors for CXCR2 and CXCR4. Moreover, increased numbers of macrophages have been reported in HNSCC with numbers correlating to poor prognosis (Fujii et al., 2012). It was therefore interesting to determine if blocking these receptors or ISO-1 would inhibit recruitment of monocytes into FaDu HNSCC. The human monocytic cell line, THP-1 (Qin, 2012), is the most used cell line to study monocytes and macrophages. THP-1 cells are positive for CXCR4 (Schols et al., 1997) and CXCR2 (Vogiatzi et al., 2013) and so were used in this study using the same protocol as described previously for neutrophils. Untreated THP-1 infiltration into FaDu MCTS at this time period was slightly lower than for neutrophils at 13%. THP-1 infiltration was significantly inhibited using the CXCR4 antagonist AMD3100 (5.5%). Surprisingly, the use of the CXCR2 antagonist, AZ-767 showed no significant inhibition of THP-1 infiltration, whereas SB265610 showed a small but significant reduction in infiltration (8%). Interestingly, the use of ISO-1 showed the greatest reduction on THP-1 infiltration to just 3% (Fig. 4.21).

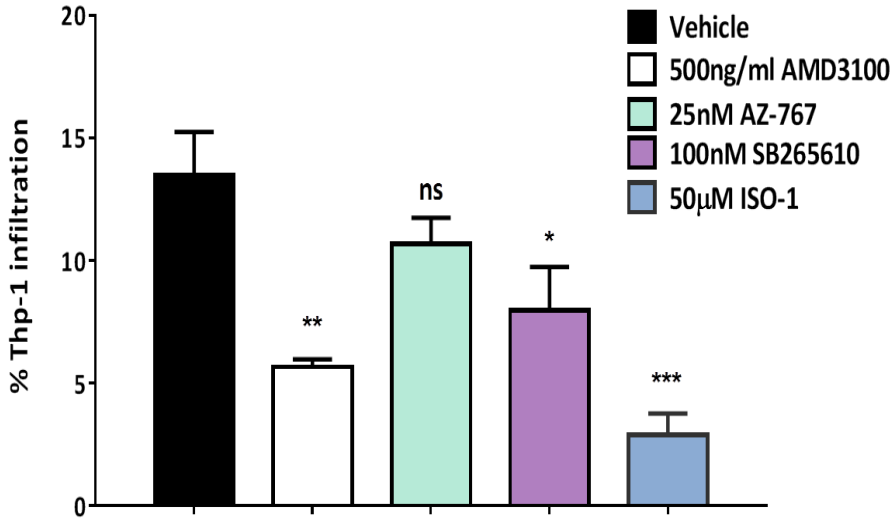

Figure 4.21 Flow cytometric analysis of THP-1 monocyte infiltration into FaDu MCTS. THP-1 cells were pre-incubated with CXCR2 antagonist (AZ-10397767 or SB-265610), CXCR4 antagonist (AMD3100) or FaDu MCTS treated with the MIF inhibitor (ISO-1). One-way ANOVA test was used to compare the statistical significance, showed CXCR4 and ISO-1 significantly reduced monocyte migration into FaDu MCTS compared to vehicle control (*P<0.05, **0.01, ***0.001). Data pooled from three individual experiments as mean % of Infiltration ± SEM.

4.4. Discussion

FaDu MCTS formation was generated using the liquid overlay method as previously described (Carlsson and Yuhas, 1984). The use of MTCS gives advantages over monolayer culture as it is more close to the *in vivo* situation. The multi-cellular, 3D MCTS structures enable MCTS to replicate various micro-environmental aspects, such as the oxygen diffusion, glucose, lactate and pH gradients, and the distribution of proliferation/quiescent cells within the spheroid (Sutherland and Durand, 1984). When tumour MCTS grow larger than 500 µm in diameter, they are frequently characterized by hypoxic regions and necrotic centres, therefore they resemble avascular tumour *in vivo* (Hirschhaeuser et al., 2010). The presence of hypoxia around a necrotic area observed in the MCTS was similar to that observed in HNSCC tissue section. This is due to failure of oxygen and nutrition delivery beyond the distance of 100-150µm (Thomlinson and Gray, 1955).

Although the use of MCTS in cancer research is widespread there has been little use of these models in studies of HNSCC. MCTS co-culture approaches have been utilised in the field of oral cancer to investigate the tumour micro-environment or in tumour therapy related work. For example, the formation of tumour (UM-SCC 14C)/fibroblast mixed MCTS were utilised to study the effect of anti-EGFR mAb on leukocyte migration towards HNSCC (Hoffmann et al., 2009). Hirschhaeuser et al, (2009) used FaDu MCTS to test the mode of action and effectiveness of catumaxomab *in vitro*. In comparison to the results presented here, the FaDu MCTS used in their study grew slower, even though they were plated at the same seeding density. In this study data generated from growth curves show that after 24 h FaDu cells aggregated together and formed a spheroid with average size of 694 µm and these continued to grow to reach approximately 1413 µm by day 13 (Hirschhaeuser et al., 2009). Whereas, Hirschhaeuser (2009) FaDu spheroids formed after 2 to 4 days, and these reached a diameter

of about 900 µm after a week of incubation and then slightly decreased in size but stayed over 400 µm the size of the day 0 MCTS. These differences may be due to the culture medium, supplements or culture conditions used. The FaDu used in this study were verified using STR analysis to rule out cell line contamination. The data provided in this chapter clearly show that FaDu MCTS display many of the micro-environmental features on an *in vivo* HNSCC tumour are good in vitro models to represent these cancers. FaDu MCTS have also been used to develop a model of oral cancer in order to facilitate the study of cancer invasion using human organotypic models (Colley et al., 2011).

It has been reported that tumour cells are able to recruit and modulate the function of neutrophils by a variety of inflammatory mediators and cytokines. For example, the expression of CXCL8, a potent neutrophil chemoattractant, was found to be increased in various tumour cells (De Larco et al., 2001). Cytokine analysis of FaDu secreted products revealed high levels of the classic neutrophil chemokines CXCL8, CXCL1 as well as CCL5 and MIF in the medium from FaDu MCTS. In addition, a small amount of CXCL6 was released from FaDu MCTS but only after stimulation with TNF-α. In two separate studies by the same group, the serum concentration of CXCL8 was found to be higher in the peripheral blood of HNSCC patients than in that of a control group and the use of neutralizing CXCL8 antibodies reduced the migration neutrophil towards FaDu conditioned medium *in vitro*. This finding was supported by a subsequent screening array of FaDu conditioned media which showed that CXCL8, CXCL6 and MIF were the most abundant cytokines released by these cells (Trellakis et al., 2011a, Dumitru et al., 2011); data that are concordant with those of this study. High levels of MIF have also been detected in HNSCC patients (Kindt et al., 2013a, Kindt et al., 2013b). These data suggest that the MCTS models are replicating those *in vivo* by secreting

chemotactic factors into the culture medium as *in vivo* tumours secrete these factors into the circulation. Data in chapter 3 show high numbers of neutrophils in biopsies of HNSCC and so the FaDu MCTS model was used to investigate neutrophil recruitment into tumours.

Neutrophil infiltration into FaDu MCTS peaked at 5 hours when pre-incubated with TNF-α, with similar levels of infiltration induced after 2 hours following pre-incubation with TNF-α for 18 h. In contrast, co-cultured FaDu MCTS with neutrophils for 24 h caused a decline in their infiltration. The likely reason for this reduction is possibly due to the limited neutrophil life-span, as many studies have reported that neutrophils do not exceed 16-24 hours *ex- vitro* before undergoing apoptosis (Dancey et al., 1976).

Neutrophil infiltration into FaDu spheroids is most likely to be chemokine and adhesion molecule-dependent, as the infiltration of neutrophils into un-stimulated spheroids was limited. FaDu MCTS were pre-treated with TNF-α because the tumour micro-environment is known to be pro-inflammatory. For instance, many studies have reported elevated levels of TNF-α in various tumours, including pancreatic (Schmiegel et al., 1993), renal cancer (Al-Lamki et al., 2010) and HNC (Soylu et al., 1994). In lung adenocarcinoma, TNF-α was able to induce expression of ICAM-1 on tumour cells in vitro and in vivo facilitating leukocyte adhesion and migration (Huang et al., 2004). When FaDu MCTS were pre-treated with TNF-α neutrophil recruitment increased several fold in a time dependent manner and this was associated with the respective increased levels of chemokines and ICAM-1 expression. ICAM-1 is an essential adhesion molecule that allows neutrophils to bind to epithelial cells (Dustin et al., 1989). It is likely that addition of TNF-α not only increases the secretion of neutrophil chemokines but also increases expression of ICAM-1 leading to increased infiltration compared to un-treated MCTS. The importance of ICAM-1 in neutrophil recruitment could

have been verified using siRNA or blocking antibodies to ICAM-1 although this was not performed in this thesis. One element missing in this tumour MCTS assay when compared to *in vivo* neutrophil recruitment into inflamed tissue or a tumour mass is the binding of neutrophils to the endothelium lining the blood vessels during the extravasation. These interactions induce activation of signalling pathway leading to alteration in integrin expression, phagocytosis and release of granule content (Zarbock and Ley, 2008). The generation of more complex assays using neutrophils delivered under flow to the endothelium with MCTS placed below the epithelium have been created (Muthana et al., 2015) but these were considered too complex for this study.

Neutrophil recruitment into tumours appears to be dependent on chemokines that bind to CXCR1 and CXCR2 expressed by neutrophils. CXCR1 binds CXCL6 and CXCL8 with high affinity but binds CXCL1-3, CXCL5 with only low affinity. On the other hand, CXCR2 binds CXCL1-3, CXCL5, CXCL6 and CXCL8 all with high affinity (Lee et al., 1992, Ahuja and Murphy, 1996a). In contrast to the role of CXCL8, CXCL1 and CXCL6 in neutrophil recruitment, little is known about MIF-induced neutrophil recruitment. MIF was originally identified as a regulator for macrophage migration *in vitro* (David, 1966). However, many studies have reported expression in different human tumours, such as breast (Larsen et al., 2008), liver (Hira et al., 2005), colorectal (Legendre et al., 0000) prostate (Meyer-Siegler et al., 2005), melanoma (Shimizu et al., 1999), oesophageal and recently increase level of MIF was detected in HNSCC patients and correlated with poor patient outcome and tumour progression (Dumitru et al., 2011, Kindt et al., 2013a, Kindt et al., 2013b). Using qPCR, we confirmed that MIF was over-expressed in a number of HNSCC cell lines suggesting that the data obtained with FaDu is common amongst all other HNSCC cells. Interestingly, HPV-negative cell lines generally

secreted more MIF than HPV-positive cell lines and this may be due to their aetiology (carcinogen-promoted mutations rather than viral mediated). This phenomenon has also been observed with chemokine secretion in the group's laboratory (Sarmad Al-Sahaf, unpublished personal communication). This study went on to confirm that MIF is over-expressed in HNSCC by measuring its expression in biopsies of human HNSCC and comparing this to normal mucosa. Interestingly, in normal oral mucosa weak MIF staining was localized in the basal/proliferating cells of mucosa and not in any of the upper differentiating cell, as reported by Cludts et al, where they showed low or absence of MIF expression in the basal cellular layer and weak stain was also detected in superficial layers of normal mucosa (CLUDTS et al., 2010). It has been reported that MIF expression in the basal layer of human skin contributes to epidermal cell proliferation and differentiation (Shimizu et al., 1996), and this may account for why isolated normal oral keratinocytes displayed MIF expression in *in vitro* culture (it is the basal cells that are isolated and grown in culture). MIF expression was significantly increased in HNSCC tissues confirming that the *in vitro* cell line data is matched *in vivo*. MIF overexpression has also been reported in hypopharyngeal carcinoma (CLUDTS et al., 2010) and Laryngeal carcinoma (Kindt et al., 2013b) and this correlated positively with disease progression.

Neutrophil migration toward FaDu conditioned media significantly increased when FaDu cells were incubated under hypoxia, suggesting that hypoxia induces the secretion of neutrophil chemoattractants from FaDu cells. Hypoxia, a common characteristic of locally advanced solid tumours, occurs due to the inability of oxygen to meet the cellular demand by the growing tumour mass (Vaupel and Mayer, 2007). In response to hypoxia, cellular adaptation is mediated by the transcription factor hypoxia-inducible factors HIF-1 and HIF-2. Hence,

activation of these transcription factors by tumour cells facilitates their progression by inducing proteomic and genomic changes that have a profound effect on tumour angiogenesis, anaerobic metabolism and other process that enable tumour cells to survive in a low oxygen concentration environment (Eales et al., 2016). Evidence shows that hypoxia can induce MIF secretion in breast cancers (Larsen et al., 2008), pancreatic adenocarcinoma (Winner et al., 2007) in both a HIF-dependent or independent manner. Although, MIF has been identified as a hypoxia inducible gene firstly in squamous cell carcinoma-derived cell line (FaDu) (Koong et al., 2000), but our gene expression data has not MIF upregulation in FaDu in response to hypoxia. However, other HNSCC cells (H357, SCC4, SCC72, SCC2 and SCC90) cultured under hypoxic conditions confirmed that MIF expression is induced by hypoxia. A recent study showed that knocking down hypoxia-inducible factors (HIF) -1α and HIF-2α I in HNSCC cells, significantly reduce the level of MIF, providing evidence that MIF is HIF dependant *in vitro* (Zhu et al., 2014). Surprisingly, silencing HIF did not affect the migration of CD11b+Gr-1+ myeloid cells to hypoxia treated HNSCC cells *in vitro* (Zhu et al., 2014). Hypoxia also induced expression of VEGF in all the cells tested and this is a well know pathway in most cancer types, including HNC (LIANG et al., 2008) and is the basis of tumour angiogenesis (Goel and Mercurio, 2013) .

Small molecule antagonists of CXCR2, a CXCR4 antagonist and a MIF activity inhibitor were used to investigate the recruitment of neutrophils and monocytes into HNSCC tumour spheroids. Neutrophil recruitment into FaDu MCTS was significantly reduced in the presence of both CXCR2 inhibitors and in the presence of AMD3100, the CXCR4 inhibitor. Concentrations of inhibitors used have previously been shown to be non-toxic to neutrophils

in previous studies (Tazzyman et al., 2011, Bradley et al., 2009, Bot et al., 2014). Moreover, at a concentration determined to be non-toxic, the MIF inhibitor ISO-1, inhibited approximately 77% of neutrophil infiltration into FaDu spheroids when compared to control. It has been showed previously that the CXCR2 small molecule inhibitor (AZ10397767) prevented neutrophil migration towards the CXCR2 specific ligands CXCL1-3 and CXCL5 but had no inhibitory effect towards CXCL8 (Tazzyman et al., 2011). These may explain the partial inhibition effect noticed using the CXCR2 antagonist in the experiment performed in this thesis and is in agreement with Hammond et al. whose findings showed that CXCL8 induces chemotaxis of neutrophils via both CXCR1 and CXCR2 (Hammond et al., 1995). At first glance, this data suggest that neutrophils are recruited to FaDu MCTS via CXCR2 along a CXCL1/CXCL6 axis. However, inhibition of CXCR4, a receptor that does not bind CXCL1, CXCL6 or CXCL8 also dramatically inhibited neutrophil recruitment, suggesting the role of another chemoattractant. Bernhagen et al (2006) found that MIF can bind to and activate signal transduction pathways via both CXCR2 and CXCR4 in monocyte and T-cells. We also found that recombinant MIF causes directed migration of neutrophils in a dose-dependent manner showing that MIF is chemotactic for neutrophils *in vitro* as reported by Bernhagen, who showed moderate chemotactic activity of neutrophils in response to MIF mainly exhibited through CXCR2 not CXCR1 (Bernhagen et al., 2007).

Since neutrophils do not express CD74 (Dumitru et al., 2011) it is likely that MIF acts via CXCR2 and/or CXCR4 expressed by neutrophils. To support this ISO-1 was used, as it is the most characterized non-toxic inhibitor of MIF function. Many have reported that this compound is effective in blocking a MIF-dependent malignant phenotype (Meyer-Siegler et al., 2006). Therefore, the action of this inhibitor on neutrophil recruitment to FaDu MCTS was tested.

ISO-1 was found to be the most potent inhibitor of neutrophil recruitment. Since inhibitors to both CXCR2, CXCR4 and ISO-1 all block neutrophil recruitment these data suggest that MIF is the major neutrophil chemoattractant in HNSCC that is mediated most likely by both CXCR2 and CXCR4. The evidence support our hypothesis is that, neutrophils isolated from MIF-/- mice showed a reduce migration index to cytokine-induced KC, homology to human CXCL1, known ligand for CXCR2 (Santos et al., 2011). On the other hand, our findings contrast to that of Dumitru et al. who showed that MIF neutrophil recruitment relied solely on CXCR2 (Dumitru et al., 2011). Most literature proposes that the CXCR4 ligand CXCL12 is overexpressed and this has been widely detected in various tumours including HNSCC (Clatot et al., 2015). However, the cytokine array analysis did not detect expression of CXCL12 and so recruitment by this mechanism is unlikely, although further analysis is required to rule out this possibility.

In contrast to neutrophils we found that monocyte (THP-1) recruitment into tumours was blocked by inhibitors to CXCR4 and ISO-1 whereas the CXCR2 inhibitors were much less effective. This suggests that for monocytes, CXCR4 is the main receptor utilised and this is most likely driven by a MIF-mediated mechanism as FaDu MCTS did not express CXCL12 or CCL2 by cytokine array (generally known to be the main monocyte chemokine acting via CCR2).

Taken together these data suggests that MIF is over-expressed in HNSCC and is the main driver of neutrophil recruitment to these tumours. However, this conclusion is based on *in vitro* functional experiments and so the next chapter will examine the potential role of MIF-mediated neutrophil recruitment in an *in vivo* model.

Chapter 5: Effect of the MIF antagonist, ISO-1 and anti-Ly6G treatment on neutrophil infiltration and subsequent growth of FaDu xenograft tumours in vivo

5.1. Introduction

Data in chapter 4 showed that neutrophil recruitment to an HNSCC MCTS model was predominantly under the control of MIF, most likely acting via CXCR2 and CXCR4. A growing body of evidence has reported the therapeutic advantage of blocking MIF activity in oncology. Thus far, the main strategies involved in cancer studies include the use of small molecule inhibitors of MIF's biological activity (He et al., 2009, Meyer-Siegler et al., 2006, Kindt et al., 2013a) or destabilization of MIF via the heat shock chaperone complex (HSP90) (Schulz et al., 2012). Furthermore, inhibition of the receptor for MIF, CD74, decreased tumour cell proliferation and invasion *in vitro* (Govindan et al., 2013, Meyer-Siegler et al., 2006). Indeed, anti-MIF therapeutic interventions are in clinical trials at the moment for solid tumours (https://clinicaltrials.gov/ct2/show/NCT01765790?term=MIF&rank=1).

Anti-MIF antibodies have been developed by Baxter and recently investigated (Kerschbaumer et al., 2012). The authors showed that out of a panel of 74 antibodies screened, 14 were able to neutralize MIF activity *in vitro* while only three monoclonal antibodies (BaxG03, BaxB01, and BaxM159) reduced the cell growth and viability of the human prostate cancer cell line (PC3) by inhibiting activation of p44/42 mitogen-activated protein kinase (MAPK)/ ERK1/2. Administration of anti-MIF antibodies in a PC3-xenograft mouse model showed a significant reduction in tumour growth in a dose-dependent manner compered to isotype control antibody (Hussain et al., 2013).

Pharmacological inhibition of MIF using ISO-1, the most studied compound that binds to the catalytic site of MIF, has shown shrinkage in tumour size and reduced vascularization in xenograft experimental models of colorectal cancer (He et al., 2009) and Prostate cancer (Meyer-Siegler et al., 2006). A similar reduction in tumour growth was also achieved using anti-MIF antibodies in colorectal cancer (He et al., 2009).

5.2. Aims

The aim of this chapter was to explore the actions of the small molecule MIF inhibitor ISO-1 as well as anti-Ly6G treatment on innate immune cell recruitment, growth and vascularity of FaDu xenografts in an *in vivo* CD-1 immunodeficient murine model of HNSCC.

5.3. Methods

5.3.1. In vivo study Design

A xenograft murine model was generated by injecting CD-1 nude mice subcutaneously with 5×10^7 FaDu cells. Tumours were allowed to develop for 3 days, at which point mice were randomly divided into treatment groups. Each group consisted of 5 tumour-bearing mice and the treatment schedule was as follows; control group were given Intraperitoneal (i.p.) injections of PBS, the neutrophil depleted group received 200 µg anti-Ly6G three times a week over a 3 week period while the ISO-1 treated group received 20 mg/kg ISO-1 twice weekly by the same route (He et al., 2009) (see section 2.2.10 for further details). Tumours were measured using measuring callipers and length, depth and width of the tumour were recorded. At the end of experiment, mice were injected with BrdU for 1 h, mice culled and the tumour and serum were collected for further analysis. Tumours were divided and FFPE

for IHC analysis (see section 2.2.7.5 and 2.2.7.6) or snap frozen for immunofluorescence analysis for presence of leukocyte populations (see section 2.2.8.2).

5.3.2. Tissue imaging and quantitative analysis

For each tumour the entire tumour section was scanned using an image acquiring system (TissueFaxs200). Images were obtained with a 20X objective that automatically creates a high-resolution digital file, which can be viewed using automated tissue analysis software HistoQuest (4.0.4.161). The HistoQuest software uses algorithms that allow cell detection based on nuclear segmentation and the intensity measurement of nuclear as well as membrane and cytoplasmic antigens. Analysis for this thesis focused on quantifying proliferating cells (BrdU+) and the microvessel density (MVD) in whole tumour sections. The area of necrosis was excluded from analysis and MVD was assessed using a modified "Hot-spot" approach proposed by Weidner (Weidner, 1995). Whole tissue was examined and eight representative non-overlapping regions of interest (ROI) with high vascular density (HVD) and eight ROI with low vascular density (LVD) were selected (Fig. 5-1). The distribution of BrdU+ cells in relation to the vascular density of tumour (HVD vs LVD) was counted in each region. Each ROI had a fixed size of (0.03 mm^2) and the mean number of BrdU + cells counted in each ROI was expressed as % of BrdU + cells / tumour tissue and between high and low vascular areas.

The cut-off value to distinguish between positive (brown) and negative (blue) for nuclear detection of BrdU was determined manually based on the threshold selected on the IgG isotype control slide (threshold = 45) and then a threshold was selected for MVD was based on intensity of red (Vector red stain) threshold of CD31 immunostaining (threshold = 60).

Data from the quantitative analysis of immunostaining were expressed as following:

$$\% \text{ cell proliferating} = \frac{\text{number of positive (brown)cells}}{\text{number of total cells}} \times 100$$

$$\% \text{ of MVD} = \frac{\text{Area of positive CD31 stain}}{\text{total area of tumour}} \times 100$$

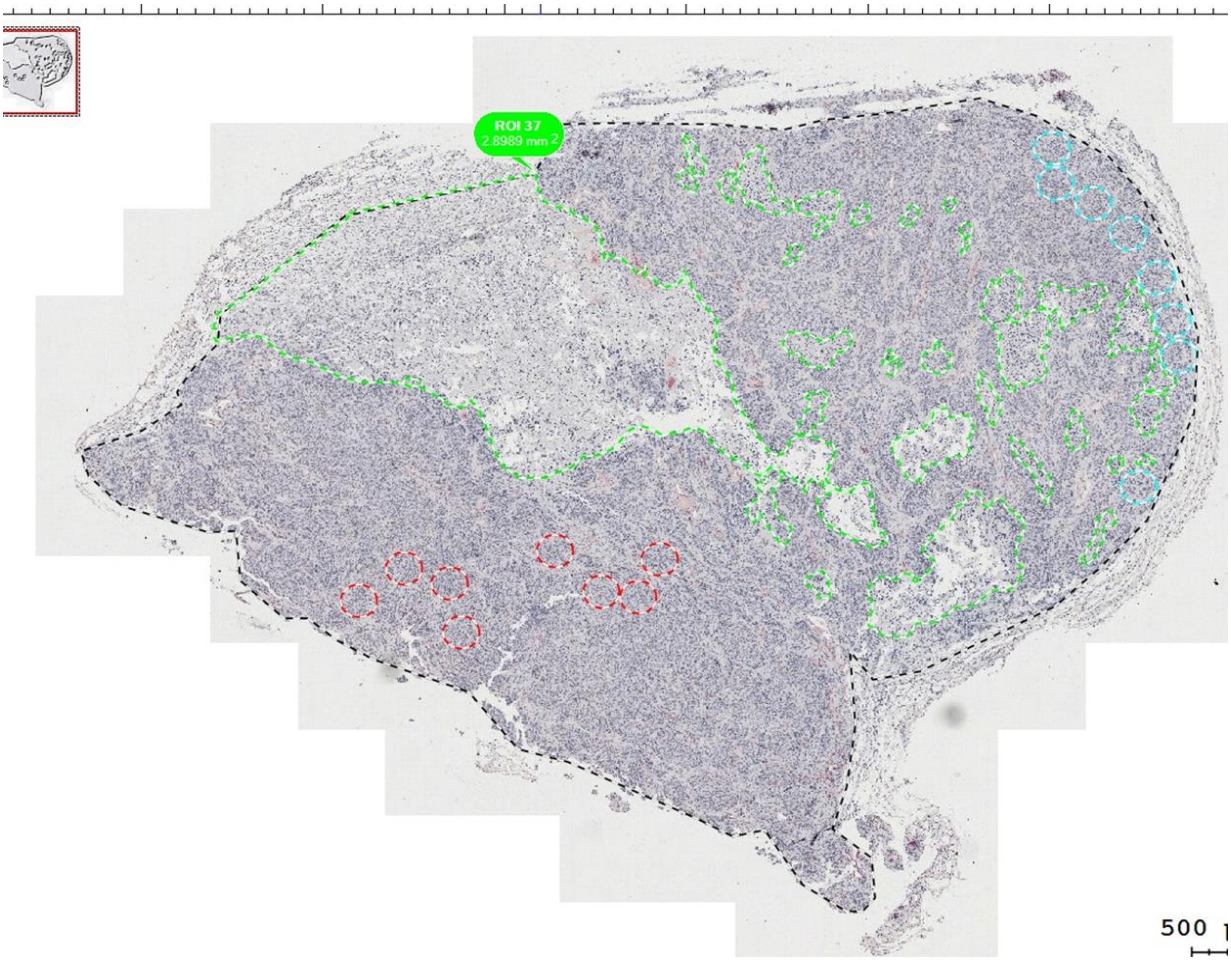

Figure 5.1 Automated Image analysis system HistoQuest was used to analyse FaDu xenograft sections. Tumour sections were scanned and area of tumour was measured (mm^2) (black dotted line) area of necrosis was defined microscopically (green dotted line) and excluded from analysis. Proliferating activity of cells (BrdU+) was quantified on the whole tumour section and correlated to Microvessel density (MVD). A detailed analysis of BrdU + cells was investigated in 8 region of interest (ROI) with HVD (red circles) and 8 ROI with LVD (blue circles). Each of ROI had a fixed size of 0.03 mm^2.

5.4. Results

5.4.1. Effects of ISO-1 and anti-Ly6G on tumour growth of FaDu xenograft tumours

Mice were implanted with 5×10^7 FaDu cells to create subcutaneous tumours and were subsequently treated with ISO-1, anti-Ly6G or PBS as control to examine the role of neutrophil depletion of MIF inhibition on FaDu growth. The onset of a measurable tumour was observed at day 11, with tumour size of 49.3±6.9 mm^3 for vehicle, 75± 18.4 mm^3 for anti-Ly6G and 37.4 ± 16.7mm^3 for ISO-1 treated mice. At the next measurement at day 13, the tumours from vehicle-treated animals had increased by approximately 31 mm^3 while the tumours from anti-Ly6G neutrophil depleted mice only increased by 8 mm^3 to around 45 mm^3. However, tumour sizes in the ISO-1 treated mice had grown to approximately 62 mm^3. Because the tumour size was variable between individual tumours, the tumour size at each time point was calculated in proportion to initial tumour volume at day 11 (Fig. 5.2-A).

All the tumours were found to be of equal size up until day 11 after which the growth of the tumour treatment groups started to diverge. Administration of vehicle control did not reduce or over promote tumour growth and these tumours grew at a consistent rate, and were significantly larger at the end of the experiment on day 21 than tumours at day 11 ($p=0.0159$). Treatment with anti-Ly6G appeared to reduce tumour growth from day 11 to day 21 compared to PBS treated controls although this was not statistically significantly different ($p=0.7606$) (Fig.5.2-B). The anti-Ly6G tumours had increased growth from day 18 to day 21. However, inhibition of MIF using ISO-1 significantly ($p<0.05$) increased tumour volume between day 13 and day 18 compared to both PBS controls and anti-Ly6G treated tumours (Fig. 5.2-A).

Measuring the tumour at the time of harvesting revealed that tumour-bearing mice treated with anti-Ly6G or ISO-1 were generally larger than tumours from untreated controls tumours with final tumour volume of 484±315mm^3 for ISO-1 compared to 308±127 mm^3 for anti-Ly6G treated tumours and 70±23 mm^3 for PBS treated animals. However, the difference was not statistically significant between groups (Fig. 5.3).

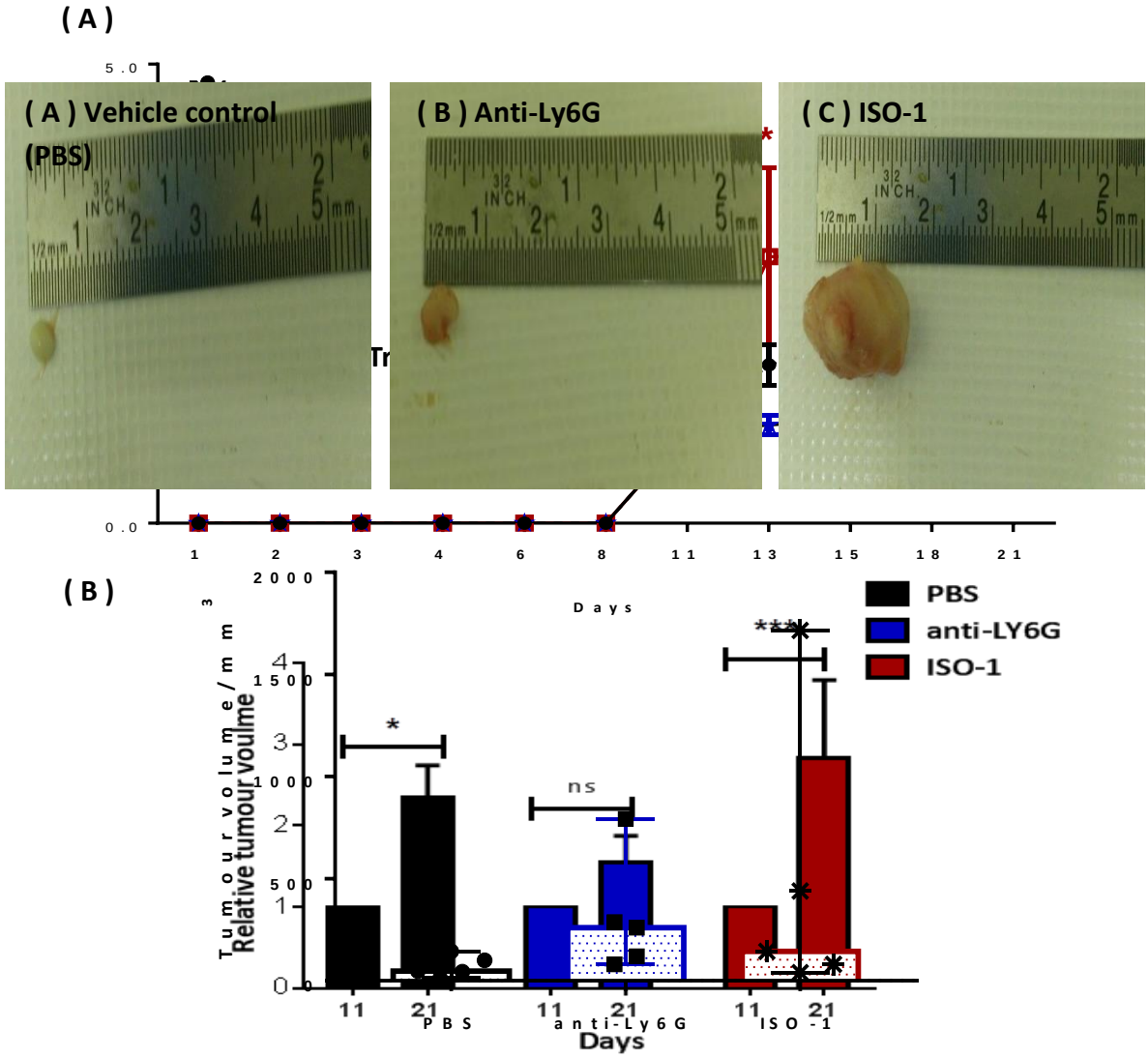

Figure 5.3 Growth of FaDu xenograft tumour in response to anti-Ly6G or ISO-1 treatment.

Figur CD-1 nude mice were inoculated with FaDu cells. Tumours were allowed to develop for 3 Grow days before mice received i.p. injection with either vehicle (PBS), anti-Ly6G or ISO-1 for 200 µ three weeks. On day 22, mice were scarified and tumours were harvested and day a photographed (A, B, C). Scatter plot represented tumour volumes calculated from the at da dimensions of each individual xenografts mice at the end point (volume = length x depth x 1 tre width). Data are expressed as range and black horizontal line represents the median (n=5). way A

tumour to

compute as

mean ± SEM (n=5).

Microscopic analysis of histological sections was carried out to further investigate the increase in tumour size in ISO-1 treated animals. The histopathology of FaDu xenograft stained sections revealed that tumours from control mice and anti-Ly6G mice appear as well circumscribed masses. In contrast, two out of five tumours excised from ISO-1 treated mice were less circumscribed masses with tumour infiltration into surrounding muscles (Fig. 5.4).

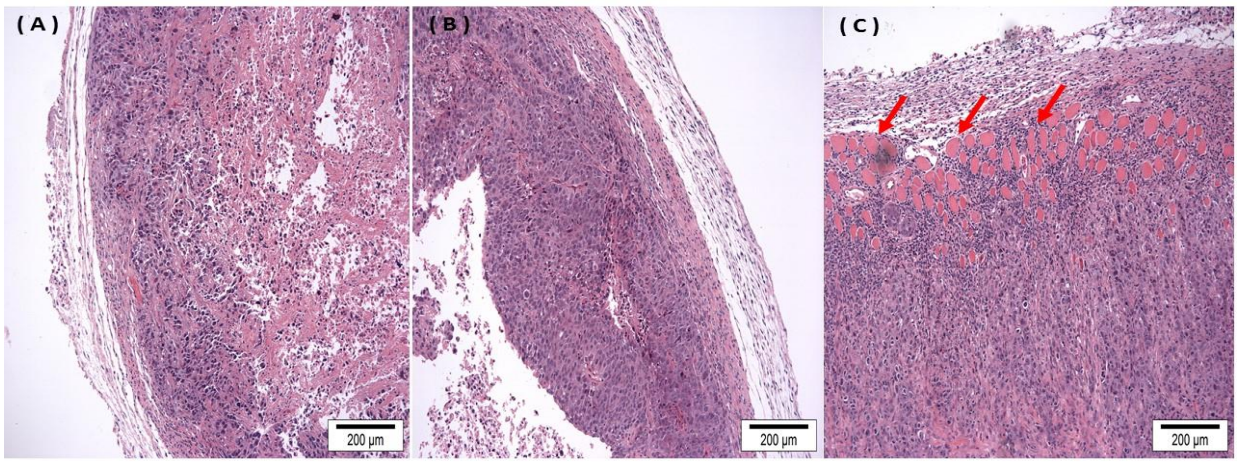

Figure 5.4 Extent of tumour infiltration at the tumour margin when harvested. Histopathology of PBS control tumours (A), anti-LY6G (B) shows that tumours are well circumscribed, whereas in ISO-1 treated mice (D) tumours were often found infiltrating into muscle tissue (red arrows).

The first objective of this examination was to assess the area of necrosis in each of treatment regimen. Tumour necrosis, a common feature of solid tumours, is usually a result of rapid tumour growth and inadequate blood supply. Areas of necrosis were identified, after consultation with an oral pathologist (Dr Keith Hunter), based on the morphology of fragmented cells, nuclear shrinkage and cellular debris (Fig. 5.5). Image analysis of the tumour area (as described in 5.3.2) from control and anti-Ly6G shows an average size of tumour of 9.51mm^2 and 9.12 mm^2, respectively. In contrast, ISO-1 tumour measurements revealed large tumours with an average size of 16.72 mm^2, with a large difference in size ranging between 2.06 mm^2 and 57.73 mm^2. Control tumours displayed small foci of necrosis covering 18.9 ± 9.7% mm^2 (Fig. 5.5A), whereas anti-Ly6G tumours contained predominantly large necrotic areas of 31 ± 4.5% (Fig. 5.5B). Images from ISO-1 treated groups contained an area of 24.3 ± 8.5% (Fig. 5.5C). Although the percentage area of necrosis was lower in control tumours than treated tumours, no statistical significance was detected between the groups ($p = 0.4749$ and 0.8535 for anti-Ly6G and ISO-1, respectively). However, when necrosis is expressed relative to tumour area (Fig. 5.6-B), the results show that the large tumour size in ISO-1 treated group was as result of the presence of large area of necrosis (37%) with less tumour cells, compared to 15% necrosis in control tumours.

.

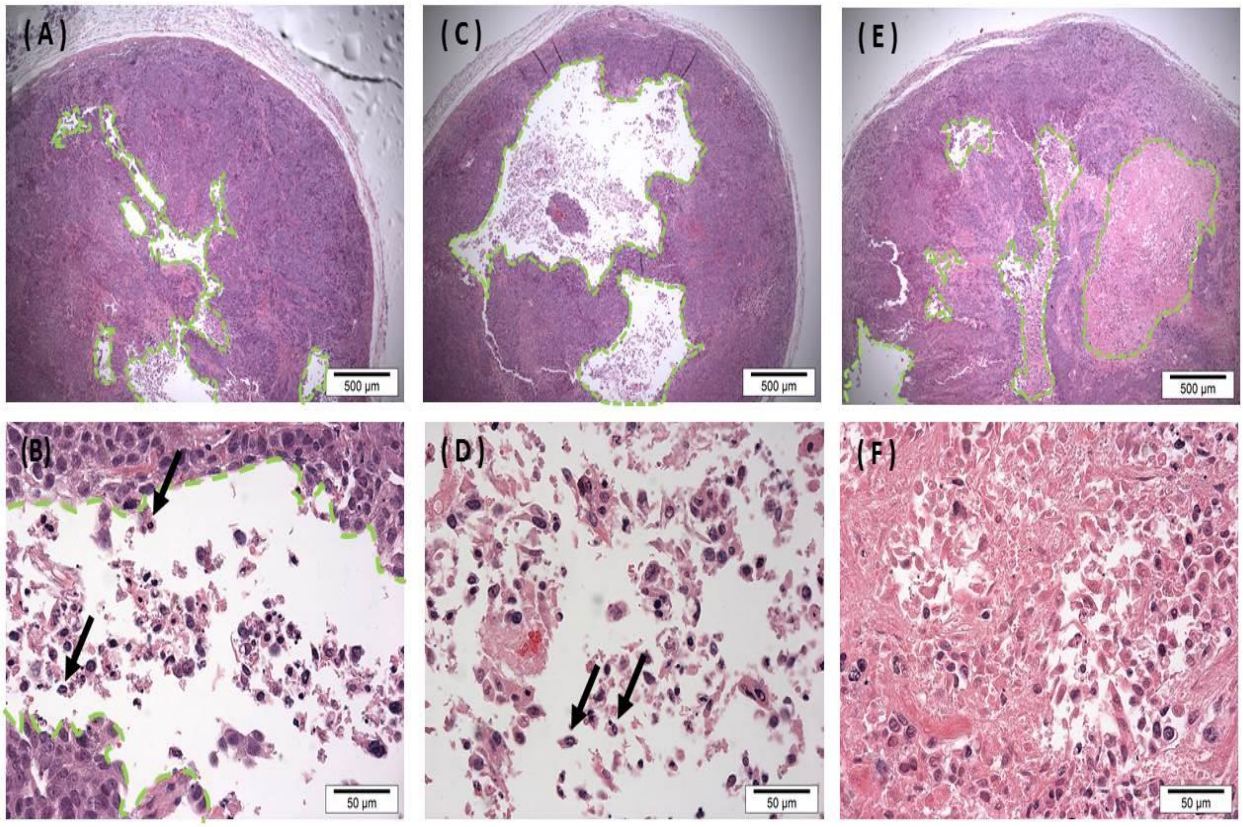

Figure 5.5 Area of necrosis present in FaDu xenograft tumour growth. Histopathology of PBS control tumours **(A, B)**, anti-Ly6G **(C, D)** and ISO-1 treated mice **(E, F)** shows the presence of necrosis (green dotted line). Necrosis was defined morphologically as change in tumour cells with nuclear shrinkage and cellular debris. The area of necrosis was measured using automated image analysis in whole tumour sections. At higher magnification images (B, D, F) neutrophils (black arrow) and other inflammatory cells could be identified by their distinctive nuclear morphology within the necrotic area. A,C,E scale bar = 500 µm,. B, D, F scale bar = 50 µm.

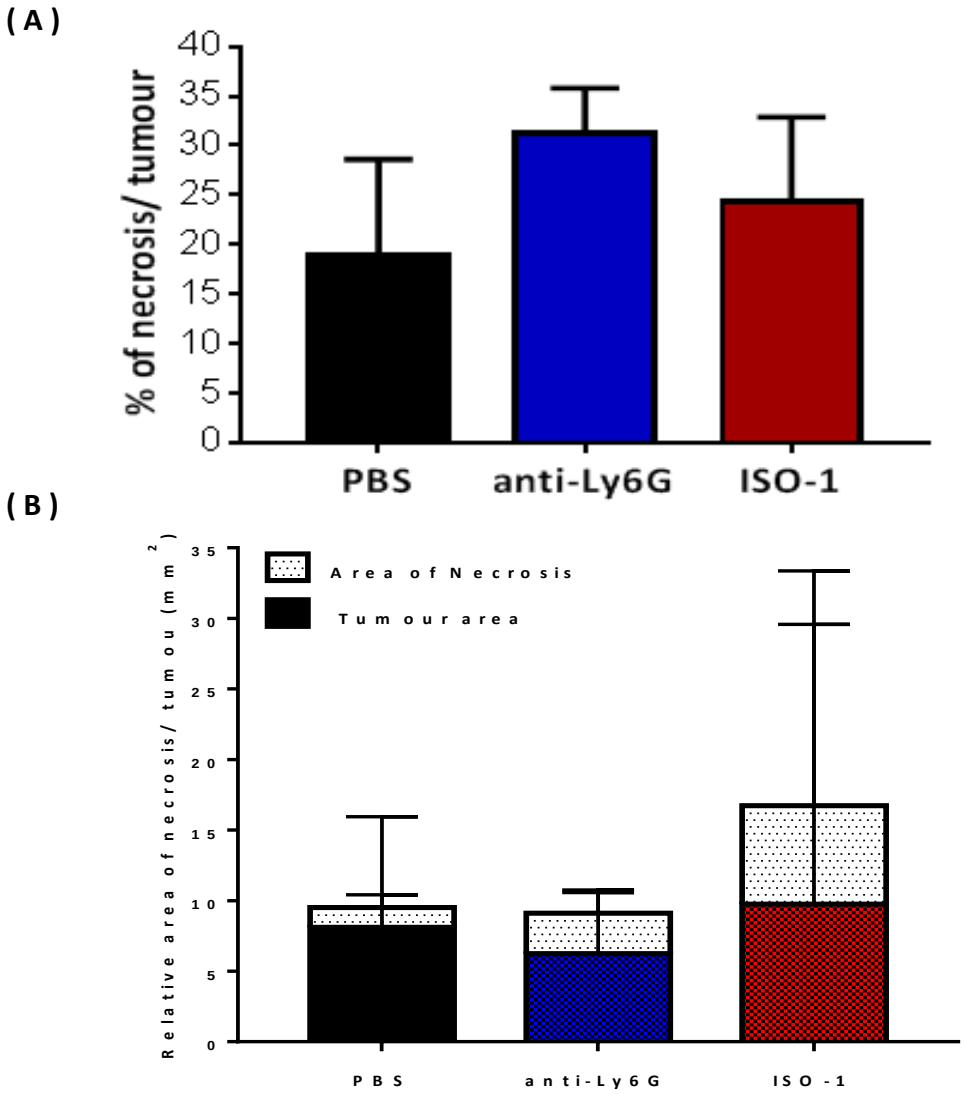

Figure 5.6 Image analysis of tumour necrosis present in FaDu xenograft tumours. (A) Presence of necrosis was assessed in whole tumour tissue and expressed as percentage relative of tumour area. One-way ANOVA showed no significance difference between control group or treated group **(B)** % Necrosis in proportion to the whole tumour area as measured by Image analysis.

5.4.2. ISO-1 or anti-Ly6G alter the number of neutrophils in FaDu xenograft tumours

To determine the importance of MIF in neutrophil recruitment that was observed *in vitro* and also in tumour progression, using the same FaDu tumour bearing mice were injected with ISO-1. Treatment with anti-Ly6G was used as a positive control for neutrophil depletion and was used alongside DMSO control treated mice. At the end of experiment, tumours were removed, snap-frozen in OCT, sectioned and immunofluorescently stained for the murine neutrophil marker Ly6G, macrophage marker F4/80 and vascularization using CD31 (see section 2.2.8.2). The intensity and area of fluorescence in mm^3/microscopic field for each of the targeted cells was analysed using velocity software (section 2.2.8.3). Image analysis (Fig. 5.7) showed an 87% reduction ($p=0.0013$) in the number of murine neutrophils in FaDu xenograft tumours treated with anti-Ly6G when compared to vehicle control (PBS). Similarly, FaDu xenograft tumours treated with ISO-1 also displayed a significant (80%) reduction ($p=0.0025$) in the number of tumour-associated neutrophils with the area of fluorescence decreasing from average 42885.2 mm^3/microscopic field with the control treated tumours to average 8896.1 mm^3/microscopic field for the ISO-1 treated tumours and average 5594.37 mm^3/microscopic for anti-Ly6G (Fig. 5.7).

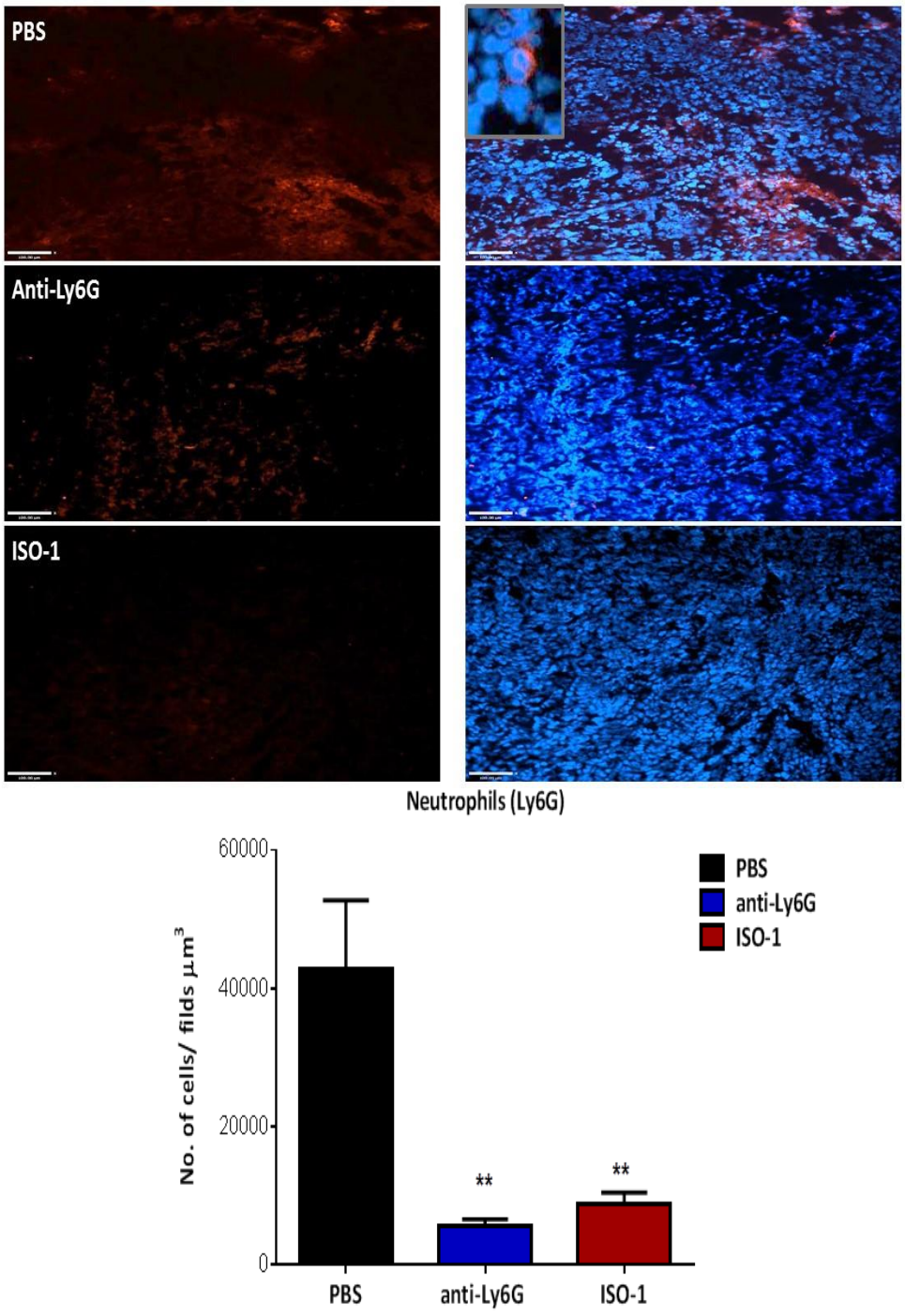

Figure 5.7 Image analysis of Ly6G$^+$ neutrophils in anti-Ly6G and ISO-1 treated FaDu xenograft tumours. A) Representative images Ly6G staining (red, neutrophils) and DAPI (blue, nuclei) in tissue sections of xenograft tumours treated with DMSO control, anti-Ly6G or ISO-1. Scale bar = 100 µm B) The number of Ly6G cells in z-stacks was measured based on intensity and area of fluorescence per microscopic field, and presented in bar chart as mean ± SEM (n=5). One-way ANOVA test was used to compute the statistical significance **= $p<0.001$.

5.4.3. Treatment of FaDu xenograft tumours with ISO-1 or anti-Ly6G affects macrophage recruitment.

MIF has been reported to elicit human monocyte chemotaxis through CXCR2 (Bernhagen et al., 2007) and mice express a homologous of CXCR2 on monocytes (Cacalano et al., 1994). In addition, inhibition of MIF in an inflammatory disease model reduced infiltrated F4/80 macrophages in diseased tissue (Leng et al., 2011). This evidence along with the data presented in chapter 4 suggests that treatment with ISO-1 or anti-Ly6G may alter macrophage recruitment into tumours. Therefore, the number of macrophages in ISO-1 and anti-Ly6G treated FaDu tumours were examined using the murine macrophage marker, F4/80 and compared to control tumours.

Image analysis showed that the number of F40/80 positive cells in both anti-Ly6G and ISO-1 treated tumour-bearing mice were lower than those observed in control mice (Fig. 5.8). Statistical analysis confirmed a significant reduction ($p=0.0427$, 40.2%) in the number of F4/80 macrophages observed in FaDu xenograft tumours receiving anti-Ly6G compared to control tumours to 25870 mm^3/microscopic field. Moreover, there was an even greater reduction in the number of F4/80 positive macrophages in ISO-1 treated FaDu tumours decreasing from 43189mm^3/microscopic field in control tumours to 6443.85 mm^3/microscopic field in ISO-1 treated tumours, equating to an 86% fold decrease in neutrophil numbers ($p=0.0003$).

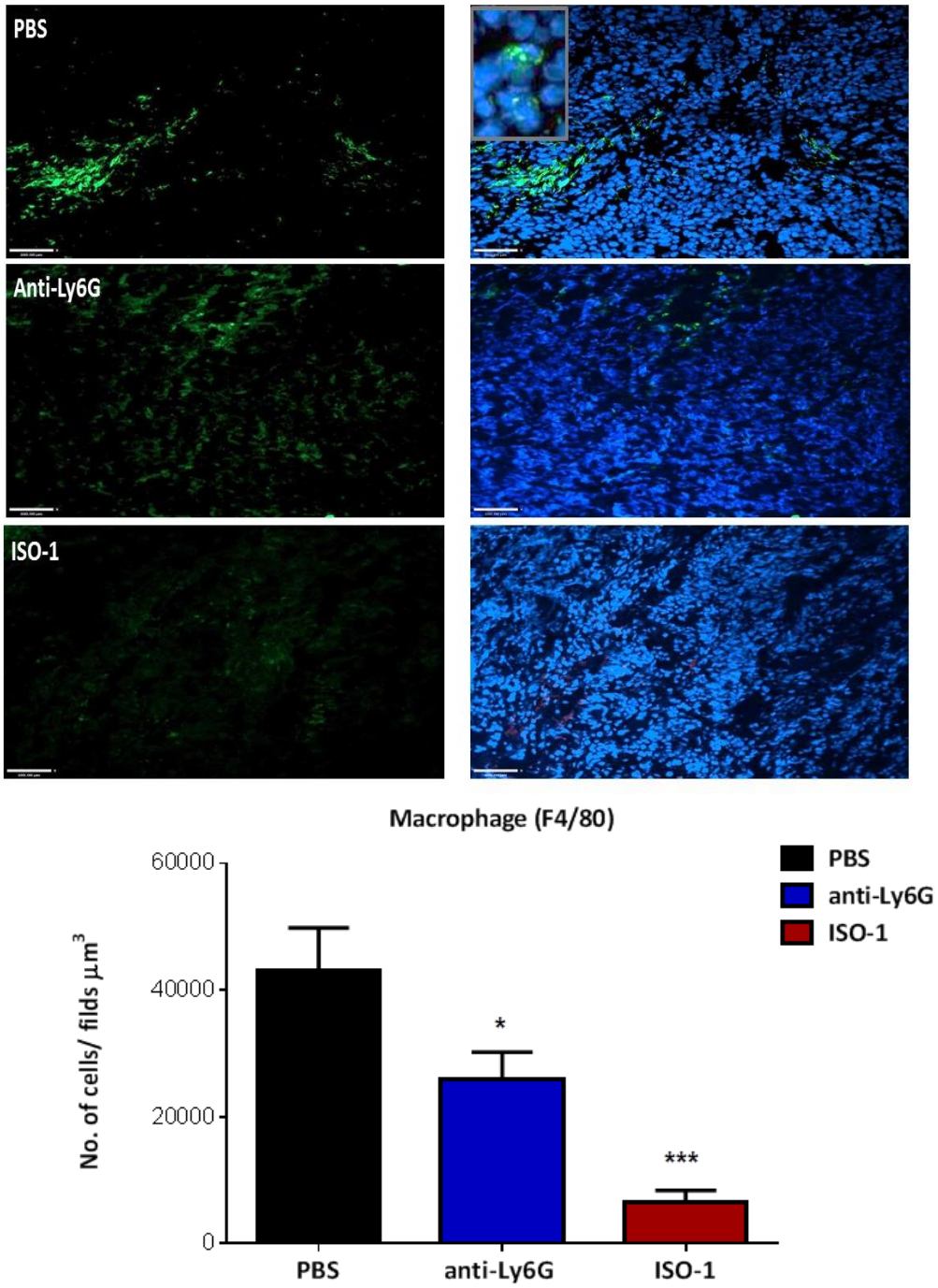

Figure 5.8 Image analysis of F4/80 macrophages in anti-Ly6G and ISO-1 treated FaDu xenograft tumours. A) Representative images F4/80 staining (green, macrophages) and DAPI (blue, nuclei) in FaDu xenograft sections treated with DMSO control, anti-Ly6G or ISO-1. Scale bar = 100 µm. B) The number of F4/80 cells in z-stacks was measured based on intensity and area of fluorescence per microscopic field, and presented in bar chart as mean ± SEM (n=5). One-way ANOVA test was used to compute the statistical significance *= P<0.05, ***= P<0.0001.

5.4.4. Effects of neutrophil depletion and ISO-1 treatment on angiogenesis in FaDu xenograft tumours

Accumulating evidence suggest that TAN play a role in the vascularization process in many types of tumours (Tazzyman et al., 2013) with one study showing an association between increased numbers of TAN detected in hepatocellular carcinoma (HCC) tissue and MVD. Zho et al showed that depletion of TAN using anti-Ly6G significantly attenuated the MVD in HCC based on immunostaining analysis of CD34-positive endothelial cells (Zhou et al., 2016). Therefore, the influence of TAN depletion by anti-Ly6G and inhibition of MIF in tumour vascularization was investigated in FaDu tumour sections using CD31, a murine endothelial cell marker. Image analysis showed that there was no significant difference in CD31 density either in ISO-1 (11097.9 mm^3/microscopic field) (P=0.1638) or anti-Ly6G (13026 mm^3/microscopic field) (p=0.2607) treated tumours compared to controls (20138.6 mm^3/microscopic field). These data exclude the possibility that the difference in tumour growth rate observed between control and treated tumours is due to an inhibitory effect on tumour angiogenesis by neutrophil or macrophage depletion.

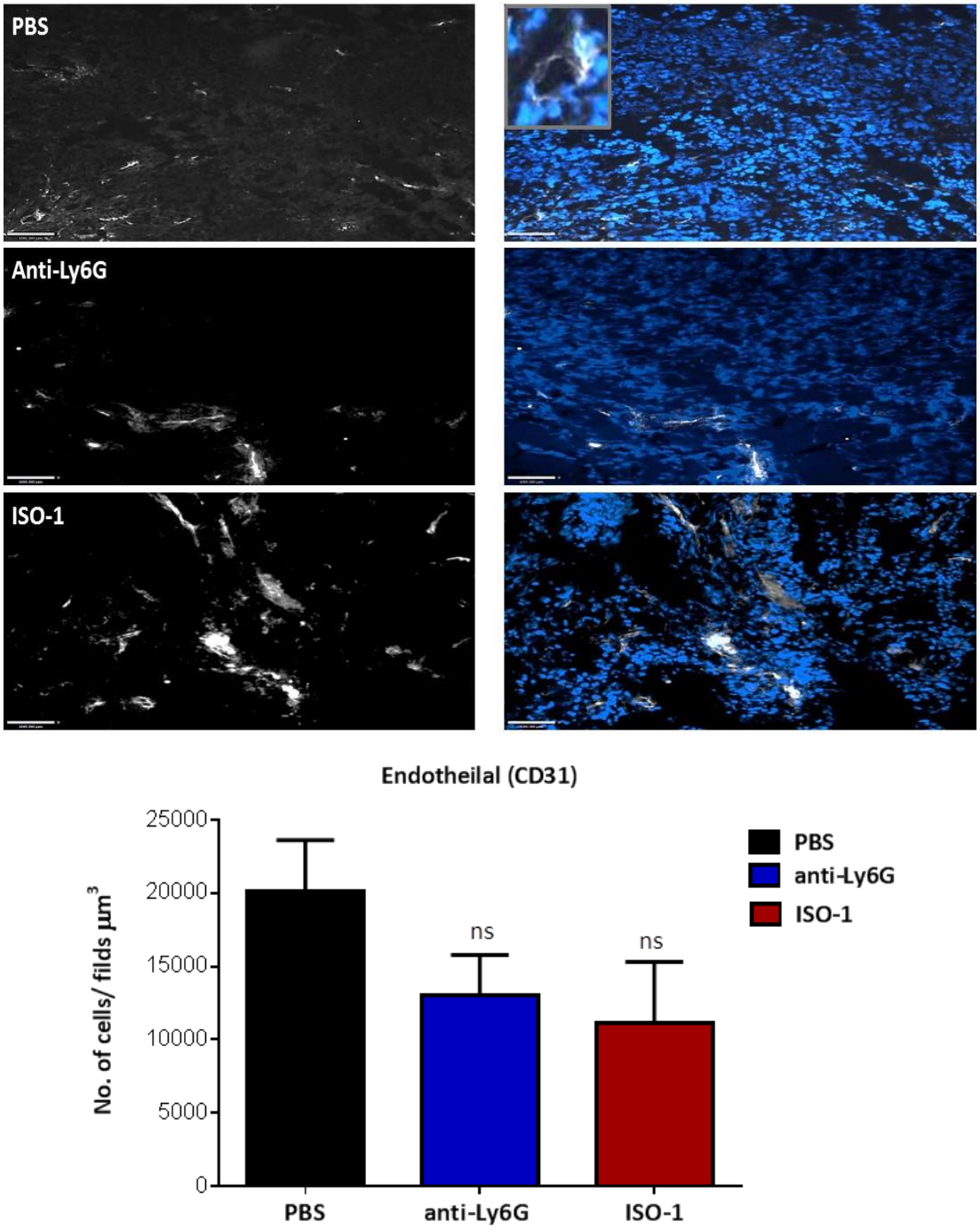

Figure 5.9 Effect of anti-Ly6G and ISO-1 on the distribution of CD31 blood vessels in FaDu xenograft tumours. A) Representative immunostaining images of vascularized CD31+ areas (white, endothelial cell) and DAPI (blue, nuclei) in FaDu xenograft sections treated with DMSO, anti-Ly6G or ISO-1. Scale bar = 100 µm. B) The number of CD31+ endothelial cells was measured based on intensity and area of fluorescence per microscopic field, and presented mean ± SEM (n=5). One-way ANOVA test was used to compute the statistical significance.

5.4.5. Effects of neutrophil depletion and ISO-1 treatment on tumour proliferation using BrdU

TAN can release factors that are capable of stimulating tumour cell proliferation and depletion of neutrophils reduced the tumour growth and microvessel density in a melanoma and fibrosarcoma murine cancer model (Jablonska et al., 2010). In section 5.4.3 it was found that the number of neutrophils was significantly diminished in both anti-Ly6G and ISO-1 treated FaDu tumours. To test if this depletion affects tumour cell proliferation mice received BrdU, a thymidine analog which is incorporated into newly synthesised DNA, an hour prior to sacrifice and tumour removal. Proliferating cells were detected in tumour sections using anti-BrdU (see section 5.3.2) and the number of BrdU+ cells counted using automated image analysis. The proliferation index was calculated by dividing the number of BrdU positively stained nuclei (Brown, Fig. 5.10) by the total number of cells detected in the same area of tumour (excluding areas of necrosis) and the value express as a percentage proliferating cell per image.

Microscopical analysis shows that BrdU+ cells were abundant in both the control and Ly6G depleted FaDu tumours with the BrdU staining co-localising to the nuclei of tumour cells. There was no significant difference ($p=0.2758$) in the abundance of proliferating cells between these two groups. In contrast, significantly ($p=0.0155$) fewer BrdU positive cells were detected in ISO-1 -treated cells (2.2%) compared to both control (8.7%) and Ly6G neutrophil depleted (11.9%) tumours (Fig. 5.11). Indeed, ISO-1 treated tumours displayed a 75-fold decrease in tumour cell proliferation compared to control and Ly6G display 35-fold increase in tumour cell proliferation compared to control (Fig. 5.11).

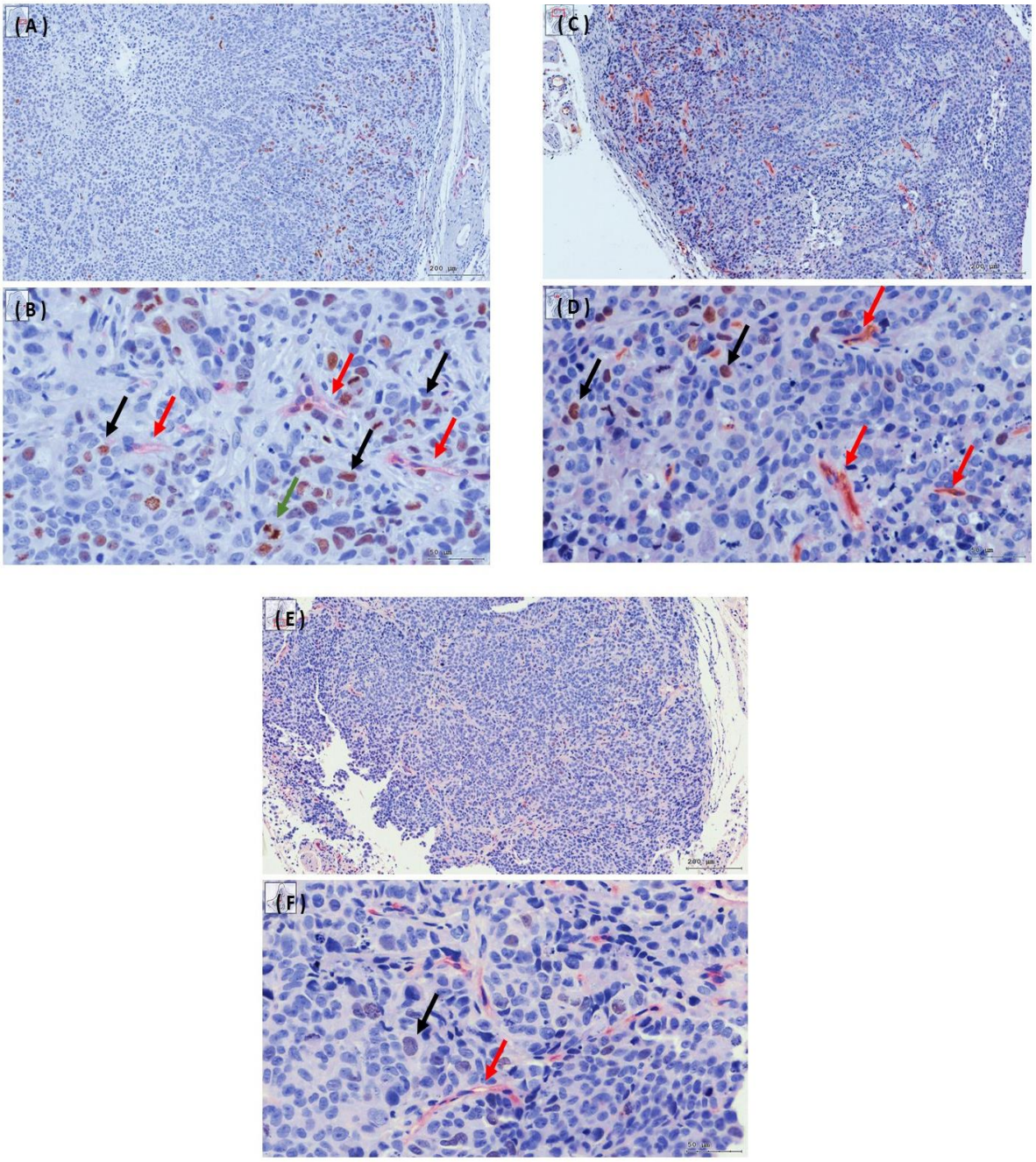

Figure 5.10 The proliferative status and vascularity of FaDu cells in control, Ly6G neutrophil depleted and ISO-1-treated xenograft murine models. Paraffin-embedded samples from tumour bearing mice were stained with anti-BrdU to measure the proliferative status of FaDu cells. **A** & **B** are representative images from vehicle control tumour, **C** & **D** are representative image from anti-Ly6G treated tumours and **E** & **F** are from ISO-1 treated tumours. Numbers of BrdU+ nuclei were counted in whole tumour sections. Scale bar A, C, E = 200 µm. Scale bar B, D, F = 50 µm. Black arrow indicated positive stain of BrdU in the nuclei of cells; red arrow indicates CD31 positive staining of blood vessels; green arrow shows a tumour cell undergoing mitosis.

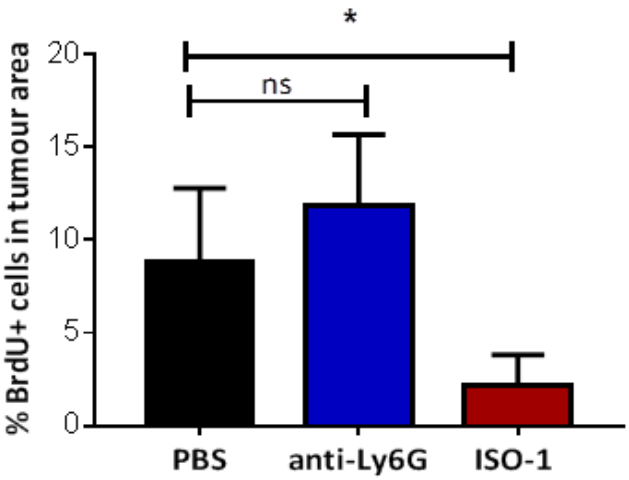

Figure 5.11 Image analysis of the proliferative status in FaDu tumour xenografts. The number of BrdU positive nuclei (brown) were evaluated using automated image analysis in whole tumour tissue and expressed as % of BrdU + cells in the whole cell population. One-way ANOVA test was used to compute the statistical significance of proliferating cells and this revealed no statistical difference in the % of BrdU+ cells between control and anti-Ly6G tumours. In contrast, the % of BrdU + cells in ISO-1 treated tumours were significantly reduced (*$p<0.05$) when compared to control. Data are mean ± SEM. n=5/group.

5.4.6. Dual analysis of tumour vascularisation and proliferation

Of note, BrdU + cells were observed to be accumulated in the tumour periphery or areas with HVD. Therefore, a detailed analysis of proliferating cells based on density of blood vessels distribution was carried out as described in section 5.3.3 (Fig 5.12 and Fig5.13). As can be seen in figure 5.14, BrdU+ accumulation was associated with areas of high vascular density (HVD) and a significant reduction ($p=0.0005$) in the number of BrdU + cells was observed in low vascular density (LVD) areas in comparison to those that were highly vascularised in control treated mice (1.52 cells and 13.47 cells respectively). Similarly, the number of proliferating cells in anti-Ly6G tumours significantly decreased from 14.42 cells in HVD areas to 2.43 cells in LVDs ($p=0.0015$). In ISO-1 treated, less proliferating cells was detected in general but more BrdU+ cells was observed around HVD with mean number of 5.3 cells, whereas no or very weak BrdU positive cells were detected in LVD.

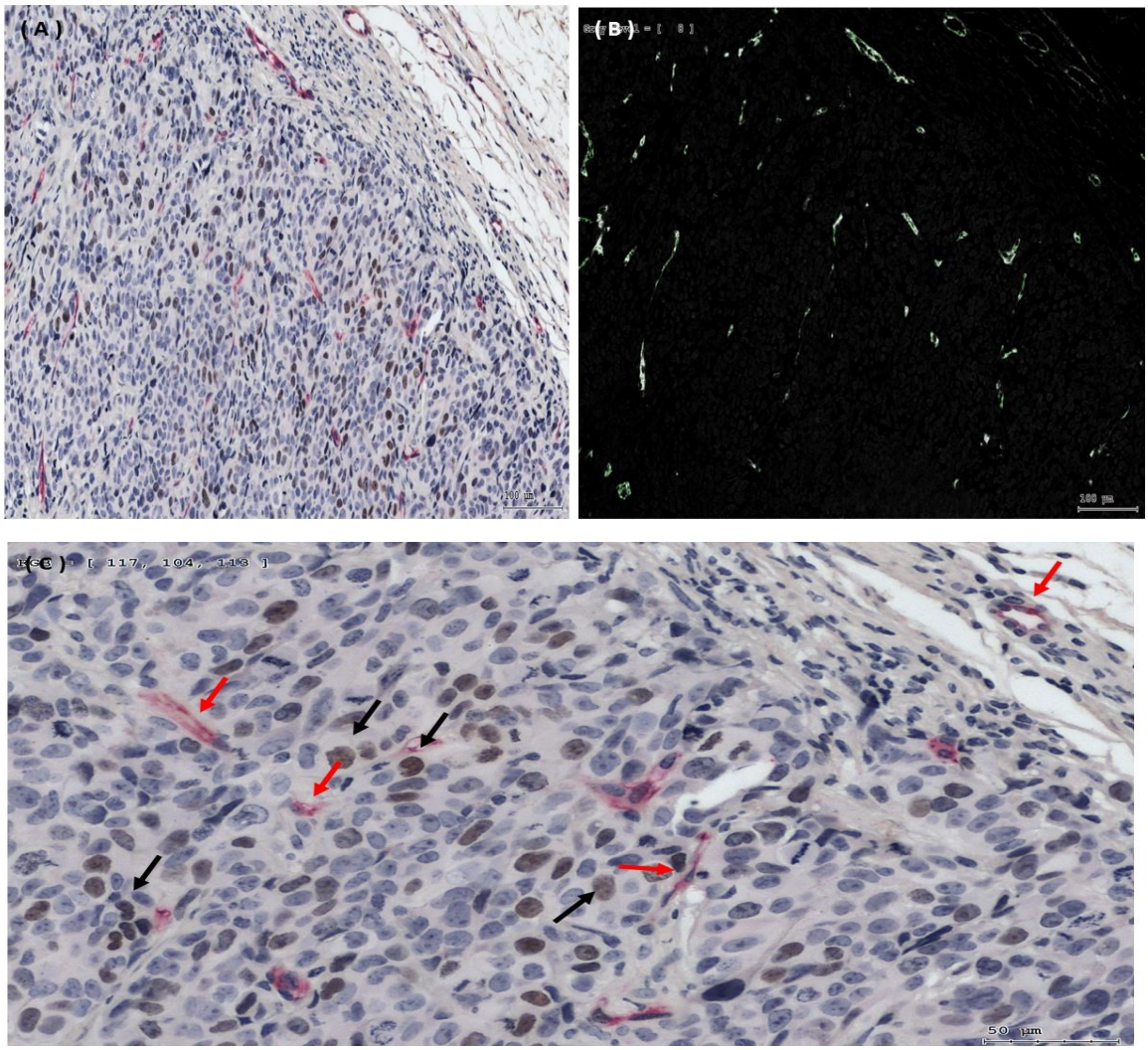

Figure 5.12 Image analysis of BrdU in correlation to CD31 distribution in FaDu tumour xenografts. Dual stained sections were scanned using HistoQuest software that detected the intensity of both CD31 (white areas in overlay image B) and BrdU (brown) Scale bar = 50 µm. (C) High magnification image showing CD31 (red staining, red arrow) and BrdU (brown nuclear stain, black arrow), Scale bar = 100 µm.

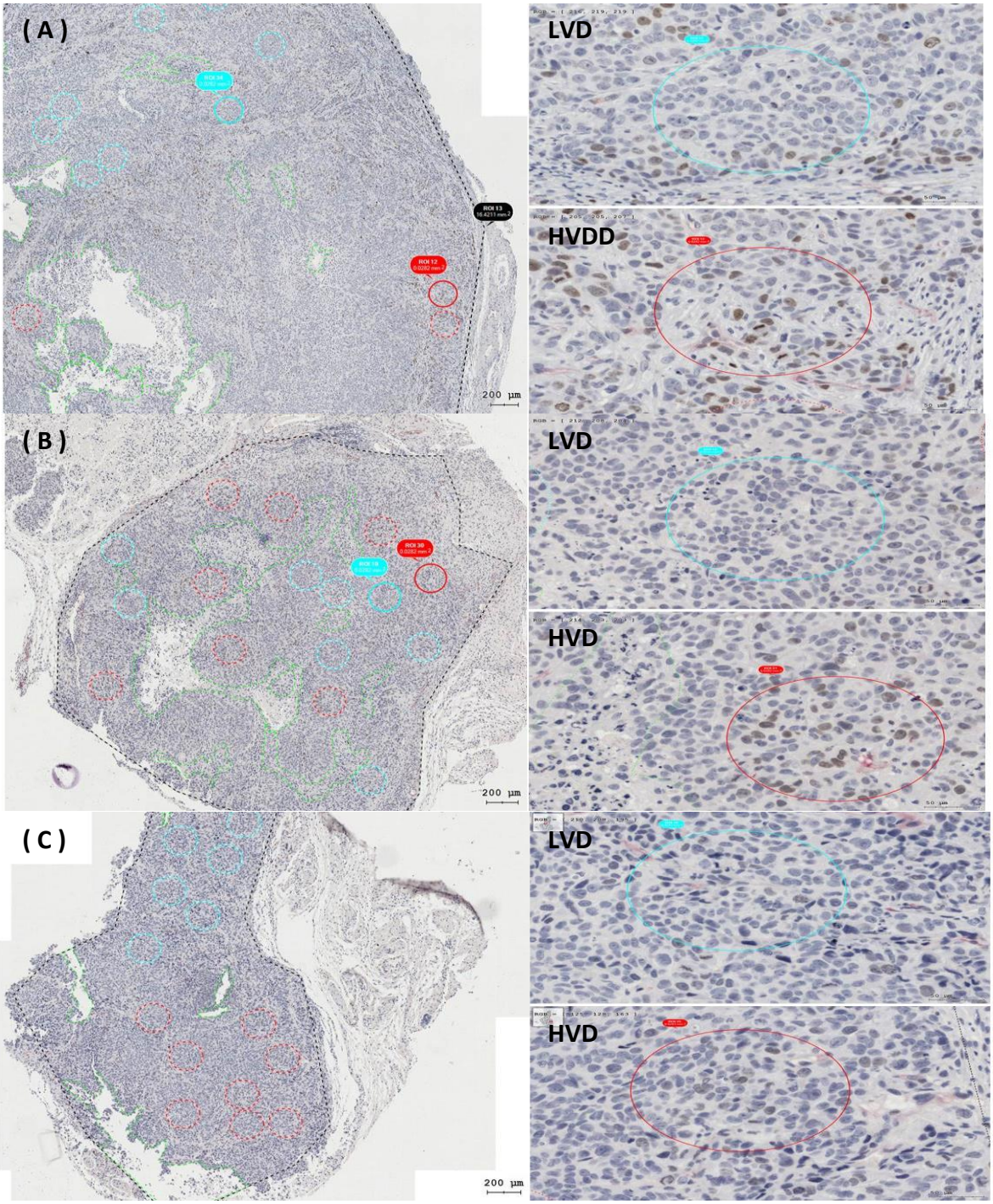

Figure 5.13. Image analysis of BrdU in FaDu tumour xenografts using the hot spot method.the intensity of BrdU+ (brown) in LVD (Aqua blue circle, left) and HVD (red circle, left) in control treted mice (A) anti-Ly6G (B) and ISO-1 treated tumour

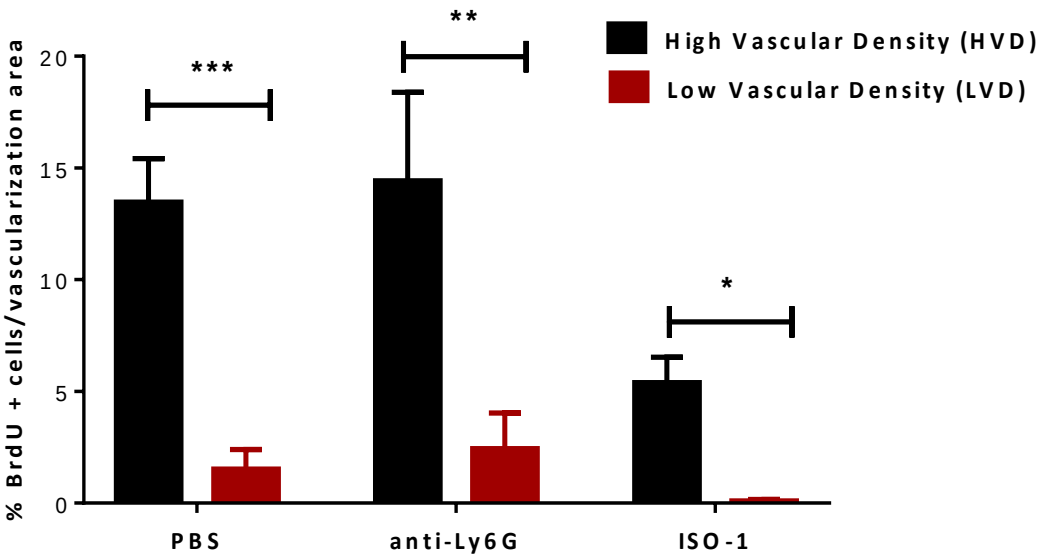

Figure 5.14 Image analysis of BrdU in FaDu tumour xenografts using the hot spot method. Bar chart of BrdU+ cells in HVD and LVD areas of FaDu tumour, showing accumulation of proliferating cells in highly vascularize areas in comparison to avascular areas of tumors. The statistical significance of proliferation index between HVD vs LVD in each of treatment regimen was calculated by Students t-test. * = $p<0.05$, ** = $p<0.005$, *** = $p<0.0001$. Data are mean ± SEM of eight fields selected for each HVD and LVD area.

5.4.7. MIF expression in FaDu xenograft control and treated tumours

MIF expression has been observed *in vivo* in tumours in this and other studies (Dumitru et al., 2011), and has been shown to correlate with disease severity (Kindt et al., 2013). Therefore, the intensity of MIF immunostaining in control and treated tumours was evaluated using a modified Quick-score method (described in section 2.2.7.5) and scoring was independently reviewed by an oral pathologist (Dr Keith Hunter). Staining analysis showed expression of MIF primarily in the cell cytoplasm. Surprisingly, the detected level of MIF in the anti-Ly6G and ISO-1 treated mice was significantly higher than control mice ($p=0.0045$ and $p=0.0005$, respectively) (Fig. 5.15).

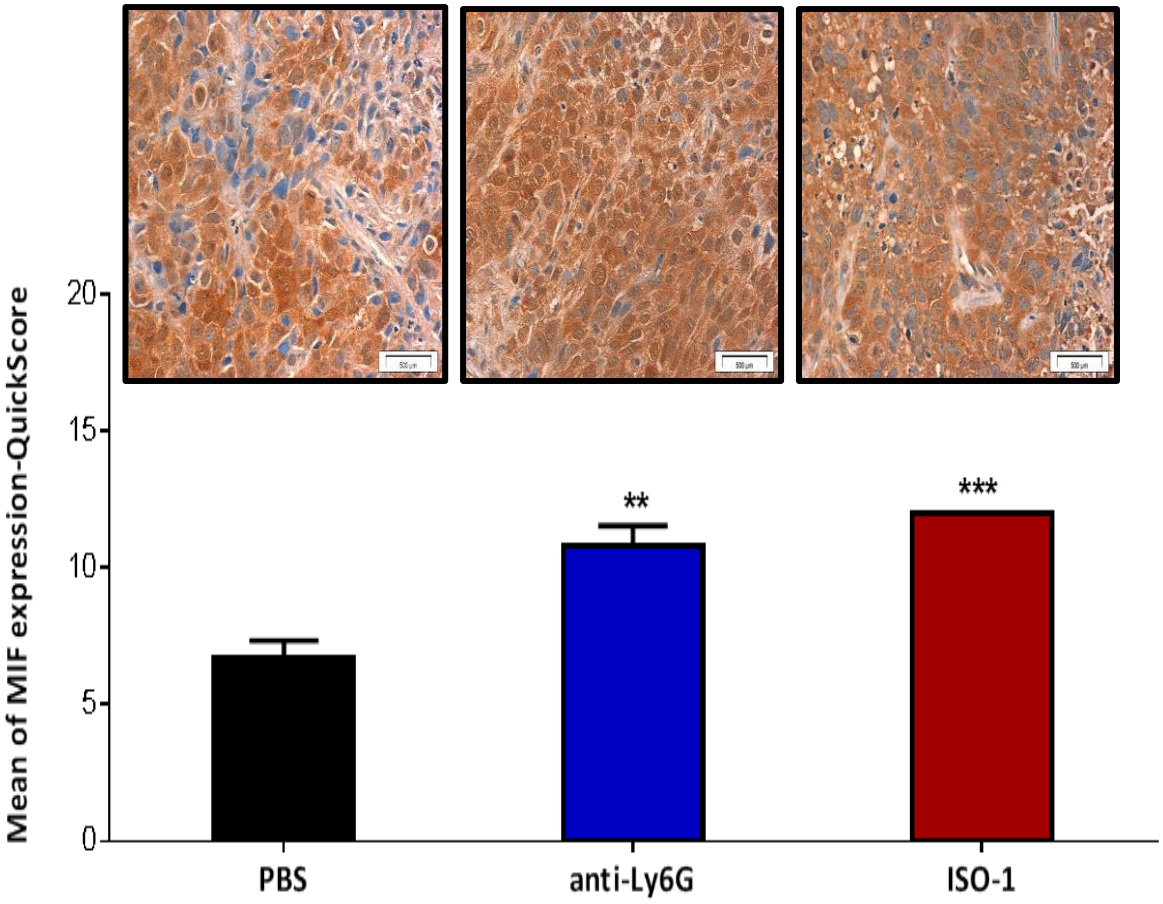

Figure 5.15 MIF protein expression levels in FaDu xenograft tumour sections. Paraffin-embedded sections from FaDu tumour bearing mice were stained with anti-human MIF antibody and the stain intensity was evaluated using a Quick-score method. The level of MIF detected in vehicle control (PBS) was lower than anti-Ly6G treated or ISO-1 treated mice model. One-way ANOVA test was used to compute the statistical significance of the scores variance of MIF cancer tissue with or without treatment. Scale bar = 500 µm.

5.4.8. MIF serum concentration in ISO-1, Ly6G-treated and control tumours

Quantitative analysis of MIF released in to the serum of mice-bearing FaDu tumours as well as non-tumour-bearing mice was assessed by ELISA. Although the ELISA was developed with antibodies raised against human MIF, this cytokine was detected in mice with no tumours, albeit at low levels, suggesting some cross-reactivity to murine MIF. However, MIF levels were greatly increased in mice bearing human FaDu tumours showing that these tumours release MIF into the bloodstream (non-tumour bearing mice vs. control tumours, p=0.0001). High levels of MIF were also detected in the serum from both anti-Ly6G and ISO-1 treated tumour-bearing mice. Interestingly, depletion of neutrophils using anti-Ly6G significantly reduced the levels of MIF in the serum of mice (p=0.0414) compared to controls (Fig. 5.15). In addition, ISO-1 treated tumour-bearing mice also displayed significantly reduced MIF levels in their serum compared to control tumours (p=0.0138, Fig. 5.15). However, there was no significant difference between the levels of MIF in the serum of ISO-1 and Ly6G-treated tumour-bearing mice.

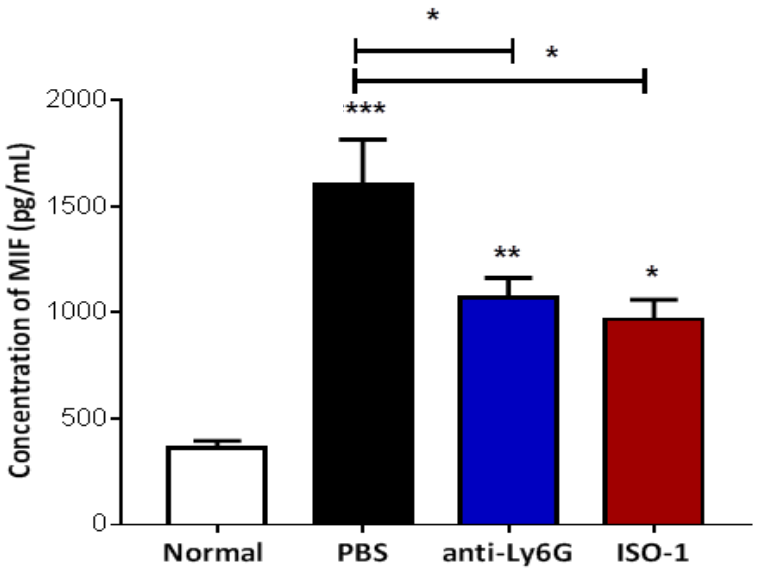

Figure 5.15 MIF levels in tumour-bearing and non-tumour-bearing mice. ELISA analysis of MIF levels in the serum collected from non-tumour bearing or mice with treated or control FaDu xenograft. Non-tumour-bearing mice showed low levels of MIF whereas the levels of MIF were significantly increased in all tumour-bearing mice. Administration of anti-Ly6G or ISO-1 significantly reduced the level of MIF in the serum compared to vehicle control tumours. Multiple comparisons One-way ANOVA test was used to compute the statistical significance for differences in MIF levels between normal and tumour-bearing mice (PBS, anti-Ly6G, ISO-1) or between untreated tumour bearing mice (PBS) and treated tumour-bearing mice (anti-Ly6G, ISO-1). The histograms represent the mean ± SEM of MIF level from 5 mice for each treatment. *= $p<0.05$, **=$p<0.005$, ***= $p<0.0001$.

5.5. Discussion

In this chapter it was demonstrated that administration of the small molecule inhibitor, ISO-1, in FaDu tumour-bearing mice did not reduce the tumour growth when compared to control tumours. Instead the sizes of tumours were observed to increase after ISO-1 treatment. In contrast, targeting MIF either by using MIF inhibitor ISO-1 in xenograft colon or prostate cancer murine models (He et al., 2009, Meyer-Siegler et al., 2006) or using anti-MIF neutralizing antibody in a prostate xenograft model (Hussain et al., 2013) was shown to reduce tumour growth. Further histological analysis showed that although the tumour burden was greater, ISO-1 tumour-bearing mice contained larger areas of necrosis and less proliferating cells. This result is in line with an *in vivo* study that used humanized anti-MIF antibodies to treat a murine prostate cancer model, which showed a reduction in proliferating tumour cells using Ki67 immunostaining in dose-dependent manner (Husaan et al., 2013). Large areas of tumour were found to be necrotic (up to 37.5%) in the ISO-1 treated group compared to control tumours (15.5%). The reduction in number of proliferating cells associated with presence of large area of necrosis in ISO-1 section indicates a higher death rate in these tumours. This could be due to the direct effect of MIF on tumour cells or an indirect effect. It must be noted that the data presented in this thesis is a snapshot of events occurring at 21 days when the tumours were excised and analysed. However, time course data suggests that differences in tumour growth first occurred at 11 days, 7 days after treatment. It is possible that MIF inhibition affects events occurring in the tumours at day 11 and 13 that have dissipated and so are not picked up by the analysis at day 21. Analysis of the early tumours would provide more insight into the reason for low proliferation with elevated necrosis but this was not possible in this study. Treatment of FaDu tumours with anti-Ly6G to deplete mice of neutrophils caused a marked reduction in tumour growth. A similar effect

was observed in a murine model of melanoma and fibrosarcoma (Jablonska et al., 2010), while neutrophil depletion did not influence tumour growth in a mammary tumour-bearing murine model (Coffelt et al., 2015). It has been demonstrated that the effect of neutrophil depletion on tumour growth is dependent on the stage of tumour development. Systemic depletion of neutrophils at an early stage of cancer development (Ly6G treatment started at the same time tumour cells were inoculated) had no effect on tumour growth. In contrast, when tumours were allowed to develop before neutrophil were depleted (as in the model described in this thesis), the authors observed a significant reduction in tumour growth in the murine model of Lewis lung cancer and mesothelioma (Mishalian et al., 2013). These data accord with the data presented in this thesis and suggest that neutrophils aid tumour progression once a tumour has been established.

The FaDu tumour xenografts were evaluated microscopically and immunohistochemically for tumour necrosis, cell proliferation, vascularisation and presence of macrophages. In this study we observed that ISO-1 treatment induced a strong inhibitory effect on recruitment of innate inflammatory cells (neutrophils and macrophage). The inhibition was not 100% suggesting that other factors aid MIF in leukocyte recruitment. Data from the *in vitro* MCTS studies suggest that CXCL1, CXCL6 and CXCL8 may aid neutrophil recruitment in human tumours. Murine neutrophils express CXCR2 (the receptor for KC, the murine equivalent of CXCL1 – mice do not have the gene for CXCL8) and so are likely to be recruited via human CXCL1 expressed by FaDu xenografts. It is possible that MIF and CXCL1 may act in concert because neutrophils from MIF-/- mice showed reduced migration toward KC (known as CXCL1 in human) *in vitro* (Santos et al., 2011), suggesting an interplay between the two molecules. Macrophages may also be recruited to tumours by chemoattractants independent of MIF, for

example by CCL2 a potent monocyte chemoattractant. In fact, CCL2 expression has been reported to be regulated by MIF in injured hepatocytes in an autocrine manner (Xie et al., 2016). However, CCL2 was not detected in the conditioned medium for FaDu MCTS in the cytokine array data suggesting that this chemokine does not play a role in monocyte recruitment in HNSCC. However, there are several other monocyte chemoattractants (CCL7, CCL8, CCL13) that were not on the cytokine array that could be involved in the recruitment of monocytes to FaDu tumours and this possibility needs further investigation.

One of the most important roles MIF has been observed to play in promoting tumour progression is stimulation of angiogenesis (He et al., 2006) and, although not statistically significant, tumours treated with ISO-1 and Ly6G displayed a marked and consistent reduction in CD31 staining (a marker of microvessel vessel density, which also expressed by endothelial cells lining lymphatic vessels). Knock-down of MIF in melanoma cells prior to implanting these cells in a syngeneic murine model showed up to a 40% reduction in CD31 staining density, without affecting tumour growth, in comparison to wild-type mice (Girard et al., 2012). A similar reduction in microvessel density, assessed by CD34, was observed in DU-145 xenograft tumours treated with ISO-1 (Meyer-Siegler et al., 2006), suggesting that MIF inhibition may affect tumour vascularisation either directly or indirectly by inhibition of leukocyte recruitment.

Immunohistochemical analysis of MIF protein expression on FaDu xenografts tumour sections showed an increased level of MIF in ISO-1 and anti-Ly6G treated tumours compared to control tumours. This result could be explained by the fact that, diverse cell types store pre-formed MIF in their cytoplasm, ready to be released upon stimulation. Since MIF has been reported to act via autocrine and paracrine loops, the increased expression of MIF could be a feedback

mechanism to compensate for the loss of the MIF producing cells, neutrophils and macrophages (Daryadel et al., 2006, Calandra et al., 1994). It could also be that neutrophils and macrophages somehow regulate MIF production by tumour cells via paracrine signalling. Further experiments are required to determine if paracrine signalling mechanisms regulate MIF expression. In fact, blocking exogenous MIF by ISO-1 in glioblastoma multiforme cells enhanced mRNA expression not only of MIF but also its receptors CD74, CXCR2, and CXCR4 *in vitro* (Baron et al., 2011).

The observation that MIF serum levels from FaDu xenograft tumour increase compared to non-tumour bearing mice show that MIF is released by the tumour into the circulation. Elevated levels of MIF in the circulation have been reported for many cancers, including, renal cancer (Du et al., 2013), HNSCC (Kindt et al., 2013b) and prostate cancer (Meyer-Siegler et al., 2005). By contrast, the levels of protein detected in the serum of ISO-1 and anti-Ly6G treated mice were reduced compared to levels seen in control tumours. This reduction in secreted MIF protein might be as a result of blocking the D-dopachrome active site of MIF (Lubetsky et al., 2002), whereas, the reduction of MIF serum levels observed in anti-Ly6G (and possibly ISO-1) treated mice may be due to the significant reduction in number of neutrophils in these tumours.

The observation that MIF levels are increased in the tumours but decreased in the circulation of ISO-1 and Ly6G treated tumours may suggest that MIF is prevented from being released into the circulation. It is possible that since MIF can be pre-stored intracellularly its presence is still detected in tumours using IHC but its secretion into the circulation is somehow reduced when neutrophils are absent or in the presence of ISO-1. It is possible that neutrophils

produce factors that regulate tumour cell secretion of MIF, although this needs to be examined experimentally.

Administration of ISO-1 in a DU-145 prostate tumour model reduced tumour growth by 40% (Meyer-Siegler et al., 2006). Further investigation showed that inhibiting MIF *in vitro* could affect tumour growth directly by reducing the downstream signalling of ERK1/2 MAPK cascade (Meyer-Siegler et al., 2006). In addition, a preliminary study using an irreversible MIF inhibitor (4-iodo-6-phenylpyrimidine (4-IPP), which is estimated to have 5-10 times more inhibitory potency than ISO-1, reduced migration of murine SCCVII squamous carcinoma cells in a Boyden chamber assay and proliferation *in vitro* (Kindt et al., 2013a), suggesting that exogenous MIF partially affects the proliferative capacity of tumour cells *in vitro*. MIF may also exert its effects indirectly by stimulating other cells. In fact, Dumitru et al (2011) showed increased proliferation and invasive properties of FaDu cells cultured as monolayers in the presence of FaDu-primed neutrophil conditioned medium. This effect was abolished when cells were co-culture with FaDu primed neutrophil conditioned medium in presence of ISO-1 inhibitor (Dumitru et al., 2011). These data suggest that MIF activated neutrophils to secrete factors that affect tumour cell proliferation.

Other possible reason for not observing an inhibitory effect generated by ISO-1 treatment *in vivo* might be dosing regimen. The *in vivo* study in this thesis followed the same treatment regimen used in a colorectal cancer xenograft model (He et al., 2009), but ISO-1 administration twice per week may be not enough to achieve sustained inhibition of MIF. Of note, a 47% reduction in tumour growth was achieved by using MIF-/- mice (Girard et al., 2012).

Chapter 6: The effect of cytokines and HNSCC-secreted factors on neutrophil phenotype

6.1. Introduction

The concept of neutrophil polarization into N1 (anti-tumour) or N2 (pro-tumour) phenotypes in response to molecules in the tumour microenvironment has been recently reported in two elegant studies using murine cancer models. In the first study, Fridlender et al, (2009) noted that upon inhibition of TGF-β in two murine cancer models (NSCLC and mesothelioma) neutrophils recruited to these tumours displayed what they characterised as an N1 phenotype. The most important features of the N1 anti-tumour phenotype are activation of cytotoxic T lymphocytes and improved ability to kill tumour cells, increased expression of pro-inflammatory cytokines such as TNF-α and their ability to stimulate the immune response with levels of immunosuppressive Arg-1 significantly reduced (Fridlender et al., 2009). In another study, when tumour-bearing *Ifnβ1*-/- mice received a low dose IFN-β therapy, neutrophils appeared to change their phenotype to one with an enhanced ability to cause tumour cell destruction (Andzinski et al., 2016); a trait of N1 neutrophils. In addition, administration of adjuvant type I IFN treatment in melanoma patients resulted in reduced expression of CXCR1 and CXCR2, up-regulation of ICAM-1 and increased apoptosis of blood-derived neutrophils, other features that were deemed characteristic for anti-tumour N1 neutrophils (Andzinski et al., 2016). Further evidence confirmed the important role that type I INFs plays in polarization of TAN. Mice lacking endogenous INF-β acquire a TAN phenotype that express increased levels of pro-angiogenic genes (VEGF, MMP9) as well as c-myc and STAT3 activation. Moreover, depletion of this type of neutrophil showed a therapeutic effect in reducing tumour

growth in both control and IFN-β–deficient mice (Jablonska et al., 2010). Such TAN have been described as displaying an N2 pro-tumour phenotype, and have immunosuppressive functions as well as increased secretion of chemokines CCL2, CCL5 and expression of chemokine receptor CXCR4 (Jablonska et al., 2010).

The major challenge in studying TAN phenotype is the fact that the proposed phenotype and function of TAN has mainly been characterized in murine tumour models that may not directly relate to humans because of species-specific differences. Currently, there is only one study that describes the characteristic phenotype of TAN isolated from freshly removed lung tumour tissue when compared to neutrophils isolated from distant non-malignant lung tissue (Eruslanov et al., 2014). Using flow cytometric analysis, the authors confirmed that human TAN show decreased expression of CXCR1, CXCR2, adhesion molecule CD62L (L-selectin) and increased expression of ICAM-1 (CD54), a previously reported neutrophil activation marker (Fortunati et al., 2009). In addition, analysis of CCR and CXCR chemokine receptor expression revealed increased levels of CXCR4, CXCR3, CCR7 and CCR5 on TAN whereas no expression was detected on peripheral blood neutrophils (Eruslanov et al., 2014). Therefore, there appears to be differences in the phenotypic markers between human and murine N1 and N2 neutrophils.

The influence of factors in the HNSCC microenvironment on the phenotype of TAN is unclear. There is evidence that the tumour-associated stroma, mainly CAF, within HNSCC induce elevated level of TGF-β *in vitro* and *in vivo* (Rosenthal et al., 2004), this study found high levels of MIF both *in vitro* and *in vivo* HNSCC tumours. Pilot study experiments described in this chapter test if stimulation with molecules found in the HNSCC environment are able to alter the phenotype of neutrophils *in vitro*.

6.2. Aims

The aim of the work described in this chapter was to determine the phenotype of freshly isolated neutrophils upon stimulation with recombinant human MIF and HNSCC-derived factors and compare these phenotypes to those driven by INFγ (N1) or TGF-β (N2) phenotype. This entailed investigating changes in cell surface marker expression in response to each stimulus by flow cytometry.

6.3. Methods

6.3.1. Neutrophil isolation using MACSexpress

Although the standard ficoll density gradient isolation method is a reliable and cost effective way to isolate neutrophils from blood, it is lengthy and prone to cause unwanted cell activation. Thus, a different technique involving the use of antibody-coated micro-beads to deplete non-target cells from anti-coagulated whole blood within 30 minutes, yielding unstimulated neutrophils of high purity was used in the studies described here (the detailed method is described in section 2.2.2.2).

6.3.2. Neutrophil polarization

To examine the neutrophil phenotype (N1 or N2 selected marker, Fig. 6.1), freshly isolated peripheral blood neutrophils from healthy donors were exposed to 100 ng/ml recombinant INF-γ to polarize neutrophils to an N1 phenotype, 25 ng/ml recombinant TGFβ to polarize neutrophils to an N2 phenotype, 100 ng/ml recombinant MIF or to conditioned medium from FaDu MCTS for 8 and 24 hours (see section 2.2.2.3).

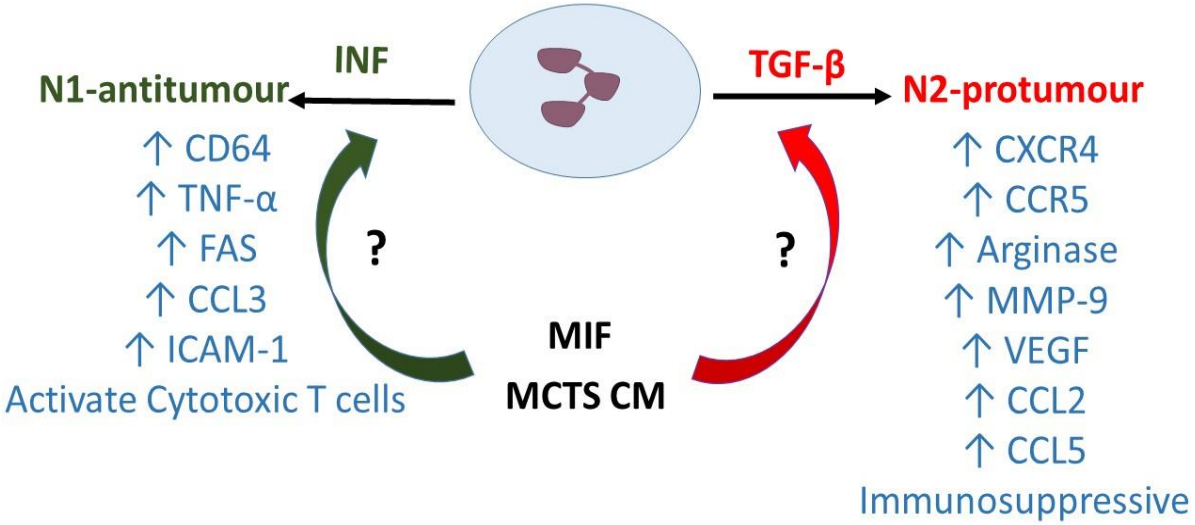

Figure 6.1 Schematic diagram for polarization of TAN in response to INF (N1 phenotype) or TGF-β (N2 phenotype) in mice and humans and characteristic alterations associated with both neutrophils phenotype.

6.3.3. Multicolour flow cytometry

At the end of incubation period neutrophils were washed with cold FACS buffer and stained according to the protocol in section 2.2.9.7. In summary, a cocktail of antibodies were selected according to antibody fluorochrome availability, receptor expression levels and classified into three groups for staining purposes; 1. CXCRs (CXCR1-FITC, CXCR2-PE, CXCR4-PE-Cyanine-7), 2. adhesion molecules (CD62-L-FITC, ICAM-1-PE), 3. CCRs (CCR5-PE) and Fcγ receptor (CD64-FITC). In addition, the neutrophil marker CD66b-APC and a LIVE/DEAD™ cell dye was used in each group so that viable CD66b-positive neutrophils could be gated for cell

surface expression analysis. Compensation beads were run for each of the antibodies used to eliminate spill-over as a result of the use of multiple fluorochromes in this experiment and BD FACSDiva software was used for analysis (section 2.2.9.8).

Neutrophils were gated based on expression of CD66b after excluding cell doublets and non-viable cells. Expression of the selected N1 and N2 markers on the neutrophil population was examined after adjusting the gating using a fluorescence-minus one (FMO) control. Expression of cell surface markers on all tested neutrophils was measured using median fluorescence values and stimulations were performed and analysed on neutrophils obtained from each donor. Unfortunately, due to time constraints, the data presented here is not complete. Although experiments have been performed from neutrophils obtained from 3 individuals, some of the analysis has only been performed for 2 individuals (further analysis is on going) whereas other experiments show data from 3 individuals (details are provided in the figure legends). In the following sections average median fluorescence values are in parentheses.

6.4. Results

6.4.1. Neutrophil activation marker

Un-treated peripheral blood neutrophils analysed directly after removal from the circulation (also called resting naïve cells) showed high expression of CXCR1 (3784), CXCR2 (2159) and CD62-L (474), low expression of ICAM-1 (266), CXCR4 (138), CCR5 (200) and CD64 (337) (Fig. 6.2). In contrast, isolated neutrophils cultured at 37^{o}C for 8 hours without stimulus (media only) displayed a reduced expression of CXCR1 (2062) CXCR2 (100) than freshly isolated neutrophils. There were no statistically significant differences in expression of CD62-L (250), CXCR4 (384), ICAM-1 (267), CCR5 (206) and CD64 (267) in freshly isolated compared to 8-hour

cultured neutrophils (Fig. 6.2-A). These cultured neutrophils showed a similar expression pattern to that described previously (Fortunati et al., 2009). Also, in order to characterise the change in expression of phenotype, the percentage of CD66b+neutrophils for each of selected marker was analysed and compered to naïve neutrophils (Fig. 6.2-B). The results showed that 100% of naïve neutrophils expressed CXCR1, 96.4% expressed CXCR2, whilst little CXCR4 expression was detected in naive neutrophils 0.76%. This result did not change after culturing neutrophils for 8 hours for CXCR1 and CXCR2 (99.6% & 82.1%, respectively) but a slight increase in number of CD66b+ expressing CXCR4 was observed (13.3%). However, less than half of the naïve neutrophil population expressed ICAM-1 (48.1%) and this was reduced after 8 hours (5.4%). Similar to CD64, which was reduced form 24% in naïve neutrophils to 14.8% after an 8-hour incubation. While no difference in the number of CD66b+ for CD62L was detected in naïve or cultured neutrophils (27.4% and 24%, respectively) (fig 6.2-B)

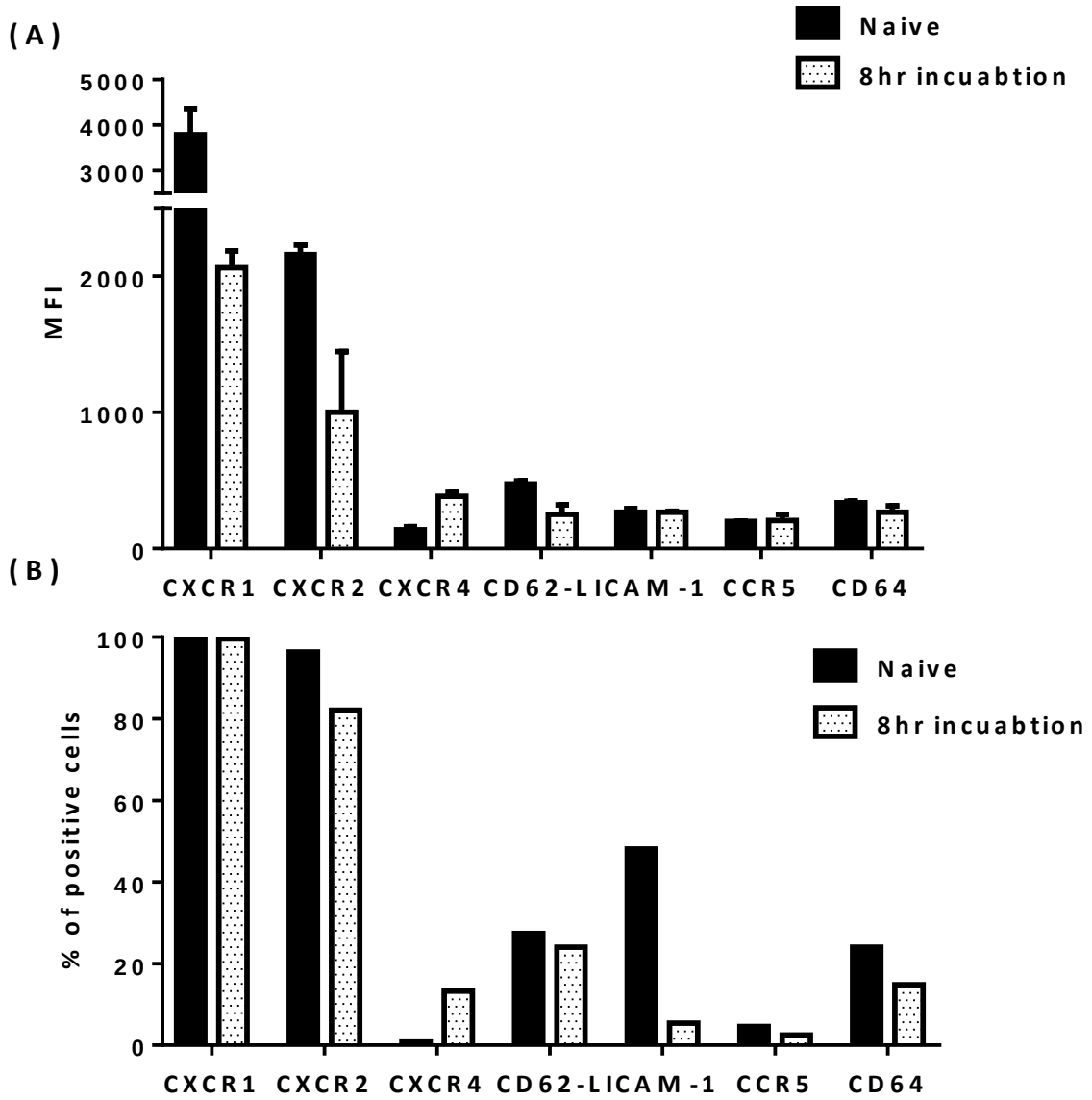

Figure 6.2 Neutrophil phenotype after 8 hours in culture. (A) Expression of CXCR (CXCR1, CXCR2 and CXCR4) adhesion molecules (ICAM-1, CD62-L) CCR5 and Fc γ receptor 1 (CD64) between freshly isolated neutrophils and neutrophils cultured in serum-free media for 8 hours then analysis by flow cytometry. Data are mean of MFI ± SD from 2 individuals. **(B)** Percentage of CD66b+ neutrophils positive for each of selected marker.

6.4.2. Phenotypic changes in polarized neutrophils

Isolated neutrophils were incubated for 8 and 24 h with recombinant MIF and HNSCC conditioned medium collected from FaDu MCTS and compared to neutrophils treated with INF-γ to stimulate an N1-like phenotype, TGF-β to stimulate an N2-like phenotype or to those cultured in medium alone. As a result of the small sample size and variability between donors, no statistically significance difference could be detected between the tested groups. However, several observations were noted in the pilot study data that will be discussed in the following section. First observation notice was that gating with the neutrophil specific marker CD66b gave a single cell population for both treated and un-treated control cells when cells were incubated for 8 hours. However, at 24 h neutrophils were split into 2 populations, one expressing high levels of CD66b and one expressing low levels and this was observed for neutrophils in all conditions tested (Fig. 6.3).

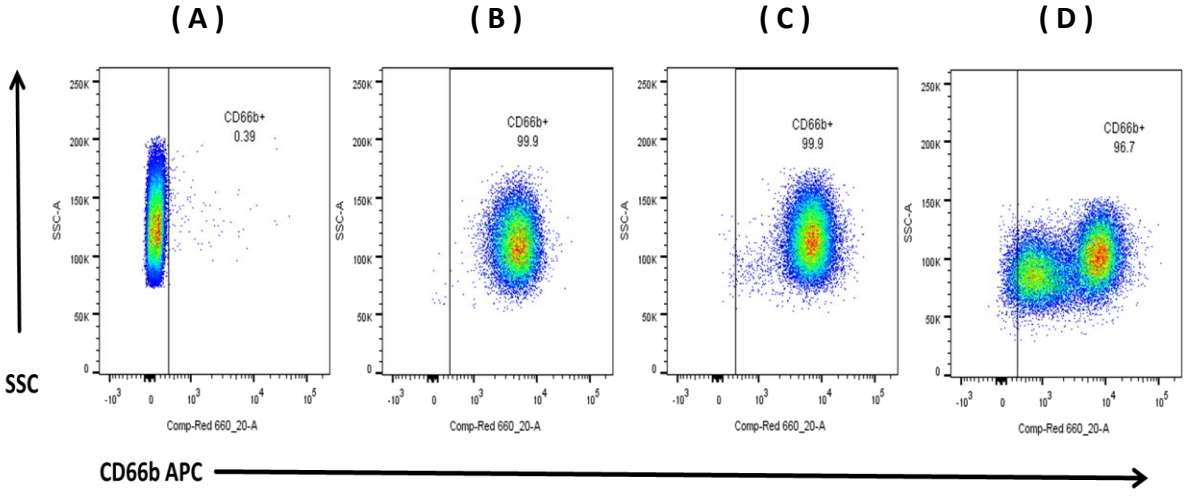

Figure 6.3 Flow cytometry analysis showing gating of neutrophils based on CD66 b in unstained cells **(A),** untreated cells **(B),** 8 hours TGF-β treated **(C)** and 24 hours TGF-β treated **(D).** Note the 2 populations of CD66b stained cells after 24 h.

Alternatively, the modulation of surface marker expression in CD66b+ neutrophils after 8 hours stimulation was expressed as % of cells positive for each marker (figure 6.4). No change in % of cells positive for CXCR1 was detected in any of treated groups after 8 hours. A slight reduction in % of CXCR2 was detected after INF-γ treatment (62.5%) followed by TGF-β (69%) and MIF (74.3%), while MCTS-CM showed same level of CXCR2 (81.8%) as control (82.1%). Massive increase in % of CD66b+ positive for CXCR4+ appeared after co-cultured with conditioned medium from FaDu MCTS (72.3% in compare to 13.3% media), while the use of single agent like TGF-β or MIF induce a slight increase (37.2% & 27.6%, respectively). Simalrly for percentage of CD6b+ positive for CD62L was increased upon MCTS-CM incubation (media 24%) to 54.8% of cells and reduce upon TGF-β treatment (9.86%). However, ICAM-1 was detected only in 5.4% of CD66b+ neutrophils but INF-γ treatment increase the population of ICAM-1 up to 48.7% and up to 36.6% after MCTS-CM, while only slight increase in %ICAM-1 was detected upon TGF-β or MIF (10%). As expected, treatment with INF-γ induce the percentage of CD64 positive cells from 14.8% to 38.7%, followed by MCTS-CM treatment (27.1%), while treatment with MIF (18.3%) and TGF-β (20.5%) show less predominant affect. Finally, although CCR5 have been suggested as a N2-TAN marker (Eruslanov et al., 2014), but only few cells was positive for CCR5 (2.53%) which only slightly up-regulte upon TGF-β (4.2%) .

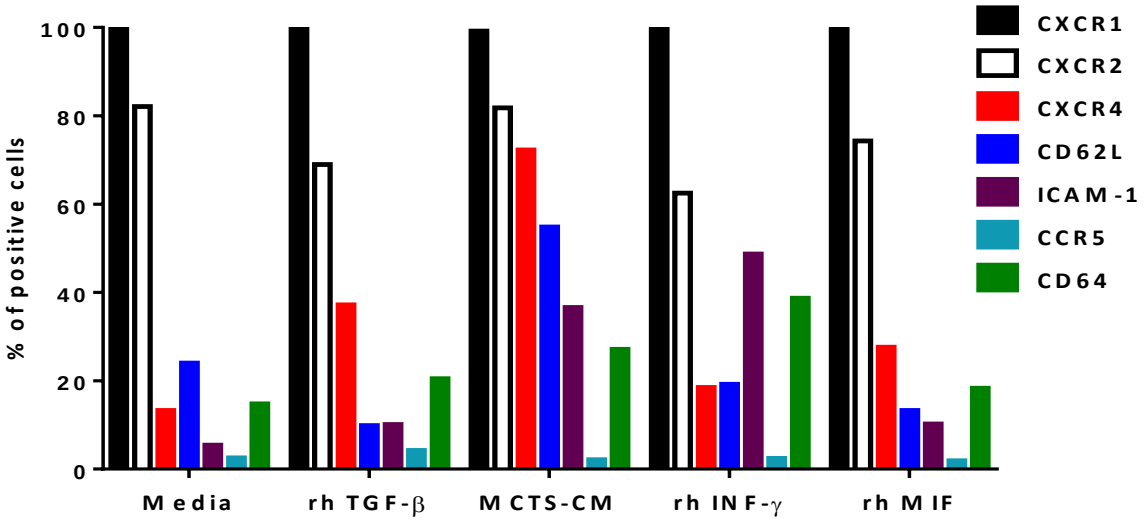

Figure 6.4 Bar chart represent percentage of cells positive for selected marker in response to different stimuli after 8 hours

Generally, the expression of both CXCR1 (2185) and CXCR2 (1001) in the media control group was almost the same as in all the treated groups (MFI for CXCR1 2055, 2030, 2146, 1931, MFI for CXCR2 895.5, 1004, 861.5, 861.5 For TGF-β, INF-γ, MIF and conditioned medium (CM), respectively; Fig. 6.5 and fig 6.6). Treatment of neutrophils with INF-γ increased the expression of ICAM-1 (409) and CD64 (279) compared to untreated cells (ICAM-1 (274) and CD64 (267) respectively), whereas none of the treatments affected the expression of CD62L (Fig. 6.4). On the other hand, when incubated with the N2 stimulant TGF-β, neutrophils presented with increased expression of CXCR4 (703.5) compared to untreated control cells (384). Cells incubated with recombinant MIF displayed slightly increased expression of CXCR4 (541), whereas conditioned medium from FaDu MCTS markedly increased the expression of neutrophil cell surface CXCR4 (1486). In addition, treatment with TGF-β also moderately increased the expression of CCR5 (248) compared to control (206) as did culture with INF-γ, recombinant MIF and conditioned medium (242, 252, 242, respectively).

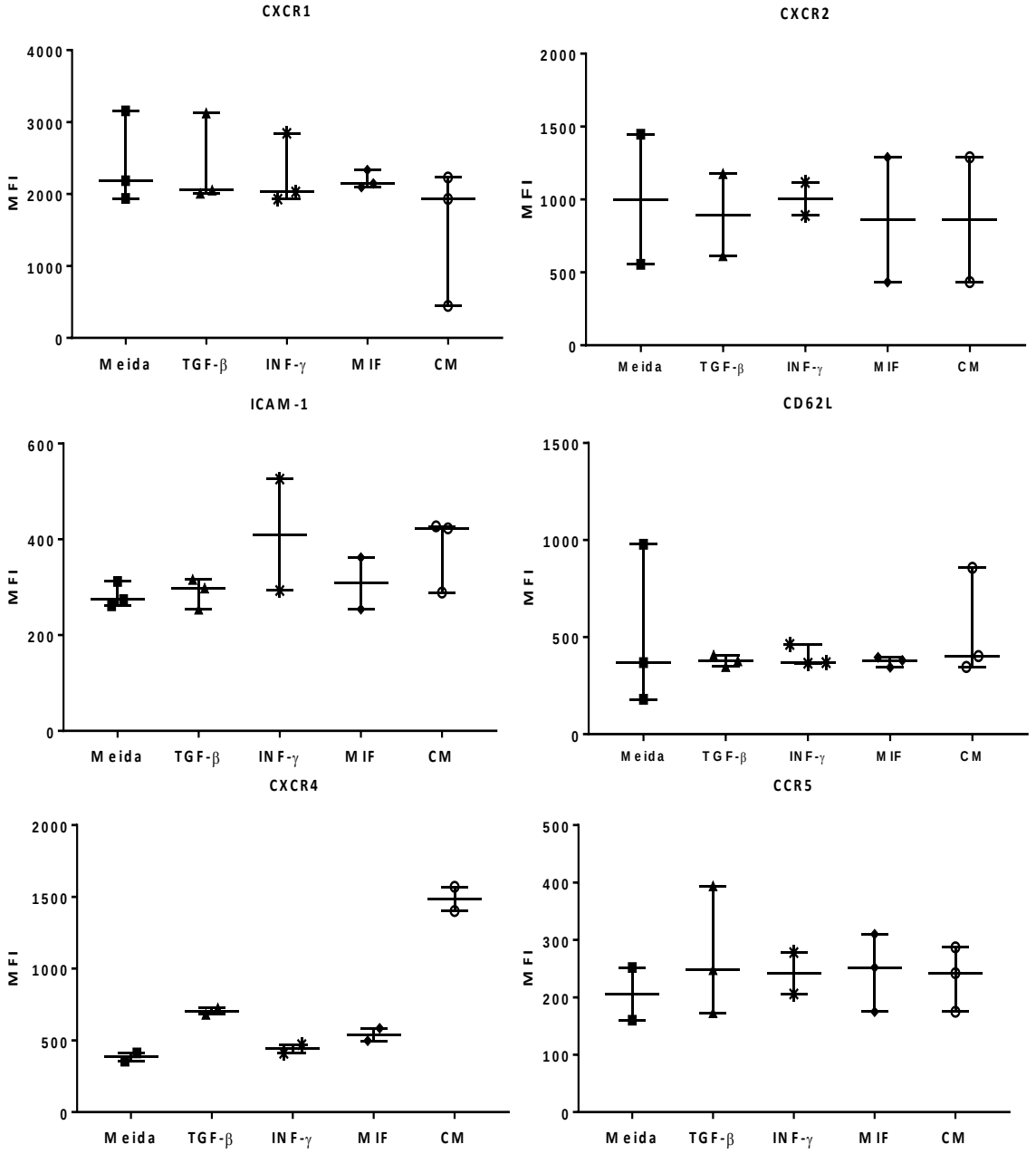

Figure 6.5 Modulation of neutrophil cell surface receptor expression in response to different stimuli. A whisker plot showing median expression with interquartile range of CXCR receptor (CXCR1, CXCR2 and CXCR4) adhesion molecules (ICAM-1, CD62-L) CCR5 and Fcγ receptor 1 (CD64) in untreated cells (media) neutrophils cultured in TGF-β, INF-γ, MIF and CM for period of 8 hours then analysis by flow cytometry. Data for 2 or 3 individuals is shown.

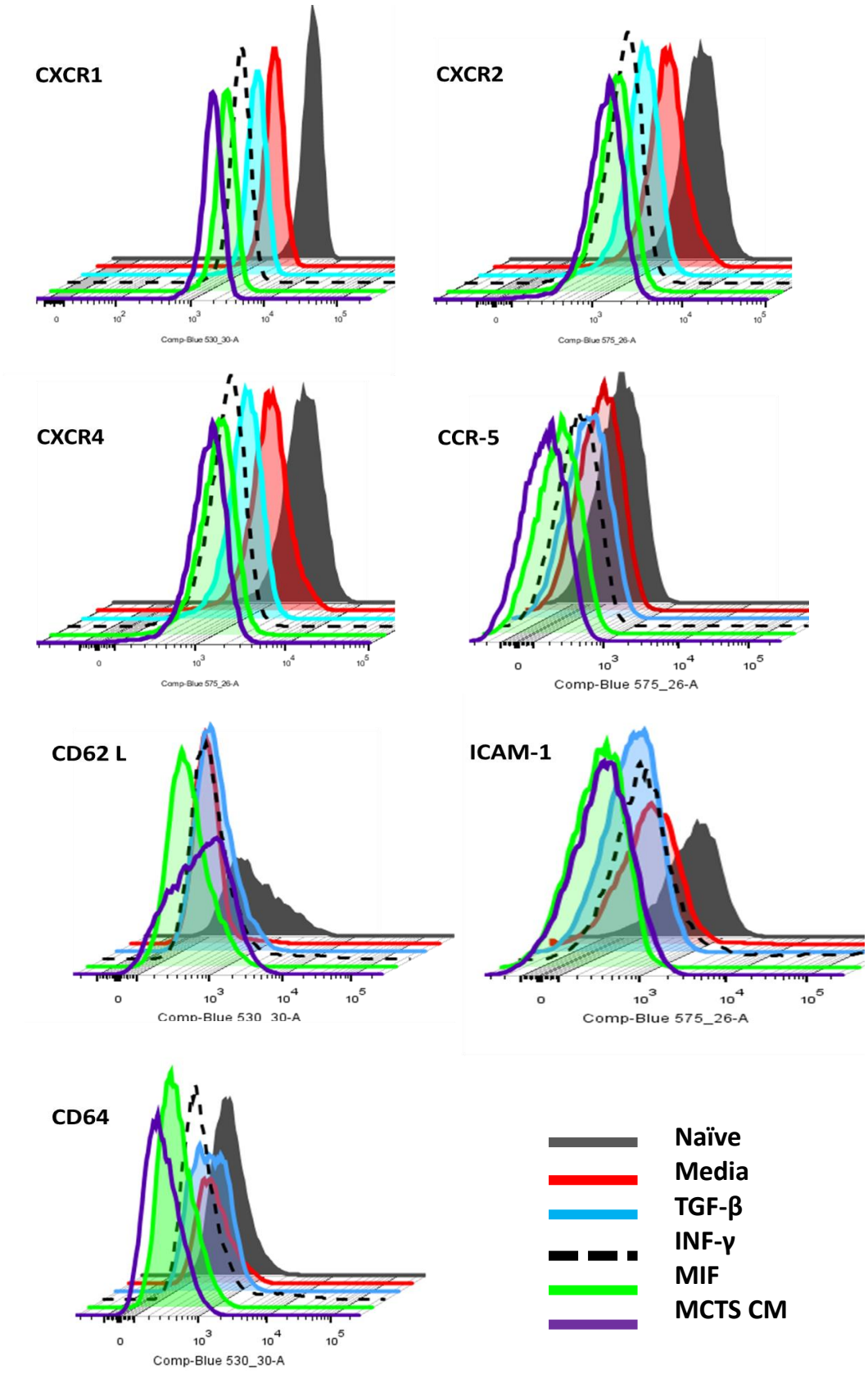

Figure 6.6 Representative histogram overlay plot of neutrophil cell surface receptor expression in unstimulated neutrophils (naïve) or in response to different stimuli after 8 hours.

6.4.3. Neutrophil phenotype after 24 hours incubation

Neutrophils incubated with same treatment regime were also analysed by flow cytometry after 24 hours. Unexpectedly, two populations were observed based on CD66b+ expression after 24 hours incubation on both control and treated neutrophils (Fig. 6.7-A). CD66b is an activation antigen that is specifically expressed on the cell surface of neutrophils and is also stored on the membrane of neutrophilic secondary granules that are released to the cell surface upon stimulation (Ducker and Skubitz, 1992). The number of CD66b+^{High} and CD66b+^{low} in each of the groups was analysed by gating each population. Untreated control neutrophils consisted of 65% CD66b+^{low} and 32% CD66b+^{High} (with 13% falling outside the gates). These levels were similar to neutrophils incubated with INF-γ (N1 phenotype) with 70% CD66b+^{low} and 26% CD66b+^{High} and neutrophils incubated with recombinant MIF (68% CD66b+^{low} and 27% CD66b+^{High}). In contrast, TGF-β stimulated (N2 phenotype) showed a decreased amount of CD66b+^{low} neutrophils (40%) but increased numbers of CD66b+^{High} neutrophils (59%). Similarly, neutrophils co-cultured in FaDu MCTS conditioned medium exhibited a similar pattern with 40% CD66b+^{low} and 60% CD66b+^{High} neutrophils (Fig. 6.7-B). Statistical analysis using one-way ANOVA highlights the major modulation of CD66b+ expression after 24 hours treatments. For example, TGF-β stimulated neutrophils significantly reduce the population of CD66b+^{low} (P= 0.0180) and induce the population of CD66b+^{High} (P= 0.0131). Treatment with FaDu MCTS conditioned medium also induce same pattern to TGF-β with significant diminish in expression of CD66b+^{low} neutrophils population (P=0.0215) and significant increase expression of CD66b+^{High} (P= 0.0214) in compare to untreated neutrophils control after 24hour *ex vivo* culture condition (Fig 6.8).

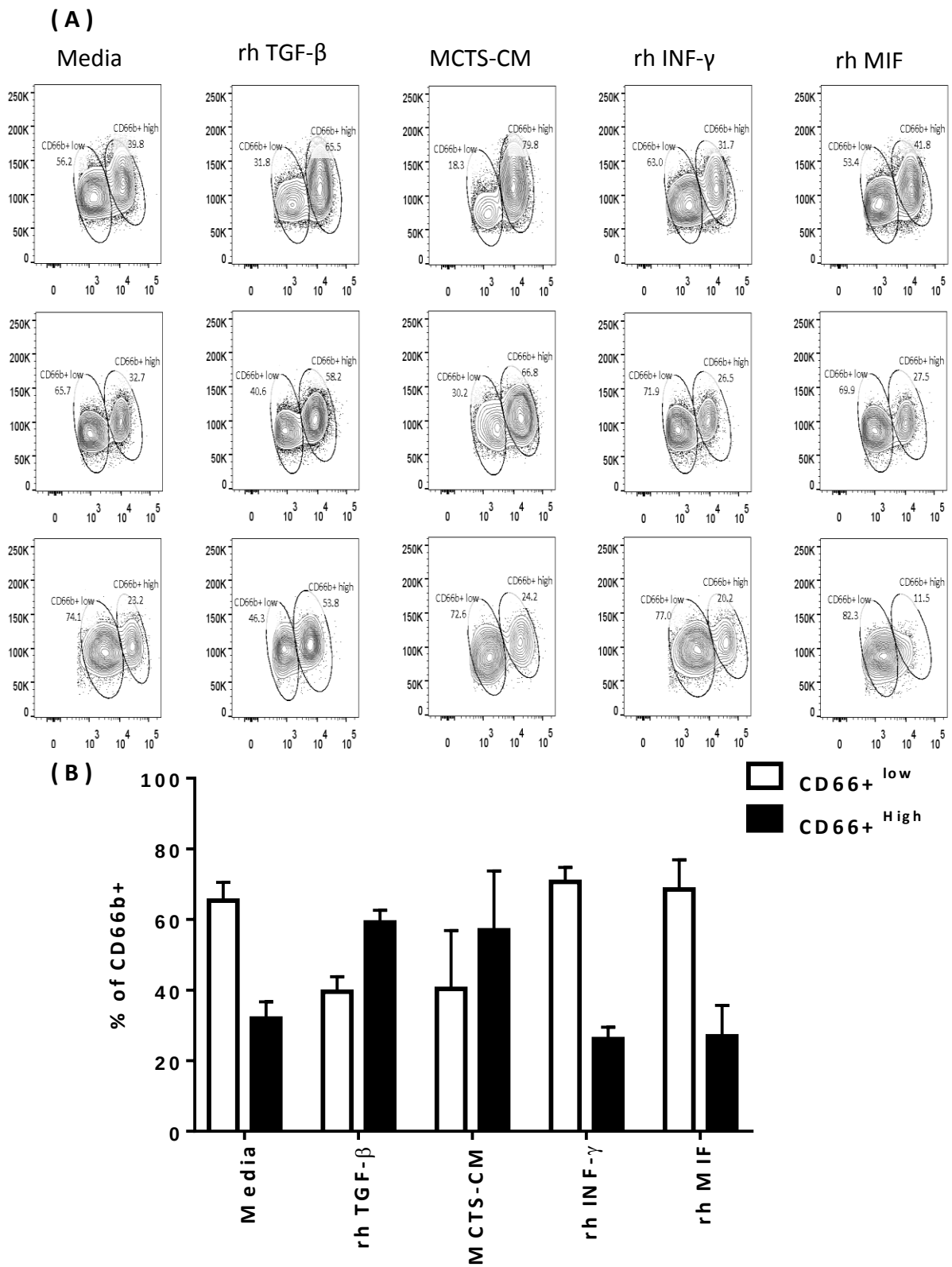

Figure 6.7 Response of neutrophils surface receptor after 24 h incubation. **(A)** Flow cytometry contour plot showing two population of cells based on CD66b+ expression. **(B)** bar chart summarising the modulation in expression of CD66b+ cells in untreated cells (media) neutrophils cultured in TGF-β, INF-γ, MIF and CM for a period of 24 hours. Data are represented from 3 individuals as Mean ± SEM.

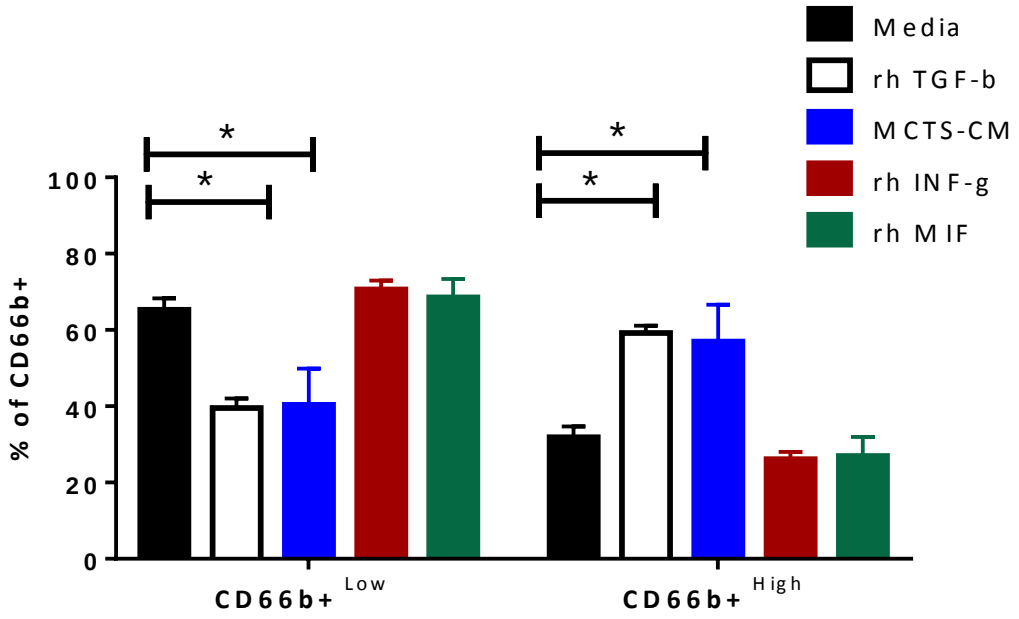

Figure 6.8 Statistical analysis comparing the change in CD66b+ expression in compared to untreated cell (media). One-way ANOVA was used to compute the modulation of CD66b+ expression after 24hours neutrophils cultured in TGF-β, INF-γ, MIF and CM for a period of 24 hours. Data are represented from 3 individuals as Mean ± SEM. *P<0.05

Unfortunately, due to time constraints, a detailed analysis for each of the surface expression markers was only carried out on one donor sample. The main observation was noticed by analysing the % of CXC4 positive cells is that after 24hours all neutrophils are CXCX4+ (83.8%) in compare to 13% of CD66b+ after 8 hours' incubation, which could indicate that neutrophils are coming to the end of their life-span. In compare to media (83.8%), MCTS-CM (99.7%), TGF-β (97.2%) followed by MIF (95.5%) are the factor induce expression of CXCR4% mainly. While CXCR1+ CD66b+ induce from 6.73% in un-treated neutrophils up to 48.9% in response to TGF-β, 43.8% in response to MIF, 31.4% in response to INF-γ and 16.2% in response to MCTS-CM. While TGF-β increase CXCR2 + population (73.8%), MCTS-CM (54%) and INF-γ (36.9%) reduce the number of CD66b+ CXCR2 in compare to control (67.5%). The CD66b+ cells that express adhesion molecules were low, where only CD62L detected in 1.21% of cells, ICAM-1 positive cells were increase mainly upon MCTS-CM stimulation (Fig 6.9). As two population of CD66b+ was detected as showed in figure 6.7-A and from histogram plot in figure 6.10 the analysis of each of the selected receptor was carried out separately.

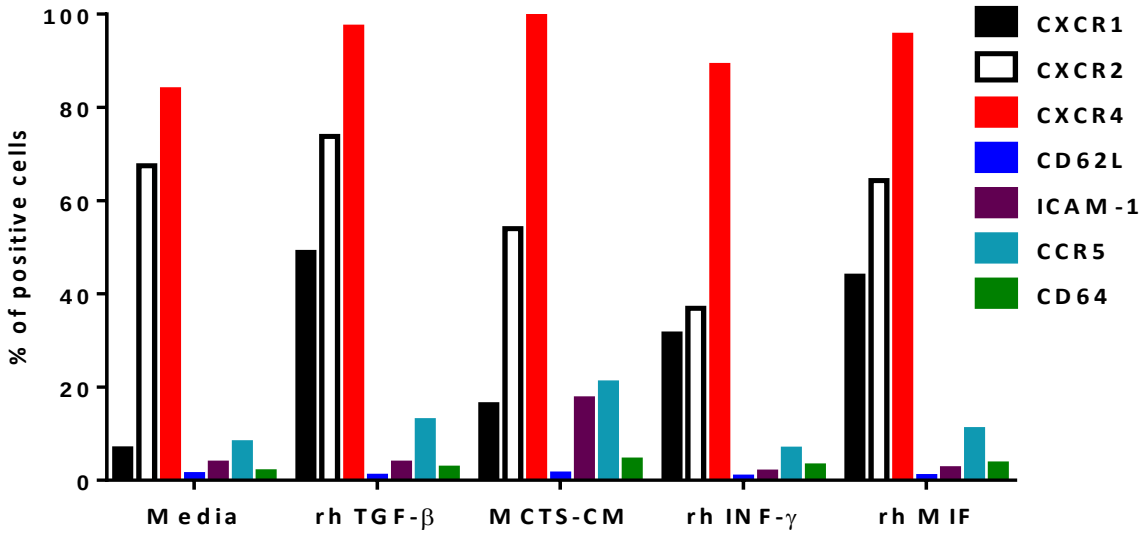

Figure 6.9 Bar chart represent percentage of cells positive for selected marker in response to different stimuli after 24 hours

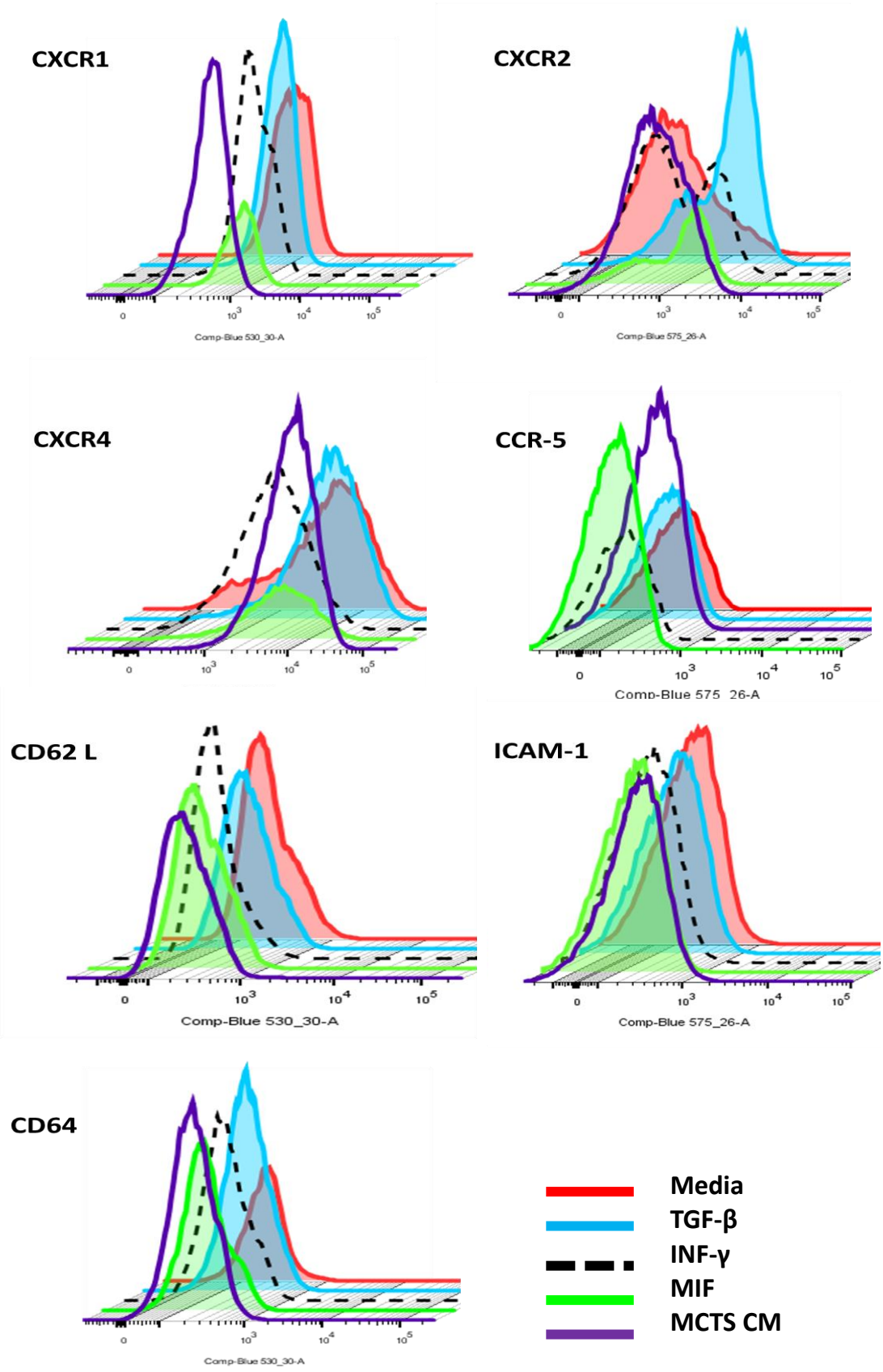

Figure 6.10 Representative histogram overlay plot of neutrophil cell surface receptor expression in in response to different stimuli after 24 hours.

In general, neutrophils that were CD66bhi displayed increased expression of all the markers tested than CD66blow neutrophils irrespective of whether they were stimulated or not. Of note, TGF-β treatment induced increased expression of CXCR4 (7114) on CD66b+High and CD66b+low (5127) neutrophils when compared to control (media) cells (CD66b+High (4270) and CD66b+low (3597) respectively). Again, this increased CXCR4 and ICAM-1 expression was observed in neutrophils treated with conditioned medium from FaDu MCTS. The conditioned medium cells also showed decreased expression of CXCR1 and CXCR2 compared to controls. In contrast, treatment with INF-γ reduced the expression of CXCR4. Recombinant MIF did not alter the expression pattern of CXCR4 (CD66b+High (4965) and CD66b+low (4017) and levels of CCR5, CD64, CD62L were unchanged in all samples at this time point (fig.6.11).

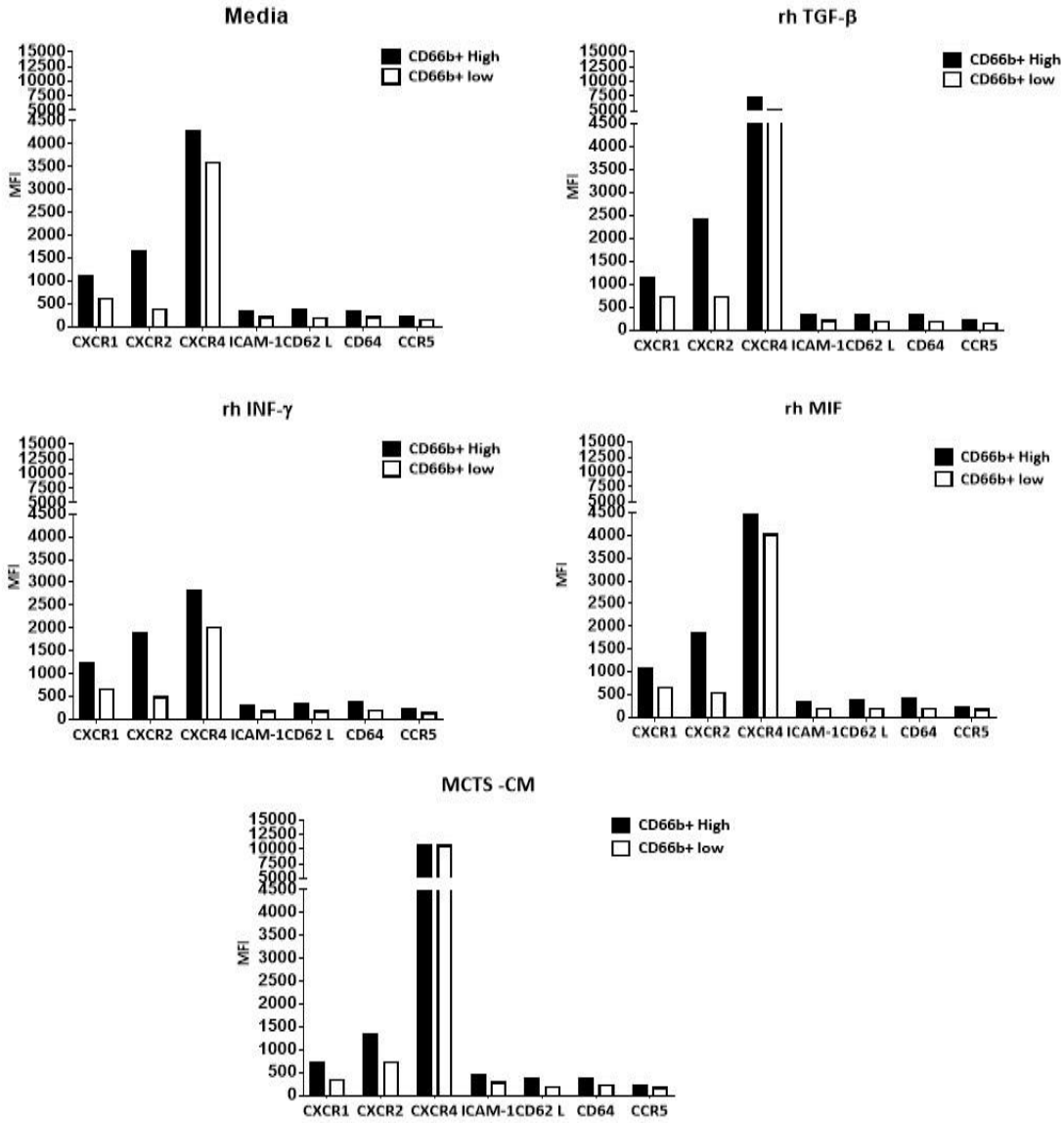

Figure 6.11 Characterisation of neutrophils by flow cytometry after 24 hours. A bar chart comparing the expression of CXCR (CXCR1, CXCR2 and CXCR4), adhesion molecules (ICAM-1, CD62-L) CCR5 and Fc γ receptor 1 (CD64) in CD66b+^{High} and CD66b+^{low} in untreated cells (media) neutrophils cultured in TGF-β, INF-γ, MIF and conditioned medium (CM) for 24 hours. Data represented MFI of one donor.

6.5. Discussion

There are currently only a few studies that have examined human neutrophil polarisation, often because of the difficulty in isolating unstimulated neutrophils from blood as well as from tumour tissue and the lack of well-characterised polarisation markers. Moreover, neutrophils are short-lived cells that do not survive well once isolated from the circulation or tissues. Indeed, cell surface expression of CXCR1, CXCR2 and CD62L decreased dramatically whereas CXCR4 increased upon 8-hour *in vitro* culture with medium alone compared to expression on freshly isolated neutrophils from the same donor. A previous study by Fortunati et al showed that cultured neutrophils acquired a phenotype characterized by decreased expression of CXCR1, CXCR2, CD62-L and up-regulation of ICAM-1 in time-dependent manner (Fortunati et al., 2009). The alteration in expression of CXCR4 is likely to be a natural response to cell survival signals as neutrophils in the circulation programmed for cell destruction in the bone marrow or spleen increase expression of CXCR4 and decrease expression of CXCR1 and CXCR2 in order to migrate back to these tissues when their life-span is coming to an end (Martin et al., 2003). Therefore, it is likely that decreased CXCR1/2 and CD62L and increased CXCR4 observed in culture are stress response signals signifying the desire for neutrophil termination.

Neutrophils cultured for 8 hours in the presence or absence of stimulants were analysed by flow cytometry for differences in N1, N2 polarisation markers. According to the few studies examining neutrophil phenotypes, N1 neutrophils should display decreased CXCR1/2 and CD62L expression, and increased ICAM-1 expression (Andzinski et al., 2016). Using the N1 stimulant INF-γ, overall we observed no change in CXCR1/2 or CD62-L expression but an increase in ICAM-1 expression compared to unstimulated neutrophils, so only one of the markers tested confirmed with previous data. Stimulation with MIF did not increase any of

the proposed N1 markers, however, incubation with FaDu MCTS conditioned medium did increase ICAM-1, suggesting at least some polarisation to an N1 phenotype if expression of these markers are believed to represent an N1 phenotype. Previously, Eruslanov *et al* (2014) characterized human TAN isolated from early stage lung cancer as $CD66b^{+}CD11b^{+}CD15^{hi}$, here TAN were characterized by ICAM-1^{hi} (in the previous study shown to be an N1 marker), CD62-L^{low}, $CXCR4^{hi}$, $CCR5^{hi}$, $CCR7^{hi}$, $CXCR3^{hi}$ (Eruslanov et al., 2014). At the mRNA level, high expression of CXCR4 as well as other cytokines (VEGF, arginase, CCL2, CCL5, MMP-9, C-MYC and STAT-3) has been detected in N2 TAN from murine tumours (Jablonska et al., 2010). Overall we found that after 8 hours human neutrophils stimulated with the N2 polarisation factor TGFβ a cytokine found to be over-expressed in HNSCC patients, (Rosenthal et al, 2004), displayed increased expression of CXCR4, with no change in the other markers analysed (CCR5, CCR7 and CXCR3 were not analysed in this study). Therefore, increases in some but not all suggested N2 markers were the same as observed in previous studies and it could be that increased expression in of CXCR4, are the most reliable markers for the human N2 phenotype. If this is the case then it could be argued that MIF and conditioned medium for FaDu MCTS in particular, skew neutrophils towards an N2 pro-tumour phenotype.

After 24 hours it was noted that there were 2 populations of CD66b+ in both control and treated neutrophils whereas at 8 hours neutrophils showed as only a single population. Expression of cell surface CD66b has been shown to increase on activated, degranulating neutrophils (Ducker and Skubitz, 1992), suggesting that over time in culture some neutrophils become activated increasing their cell surface expression of CD66b. Interestingly, the ratio of high/low expressing neutrophils was similar for medium control, INFY and MIF-treatment with more $CD66b^{low}$ than $CD66b^{hi}$ cells. In contrast, treatment with the N2 cytokine TGFβ and

FaDu conditioned medium displayed elevated numbers of $CD66b^{hi}$ compared to $CD66b^{low}$ neutrophils. This suggests that TGFβ and FaDu conditioned medium may be able to further stimulate neutrophil degranulation and therefore their activation status increasing expression of CD66b. Expression of polarisation markers on both $CD66b^{low}$ and $CD66b^{hi}$ neutrophils was conducted for only one of the donor samples due to time constraints and so interpretation of this data must be taken lightly. The data showed that in nearly all cases $CD66b^{hi}$ neutrophils expressed more sell surface markers than $CD66b^{low}$ neutrophils and this may be linked with differences in their activation status. On the whole data at 24 hours matched those at 8 hours with TGFβ and conditioned medium from FaDu displaying increased expression of CXCR4 (and ICAM-1 for conditioned medium) suggesting polarisation to an N2 phenotype. Treatment with MIF did not alter any polarisation markers at this time point.

The use of specific cell surface markers to characterise neutrophil polarisation into N1 or N2 phenotypes is controversial and at best can be described as in an early stage of development. Because only a few studies have been performed in this area there is currently no consensus as to which markers are N1 and which are N2. However, if the current paradigm is to be believed, the pilot data generated in this chapter tentatively suggest that the tumour microenvironment from HNSCC may polarise neutrophils to an N2 phenotype although this seems to be independent of MIF and may be due to TGFβ amongst other cytokines. Clearly, further experiments are required on more individuals to overcome individual-to-individual variability in cell surface expression of these markers and to gain a consensus of neutrophil polarisation. In addition, analysing the phenotype of neutrophils within HNSCC or even within specific areas of these tumours (necrotic, invasive front) and comparing these to the

neutrophil phenotype in non-diseased tissue would further clarify phenotypic markers and if these have any meaning in tumour progression or for diagnostic purposes.

Unfortunately, this study was not able to investigate functional changes in neutrophil activity or cytokine secretion upon polarised as suggested in the literature (Fridlender et al., 2009 and Jablonska et al., 2010). Clearly, this is an emerging field and further extensive and detailed analysis of the change (or not) in polarised human TAN and their roles in tumour progression are required.

Chapter 7: General Discussion

Several studies have linked the number of TAN in various types of cancer, including HNSCC, with poor patient prognosis, suggesting that the presence of neutrophils within tumours has an impact on tumour progression and outcome. However, only a few of these studies have evaluated TAN localization within cancer tissue. In chapter 3, the spatial distribution of TAN within HNSCC tissue of a small cohort of patients showed that TAN mainly accumulate in necrotic and stromal areas. The tumour stroma is the area that probably has the most cell diversity within the tumour microenvironment. It is composed of fibrous connective tissue and various types of non-cancerous cells that secrete factors, which continuously interact with the tumour cells. This process is often termed desmoplastic reaction (DR), which is characterized by a connective tissue densely packed with fibroblasts, inflammatory and endothelial cells. DR has been reported in HNSCC (Janot et al., 1996), but the contribution of neutrophils in the tumour stroma is poorly understood. Most studies have focused on the communication between CAFs, the most predominant component of the stroma, and the adjacent tumour cells to provide evidence that this cell-cell interaction modulates tumour growth and facilitates HNSCC invasion (Rosenthal et al, 2004, Kawahiri et al 2009). However, this study observed many neutrophils in the tumour stroma of HNSCC patient biopsies; an observation reported in hepatocellular carcinoma (HCC) (Kuang et al., 2011). In HCC the $CD15^+$ neutrophils found in tumour stroma was associated with increased MMP-9 expression, a known regulator of the angiogenic switch. An *in vivo* study has showed that co-culture of $Gr\text{-}1^+CD11b^+$ neutrophils isolated from tumour-bearing mice promoted the activation of CAF and displayed enhanced survival and increased expression of cytokines, indicating the importance of cell communication between many cell types, including neutrophils within in the tumour

stroma. Furthermore, these interactions highlight the possibility of targeting tumour growth by disturbing the tumour stroma, indeed, treatment with the immunomodulatory drug dexamethasone reduced DR and attenuated tumour growth in a murine tumour model (Stairs et al., 2011). Collectively, these data support the notion that the presence of neutrophils in the tumour stroma is important in tumour progression and so further *in vivo* studies ideally using orthotropic HNSCC tumours along with Ly6G-depleted neutrophils and knock-out mice deficient in fibroblast-derived factors are required to substantiate these observations.

TAN were found to accumulate in necrotic areas of HNSCC tumours. Necrotic tissue develops as a result of chronic stress due to the lack of oxygen within tissue. The presence of necrosis has been observed in HNSCC and patients with low levels of tumour necrosis were found to have a better prognosis and responded better to chemotherapy than patients with large areas of necrosis who tended to develop chemoresistant tumours (Kuhnt et al., 2005). Data in this thesis found that neutrophils were recruited in large numbers to areas of tumour necrosis. Although the mechanism of neutrophil recruitment to necrotic areas is largely unknown it is likely due to increased expression of hypoxia-regulated chemoattractants or factors released from necrotic tissue. This was substantiated to a degree by the finding that FaDu hypoxic conditioned medium was more chemotactic than that produced from cells cultured under normoxic conditions, and that MIF gene expression was up-regulated by hypoxia. Zhu et al also observed accumulation of Gr-1+CD11b+ neutrophils around the necrotic zone in a xenograft HNSCC tumour model, and confirmed the increased migration of Gr-1+CD11b+ to hypoxic derived conditioned medium *in vitro.* Similar to our MCTS cytokine array analysis, the authors detected MIF, IL-6, sICAM-1, and PAI-1 release from HNSCC from under normoxic conditions with increased expression under hypoxia (Zhu et al., 2014). Knock-down of HIF-1α

and HIF-2α, the main regulatory mechanism for hypoxia in HNSSC cells, reduced the level of MIF but, in contrast to the data presented here, did not affect Gr-1+CD11b+ migration towards hypoxic condition medium *in vitro*, suggesting that other factors were responsible for the recruitment of neutrophils (Zhu et al., 2014). Other factors may also aid recruitment of neutrophils to necrotic areas such as HMGB1, a protein released by necrotic tissue (Scaffidi et al., 2002). HMGB1 specifically triggers neutrophil but not macrophage migration to necrotic tissue and this is independent of CXCR4 (Scaffidi et al., 2002). Whereas migration of neutrophils lacking RAGE (receptor for advanced glycation end-products), the HMGB1 receptor, was reduced by 80% toward liver necrotic lysate compared to control neutrophils (Huebener et al., 2015). Further investigation using laser capture microdissection to isolate neutrophils from stroma and necrotic tissue of HNSCC patient tissue will help understand the molecular mechanism of recruitment and the cross-talk between TAN and cancer cells. It is likely that neutrophils accumulating in large numbers in HNSCC biopsies in this study do so by a combination of hypoxia regulated chemoattractants such as MIF and CXCL12 and the actions of HMGB1 within the necrotic debris. This study is limited by the number of patient samples analysed and inability to link neutrophil numbers and MIF expression in various areas of the tumour to patient outcome. Access to further patient samples and clinical data would have allowed a more in-depth statistical analysis and further investigation in this area is required.

In chapter 4, MCTS generated from HNSCC carcinoma cells were utilized to investigate the complex phenomena of neutrophil recruitment and factors responsible for this process. The use of an *in vitro* 3D model to study the immune cell-tumour cell interaction provides an excellent alternative to conventional monolayer culture and experimental murine models where species differences occur. For example, neutrophils account for 50-70% of peripheral

blood leukocytes in humans, while they only make up 15-20% of peripheral blood leukocytes in mice (Haley, 2003). The key observation was that MCTS secrete multiple neutrophil chemoattractant factors, such as MIF, CXCL1 and CXCL8. MIF overexpression was detected in HNSCC patient biopsies and FaDu cells and has been reported previously by others (Kindt et al., 2013b, CLUDTS et al., 2010, Dumitru et al., 2011). Pre-incubation of neutrophils with a pharmacological inhibitor of CXCR4 and CXCR2 significantly inhibited neutrophil recruitment suggesting that ligands binding to these receptors (MIF, CXCL1, CXCL8, CXCL12) are important in this process. FaDu MCTS express little CXCL12 (array data) suggesting that factor is not crucial for neutrophil recruitment. Moreover, the MIF specific inhibitor ISO-1 caused a dramatic inhibition of neutrophil infiltration that was greater than blocking CXCR2 or CXCR4. This observation and the fact that neutrophils do not express the MIF receptor CD74 (Dumitru et al., 2011) strongly suggest that MIF is the main neutrophil chemoattractant and this is via a CXCR2/CXCR4 axis. Similar findings were observed when MIF expression was prevented in knock down studies using HNSCC cell lines Cal-27 and Tca8113. When MIF expression was blocked, Gr-1+CD11b+ neutrophil recruitment was reduced from 10% to 4% (61% reduction) in a nude mouse xenograft model (Zhu et al., 2014). Using ISO-1 the data presented in this thesis showed reduced Ly6G neutrophil infiltration up to 80% *in vivo* and 87% *in vitro* MCTS FaDu model. The difference between these studies could be due to the different HNSCC cell types employed. The involvement of CXCR4 in neutrophil chemotaxis has not reported before but migration of B lymphocyte towards MIF or CXCL12 was reduced significantly upon treatment of B cells with AMD3100 (Klasen et al., 2014). Interestingly, *in vitro* and *in vivo* data in this study showed that THP-1 monocyte recruitment to HNSCC might also by MIF-dependent, or at least partially. Previous studies examining other tumour-derived factors have pointed to CCL2 and/or CXCL12 amongst other molecules as the main ligands that recruit

monocytes to tumours (Kitamura et al., 2015, Murdoch et al., 2004). This is the first report citing MIF as an important tumour-derived factor to recruit monocytes to HNSCC tumours. However, these data must be taken with caution as the THP-1 monocytic cell line was used in this study and there are several reports that THP-1 cells are not good models of peripheral blood monocytes (Heil et al., 2002) and so these data need to be repeated using human peripheral blood monocytes. Clearly, further investigations are required to confirm these findings but it does raise the possibility that MIF inhibition may reduce recruitment of both TAN and TAM.

This hypothesis was further investigated in chapter 5 where depletion of neutrophils using anti-Ly6G caused a decrease in tumour volume compared to PBS controls. Similarly, Ly6G depletion of neutrophils caused a reduction in tumour growth in melanoma and fibroosarcoma *in vivo* tumour models (Jablonska et al., 2010) supporting the tumour-facilitating role of TAN. Administration of ISO-1 in CD-1 mice bearing subcutaneous FaDu tumours caused a significant reduction in the number of TAN and TAM but increased the size of tumour. This result was unexpected as a reduction in tumour size upon ISO-1 treatment was previously reported in a murine model of colon and prostate cancer (He et al, 2009, Meyer-Siegler 2006). Histological examination showed large areas of necrosis in ISO-1 treated tumours when compared to PBS-treated controls and unexpectedly this observation was associated with a reduction in the number of proliferative (BrdU+) cells in ISO-1-treated compared to control tumours. These results were opposite to those found with neutrophil depletion using Ly6G and points to the involvement of MIF in other tumour processes as well as leukocyte recruitment. For example, the reduction of tumour cell proliferation could be a direct effect of blocking the actions of MIF on tumour cells and not as a result of neutrophil

depletion. Several *in vitro* studies have shown that MIF inhibition using ISO-1 in lung (A549) (Rendon et al., 2007) prostate (DU145) (Meyer-Siegler et al., 2006) and glioblastoma (LN229) (Schrader et al., 2009) affected the migration, proliferation and invasiveness of these cancer cells. Accordingly, blocking exogenous MIF may diminish the proliferation ability of HNSCC tumour cells. This is supported by evidence showing that blocking endogenous MIF using shRNA in HNSCC cells resulted in a significant inhibition of tumour cell proliferation and motility, suggesting that endogenous MIF acts in an autocrine feedback mechanism to promote cell division and migration (Kindt et al., 2013b). Therefore, it is possible that MIF acts to accelerate tumour growth in an autocrine fashion in early tumours leading to increased tumour growth, and increased hypoxia and necrosis but then tumour cell proliferation is inhibited by ISO-1 treatment leading to low tumour cell proliferation rates observed in later *in vivo* tumours. In other words, the effect of inhibiting MIF in other aspects of tumour biology in addition to the recruitment of leukocytes may significantly impact on tumour growth. Further investigations are required specifically looking at the early stage tumours to examine the precise role of MIF during HNSCC tumour progression. These studies could include the use of MIF knockout mice or MIF knock-out HNSCC cell lines, preferably implanted orthotopically as these will be more representative of tumours in humans.

Although differences in vascularisation (CD31) were not found in this study between neutrophil-depleted and control tumours, there is much evidence to suggest that neutrophils can express pro-angiogenic factors and therefore have a significant impact tumour angiogenesis (Tazzyman et al, 2013). For example, $CXCR4^{hi}$ neutrophils are rapidly recruited to pancreatic islets that have been grafted into striated muscles. These $CXCR4^{hi}$ neutrophils produced 10 times more MMP-9 than neutrophils recruited to inflammatory stimuli with this

factor mediating islet revascularization (Christoffersson et al., 2012). A further investigation by same group using a different mouse model showed that hypoxia-induced secretion of VEGF-A identified distinct cell surface receptor expression on circulating pro-angiogenic neutrophils, such as VEGF receptor1 (VEGFR1), CXCR4 and integrin a4 subunit (CD49d) in both humans and mice (Massena et al., 2015). This observation may explain the increase in CXCR4 expression that we reported upon neutrophil stimulation with TGF-ß and conditioned medium from FaDu MCTS.

In chapter 6, the effect of MIF and HNSCC-derived molecules on TAN polarization *ex vivo* was examined by flow cytometry. Neutrophils acquired an activated phenotype, characterized by decreased expression of CXCR1, CXCR2, CD62L and up-regulation of ICAM-1 in time-dependent manner. Stimulation with the N2 polarisation factor TGFβ increased expression of CXCR4 and to a lesser extent CCR5. Prolonged culture of neutrophils for 24 hours resulted in two populations of CD66b+ neutrophils in both control and treated groups whereas at 8 hours only one population was observed. Although only based on three (and in some instances two) blood samples this study provides pilot data that healthy neutrophils can change their phenotype based on their cell surface marker expression when stimulated. However, since there are very few studies to analyse and validate neutrophil polarisation markers it is difficult to determine what exactly constitutes a N1 or N2 phenotype. Expression of cell surface CD66b has been shown to increase on activated neutrophils (Ducker and Skubitz, 1992), suggesting that over time in culture all neutrophils become activated. This is a very preliminary study and neutrophil polarisation into N1 or N2 phenotypes is controversial as most of the evidence for TAN polarization comes from murine studies and these markers may not translate to a human setting. To date, only one study has attempted to characterise TAN

polarisation markers in neutrophils isolated from early stage lung cancer tissue. These cells were described as CD66b+CD11b+CD15^{hi} and characterized by ICAM-1^{hi}, CD62L^{low}, CXCR4^{hi}, CCR5^{hi}, CCR7^{hi}, CXCR3^{hi} (Eruslanov et al., 2014). This study is unable to confirm that TGFβ induces an N2 phenotype or that INFγ treatment induces an N1 anti-tumour phenotype and more studies from the field need to be published to validate and confirm these markers. However, for the first time, this study shows that neutrophils from healthy volunteers can be polarised, in particular by culturing them with HNSCC tumour-derived factors where elevated expression of CXCR4 was evident, pointing to an N2 phenotype. This is strong evidence that tumour factors as a whole can modulate the gene and protein expression of neutrophils; the implications of these changes require further examination.

Overall the data provided in this thesis show that MIF is overexpressed in HNSCC tumours and this factor appears to be central for the recruitment of TAN and possibly TAM into HNSCC, and that this occurs by activation of CXCR2 and CXCR4. There is very good evidence that leukocyte (TAN and TAM) recruitment into HNSCC is closely linked with poor prognosis, and although not identified in this study, this appears to be due to pro-angiogenic factors that these cells secrete within the tumour microenvironment that aids tumour progression. Therefore, inhibiting the actions of MIF may be a potential adjunctive therapy aimed at increasing the survival rates of individuals presenting with HNSCC.

REFERENCES

AARBIOU, J., ERTMANN, M., VAN WETERING, S., VAN NOORT, P., ROOK, D., RABE, K. F., LITVINOV, S. V., VAN KRIEKEN, J. H., DE BOER, W. I. & HIEMSTRA, P. S. 2002. Human

neutrophil defensins induce lung epithelial cell proliferation in vitro. *Journal of leukocyte biology,* 72**,** 167-74.

ACOSTA, J. C., O'LOGHLEN, A., BANITO, A., GUIJARRO, M. V., AUGERT, A., RAGUZ, S., FUMAGALLI, M., DA COSTA, M., BROWN, C., POPOV, N., TAKATSU, Y., MELAMED, J., D'ADDA DI FAGAGNA, F., BERNARD, D., HERNANDO, E. & GIL, J. 2008. Chemokine Signaling via the CXCR2 Receptor Reinforces Senescence. *Cell,* 133**,** 1006-1018.

ADDISON, C. L., BELPERIO, J. A., BURDICK, M. D. & STRIETER, R. M. 2004. Overexpression of the duffy antigen receptor for chemokines (DARC) by NSCLC tumor cells results in increased tumor necrosis. *BMC Cancer,* 4**,** 28-28.

ADDISON, C. L., DANIEL, T. O., BURDICK, M. D., LIU, H., EHLERT, J. E., XUE, Y. Y., BUECHI, L., WALZ, A., RICHMOND, A. & STRIETER, R. M. 2000. The CXC Chemokine Receptor 2, CXCR2, Is the Putative Receptor for ELR⁺ CXC Chemokine-Induced Angiogenic Activity. *The Journal of Immunology,* 165**,** 5269-5277.

AHUJA, S. K. & MURPHY, P. M. 1996a. The CXC chemokines growth-regulated oncogene (GRO) alpha, GRObeta, GROgamma, neutrophil-activating peptide-2, and epithelial cell-derived neutrophil-activating peptide-78 are potent agonists for the type B, but not the type A, human interleukin-8 receptor. *The Journal of biological chemistry,* 271**,** 20545-50.

AHUJA, S. K. & MURPHY, P. M. 1996b. The CXC Chemokines Growth-regulated Oncogene (GRO) α, GROβ, GROγ, Neutrophil-activating Peptide-2, and Epithelial Cell-derived Neutrophil-activating Peptide-78 Are Potent Agonists for the Type B, but Not the Type A, Human Interleukin-8 Receptor. *Journal of Biological Chemistry,* 271**,** 20545-20550.

AL-ABED, Y., DABIDEEN, D., ALJABARI, B., VALSTER, A., MESSMER, D., OCHANI, M., TANOVIC, M., OCHANI, K., BACHER, M., NICOLETTI, F., METZ, C., PAVLOV, V. A., MILLER, E. J. & TRACEY, K. J. 2005. ISO-1 Binding to the Tautomerase Active Site of MIF Inhibits Its Pro-inflammatory Activity and Increases Survival in Severe Sepsis. *Journal of Biological Chemistry,* 280**,** 36541-36544.

AL-LAMKI, R. S., SADLER, T. J., WANG, J., REID, M. J., WARREN, A. Y., MOVASSAGH, M., LU, W., MILLS, I. G., NEAL, D. E., BURGE, J., VANDENEBEELE, P., POBER, J. S. & BRADLEY, J. R. 2010. Tumor Necrosis Factor Receptor Expression and Signaling in Renal Cell Carcinoma. *The American Journal of Pathology,* 177**,** 943-954.

ALCOLEA, S., ANTON, R., CAMACHO, M., SOLER, M., ALFRANCA, A., AVILES-JURADO, F. X., REDONDO, J. M., QUER, M., LEON, X. & VILA, L. 2012. Interaction between head and neck squamous cell carcinoma cells and fibroblasts in the biosynthesis of PGE2. *J Lipid Res,* 53**,** 630-42.

ALDO, P. B., CRAVEIRO, V., GULLER, S. & MOR, G. 2013. Effect of culture conditions on the phenotype of THP-1 monocyte cell line. *Am J Reprod Immunol,* 70**,** 80-6.

ALKUREISHI, L. W. T., ROSS, G. L., SHOAIB, T., SOUTAR, D. S., ROBERTSON, A. G., THOMPSON, R., HUNTER, K. D., SORENSEN, J. A., THOMSEN, J., KROGDAHL, A., ALVAREZ, J., BARBIER, L., SANTAMARIA, J., POLI, T., SESENNA, E., KOVÁCS, A. F., GRÜNWALD, F., BARZAN, L., SULFARO, S. & ALBERTI, F. 2010. Sentinel Node Biopsy in Head and Neck Squamous Cell Cancer: 5-Year Follow-Up of a European Multicenter Trial. *Annals of Surgical Oncology,* 17**,** 2459-2464.

AN, X., DING, P. R., WANG, F. H., JIANG, W. Q. & LI, Y. H. 2011. Elevated neutrophil to lymphocyte ratio predicts poor prognosis in nasopharyngeal carcinoma. *Tumour biology : the journal of the International Society for Oncodevelopmental Biology and Medicine,* 32**,** 317-24.

ANDZINSKI, L., KASNITZ, N., STAHNKE, S., WU, C. F., GEREKE, M., VON KOCKRITZ-BLICKWEDE, M., SCHILLING, B., BRANDAU, S., WEISS, S. & JABLONSKA, J. 2016. Type I IFNs induce anti-tumor polarization of tumor associated neutrophils in mice and human. *Int J Cancer,* 138**,** 1982-93.

APTE, R. S., SINHA, D., MAYHEW, E., WISTOW, G. J. & NIEDERKORN, J. Y. 1998. Cutting Edge: Role of Macrophage Migration Inhibitory Factor in Inhibiting NK Cell Activity and Preserving Immune Privilege. *The Journal of Immunology,* 160**,** 5693-5696.

ARDI, V. C., KUPRIYANOVA, T. A., DERYUGINA, E. I. & QUIGLEY, J. P. 2007. Human neutrophils uniquely release TIMP-free MMP-9 to provide a potent catalytic stimulator of angiogenesis. *Proc Natl Acad Sci U S A,* 104**,** 20262-7.

AZAB, B., BHATT, V. R., PHOOKAN, J., MURUKUTLA, S., KOHN, N., TERJANIAN, T. & WIDMANN, W. D. 2012. Usefulness of the neutrophil-to-lymphocyte ratio in predicting short- and long-term mortality in breast cancer patients. *Annals of surgical oncology,* 19**,** 217-24.

BAAL, N., WIDMER-TESKE, R., MCKINNON, T., PREISSNER, K. T. & ZYGMUNT, M. T. 2009. In vitro spheroid model of placental vasculogenesis: does it work? *Lab Invest,* 89**,** 152-63.

BACHER, M., MEINHARDT, A., LAN, H. Y., MU, W., METZ, C. N., CHESNEY, J. A., CALANDRA, T., GEMSA, D., DONNELLY, T., ATKINS, R. C. & BUCALA, R. 1997. Migration inhibitory factor expression in experimentally induced endotoxemia. *The American Journal of Pathology,* 150**,** 235-246.

BADDELA, V. S., BAUFELD, A., YENUGANTI, V. R., VANSELOW, J. & SINGH, D. 2014. Suitable housekeeping genes for normalization of transcript abundance analysis by real-time RT-PCR in cultured bovine granulosa cells during hypoxia and differential cell plating density. *Reprod Biol Endocrinol,* 12**,** 118.

BAGAN, J., SARRION, G. & JIMENEZ, Y. 2010. Oral cancer: clinical features. *Oral Oncol,* 46**,** 414-7.

BALUK, P., HASHIZUME, H. & MCDONALD, D. M. 2005. Cellular abnormalities of blood vessels as targets in cancer. *Current opinion in genetics & development,* 15**,** 102-11.

BARON, N., DEUSTER, O., NOELKER, C., STÜER, C., STRIK, H., SCHALLER, C., DODEL, R., MEYER, B. & BACHER, M. 2011. Role of macrophage migration inhibitory factor in primary glioblastoma multiforme cells. *Journal of Neuroscience Research,* 89**,** 711-717.

BECKER, A., KUHNT, T., LIEDTKE, H., KRIVOKUCA, A., BLOCHING, M. & DUNST, J. 2002. Oxygenation measurements in head and neck cancers during hyperbaric oxygenation. *Strahlenther Onkol,* 178**,** 105-8.

BEKES, E. M., SCHWEIGHOFER, B., KUPRIYANOVA, T. A., ZAJAC, E., ARDI, V. C., QUIGLEY, J. P. & DERYUGINA, E. I. 2011. Tumor-recruited neutrophils and neutrophil TIMP-free MMP-9 regulate coordinately the levels of tumor angiogenesis and efficiency of malignant cell intravasation. *The American journal of pathology,* 179**,** 1455-70.

BELLOCQ, A., ANTOINE, M., FLAHAULT, A., PHILIPPE, C., CRESTANI, B., BERNAUDIN, J. F., MAYAUD, C., MILLERON, B., BAUD, L. & CADRANEL, J. 1998. Neutrophil alveolitis in bronchioloalveolar carcinoma: induction by tumor-derived interleukin-8 and relation to clinical outcome. *The American journal of pathology,* 152**,** 83-92.

BENDRAT, K., AL-ABED, Y., CALLAWAY, D. J. E., PENG, T., CALANDRA, T., METZ, C. N. & BUCALA, R. 1997. Biochemical and Mutational Investigations of the Enzymatic Activity of Macrophage Migration Inhibitory Factor. *Biochemistry,* 36**,** 15356-15362.

BERNHAGEN, J., KROHN, R., LUE, H., GREGORY, J. L., ZERNECKE, A., KOENEN, R. R., DEWOR, M., GEORGIEV, I., SCHOBER, A., LENG, L., KOOISTRA, T., FINGERLE-ROWSON, G.,

GHEZZI, P., KLEEMANN, R., MCCOLL, S. R., BUCALA, R., HICKEY, M. J. & WEBER, C. 2007. MIF is a noncognate ligand of CXC chemokine receptors in inflammatory and atherogenic cell recruitment. *Nature medicine,* 13**,** 587-96.

BEYRAU, M., BODKIN, J. V. & NOURSHARGH, S. 2012. Neutrophil heterogeneity in health and disease: a revitalized avenue in inflammation and immunity. *Open biology,* 2**,** 120134.

BLAISDELL, A., CREQUER, A., COLUMBUS, D., DAIKOKU, T., MITTAL, K., DEY, S. K. & ERLEBACHER, A. 2015. Neutrophils Oppose Uterine Epithelial Carcinogenesis via Debridement of Hypoxic Tumor Cells. *Cancer Cell,* 28**,** 785-99.

BLOUNT, B. C., MACK, M. M., WEHR, C. M., MACGREGOR, J. T., HIATT, R. A., WANG, G., WICKRAMASINGHE, S. N., EVERSON, R. B. & AMES, B. N. 1997. Folate deficiency causes uracil misincorporation into human DNA and chromosome breakage: Implications for cancer and neuronal damage. *Proceedings of the National Academy of Sciences,* 94**,** 3290-3295.

BOT, I., DAISSORMONT, I. T., ZERNECKE, A., VAN PUIJVELDE, G. H., KRAMP, B., DE JAGER, S. C., SLUIMER, J. C., MANCA, M., HERIAS, V., WESTRA, M. M., BOT, M., VAN SANTBRINK, P. J., VAN BERKEL, T. J., SU, L., SKJELLAND, M., GULLESTAD, L., KUIPER, J., HALVORSEN, B., AUKRUST, P., KOENEN, R. R., WEBER, C. & BIESSEN, E. A. 2014. CXCR4 blockade induces atherosclerosis by affecting neutrophil function. *J Mol Cell Cardiol,* 74**,** 44-52.

BOZZA, M., SATOSKAR, A. R., LIN, G., LU, B., HUMBLES, A. A., GERARD, C. & DAVID, J. R. 1999. Targeted disruption of migration inhibitory factor gene reveals its critical role in sepsis. *Journal of Experimental Medicine,* 189**,** 341-346.

BRADLEY, M. E., BOND, M. E., MANINI, J., BROWN, Z. & CHARLTON, S. J. 2009. SB265610 is an allosteric, inverse agonist at the human CXCR2 receptor. *Br J Pharmacol,* 158**,** 328-38.

BRANDAU, S., TRELLAKIS, S., BRUDEREK, K., SCHMALTZ, D., STELLER, G., ELIAN, M., SUTTMANN, H., SCHENCK, M., WELLING, J., ZABEL, P. & LANG, S. 2011. Myeloid-derived suppressor cells in the peripheral blood of cancer patients contain a subset of immature neutrophils with impaired migratory properties. *Journal of leukocyte biology,* 89**,** 311-7.

BRINKMANN, V., REICHARD, U., GOOSMANN, C., FAULER, B., UHLEMANN, Y., WEISS, D. S., WEINRAUCH, Y. & ZYCHLINSKY, A. 2004. Neutrophil extracellular traps kill bacteria. *Science,* 303**,** 1532-5.

BROXMEYER, H. E., ORSCHELL, C. M., CLAPP, D. W., HANGOC, G., COOPER, S., PLETT, P. A., LILES, W. C., LI, X., GRAHAM-EVANS, B., CAMPBELL, T. B., CALANDRA, G., BRIDGER, G., DALE, D. C. & SROUR, E. F. 2005. Rapid mobilization of murine and human hematopoietic stem and progenitor cells with AMD3100, a CXCR4 antagonist. *The Journal of experimental medicine,* 201**,** 1307-18.

BRU, A., SOUTO, J. C., ALCOLEA, S., ANTON, R., REMACHA, A., CAMACHO, M., SOLER, M., BRU, I., PORRES, A. & VILA, L. 2009. Tumour cell lines HT-29 and FaDu produce proinflammatory cytokines and activate neutrophils in vitro: possible applications for neutrophil-based antitumour treatment. *Mediators of inflammation,* 2009**,** 817498.

BUCHLER, P., REBER, H. A., BUCHLER, M., SHRINKANTE, S., BUCHLER, M. W., FRIESS, H., SEMENZA, G. L. & HINES, O. J. 2003. Hypoxia-inducible factor 1 regulates vascular endothelial growth factor expression in human pancreatic cancer. *Pancreas,* 26**,** 56-64.

BURKE-GAFFNEY, A. & HELLEWELL, P. G. 1996. Tumour necrosis factor-alpha-induced ICAM-1 expression in human vascular endothelial and lung epithelial cells: modulation by tyrosine kinase inhibitors. *Br J Pharmacol,* 119**,** 1149-58.

BÀNKFALVI, A. & PIFFKÒ, J. 2000. Prognostic and predictive factors in oral cancer: the role of the invasive tumour front. *Journal of Oral Pathology & Medicine,* 29**,** 291-298.

CACALANO, G., LEE, J., KIKLY, K., RYAN, A., PITTS-MEEK, S., HULTGREN, B., WOOD, W. & MOORE, M. 1994. Neutrophil and B cell expansion in mice that lack the murine IL-8 receptor homolog. *Science,* 265**,** 682-684.

CALANDRA, T., BERNHAGEN, J., MITCHELL, R. A. & BUCALA, R. 1994. The macrophage is an important and previously unrecognized source of macrophage migration inhibitory factor. *The Journal of Experimental Medicine,* 179**,** 1895-1902.

CALDEIRA, P. C., DE ANDRADE SOUSA, A. & DE AGUIAR, M. C. 2015. Differential infiltration of neutrophils in T1-T2 versus T3-T4 oral squamous cell carcinomas: a preliminary study. *BMC Res Notes,* 8**,** 569.

CAMPBELL, E. L., BRUYNINCKX, W. J., KELLY, C. J., GLOVER, L. E., MCNAMEE, E. N., BOWERS, B. E., BAYLESS, A. J., SCULLY, M., SAEEDI, B. J., GOLDEN-MASON, L., EHRENTRAUT, S. F., CURTIS, V. F., BURGESS, A., GARVEY, J. F., SORENSEN, A., NEMENOFF, R., JEDLICKA, P., TAYLOR, C. T., KOMINSKY, D. J. & COLGAN, S. P. 2014. Transmigrating neutrophils shape the mucosal microenvironment through localized oxygen depletion to influence resolution of inflammation. *Immunity,* 40**,** 66-77.

CAMPREGHER, C., LUCIANI, M. G. & GASCHE, C. 2008. Activated neutrophils induce an hMSH2-dependent G2/M checkpoint arrest and replication errors at a (CA)13-repeat in colon epithelial cells. *Gut,* 57**,** 780-7.

CARLSSON, J. & YUHAS, J. M. 1984. Liquid-overlay culture of cellular spheroids. *Recent Results Cancer Res,* 95**,** 1-23.

CEDRES, S., TORREJON, D., MARTINEZ, A., MARTINEZ, P., NAVARRO, A., ZAMORA, E., MULET-MARGALEF, N. & FELIP, E. 2012. Neutrophil to lymphocyte ratio (NLR) as an indicator of poor prognosis in stage IV non-small cell lung cancer. *Clinical & translational oncology : official publication of the Federation of Spanish Oncology Societies and of the National Cancer Institute of Mexico,* 14**,** 864-9.

CHESNEY, J., METZ, C., BACHER, M., PENG, T., MEINHARDT, A. & BUCALA, R. 1999. An essential role for macrophage migration inhibitory factor (MIF) in angiogenesis and the growth of a murine lymphoma. *Mol Med,* 5**,** 181-91.

CHIU, J. J., LEE, P. L., CHEN, C. N., LEE, C. I., CHANG, S. F., CHEN, L. J., LIEN, S. C., KO, Y. C., USAMI, S. & CHIEN, S. 2004. Shear stress increases ICAM-1 and decreases VCAM-1 and E-selectin expressions induced by tumor necrosis factor-[alpha] in endothelial cells. *Arterioscler Thromb Vasc Biol,* 24**,** 73-9.

CHO, H., HUR, H. W., KIM, S. W., KIM, S. H., KIM, J. H., KIM, Y. T. & LEE, K. 2009. Pre-treatment neutrophil to lymphocyte ratio is elevated in epithelial ovarian cancer and predicts survival after treatment. *Cancer immunology, immunotherapy : CII,* 58**,** 15-23.

CHOSAY, J. G., FISHER, M. A., FARHOOD, A., READY, K. A., DUNN, C. J. & JAESCHKE, H. 1998. Role of PECAM-1 (CD31) in neutrophil transmigration in murine models of liver and peritoneal inflammation. *American Journal of Physiology - Gastrointestinal and Liver Physiology,* 274**,** G776-G782.

CHRISTOFFERSSON, G., VÅGESJÖ, E., VANDOOREN, J., LIDÉN, M., MASSENA, S., REINERT, R. B., BRISSOVA, M., POWERS, A. C., OPDENAKKER, G. & PHILLIPSON, M. 2012. VEGF-A recruits a proangiogenic MMP-9–delivering neutrophil subset that induces angiogenesis in transplanted hypoxic tissue. *Blood,* 120**,** 4653-4662.

CLATOT, F., CORNIC, M., BERGHIAN, A., MARCHAND, V., CHOUSSY, O., EL OUAKIF, F., FRANCOIS, A., RUMINY, P., LABERGE-LE-COUTEULX, S., PICQUENOT, J. M. & JARDIN, F.

2015. CXCL12 and CXCR4, but not CXCR7, are primarily expressed by the stroma in head and neck squamous cell carcinoma. *Pathology,* 47**,** 45-50.

CLUDTS, S., DECAESTECKER, C., JOHNSON, B., LECHIEN, J., LEROY, X., KINDT, N., KALTNER, H., ANDRÉ, S., GABIUS, H.-J. & SAUSSEZ, S. 2010. Increased Expression of Macrophage Migration Inhibitory Factor During Progression to Hypopharyngeal Squamous Cell Carcinoma. *Anticancer Research,* 30**,** 3313-3319.

COFFELT, S. B., KERSTEN, K., DOORNEBAL, C. W., WEIDEN, J., VRIJLAND, K., HAU, C. S., VERSTEGEN, N. J., CIAMPRICOTTI, M., HAWINKELS, L. J., JONKERS, J. & DE VISSER, K. E. 2015. IL-17-producing gammadelta T cells and neutrophils conspire to promote breast cancer metastasis. *Nature,* 522**,** 345-8.

COLLEY, H. E., HEARNDEN, V., JONES, A. V., WEINREB, P. H., VIOLETTE, S. M., MACNEIL, S., THORNHILL, M. H. & MURDOCH, C. 2011. Development of tissue-engineered models of oral dysplasia and early invasive oral squamous cell carcinoma. *Br J Cancer,* 105**,** 1582-92.

COLOTTA, F., ALLAVENA, P., SICA, A., GARLANDA, C. & MANTOVANI, A. 2009. Cancer-related inflammation, the seventh hallmark of cancer: links to genetic instability. *Carcinogenesis,* 30**,** 1073-81.

CONDEELIS, J. & POLLARD, J. W. 2006. Macrophages: obligate partners for tumor cell migration, invasion, and metastasis. *Cell,* 124**,** 263-6.

CRUZ, I. B., SNIJDERS, P. J., MEIJER, C. J., BRAAKHUIS, B. J., SNOW, G. B., WALBOOMERS, J. M. & VAN DER WAAL, I. 1998. p53 expression above the basal cell layer in oral mucosa is an early event of malignant transformation and has predictive value for developing oral squamous cell carcinoma. *The Journal of pathology,* 184**,** 360-8.

CURRY, J. M., SPRANDIO, J., COGNETTI, D., LUGINBUHL, A., BAR-AD, V., PRIBITKIN, E. & TULUC, M. 2014. Tumor microenvironment in head and neck squamous cell carcinoma. *Semin Oncol,* 41**,** 217-34.

CZEPIELEWSKI, R. S., PORTO, B. N., RIZZO, L. B., ROESLER, R., ABUJAMRA, A. L., PINTO, L. G., SCHWARTSMANN, G., CUNHA FDE, Q. & BONORINO, C. 2012. Gastrin-releasing peptide receptor (GRPR) mediates chemotaxis in neutrophils. *Proceedings of the National Academy of Sciences of the United States of America,* 109**,** 547-52.

DALY, A. J., MCILREAVEY, L. & IRWIN, C. R. 2008. Regulation of HGF and SDF-1 expression by oral fibroblasts--implications for invasion of oral cancer. *Oral Oncol,* 44**,** 646-51.

DANAEI, G., VANDER HOORN, S., LOPEZ, A. D., MURRAY, C. J. & EZZATI, M. 2005. Causes of cancer in the world: comparative risk assessment of nine behavioural and environmental risk factors. *Lancet,* 366**,** 1784-93.

DANCEY, J. T., DEUBELBEISS, K. A., HARKER, L. A. & FINCH, C. A. 1976. Neutrophil kinetics in man. *J Clin Invest,* 58**,** 705-15.

DARBONNE, W. C., RICE, G. C., MOHLER, M. A., APPLE, T., XE, BERT, C. A., VALENTE, A. J. & BAKER, J. B. 1991. Red blood cells are a sink for interleukin 8, a leukocyte chemotaxin. *The Journal of Clinical Investigation,* 88**,** 1362-1369.

DARYADEL, A., GRIFONE, R. F., SIMON, H. U. & YOUSEFI, S. 2006. Apoptotic neutrophils release macrophage migration inhibitory factor upon stimulation with tumor necrosis factor-alpha. *J Biol Chem,* 281**,** 27653-61.

DAS, R., KOO, M.-S., KIM, B. H., JACOB, S. T., SUBBIAN, S., YAO, J., LENG, L., LEVY, R., MURCHISON, C., BURMAN, W. J., MOORE, C. C., SCHELD, W. M., DAVID, J. R., KAPLAN, G., MACMICKING, J. D. & BUCALA, R. 2013. Macrophage migration inhibitory factor

(MIF) is a critical mediator of the innate immune response to Mycobacterium tuberculosis. *Proceedings of the National Academy of Sciences,* 110**,** E2997-E3006.

DAS, S., KAR MAHAPATRA, S., GAUTAM, N., DAS, A. & ROY, S. 2007. Oxidative stress in lymphocytes, neutrophils, and serum of oral cavity cancer patients: modulatory array of L-glutamine. *Support Care Cancer,* 15**,** 1399-405.

DAVID, J. R. 1966. Delayed hypersensitivity in vitro: its mediation by cell-free substances formed by lymphoid cell-antigen interaction. *Proceedings of the National Academy of Sciences of the United States of America,* 56**,** 72-7.

DE LARCO, J. E., WUERTZ, B. R. K., MANIVEL, J. C. & FURCHT, L. T. 2001. Progression and Enhancement of Metastatic Potential after Exposure of Tumor Cells to Chemotherapeutic Agents. *Cancer Research,* 61**,** 2857-2861.

DESURMONT, T., SKRYPEK, N., DUHAMEL, A., JONCKHEERE, N., MILLET, G., LETEURTRE, E., GOSSET, P., DUCHENE, B., RAMDANE, N., HEBBAR, M., VAN SEUNINGEN, I., PRUVOT, F.-R., HUET, G. & TRUANT, S. 2015. Overexpression of chemokine receptor CXCR2 and ligand CXCL7 in liver metastases from colon cancer is correlated to shorter disease-free and overall survival. *Cancer Science,* 106**,** 262-269.

DETRE, S., SACLANI JOTTI, G. & DOWSETT, M. 1995. A "quickscore" method for immunohistochemical semiquantitation: validation for oestrogen receptor in breast carcinomas. *J Clin Pathol,* 48**,** 876-8.

DING, P. R., AN, X., ZHANG, R. X., FANG, Y. J., LI, L. R., CHEN, G., WU, X. J., LU, Z. H., LIN, J. Z., KONG, L. H., WAN, D. S. & PAN, Z. Z. 2010. Elevated preoperative neutrophil to lymphocyte ratio predicts risk of recurrence following curative resection for stage IIA colon cancer. *International journal of colorectal disease,* 25**,** 1427-33.

DIXON, G., ELKS, P. M., LOYNES, C. A., WHYTE, M. K. & RENSHAW, S. A. 2012. A method for the in vivo measurement of zebrafish tissue neutrophil lifespan. *ISRN hematology,* 2012**,** 915868.

DU, W., WRIGHT, B. M., LI, X., FINKE, J., RINI, B. I., ZHOU, M., HE, H., LAL, P. & WELFORD, S. M. 2013. Tumor-derived macrophage migration inhibitory factor promotes an autocrine loop that enhances renal cell carcinoma. *Oncogene,* 32**,** 1469-74.

DUCKER, T. P. & SKUBITZ, K. M. 1992. Subcellular localization of CD66, CD67, and NCA in human neutrophils. *Journal of Leukocyte Biology,* 52**,** 11-6.

DUDAS, J., BITSCHE, M., SCHARTINGER, V., FALKEIS, C., SPRINZL, G. M. & RIECHELMANN, H. 2011a. Fibroblasts produce brain-derived neurotrophic factor and induce mesenchymal transition of oral tumor cells. *Oral Oncol,* 47**,** 98-103.

DUDAS, J., FULLAR, A., BITSCHE, M., SCHARTINGER, V., KOVALSZKY, I., SPRINZL, G. M. & RIECHELMANN, H. 2011b. Tumor-produced, active interleukin-1beta regulates gene expression in carcinoma-associated fibroblasts. *Exp Cell Res,* 317**,** 2222-9.

DUMITRU, C. A., BANKFALVI, A., GU, X., EBERHARDT, W. E., ZEIDLER, R., LANG, S. & BRANDAU, S. 2013. Neutrophils Activate Tumoral CORTACTIN to Enhance Progression of Orohypopharynx Carcinoma. *Front Immunol,* 4**,** 33.

DUMITRU, C. A., FECHNER, M. K., HOFFMANN, T. K., LANG, S. & BRANDAU, S. 2012. A novel p38-MAPK signaling axis modulates neutrophil biology in head and neck cancer. *Journal of leukocyte biology,* 91**,** 591-8.

DUMITRU, C. A., GHOLAMAN, H., TRELLAKIS, S., BRUDEREK, K., DOMINAS, N., GU, X., BANKFALVI, A., WHITESIDE, T. L., LANG, S. & BRANDAU, S. 2011. Tumor-derived macrophage migration inhibitory factor modulates the biology of head and neck

cancer cells via neutrophil activation. *International journal of cancer. Journal international du cancer,* 129**,** 859-69.

DUNST, J., STADLER, P., BECKER, A., LAUTENSCHLÄGER, C., PELZ, T., HÄNSGEN, G., MOLLS, M. & KUHNT, T. 2003. Tumor Volume and Tumor Hypoxia in Head and Neck Cancers. *Strahlentherapie und Onkologie,* 179**,** 521-526.

DUSTIN, M. L., GARCIA-AGUILAR, J., HIBBS, M. L., LARSON, R. S., STACKER, S. A., STAUNTON, D. E., WARDLAW, A. J. & SPRINGER, T. A. 1989. Structure and regulation of the leukocyte adhesion receptor LFA-1 and its counterreceptors, ICAM-1 and ICAM-2. *Cold Spring Harb Symp Quant Biol,* 54 Pt 2**,** 753-65.

DVORAK, H. F. 1986. Tumors: wounds that do not heal. Similarities between tumor stroma generation and wound healing. *The New England journal of medicine,* 315**,** 1650-9.

EADEN, J. A., ABRAMS, K. R. & MAYBERRY, J. F. 2001. The risk of colorectal cancer in ulcerative colitis: a meta-analysis. *Gut,* 48**,** 526-35.

EALES, K. L., HOLLINSHEAD, K. E. R. & TENNANT, D. A. 2016. Hypoxia and metabolic adaptation of cancer cells. *Oncogenesis,* 5**,** e190.

EASH, K. J., GREENBAUM, A. M., GOPALAN, P. K. & LINK, D. C. 2010. CXCR2 and CXCR4 antagonistically regulate neutrophil trafficking from murine bone marrow. *J Clin Invest,* 120**,** 2423-31.

EASH, K. J., MEANS, J. M., WHITE, D. W. & LINK, D. C. 2009. CXCR4 is a key regulator of neutrophil release from the bone marrow under basal and stress granulopoiesis conditions. *Blood,* 113**,** 4711-9.

ERLER, J. T., BENNEWITH, K. L., NICOLAU, M., DORNHOFER, N., KONG, C., LE, Q.-T., CHI, J.-T. A., JEFFREY, S. S. & GIACCIA, A. J. 2006. Lysyl oxidase is essential for hypoxia-induced metastasis. *Nature,* 440**,** 1222-1226.

ERNST, P. B. & GOLD, B. D. 2000. The disease spectrum of Helicobacter pylori: the immunopathogenesis of gastroduodenal ulcer and gastric cancer. *Annual review of microbiology,* 54**,** 615-40.

ERUSLANOV, E. B., BHOJNAGARWALA, P. S., QUATROMONI, J. G., STEPHEN, T. L., RANGANATHAN, A., DESHPANDE, C., AKIMOVA, T., VACHANI, A., LITZKY, L., HANCOCK, W. W., CONEJO-GARCIA, J. R., FELDMAN, M., ALBELDA, S. M. & SINGHAL, S. 2014. Tumor-associated neutrophils stimulate T cell responses in early-stage human lung cancer. *J Clin Invest,* 124**,** 5466-80.

FAN, X., PATERA, A. C., PONG-KENNEDY, A., DENO, G., GONSIOREK, W., MANFRA, D. J., VASSILEVA, G., ZENG, M., JACKSON, C., SULLIVAN, L., SHARIF-RODRIGUEZ, W., OPDENAKKER, G., VAN DAMME, J., HEDRICK, J. A., LUNDELL, D., LIRA, S. A. & HIPKIN, R. W. 2007. Murine CXCR1 Is a Functional Receptor for GCP-2/CXCL6 and Interleukin-8/CXCL8. *Journal of Biological Chemistry,* 282**,** 11658-11666.

FERLAY, J., SHIN, H. R., BRAY, F., FORMAN, D., MATHERS, C. & PARKIN, D. M. 2010. Estimates of worldwide burden of cancer in 2008: GLOBOCAN 2008. *International journal of cancer. Journal international du cancer,* 127**,** 2893-917.

FERRANTE, A. & THONG, Y. H. 1978. A rapid one-step procedure for purification of mononuclear and polymorphonuclear leukocytes from human blood using a modification of the Hypaque-Ficoll technique. *J Immunol Methods,* 24**,** 389-93.

FIALKOW, L., WANG, Y. & DOWNEY, G. P. 2007. Reactive oxygen and nitrogen species as signaling molecules regulating neutrophil function. *Free radical biology & medicine,* 42**,** 153-64.

FOLKMAN, J. 2002. Role of angiogenesis in tumor growth and metastasis. *Seminars in oncology,* 29**,** 15-8.

FOOTE, A., BRIGANTI, E. M., KIPEN, Y., SANTOS, L., LEECH, M. & MORAND, E. F. 2004. Macrophage migration inhibitory factor in systemic lupus erythematosus. *The Journal of Rheumatology,* 31**,** 268-273.

FORTUNATI, E., KAZEMIER, K. M., GRUTTERS, J. C., KOENDERMAN, L. & VAN DEN BOSCH V, J. 2009. Human neutrophils switch to an activated phenotype after homing to the lung irrespective of inflammatory disease. *Clinical and experimental immunology,* 155**,** 559-66.

FRIDLENDER, Z. G., SUN, J., KIM, S., KAPOOR, V., CHENG, G., LING, L., WORTHEN, G. S. & ALBELDA, S. M. 2009. Polarization of tumor-associated neutrophil phenotype by TGF-beta: "N1" versus "N2" TAN. *Cancer cell,* 16**,** 183-94.

FRIDLENDER, Z. G., SUN, J., MISHALIAN, I., SINGHAL, S., CHENG, G., KAPOOR, V., HORNG, W., FRIDLENDER, G., BAYUH, R., WORTHEN, G. S. & ALBELDA, S. M. 2012. Transcriptomic analysis comparing tumor-associated neutrophils with granulocytic myeloid-derived suppressor cells and normal neutrophils. *PloS one,* 7**,** e31524.

FRIEDMAN, A. D. 2002. Transcriptional regulation of granulocyte and monocyte development. *Oncogene,* 21**,** 3377-90.

FUJII, N., SHOMORI, K., SHIOMI, T., NAKABAYASHI, M., TAKEDA, C., RYOKE, K. & ITO, H. 2012. Cancer-associated fibroblasts and CD163-positive macrophages in oral squamous cell carcinoma: their clinicopathological and prognostic significance. *J Oral Pathol Med,* 41**,** 444-51.

FUNAMIZU, N., HU, C., LACY, C., SCHETTER, A., ZHANG, G., HE, P., GAEDCKE, J., GHADIMI, M. B., RIED, T., YFANTIS, H. G., LEE, D. H., SUBLESKI, J., CHAN, T., WEISS, J. M., BACK, T. C., YANAGA, K., HANNA, N., ALEXANDER, H. R., MAITRA, A. & HUSSAIN, S. P. 2013. Macrophage migration inhibitory factor induces epithelial to mesenchymal transition, enhances tumor aggressiveness and predicts clinical outcome in resected pancreatic ductal adenocarcinoma. *International journal of cancer,* 132**,** 785-794.

GALDIERO, M. R., GARLANDA, C., JAILLON, S., MARONE, G. & MANTOVANI, A. 2012. Tumor associated macrophages and neutrophils in tumor progression. *Journal of cellular physiology*,228, 1404-1412

GALLIMIDI, A. B., FISCHMAN, S., REVACH, B., BULVIK, R., MALIUTINA, A., RUBINSTEIN, A. M., NUSSBAUM, G. & ELKIN, M. 2015. Periodontal pathogens Porphyromonas gingivalis and Fusobacterium nucleatum promote tumor progression in an oral-specific chemical carcinogenesis model. *Oncotarget,* 6**,** 22613-22623.

GAO, Q., ZHAO, Y. J., WANG, X. Y., QIU, S. J., SHI, Y. H., SUN, J., YI, Y., SHI, J. Y., SHI, G. M., DING, Z. B., XIAO, Y. S., ZHAO, Z. H., ZHOU, J., HE, X. H. & FAN, J. 2012. CXCR6 upregulation contributes to a proinflammatory tumor microenvironment that drives metastasis and poor patient outcomes in hepatocellular carcinoma. *Cancer research,* 72**,** 3546-56.

GARLEY, M., JABLONSKA, E., GRABOWSKA, S. & PIOTROWSKI, L. 2009. L-17 family cytokines in neutrophils of patients with oral epithelial squamous cell carcinoma. *Neoplasma,* 56**,** 96-100.

GAUDRY, M., BREGERIE, O., ANDRIEU, V., EL BENNA, J., POCIDALO, M. A. & HAKIM, J. 1997. Intracellular pool of vascular endothelial growth factor in human neutrophils. *Blood,* 90**,** 4153-61.

GEORGE, S. M., PARK, Y., LEITZMANN, M. F., FREEDMAN, N. D., DOWLING, E. C., REEDY, J., SCHATZKIN, A., HOLLENBECK, A. & SUBAR, A. F. 2009. Fruit and vegetable intake and risk of cancer: a prospective cohort study. *Am J Clin Nutr,* 89**,** 347-53.

GIJSBERS, K., GOUWY, M., STRUYF, S., WUYTS, A., PROOST, P., OPDENAKKER, G., PENNINCKX, F., ECTORS, N., GEBOES, K. & VAN DAMME, J. 2005. GCP-2/CXCL6 synergizes with other endothelial cell-derived chemokines in neutrophil mobilization and is associated with angiogenesis in gastrointestinal tumors. *Experimental cell research,* 303**,** 331-42.

GIRARD, E., STRATHDEE, C., TRUEBLOOD, E. & QUEVA, C. 2012. Macrophage migration inhibitory factor produced by the tumour stroma but not by tumour cells regulates angiogenesis in the B16-F10 melanoma model. *Br J Cancer,* 107**,** 1498-1505.

GOEL, H. L. & MERCURIO, A. M. 2013. VEGF targets the tumour cell. *Nat Rev Cancer,* 13**,** 871-82.

GONÇALVES, A. S. & APPELBERG, R. 2002. The Involvement of the Chemokine Receptor CXCR2 in Neutrophil Recruitment in LPS-Induced Inflammation and in Mycobacterium avium Infection. *Scandinavian Journal of Immunology,* 55**,** 585-591.

GOVINDAN, S. V., CARDILLO, T. M., SHARKEY, R. M., TAT, F., GOLD, D. V. & GOLDENBERG, D. M. 2013. Milatuzumab-SN-38 conjugates for the treatment of CD74+ cancers. *Mol Cancer Ther,* 12**,** 968-78.

GRANATA, F., FRATTINI, A., LOFFREDO, S., STAIANO, R. I., PETRAROLI, A., RIBATTI, D., OSLUND, R., GELB, M. H., LAMBEAU, G., MARONE, G. & TRIGGIANI, M. 2010. Production of vascular endothelial growth factors from human lung macrophages induced by group IIA and group X secreted phospholipases A2. *J Immunol,* 184**,** 5232-41.

GREGORY, J. L., LEECH, M. T., DAVID, J. R., YANG, Y. H., DACUMOS, A. & HICKEY, M. J. 2004. Reduced leukocyte–endothelial cell interactions in the inflamed microcirculation of macrophage migration inhibitory factor–deficient mice. *Arthritis & Rheumatism,* 50**,** 3023-3034.

GRETEN, T. F., MANNS, M. P. & KORANGY, F. 2011. Myeloid derived suppressor cells in human diseases. *International immunopharmacology,* 11**,** 802-7.

GRIFFIN, J. D., RITZ, J., NADLER, L. M. & SCHLOSSMAN, S. F. 1981. Expression of myeloid differentiation antigens on normal and malignant myeloid cells. *Journal of Clinical Investigation,* 68**,** 932-941.

GROEBE, K. & MUELLER-KLIESER, W. 1991. Distributions of oxygen, nutrient, and metabolic waste concentrations in multicellular spheroids and their dependence on spheroid parameters. *European Biophysics Journal,* 19**,** 169-181.

GUO, P., WANG, J., LIU, J., XIA, M., LI, W. & HE, M. 2015. Macrophage immigration inhibitory factor promotes cell proliferation and inhibits apoptosis of cervical adenocarcinoma. *Tumor Biology,* 36**,** 5095-5102.

GUSTAVSSON, P., JAKOBSSON, R., JOHANSSON, H., LEWIN, F., NORELL, S. & RUTKVIST, L. E. 1998. Occupational exposures and squamous cell carcinoma of the oral cavity, pharynx, larynx, and oesophagus: a case-control study in Sweden. *Occup Environ Med,* 55**,** 393-400.

HADLEY, T. J. & PEIPER, S. C. 1997. From Malaria to Chemokine Receptor: The Emerging Physiologic Role of the Duffy Blood Group Antigen. *Blood,* 89**,** 3077-3091.

HALEY, P. J. 2003. Species differences in the structure and function of the immune system. *Toxicology,* 188**,** 49-71.

HAMMOND, M. E., LAPOINTE, G. R., FEUCHT, P. H., HILT, S., GALLEGOS, C. A., GORDON, C. A., GIEDLIN, M. A., MULLENBACH, G. & TEKAMP-OLSON, P. 1995. IL-8 induces neutrophil

chemotaxis predominantly via type I IL-8 receptors. *The Journal of Immunology,* 155**,** 1428-33.

HAN, I., LEE, M. R., NAM, K. W., OH, J. H., MOON, K. C. & KIM, H. S. 2008. Expression of macrophage migration inhibitory factor relates to survival in high-grade osteosarcoma. *Clin Orthop Relat Res,* 466**,** 2107-13.

HANAHAN, D. & WEINBERG, ROBERT A. 2011. Hallmarks of Cancer: The Next Generation. *Cell,* 144**,** 646-674.

HAQQANI, A. S., SANDHU, J. K. & BIRNBOIM, H. C. 2000. Expression of interleukin-8 promotes neutrophil infiltration and genetic instability in mutatect tumors. *Neoplasia,* 2**,** 561-8.

HARTL, D., KRAUSS-ETSCHMANN, S., KOLLER, B., HORDIJK, P. L., KUIJPERS, T. W., HOFFMANN, F., HECTOR, A., EBER, E., MARCOS, V., BITTMANN, I., EICKELBERG, O., GRIESE, M. & ROOS, D. 2008. Infiltrated neutrophils acquire novel chemokine receptor expression and chemokine responsiveness in chronic inflammatory lung diseases. *Journal of immunology,* 181**,** 8053-67.

HE, X. X., CHEN, K., YANG, J., LI, X. Y., GAN, H. Y., LIU, C. Y., COLEMAN, T. R. & AL-ABED, Y. 2009. Macrophage migration inhibitory factor promotes colorectal cancer. *Mol Med,* 15**,** 1-10.

HE, X. X., YANG, J., DING, Y. W., LIU, W., SHEN, Q. Y. & XIA, H. H. 2006. Increased epithelial and serum expression of macrophage migration inhibitory factor (MIF) in gastric cancer: potential role of MIF in gastric carcinogenesis. *Gut,* 55**,** 797-802.

HEIDEMANN, J., OGAWA, H., DWINELL, M. B., RAFIEE, P., MAASER, C., GOCKEL, H. R., OTTERSON, M. F., OTA, D. M., LÜGERING, N., DOMSCHKE, W. & BINION, D. G. 2003. Angiogenic Effects of Interleukin 8 (CXCL8) in Human Intestinal Microvascular Endothelial Cells Are Mediated by CXCR2. *Journal of Biological Chemistry,* 278**,** 8508-8515.

HEIL, T. L., VOLKMANN, K. R., WATAHA, J. C. & LOCKWOOD, P. E. 2002. Human peripheral blood monocytes versus THP-1 monocytes for in vitro biocompatibility testing of dental material components. *Journal of Oral Rehabilitation,* 29**,** 401-407.

HIGGINS, D. F., BIJU, M. P., AKAI, Y., WUTZ, A., JOHNSON, R. S. & HAASE, V. H. 2004. Hypoxic induction of Ctgf is directly mediated by Hif-1. *American Journal of Physiology - Renal Physiology,* 287**,** F1223-F1232.

HIGHFILL, S. L., CUI, Y., GILES, A. J., SMITH, J. P., ZHANG, H., MORSE, E., KAPLAN, R. N. & MACKALL, C. L. 2014. Disruption of CXCR2-Mediated MDSC Tumor Trafficking Enhances Anti-PD1 Efficacy. *Science Translational Medicine,* 6**,** 237ra67-237ra67.

HIRA, E., ONO, T., DHAR, D. K., EL-ASSAL, O. N., HISHIKAWA, Y., YAMANOI, A. & NAGASUE, N. 2005. Overexpression of macrophage migration inhibitory factor induces angiogenesis and deteriorates prognosis after radical resection for hepatocellular carcinoma. *Cancer,* 103**,** 588-598.

HIRSCHHAEUSER, F., LEIDIG, T., RODDAY, B., LINDEMANN, C. & MUELLER-KLIESER, W. 2009. Test system for trifunctional antibodies in 3D MCTS culture. *J Biomol Screen,* 14**,** 980-90.

HIRSCHHAEUSER, F., MENNE, H., DITTFELD, C., WEST, J., MUELLER-KLIESER, W. & KUNZ-SCHUGHART, L. A. 2010. Multicellular tumor spheroids: an underestimated tool is catching up again. *Journal of biotechnology,* 148**,** 3-15.

HOFFMANN, T. K., SCHIRLAU, K., SONKOLY, E., BRANDAU, S., LANG, S., PIVARCSI, A., BALZ, V., MULLER, A., HOMEY, B., BOELKE, E., REICHERT, T., FRIEBE-HOFFMANN, U., GREVE, J., SCHULER, P., SCHECKENBACH, K., SCHIPPER, J., BAS, M., WHITESIDE, T. L. & BIER, H.

2009. A novel mechanism for anti-EGFR antibody action involves chemokine-mediated leukocyte infiltration. *Int J Cancer,* 124**,** 2589-96.

HOUGHTON, A. M., RZYMKIEWICZ, D. M., JI, H., GREGORY, A. D., EGEA, E. E., METZ, H. E., STOLZ, D. B., LAND, S. R., MARCONCINI, L. A., KLIMENT, C. R., JENKINS, K. M., BEAULIEU, K. A., MOUDED, M., FRANK, S. J., WONG, K. K. & SHAPIRO, S. D. 2010. Neutrophil elastase-mediated degradation of IRS-1 accelerates lung tumor growth. *Nature medicine,* 16**,** 219-23.

HUANG, S., VAN ARSDALL, M., TEDJARATI, S., MCCARTY, M., WU, W., LANGLEY, R. & FIDLER, I. J. 2002. Contributions of stromal metalloproteinase-9 to angiogenesis and growth of human ovarian carcinoma in mice. *J Natl Cancer Inst,* 94**,** 1134-42.

HUANG, W.-C., CHAN, S.-T., YANG, T.-L., TZENG, C.-C. & CHEN, C.-C. 2004. Inhibition of ICAM-1 gene expression, monocyte adhesion and cancer cell invasion by targeting IKK complex: molecular and functional study of novel α-methylene-γ-butyrolactone derivatives. *Carcinogenesis,* 25**,** 1925-1934.

HUANG, X.-H., JIAN, W.-H., WU, Z.-F., ZHAO, J., WANG, H., LI, W. & XIA, J.-T. 2014. Small interfering RNA (siRNA)-mediated knockdown of macrophage migration inhibitory factor (MIF) suppressed cyclin D1 expression and hepatocellular carcinoma cell proliferation. *Oncotarget,* 5.

HUDSON, J. D., SHOAIBI, M. A., MAESTRO, R., CARNERO, A., HANNON, G. J. & BEACH, D. H. 1999. A Proinflammatory Cytokine Inhibits P53 Tumor Suppressor Activity. *The Journal of Experimental Medicine,* 190**,** 1375-1382.

HUEBENER, P., PRADERE, J. P., HERNANDEZ, C., GWAK, G. Y., CAVIGLIA, J. M., MU, X., LOIKE, J. D., JENKINS, R. E., ANTOINE, D. J. & SCHWABE, R. F. 2015. The HMGB1/RAGE axis triggers neutrophil-mediated injury amplification following necrosis. *J Clin Invest,* 125**,** 539-50.

HUH, S. J., LIANG, S., SHARMA, A., DONG, C. & ROBERTSON, G. P. 2010. Transiently entrapped circulating tumor cells interact with neutrophils to facilitate lung metastasis development. *Cancer research,* 70**,** 6071-82.

HUNTLEY, S. P., DAVIES, M., MATTHEWS, J. B., THOMAS, G., MARSHALL, J., ROBINSON, C. M., EVESON, J. W., PATERSON, I. C. & PRIME, S. S. 2004. Attenuated type II TGF-β receptor signalling in human malignant oral keratinocytes induces a less differentiated and more aggressive phenotype that is associated with metastatic dissemination. *International Journal of Cancer,* 110**,** 170-176.

HUSSAIN, F., FREISSMUTH, M., VOLKEL, D., THIELE, M., DOUILLARD, P., ANTOINE, G., THURNER, P., EHRLICH, H., SCHWARZ, H. P., SCHEIFLINGER, F. & KERSCHBAUMER, R. J. 2013. Human anti-macrophage migration inhibitory factor antibodies inhibit growth of human prostate cancer cells in vitro and in vivo. *Mol Cancer Ther,* 12**,** 1223-34.

HÉBERT, C. A., VITANGCOL, R. V. & BAKER, J. B. 1991. Scanning mutagenesis of interleukin-8 identifies a cluster of residues required for receptor binding. *Journal of Biological Chemistry,* 266**,** 18989-18994.

ILIE, M., HOFMAN, V., ORTHOLAN, C., BONNETAUD, C., COELLE, C., MOUROUX, J. & HOFMAN, P. 2012. Predictive clinical outcome of the intratumoral CD66b-positive neutrophil-to-CD8-positive T-cell ratio in patients with resectable nonsmall cell lung cancer. *Cancer,* 118**,** 1726-37.

IMAMURA, K., NISHIHIRA, J., SUZUKI, M., YASUDA, K., SASAKI, S., KUSUNOKI, Y., TOCHIMARU, H. & TAKEKOSHI, Y. 1996. Identification and immunohistochemical localization of

macrophage migration inhibitory factor in human kidney. *Biochem Mol Biol Int,* 40**,** 1233-42.

JABLONSKA, E., GARLEY, M. & JABLONSKI, J. 2009. The expressions of intrinsic and extrinsic apoptotic pathway proteins in neutrophils of oral cavity cancer patients: a preliminary study. *Archivum immunologiae et therapiae experimentalis,* 57**,** 229-34.

JABLONSKA, J., LESCHNER, S., WESTPHAL, K., LIENENKLAUS, S. & WEISS, S. 2010. Neutrophils responsive to endogenous IFN-beta regulate tumor angiogenesis and growth in a mouse tumor model. *The Journal of clinical investigation,* 120**,** 1151-64.

JABLONSKA, J., WU, C. F., ANDZINSKI, L., LESCHNER, S. & WEISS, S. 2014. CXCR2-mediated tumor-associated neutrophil recruitment is regulated by IFN-β. *International Journal of Cancer,* 134**,** 1346-1358.

JANOT, F., KLIJANIENKO, J., RUSSO, A., MAMET, J. P., DE BRAUD, F., EL-NAGGAR, A. K., PIGNON, J. P., LUBOINSKI, B. & CVITKOVIC, E. 1996. Prognostic value of clinicopathological parameters in head and neck squamous cell carcinoma: a prospective analysis. *Br J Cancer,* 73**,** 531-8.

JENSEN, H. K., DONSKOV, F., MARCUSSEN, N., NORDSMARK, M., LUNDBECK, F. & VON DER MAASE, H. 2009a. Presence of intratumoral neutrophils is an independent prognostic factor in localized renal cell carcinoma. *Journal of clinical oncology : official journal of the American Society of Clinical Oncology,* 27**,** 4709-17.

JENSEN, H. K., DONSKOV, F., MARCUSSEN, N., NORDSMARK, M., LUNDBECK, F. & VON DER MAASE, H. 2009b. Presence of intratumoral neutrophils is an independent prognostic factor in localized renal cell carcinoma. *J Clin Oncol,* 27**,** 4709-17.

JENSEN, T. O., SCHMIDT, H., MOLLER, H. J., DONSKOV, F., HOYER, M., SJOEGREN, P., CHRISTENSEN, I. J. & STEINICHE, T. 2012. Intratumoral neutrophils and plasmacytoid dendritic cells indicate poor prognosis and are associated with pSTAT3 expression in AJCC stage I/II melanoma. *Cancer,* 118**,** 2476-85.

JR, S. S., GORSKY, M. & MS, F. L. D. 1984. Oral leukoplakia and malignant transformation. A follow-up study of 257 patients. *Cancer,* 53**,** 563-568.

KALYANKRISHNA, S. & GRANDIS, J. R. 2006. Epidermal Growth Factor Receptor Biology in Head and Neck Cancer. *Journal of Clinical Oncology,* 24**,** 2666-2672.

KATOH, H., WANG, D., DAIKOKU, T., SUN, H., DEY, SUDHANSU K. & DUBOIS, RAYMOND N. 2013. CXCR2-Expressing Myeloid-Derived Suppressor Cells Are Essential to Promote Colitis-Associated Tumorigenesis. *Cancer Cell,* 24**,** 631-644.

KEANE, M. P., BELPERIO, J. A., XUE, Y. Y., BURDICK, M. D. & STRIETER, R. M. 2004. Depletion of CXCR2 Inhibits Tumor Growth and Angiogenesis in a Murine Model of Lung Cancer. *The Journal of Immunology,* 172**,** 2853-2860.

KERSCHBAUMER, R. J., RIEGER, M., VÖLKEL, D., LE ROY, D., ROGER, T., GARBARAVICIENE, J., BOEHNCKE, W.-H., MÜLLBERG, J., HOET, R. M., WOOD, C. R., ANTOINE, G., THIELE, M., SAVIDIS-DACHO, H., DOCKAL, M., EHRLICH, H., CALANDRA, T. & SCHEIFLINGER, F. 2012. Neutralization of Macrophage Migration Inhibitory Factor (MIF) by Fully Human Antibodies Correlates with Their Specificity for the β-Sheet Structure of MIF. *The Journal of Biological Chemistry,* 287**,** 7446-7455.

KINDT, N., LAURENT, G., NONCLERCQ, D., JOURNE, F., GHANEM, G., DUVILLIER, H., GABIUS, H. J., LECHIEN, J. & SAUSSEZ, S. 2013a. Pharmacological inhibition of macrophage migration inhibitory factor interferes with the proliferation and invasiveness of squamous carcinoma cells. *Int J Oncol,* 43**,** 185-93.

KINDT, N., PREILLON, J., KALTNER, H., GABIUS, H. J., CHEVALIER, D., RODRIGUEZ, A., JOHNSON, B. D., MEGALIZZI, V., DECAESTECKER, C., LAURENT, G. & SAUSSEZ, S. 2013b. Macrophage migration inhibitory factor in head and neck squamous cell carcinoma: clinical and experimental studies. *J Cancer Res Clin Oncol,* 139**,** 727-37.

KITAMURA, T., QIAN, B.-Z., SOONG, D., CASSETTA, L., NOY, R., SUGANO, G., KATO, Y., LI, J. & POLLARD, J. W. 2015. CCL2-induced chemokine cascade promotes breast cancer metastasis by enhancing retention of metastasis-associated macrophages. *The Journal of Experimental Medicine,* 212**,** 1043-1059.

KLASEN, C., OHL, K., STERNKOPF, M., SHACHAR, I., SCHMITZ, C., HEUSSEN, N., HOBEIKA, E., LEVIT-ZERDOUN, E., TENBROCK, K., RETH, M., BERNHAGEN, J. & EL BOUNKARI, O. 2014. MIF promotes B cell chemotaxis through the receptors CXCR4 and CD74 and ZAP-70 signaling. *J Immunol,* 192**,** 5273-84.

KOONG, A. C., DENKO, N. C., HUDSON, K. M., SCHINDLER, C., SWIERSZ, L., KOCH, C., EVANS, S., IBRAHIM, H., LE, Q. T., TERRIS, D. J. & GIACCIA, A. J. 2000. Candidate genes for the hypoxic tumor phenotype. *Cancer Res,* 60**,** 883-7.

KOPNIN, B. P. 2000. Targets of oncogenes and tumor suppressors: key for understanding basic mechanisms of carcinogenesis. *Biochemistry. Biokhimiia,* 65**,** 2-27.

KOZAKI, K.-I., IMOTO, I., PIMKHAOKHAM, A., HASEGAWA, S., TSUDA, H., OMURA, K. & INAZAWA, J. 2006. PIK3CA mutation is an oncogenic aberration at advanced stages of oral squamous cell carcinoma. *Cancer Science,* 97**,** 1351-1358.

KRAEMER, S., LUE, H., ZERNECKE, A., KAPURNIOTU, A., ANDREETTO, E., FRANK, R., LENNARTZ, B., WEBER, C. & BERNHAGEN, J. 2011. MIF-chemokine receptor interactions in atherogenesis are dependent on an N-loop-based 2-site binding mechanism. *The FASEB Journal,* 25**,** 894-906.

KROCKENBERGER, M., DOMBROWSKI, Y., WEIDLER, C., OSSADNIK, M., HÖNIG, A., HÄUSLER, S., VOIGT, H., BECKER, J. C., LENG, L., STEINLE, A., WELLER, M., BUCALA, R., DIETL, J. & WISCHHUSEN, J. 2008. Macrophage Migration Inhibitory Factor (MIF) Contributes to the Immune Escape of Ovarian Cancer by Downregulating NKG2D(). *Journal of immunology (Baltimore, Md. : 1950),* 180**,** 7338-7348.

KUANG, D. M., ZHAO, Q., WU, Y., PENG, C., WANG, J., XU, Z., YIN, X. Y. & ZHENG, L. 2011. Peritumoral neutrophils link inflammatory response to disease progression by fostering angiogenesis in hepatocellular carcinoma. *Journal of hepatology,* 54**,** 948-55.

KUHNT, T., MUELLER, A. C., PELZ, T., HAENSGEN, G., BLOCHING, M., KOESLING, S., SCHUBERT, J. & DUNST, J. 2005. Impact of tumor control and presence of visible necrosis in head and neck cancer patients treated with radiotherapy or radiochemotherapy. *J Cancer Res Clin Oncol,* 131**,** 758-64.

KUILMAN, T., MICHALOGLOU, C., VREDEVELD, L. C. W., DOUMA, S., VAN DOORN, R., DESMET, C. J., AARDEN, L. A., MOOI, W. J. & PEEPER, D. S. 2008. Oncogene-Induced Senescence Relayed by an Interleukin-Dependent Inflammatory Network. *Cell,* 133**,** 1019-1031.

KUMAR, B., KOUL, S., KHANDRIKA, L., MEACHAM, R. B. & KOUL, H. K. 2008a. Oxidative stress is inherent in prostate cancer cells and is required for aggressive phenotype. *Cancer Res,* 68**,** 1777-85.

KUMAR, H. R., ZHONG, X., HOELZ, D. J., RESCORLA, F. J., HICKEY, R. J., MALKAS, L. H. & SANDOVAL, J. A. 2008b. Three-dimensional neuroblastoma cell culture: proteomic analysis between monolayer and multicellular tumor spheroids. *Pediatr Surg Int,* 24**,** 1229-34.

KYZAS, P. A., CUNHA, I. W. & IOANNIDIS, J. P. A. 2005. Prognostic Significance of Vascular Endothelial Growth Factor Immunohistochemical Expression in Head and Neck Squamous Cell Carcinoma: A Meta-Analysis. *Clinical Cancer Research,* 11**,** 1434-1440.

LAI, K. N., LEUNG, J. C. K., METZ, C. N., LAI, F. M., BUCALA, R. & LAN, H. Y. 2003. Role for macrophage migration inhibitory factor in acute respiratory distress syndrome. *The Journal of Pathology,* 199**,** 496-508.

LAKSCHEVITZ, F. S., ABOODI, G. M. & GLOGAUER, M. 2013. Oral neutrophil transcriptome changes result in a pro-survival phenotype in periodontal diseases. *PLoS One,* 8**,** e68983.

LARSEN, M., TAZZYMAN, S., LUND, E. L., JUNKER, N., LEWIS, C. E., KRISTJANSEN, P. E. & MURDOCH, C. 2008. Hypoxia-induced secretion of macrophage migration-inhibitory factor from MCF-7 breast cancer cells is regulated in a hypoxia-inducible factor-independent manner. *Cancer Lett,* 265**,** 239-49.

LEE, J., HORUK, R., RICE, G. C., BENNETT, G. L., CAMERATO, T. & WOOD, W. I. 1992. Characterization of two high affinity human interleukin-8 receptors. *The Journal of biological chemistry,* 267**,** 16283-7.

LEGENDRE, H., DECAESTECKER, C., NAGY, N., HENDLISZ, A., SCHURING, M.-P., SALMON, I., GABIUS, H.-J., PECTOR, J.-C. & KISS, R. 0000. Prognostic Values of Galectin-3 and the Macrophage Migration Inhibitory Factor (MIF) in Human Colorectal Cancers. *Mod Pathol,* 16**,** 491-504.

LENG, L., CHEN, L., FAN, J., GREVEN, D., ARJONA, A., DU, X., AUSTIN, D., KASHGARIAN, M., YIN, Z., HUANG, X. R., LAN, H. Y., LOLIS, E., NIKOLIC-PATERSON, D. & BUCALA, R. 2011. A small-molecule macrophage migration inhibitory factor antagonist protects against glomerulonephritis in lupus-prone NZB/NZW F1 and MRL/lpr mice. *J Immunol,* 186**,** 527-38.

LENG, L., METZ, C. N., FANG, Y., XU, J., DONNELLY, S., BAUGH, J., DELOHERY, T., CHEN, Y., MITCHELL, R. A. & BUCALA, R. 2003. MIF signal transduction initiated by binding to CD74. *J Exp Med,* 197**,** 1467-76.

LEVINE, A. J. 1997. p53, the cellular gatekeeper for growth and division. *Cell,* 88**,** 323-31.

LIANG, X., YANG, D., HU, J., HAO, X., GAO, J. & MAO, Z. 2008. Hypoxia Inducible Factor-1alpha Expression Correlates with Vascular Endothelial Growth Factor-C Expression and Lymphangiogenesis/Angiogenesis in Oral Squamous Cell Carcinoma. *Anticancer Research,* 28**,** 1659-1666.

LILES, W. C., BROXMEYER, H. E., RODGER, E., WOOD, B., HUBEL, K., COOPER, S., HANGOC, G., BRIDGER, G. J., HENSON, G. W., CALANDRA, G. & DALE, D. C. 2003. Mobilization of hematopoietic progenitor cells in healthy volunteers by AMD3100, a CXCR4 antagonist. *Blood,* 102**,** 2728-30.

LIN, J., LIU, C., GE, L., GAO, Q., HE, X., LIU, Y., LI, S., ZHOU, M., CHEN, Q. & ZHOU, H. 2011. Carcinoma-associated fibroblasts promotes the proliferation of a lingual carcinoma cell line by secreting keratinocyte growth factor. *Tumour Biol,* 32**,** 597-602.

LUBETSKY, J. B., DIOS, A., HAN, J., ALJABARI, B., RUZSICSKA, B., MITCHELL, R., LOLIS, E. & AL-ABED, Y. 2002. The tautomerase active site of macrophage migration inhibitory factor is a potential target for discovery of novel anti-inflammatory agents. *J Biol Chem,* 277**,** 24976-82.

LUE, H., KAPURNIOTU, A., FINGERLE-ROWSON, G., ROGER, T., LENG, L., THIELE, M., CALANDRA, T., BUCALA, R. & BERNHAGEN, J. 2006. Rapid and transient activation of

the ERK MAPK signalling pathway by macrophage migration inhibitory factor (MIF) and dependence on JAB1/CSN5 and Src kinase activity. *Cellular Signalling,* 18**,** 688-703.

MAINARDI, C. L., DIXIT, S. N. & KANG, A. H. 1980. Degradation of type IV (basement membrane) collagen by a proteinase isolated from human polymorphonuclear leukocyte granules. *The Journal of biological chemistry,* 255**,** 5435-41.

MANTOVANI, A., CASSATELLA, M. A., COSTANTINI, C. & JAILLON, S. 2011. Neutrophils in the activation and regulation of innate and adaptive immunity. *Nature reviews. Immunology,* 11**,** 519-31.

MARSH, D., SUCHAK, K., MOUTASIM, K. A., VALLATH, S., HOPPER, C., JERJES, W., UPILE, T., KALAVREZOS, N., VIOLETTE, S. M., WEINREB, P. H., CHESTER, K. A., CHANA, J. S., MARSHALL, J. F., HART, I. R., HACKSHAW, A. K., PIPER, K. & THOMAS, G. J. 2011. Stromal features are predictive of disease mortality in oral cancer patients. *J Pathol,* 223**,** 470-81.

MARTIN, C., BURDON, P. C., BRIDGER, G., GUTIERREZ-RAMOS, J. C., WILLIAMS, T. J. & RANKIN, S. M. 2003. Chemokines acting via CXCR2 and CXCR4 control the release of neutrophils from the bone marrow and their return following senescence. *Immunity,* 19**,** 583-93.

MARTIN, J., DUNCAN, F. J., KEISER, T., SHIN, S., KUSEWITT, D. F., OBERYSZYN, T., SATOSKAR, A. R. & VANBUSKIRK, A. M. 2009. Macrophage migration inhibitory factor (MIF) plays a critical role in pathogenesis of ultraviolet-B (UVB) -induced nonmelanoma skin cancer (NMSC). *FASEB journal : official publication of the Federation of American Societies for Experimental Biology,* 23**,** 720-30.

MASHBERG, A., MERLETTI, F., BOFFETTA, P., GANDOLFO, S., OZZELLO, F., FRACCHIA, F. & TERRACINI, B. 1989. Appearance, site of occurrence, and physical and clinical characteristics of oral carcinoma in Torino, Italy. *Cancer,* 63**,** 2522-7.

MASSENA, S., CHRISTOFFERSSON, G., VAGESJO, E., SEIGNEZ, C., GUSTAFSSON, K., BINET, F., HERRERA HIDALGO, C., GIRAUD, A., LOMEI, J., WESTROM, S., SHIBUYA, M., CLAESSON-WELSH, L., GERWINS, P., WELSH, M., KREUGER, J. & PHILLIPSON, M. 2015. Identification and characterization of VEGF-A-responsive neutrophils expressing CD49d, VEGFR1, and CXCR4 in mice and humans. *Blood,* 126**,** 2016-26.

MCGETTRICK, H. M., LORD, J. M., WANG, K. Q., RAINGER, G. E., BUCKLEY, C. D. & NASH, G. B. 2006. Chemokine- and adhesion-dependent survival of neutrophils after transmigration through cytokine-stimulated endothelium. *Journal of leukocyte biology,* 79**,** 779-88.

MEYER-SIEGLER, K. L., ICZKOWSKI, K. A., LENG, L., BUCALA, R. & VERA, P. L. 2006. Inhibition of Macrophage Migration Inhibitory Factor or Its Receptor (CD74) Attenuates Growth and Invasion of DU-145 Prostate Cancer Cells. *The Journal of Immunology,* 177**,** 8730-8739.

MEYER-SIEGLER, K. L., ICZKOWSKI, K. A. & VERA, P. L. 2005. Further evidence for increased macrophage migration inhibitory factor expression in prostate cancer. *BMC Cancer,* 5**,** 73.

MISHALIAN, I., BAYUH, R., LEVY, L., ZOLOTAROV, L., MICHAELI, J. & FRIDLENDER, Z. G. 2013. Tumor-associated neutrophils (TAN) develop pro-tumorigenic properties during tumor progression. *Cancer Immunol Immunother,* 62**,** 1745-56.

MITTELBRONN, M., PLATTEN, M., ZEINER, P., DOMBROWSKI, Y., FRANK, B., ZACHSKORN, C., HARTER, P. N., WELLER, M. & WISCHHUSEN, J. 2011. Macrophage migration inhibitory factor (MIF) expression in human malignant gliomas contributes to immune escape and tumour progression. *Acta Neuropathol,* 122**,** 353-65.

MOLLINEDO, F., NAKAJIMA, M., LLORENS, A., BARBOSA, E., CALLEJO, S., GAJATE, C. & FABRA, A. 1997. Major co-localization of the extracellular-matrix degradative enzymes heparanase and gelatinase in tertiary granules of human neutrophils. *The Biochemical journal,* 327 (Pt 3)**,** 917-23.

MORAND, E. F., LEECH, M. & BERNHAGEN, J. 2006. MIF: a new cytokine link between rheumatoid arthritis and atherosclerosis. *Nat Rev Drug Discov,* 5**,** 399-411.

MORI, K., HIROI, M., SHIMADA, J. & OHMORI, Y. 2011. Infiltration of m2 tumor-associated macrophages in oral squamous cell carcinoma correlates with tumor malignancy. *Cancers (Basel),* 3**,** 3726-39.

MUELLER, M. D., LEBOVIC, D. I., GARRETT, E. & TAYLOR, R. N. 2000. Neutrophils infiltrating the endometrium express vascular endothelial growth factor: potential role in endometrial angiogenesis. *Fertility and sterility,* 74**,** 107-12.

MURDOCH, MONK & FINN 1999. Functional expression of chemokine receptor CXCR4 on human epithelial cells. *Immunology,* 98**,** 36-41.

MURDOCH, C., GIANNOUDIS, A. & LEWIS, C. E. 2004. Mechanisms regulating the recruitment of macrophages into hypoxic areas of tumors and other ischemic tissues. *Blood,* 104**,** 2224-2234.

MURDOCH, C., MUTHANA, M., COFFELT, S. B. & LEWIS, C. E. 2008. The role of myeloid cells in the promotion of tumour angiogenesis. *Nat Rev Cancer,* 8**,** 618-31.

MUTHANA, M., KENNERLEY, A. J., HUGHES, R., FAGNANO, E., RICHARDSON, J., PAUL, M., MURDOCH, C., WRIGHT, F., PAYNE, C., LYTHGOE, M. F., FARROW, N., DOBSON, J., CONNER, J., WILD, J. M. & LEWIS, C. 2015. Directing cell therapy to anatomic target sites in vivo with magnetic resonance targeting. *Nature Communications,* 6**,** 8009.

NING, Y., MANEGOLD, P. C., HONG, Y. K., ZHANG, W., POHL, A., LURJE, G., WINDER, T., YANG, D., LABONTE, M. J., WILSON, P. M., LADNER, R. D. & LENZ, H.-J. 2011. Interleukin-8 is associated with proliferation, migration, angiogenesis and chemosensitivity in vitro and in vivo in colon cancer cell line models. *International Journal of Cancer,* 128**,** 2038-2049.

NISHIHIRA, J., KOYAMA, Y. & MIZUE, Y. 1998. IDENTIFICATION OF MACROPHAGE MIGRATION INHIBITORY FACTOR (MIF) IN HUMAN VASCULAR ENOTHELIAL CELLS AND ITS INDUCTION BY LIPOPOLYSACCHARIDE. *Cytokine,* 10**,** 199-205.

NORDSMARK, M. & OVERGAARD, J. 2000. A confirmatory prognostic study on oxygenation status and loco-regional control in advanced head and neck squamous cell carcinoma treated by radiation therapy. *Radiother Oncol,* 57**,** 39-43.

NOZAWA, H., CHIU, C. & HANAHAN, D. 2006. Infiltrating neutrophils mediate the initial angiogenic switch in a mouse model of multistage carcinogenesis. *Proceedings of the National Academy of Sciences of the United States of America,* 103**,** 12493-8.

ONODERA, S., NISHIHIRA, J., KOYAMA, Y., MAJIMA, T., AOKI, Y., ICHIYAMA, H., ISHIBASHI, T. & MINAMI, A. 2004. Macrophage migration inhibitory factor up-regulates the expression of interleukin-8 messenger RNA in synovial fibroblasts of rheumatoid arthritis patients: Common transcriptional regulatory mechanism between interleukin-8 and interleukin-1β. *Arthritis & Rheumatism,* 50**,** 1437-1447.

ORBAK, R., BAYRAKTAR, C., KAVRUT, F. & GÜNDOGDU, C. 2005. Poor oral hygiene and dental trauma as the precipitating factors of squamous cell carcinoma. *Oral Oncology Extra,* 41**,** 109-113.

ORLOVA, V. V., CHOI, E. Y., XIE, C., CHAVAKIS, E., BIERHAUS, A., IHANUS, E., BALLANTYNE, C. M., GAHMBERG, C. G., BIANCHI, M. E., NAWROTH, P. P. & CHAVAKIS, T. 2007. A novel

pathway of HMGB1-mediated inflammatory cell recruitment that requires Mac-1-integrin. *The EMBO journal,* 26**,** 1129-39.

PAI, S. I. & WESTRA, W. H. 2009. Molecular pathology of head and neck cancer: implications for diagnosis, prognosis, and treatment. *Annual review of pathology,* 4**,** 49-70.

PELUCCHI, C., TALAMINI, R., NEGRI, E., LEVI, F., CONTI, E., FRANCESCHI, S. & LA VECCHIA, C. 2003. Folate intake and risk of oral and pharyngeal cancer. *Ann Oncol,* 14**,** 1677-81.

PERISANIDIS, C., KORNEK, G., POSCHL, P. W., HOLZINGER, D., PIRKLBAUER, K., SCHOPPER, C. & EWERS, R. 2013. High neutrophil-to-lymphocyte ratio is an independent marker of poor disease-specific survival in patients with oral cancer. *Medical oncology,* 30**,** 334.

PIFFKO, J., BANKFALVI, A., OFNER, D., BRYNE, M., RASCH, D., JOOS, U., BOCKER, W. & SCHMID, K. W. 1997. Prognostic value of histobiological factors (malignancy grading and AgNOR content) assessed at the invasive tumour front of oral squamous cell carcinomas. *Br J Cancer,* 75**,** 1543-6.

PILLAY, J., DEN BRABER, I., VRISEKOOP, N., KWAST, L. M., DE BOER, R. J., BORGHANS, J. A., TESSELAAR, K. & KOENDERMAN, L. 2010. In vivo labeling with 2H2O reveals a human neutrophil lifespan of 5.4 days. *Blood,* 116**,** 625-7.

PROOST, P., DE WOLF-PEETERS, C., CONINGS, R., OPDENAKKER, G., BILLIAU, A. & VAN DAMME, J. 1993. Identification of a novel granulocyte chemotactic protein (GCP-2) from human tumor cells. In vitro and in vivo comparison with natural forms of GRO, IP-10, and IL-8. *Journal of immunology,* 150**,** 1000-10.

QIN, Z. 2012. The use of THP-1 cells as a model for mimicking the function and regulation of monocytes and macrophages in the vasculature. *Atherosclerosis,* 221**,** 2-11.

QUEEN, M. M., RYAN, R. E., HOLZER, R. G., KELLER-PECK, C. R. & JORCYK, C. L. 2005. Breast cancer cells stimulate neutrophils to produce oncostatin M: potential implications for tumor progression. *Cancer research,* 65**,** 8896-904.

RAGIN, C. C., MODUGNO, F. & GOLLIN, S. M. 2007. The epidemiology and risk factors of head and neck cancer: a focus on human papillomavirus. *Journal of dental research,* 86**,** 104-14.

RAGIN, C. C. & TAIOLI, E. 2007. Survival of squamous cell carcinoma of the head and neck in relation to human papillomavirus infection: review and meta-analysis. *International journal of cancer. Journal international du cancer,* 121**,** 1813-20.

RALEIGH, J. A., FRANKO, A. J., KELLY, D. A., TRIMBLE, L. A. & ALLEN, P. S. 1991. Development of an in vivo 19F magnetic resonance method for measuring oxygen deficiency in tumors. *Magn Reson Med,* 22**,** 451-66.

RAO, H. L., CHEN, J. W., LI, M., XIAO, Y. B., FU, J., ZENG, Y. X., CAI, M. Y. & XIE, D. 2012. Increased intratumoral neutrophil in colorectal carcinomas correlates closely with malignant phenotype and predicts patients' adverse prognosis. *PloS one,* 7**,** e30806.

REN, Y., TSUI, H.-T., POON, R. T.-P., NG, I. O.-L., LI, Z., CHEN, Y., JIANG, G., LAU, C., YU, W.-C., BACHER, M. & FAN, S.-T. 2003. Macrophage migration inhibitory factor: Roles in regulating tumor cell migration and expression of angiogenic factors in hepatocellular carcinoma. *International Journal of Cancer,* 107**,** 22-29.

RENDON, B. E., ROGER, T., TENENG, I., ZHAO, M., AL-ABED, Y., CALANDRA, T. & MITCHELL, R. A. 2007. Regulation of Human Lung Adenocarcinoma Cell Migration and Invasion by Macrophage Migration Inhibitory Factor. *Journal of Biological Chemistry,* 282**,** 29910-29918.

RIVERA, C. & VENEGAS, B. 2014. Histological and molecular aspects of oral squamous cell carcinoma (Review). *Oncology Letters,* 8**,** 7-11.

RODRIGUEZ, P. C., ERNSTOFF, M. S., HERNANDEZ, C., ATKINS, M., ZABALETA, J., SIERRA, R. & OCHOA, A. C. 2009. Arginase I-producing myeloid-derived suppressor cells in renal cell carcinoma are a subpopulation of activated granulocytes. *Cancer research,* 69**,** 1553-60.

ROGER, T., DAVID, J., GLAUSER, M. P. & CALANDRA, T. 2001. MIF regulates innate immune responses through modulation of Toll-like receptor 4. *Nature,* 414**,** 920-924.

ROSENGREN, E., BUCALA, R., AMAN, P., JACOBSSON, L., ODH, G., METZ, C. N. & RORSMAN, H. 1996. The immunoregulatory mediator macrophage migration inhibitory factor (MIF) catalyzes a tautomerization reaction. *Molecular Medicine,* 2**,** 143-149.

ROSENTHAL, E., MCCRORY, A., TALBERT, M., YOUNG, G., MURPHY-ULLRICH, J. & GLADSON, C. 2004. Elevated expression of TGF-beta1 in head and neck cancer-associated fibroblasts. *Mol Carcinog,* 40**,** 116-21.

ROSSI, A. G., HASLETT, C., HIRANI, N., GREENING, A. P., RAHMAN, I., METZ, C. N., BUCALA, R. & DONNELLY, S. C. Human circulating eosinophils secrete macrophage migration inhibitory factor (MIF). Potential role in asthma. *The Journal of Clinical Investigation,* 101**,** 2869-2874.

ROTONDO, R., BARISIONE, G., MASTRACCI, L., GROSSI, F., ORENGO, A. M., COSTA, R., TRUINI, M., FABBI, M., FERRINI, S. & BARBIERI, O. 2009. IL-8 induces exocytosis of arginase 1 by neutrophil polymorphonuclears in nonsmall cell lung cancer. *International journal of cancer. Journal international du cancer,* 125**,** 887-93.

RUSSELL, S. M., ANGELL, T. E., LECHNER, M. G., LIEBERTZ, D. J., CORREA, A. J., SINHA, U. K., KOKOT, N. & EPSTEIN, A. L. 2013. Immune cell infiltration patterns and survival in head and neck squamous cell carcinoma. *Head & neck oncology,* 5**,** 24.

SAKAKURA, K. & CHIKAMATSU, K. 2013. Immune suppression and evasion in patients with head and neck cancer. *2013,* 1.

SAMAN, D. M. 2012. A review of the epidemiology of oral and pharyngeal carcinoma: update. *Head & neck oncology,* 4**,** 1.

SANDHU, J. K., PRIVORA, H. F., WENCKEBACH, G. & BIRNBOIM, H. C. 2000. Neutrophils, nitric oxide synthase, and mutations in the mutatect murine tumor model. *The American journal of pathology,* 156**,** 509-18.

SANTOS, L. L., FAN, H., HALL, P., NGO, D., MACKAY, C. R., FINGERLE-ROWSON, G., BUCALA, R., HICKEY, M. J. & MORAND, E. F. 2011. Macrophage migration inhibitory factor regulates neutrophil chemotactic responses in inflammatory arthritis in mice. *Arthritis & Rheumatism,* 63**,** 960-970.

SCAFFIDI, P., MISTELI, T. & BIANCHI, M. E. 2002. Release of chromatin protein HMGB1 by necrotic cells triggers inflammation. *Nature,* 418**,** 191-5.

SCHAIDER, H., OKA, M., BOGENRIEDER, T., NESBIT, M., SATYAMOORTHY, K., BERKING, C., MATSUSHIMA, K. & HERLYN, M. 2003. Differential response of primary and metastatic melanomas to neutrophils attracted by IL-8. *International journal of cancer. Journal international du cancer,* 103**,** 335-43.

SCHMIEGEL, W., ROEDER, C., SCHMIELAU, J., RODECK, U. & KALTHOFF, H. 1993. Tumor necrosis factor alpha induces the expression of transforming growth factor alpha and the epidermal growth factor receptor in human pancreatic cancer cells. *Proceedings of the National Academy of Sciences,* 90**,** 863-867.

SCHOLS, D., STRUYF, S., VAN DAMME, J., ESTE, J. A., HENSON, G. & DE CLERCQ, E. 1997. Inhibition of T-tropic HIV strains by selective antagonization of the chemokine receptor CXCR4. *J Exp Med,* 186**,** 1383-8.

SCHRADER, J., DEUSTER, O., RINN, B., SCHULZ, M., KAUTZ, A., DODEL, R., MEYER, B., AL-ABED, Y., BALAKRISHNAN, K., REESE, J. P. & BACHER, M. 2009. Restoration of contact inhibition in human glioblastoma cell lines after MIF knockdown. *BMC Cancer,* 9**,** 464.

SCHULZ, R., MARCHENKO, N. D., HOLEMBOWSKI, L., FINGERLE-ROWSON, G., PESIC, M., ZENDER, L., DOBBELSTEIN, M. & MOLL, U. M. 2012. Inhibiting the HSP90 chaperone destabilizes macrophage migration inhibitory factor and thereby inhibits breast tumor progression. *J Exp Med,* 209**,** 275-89.

SCHWALLER, J., SCHNEIDER, P., MHAWECH-FAUCEGLIA, P., MCKEE, T., MYIT, S., MATTHES, T., TSCHOPP, J., DONZE, O., LE GAL, F. A. & HUARD, B. 2007. Neutrophil-derived APRIL concentrated in tumor lesions by proteoglycans correlates with human B-cell lymphoma aggressiveness. *Blood,* 109**,** 331-8.

SEMERAD, C. L., LIU, F., GREGORY, A. D., STUMPF, K. & LINK, D. C. 2002. G-CSF is an essential regulator of neutrophil trafficking from the bone marrow to the blood. *Immunity,* 17**,** 413-23.

SHAMAMIAN, P., POCOCK, B. J., SCHWARTZ, J. D., MONEA, S., CHUANG, N., WHITING, D., MARCUS, S. G., GALLOWAY, A. C. & MIGNATTI, P. 2000. Neutrophil-derived serine proteinases enhance membrane type-1 matrix metalloproteinase-dependent tumor cell invasion. *Surgery,* 127**,** 142-7.

SHEKHAR, M. P., WERDELL, J., SANTNER, S. J., PAULEY, R. J. & TAIT, L. 2001. Breast stroma plays a dominant regulatory role in breast epithelial growth and differentiation: implications for tumor development and progression. *Cancer Res,* 61**,** 1320-6.

SHI, X., LENG, L., WANG, T., WANG, W., DU, X., LI, J., MCDONALD, C., CHEN, Z., MURPHY, J. W., LOLIS, E., NOBLE, P., KNUDSON, W. & BUCALA, R. 2006. CD44 Is the Signaling Component of the Macrophage Migration Inhibitory Factor-CD74 Receptor Complex. *Immunity,* 25**,** 595-606.

SHIMIZU, T., ABE, R., NAKAMURA, H., OHKAWARA, A., SUZUKI, M. & NISHIHIRA, J. 1999. High Expression of Macrophage Migration Inhibitory Factor in Human Melanoma Cells and Its Role in Tumor Cell Growth and Angiogenesis. *Biochemical and Biophysical Research Communications,* 264**,** 751-758.

SHIMIZU, T., OHKAWARA, A., NISHIHIRA, J. & SAKAMOTO, W. 1996. Identification of macrophage migration inhibitory factor (MIF) in human skin and its immunohistochemical localization. *FEBS Letters,* 381**,** 199-202.

SHIN, D. M., CHARURUKS, N., LIPPMAN, S. M., LEE, J. J., RO, J. Y., HONG, W. K. & HITTELMAN, W. N. 2001. p53 protein accumulation and genomic instability in head and neck multistep tumorigenesis. *Cancer epidemiology, biomarkers & prevention : a publication of the American Association for Cancer Research, cosponsored by the American Society of Preventive Oncology,* 10**,** 603-9.

SHOJAEI, F., WU, X., ZHONG, C., YU, L., LIANG, X. H., YAO, J., BLANCHARD, D., BAIS, C., PEALE, F. V., VAN BRUGGEN, N., HO, C., ROSS, J., TAN, M., CARANO, R. A., MENG, Y. G. & FERRARA, N. 2007. Bv8 regulates myeloid-cell-dependent tumour angiogenesis. *Nature,* 450**,** 825-31.

SHWEIKI, D., ITIN, A., SOFFER, D. & KESHET, E. 1992. Vascular endothelial growth factor induced by hypoxia may mediate hypoxia-initiated angiogenesis. *Nature,* 359**,** 843-845.

SICA, A., SACCANI, A., BOTTAZZI, B., POLENTARUTTI, N., VECCHI, A., DAMME, J. V. & MANTOVANI, A. 2000. Autocrine Production of IL-10 Mediates Defective IL-12

Production and NF- B Activation in Tumor-Associated Macrophages. *The Journal of Immunology,* 164**,** 762-767.

SLATTERY, M. J. & DONG, C. 2003. Neutrophils influence melanoma adhesion and migration under flow conditions. *International journal of cancer. Journal international du cancer,* 106**,** 713-22.

SMITH, E. M., RITCHIE, J. M., SUMMERSGILL, K. F., KLUSSMANN, J. P., LEE, J. H., WANG, D., HAUGEN, T. H. & TUREK, L. P. 2004. Age, sexual behavior and human papillomavirus infection in oral cavity and oropharyngeal cancers. *International journal of cancer. Journal international du cancer,* 108**,** 766-72.

SOYLU, L., OZCAN, C., CETIK, F., PAYDAS, S., KIROGLU, M., AYDOGAN, B., SARGIN, O., OZSAHINOGLU, C. & SEYREK, E. 1994. Serum levels of tumor necrosis factor in squamous cell carcinoma of the head and neck. *Am J Otolaryngol,* 15**,** 281-5.

SPICER, J. D., MCDONALD, B., COOLS-LARTIGUE, J. J., CHOW, S. C., GIANNIAS, B., KUBES, P. & FERRI, L. E. 2012. Neutrophils promote liver metastasis via Mac-1-mediated interactions with circulating tumor cells. *Cancer research,* 72**,** 3919-27.

ST HILL, C. A., KRIESER, K. & FAROOQUI, M. 2011. Neutrophil interactions with sialyl Lewis X on human nonsmall cell lung carcinoma cells regulate invasive behavior. *Cancer,* 117**,** 4493-505.

STAIRS, D. B., BAYNE, L. J., RHOADES, B., VEGA, M. E., WALDRON, T. J., KALABIS, J., KLEIN-SZANTO, A., LEE, J. S., KATZ, J. P., DIEHL, J. A., REYNOLDS, A. B., VONDERHEIDE, R. H. & RUSTGI, A. K. 2011. Deletion of p120-catenin results in a tumor microenvironment with inflammation and cancer that establishes it as a tumor suppressor gene. *Cancer Cell,* 19**,** 470-83.

STAMPS, S. L., FITZGERALD, M. C. & WHITMAN, C. P. 1998. Characterization of the Role of the Amino-Terminal Proline in the Enzymatic Activity Catalyzed by Macrophage Migration Inhibitory Factor. *Biochemistry,* 37**,** 10195-10202.

STEELE, COLIN W., KARIM, SAADIA A., LEACH, JOSHUA D., BAILEY, P., UPSTILL-GODDARD, R., RISHI, L., FOTH, M., BRYSON, S., MCDAID, K., WILSON, Z., EBERLEIN, C., CANDIDO, JULIANA B., CLARKE, M., NIXON, C., CONNELLY, J., JAMIESON, N., CARTER, C R., BALKWILL, F., CHANG, DAVID K., EVANS, TR J., STRATHDEE, D., BIANKIN, ANDREW V., NIBBS, ROBERT J., BARRY, SIMON T., SANSOM, OWEN J. & MORTON, JENNIFER P. 2016. CXCR2 Inhibition Profoundly Suppresses Metastases and Augments Immunotherapy in Pancreatic Ductal Adenocarcinoma. *Cancer Cell,* 29**,** 832-845.

SUTHERLAND, R. M. & DURAND, R. E. 1984. Growth and cellular characteristics of multicell spheroids. *Recent Results Cancer Res,* 95**,** 24-49.

SUTHERLAND, R. M., MCCREDIE, J. A. & INCH, W. R. 1971. Growth of Multicell Spheroids in Tissue Culture as a Model of Nodular Carcinomas. *Journal of the National Cancer Institute,* 46**,** 113-120.

SUZUKI, M., SUGIMOTO, H., NAKAGAWA, A., TANAKA, I., NISHIHIRA, J. & SAKAI, M. 1996. Crystal structure of the macrophage migration inhibitory factor from rat liver. *Nat Struct Biol,* 3**,** 259-66.

SWARTZ, J. E., POTHEN, A. J., STEGEMAN, I., WILLEMS, S. M. & GROLMAN, W. 2015. Clinical implications of hypoxia biomarker expression in head and neck squamous cell carcinoma: a systematic review. *Cancer Med,* 4**,** 1101-16.

SWOPE, M., SUN, H. W., BLAKE, P. R. & LOLIS, E. 1998. Direct link between cytokine activity and a catalytic site for macrophage migration inhibitory factor. *The EMBO Journal,* 17**,** 3534-3541.

TAKEYA, M. & KOMOHARA, Y. 2016. Role of tumor-associated macrophages in human malignancies: friend or foe? *Pathol Int,* 66**,** 491-505.

TANIMOTO, N., TERASAWA, M., NAKAMURA, M., KEGAI, D., AOSHIMA, N., KOBAYASHI, Y. & NAGATA, K. 2007. Involvement of KC, MIP-2, and MCP-1 in leukocyte infiltration following injection of necrotic cells into the peritoneal cavity. *Biochem Biophys Res Commun,* 361**,** 533-6.

TAZZYMAN, S., BARRY, S. T., ASHTON, S., WOOD, P., BLAKEY, D., LEWIS, C. E. & MURDOCH, C. 2011. Inhibition of neutrophil infiltration into A549 lung tumors in vitro and in vivo using a CXCR2-specific antagonist is associated with reduced tumor growth. *International journal of cancer. Journal international du cancer,* 129**,** 847-58.

TAZZYMAN, S., LEWIS, C. E. & MURDOCH, C. 2009. Neutrophils: key mediators of tumour angiogenesis. *International journal of experimental pathology,* 90**,** 222-31.

TAZZYMAN, S., NIAZ, H. & MURDOCH, C. 2013. Neutrophil-mediated tumour angiogenesis: Subversion of immune responses to promote tumour growth. *Seminars in Cancer Biology,* 23**,** 149-158.

THOMLINSON, R. H. & GRAY, L. H. 1955. The Histological Structure of Some Human Lung Cancers and the Possible Implications for Radiotherapy. *British Journal of Cancer,* 9**,** 539-549.

TILLMANN, S., BERNHAGEN, J. & NOELS, H. 2013. Arrest Functions of the MIF Ligand/Receptor Axes in Atherogenesis. *Front Immunol,* 4**,** 115.

TORSTEINSDÓTTIR, ARVIDSON, HÄLLGREN & HÅKANSSON 1999. Enhanced Expression of Integrins and CD66b on Peripheral Blood Neutrophils and Eosinophils in Patients with Rheumatoid Arthritis, and the Effect of Glucocorticoids. *Scandinavian Journal of Immunology,* 50**,** 433-439.

TRELLAKIS, S., BRUDEREK, K., DUMITRU, C. A., GHOLAMAN, H., GU, X., BANKFALVI, A., SCHERAG, A., HUTTE, J., DOMINAS, N., LEHNERDT, G. F., HOFFMANN, T. K., LANG, S. & BRANDAU, S. 2011a. Polymorphonuclear granulocytes in human head and neck cancer: enhanced inflammatory activity, modulation by cancer cells and expansion in advanced disease. *International journal of cancer. Journal international du cancer,* 129**,** 2183-93.

TRELLAKIS, S., FARJAH, H., BRUDEREK, K., DUMITRU, C. A., HOFFMANN, T. K., LANG, S. & BRANDAU, S. 2011b. Peripheral blood neutrophil granulocytes from patients with head and neck squamous cell carcinoma functionally differ from their counterparts in healthy donors. *International journal of immunopathology and pharmacology,* 24**,** 683-93.

ULLMAN, T. A. & ITZKOWITZ, S. H. 2011. Intestinal inflammation and cancer. *Gastroenterology,* 140**,** 1807-16.

URBAN, C. F., ERMERT, D., SCHMID, M., ABU-ABED, U., GOOSMANN, C., NACKEN, W., BRINKMANN, V., JUNGBLUT, P. R. & ZYCHLINSKY, A. 2009. Neutrophil extracellular traps contain calprotectin, a cytosolic protein complex involved in host defense against Candida albicans. *PLoS Pathog,* 5**,** e1000639.

VAN DONGEN, J. J., QUERTERMOUS, T., BARTRAM, C. R., GOLD, D. P., WOLVERS-TETTERO, I. L., COMANS-BITTER, W. M., HOOIJKAAS, H., ADRIAANSEN, H. J., DE KLEIN, A., RAGHAVACHAR, A. & ET AL. 1987. T cell receptor-CD3 complex during early T cell differentiation. Analysis of immature T cell acute lymphoblastic leukemias (T-ALL) at DNA, RNA, and cell membrane level. *J Immunol,* 138**,** 1260-9.

VAN EGMOND, M., VAN SPRIEL, A. B., VERMEULEN, H., HULS, G., VAN GARDEREN, E. & VAN DE WINKEL, J. G. J. 2001. Enhancement of Polymorphonuclear Cell-mediated Tumor Cell Killing on Simultaneous Engagement of FcγRI (CD64) and FcαRI (CD89). *Cancer Research,* 61**,** 4055-4060.

VAN OVERMEIRE, E., LAOUI, D., KEIRSSE, J., VAN GINDERACHTER, J. A. & SARUKHAN, A. 2014. Mechanisms driving macrophage diversity and specialization in distinct tumor microenvironments and parallelisms with other tissues. *Front Immunol,* 5**,** 127.

VARNEY, M. L., SINGH, S., LI, A., MAYER-EZELL, R., BOND, R. & SINGH, R. K. 2011. Small molecule antagonists for CXCR2 and CXCR1 inhibit human colon cancer liver metastases. *Cancer Letters,* 300**,** 180-188.

VAUPEL, P. & MAYER, A. 2007. Hypoxia in cancer: significance and impact on clinical outcome. *Cancer and Metastasis Reviews,* 26**,** 225-239.

VERBEKE, H., STRUYF, S., BERGHMANS, N., VAN COILLIE, E., OPDENAKKER, G., UYTTENHOVE, C., VAN SNICK, J. & VAN DAMME, J. 2011. Isotypic neutralizing antibodies against mouse GCP-2/CXCL6 inhibit melanoma growth and metastasis. *Cancer letters,* 302**,** 54-62.

VERED, M., DAYAN, D., YAHALOM, R., DOBRIYAN, A., BARSHACK, I., BELLO, I. O., KANTOLA, S. & SALO, T. 2010. Cancer-associated fibroblasts and epithelial-mesenchymal transition in metastatic oral tongue squamous cell carcinoma. *Int J Cancer,* 127**,** 1356-62.

VOGIATZI, K., APOSTOLAKIS, S., VLATA, Z., KRABOVITIS, E. & SPANDIDOS, D. A. 2013. Opposite effect of angiotensin receptor blockade on CXCL8 production and CXCR1/2 expression of angiotensin II-treated THP-1 monocytes. *Experimental and Therapeutic Medicine,* 5**,** 987-991.

WALMSLEY, S. R., PRINT, C., FARAHI, N., PEYSSONNAUX, C., JOHNSON, R. S., CRAMER, T., SOBOLEWSKI, A., CONDLIFFE, A. M., COWBURN, A. S., JOHNSON, N. & CHILVERS, E. R. 2005. Hypoxia-induced neutrophil survival is mediated by HIF-1α–dependent NF-κB activity. *The Journal of Experimental Medicine,* 201**,** 105-115.

WANG, D., SONG, H., EVANS, J. A., LANG, J. C., SCHULLER, D. E. & WEGHORST, C. M. 1997. Mutation and downregulation of the transforming growth factor beta type II receptor gene in primary squamous cell carcinomas of the head and neck. *Carcinogenesis,* 18**,** 2285-2290.

WANG, J., OU, Z. L., HOU, Y. F., LUO, J. M., SHEN, Z. Z., DING, J. & SHAO, Z. M. 2006. Enhanced expression of Duffy antigen receptor for chemokines by breast cancer cells attenuates growth and metastasis potential. *Oncogene,* 25**,** 7201-7211.

WANG, L., CHEN, C., LI, F., HUA, Q., CHEN, S., XIAO, B., DAI, M., LI, M., ZHENG, A., YU, D., HU, Z. & TAO, Z. 2015. Down-regulation of neutrophil gelatinase-associated lipocalin in head and neck squamous cell carcinoma correlated with tumorigenesis, not with metastasis. *Int J Clin Exp Pathol,* 8**,** 8857-68.

WANG, N., FENG, Y., WANG, Q., LIU, S., XIANG, L., SUN, M., ZHANG, X., LIU, G., QU, X. & WEI, F. 2014. Neutrophils Infiltration in the Tongue Squamous Cell Carcinoma and Its Correlation with CEACAM1 Expression on Tumor Cells. *PLoS ONE,* 9**,** e89991.

WARNAKULASURIYA, S. 2009. Global epidemiology of oral and oropharyngeal cancer. *Oral oncology,* 45**,** 309-16.

WEBER, C., KRAEMER, S., DRECHSLER, M., LUE, H., KOENEN, R. R., KAPURNIOTU, A., ZERNECKE, A. & BERNHAGEN, J. 2008. Structural determinants of MIF functions in CXCR2-mediated inflammatory and atherogenic leukocyte recruitment. *Proceedings*

of the National Academy of Sciences of the United States of America, 105**,** 16278-16283.

WEIDNER, N. 1995. Intratumor microvessel density as a prognostic factor in cancer. *The American Journal of Pathology,* 147**,** 9-19.

WELCH, D. R., SCHISSEL, D. J., HOWREY, R. P. & AEED, P. A. 1989. Tumor-elicited polymorphonuclear cells, in contrast to "normal" circulating polymorphonuclear cells, stimulate invasive and metastatic potentials of rat mammary adenocarcinoma cells. *Proceedings of the National Academy of Sciences of the United States of America,* 86**,** 5859-63.

WELLER, M. D., NANKIVELL, P. C., MCCONKEY, C., PALERI, V. & MEHANNA, H. M. 2010. The risk and interval to malignancy of patients with laryngeal dysplasia; a systematic review of case series and meta-analysis. *Clin Otolaryngol,* 35**,** 364-72.

WERNER, S. & GROSE, R. 2003. Regulation of wound healing by growth factors and cytokines. *Physiological reviews,* 83**,** 835-70.

WHITE, E. S., STROM, S. R. B., WYS, N. L. & ARENBERG, D. A. 2001. Non-Small Cell Lung Cancer Cells Induce Monocytes to Increase Expression of Angiogenic Activity. *The Journal of Immunology,* 166**,** 7549-7555.

WILLIAMS, M. R., AZCUTIA, V., NEWTON, G., ALCAIDE, P. & LUSCINSKAS, F. W. 2011. Emerging mechanisms of neutrophil recruitment across endothelium. *Trends in immunology,* 32**,** 461-9.

WINNER, M., KOONG, A. C., RENDON, B. E., ZUNDEL, W. & MITCHELL, R. A. 2007. Amplification of Tumor Hypoxic Responses by Macrophage Migration Inhibitory Factor–Dependent Hypoxia-Inducible Factor Stabilization. *Cancer Research,* 67**,** 186-193.

WISLEZ, M., FLEURY-FEITH, J., RABBE, N., MOREAU, J., CESARI, D., MILLERON, B., MAYAUD, C., ANTOINE, M., SOLER, P. & CADRANEL, J. 2001. Tumor-derived granulocyte-macrophage colony-stimulating factor and granulocyte colony-stimulating factor prolong the survival of neutrophils infiltrating bronchoalveolar subtype pulmonary adenocarcinoma. *The American journal of pathology,* 159**,** 1423-33.

XIE, J., YANG, L., TIAN, L., LI, W., YANG, L. & LI, L. 2016. Macrophage Migration Inhibitor Factor Upregulates MCP-1 Expression in an Autocrine Manner in Hepatocytes during Acute Mouse Liver Injury. *Scientific Reports,* 6**,** 27665.

XIE, K. 2001. Interleukin-8 and human cancer biology. *Cytokine & growth factor reviews,* 12**,** 375-91.

XU, X., WANG, B., YE, C., YAO, C., LIN, Y., HUANG, X., ZHANG, Y. & WANG, S. 2008. Overexpression of macrophage migration inhibitory factor induces angiogenesis in human breast cancer. *Cancer Lett,* 261**,** 147-57.

YADDANAPUDI, K., RENDON, B. E., LAMONT, G., KIM, E. J., AL RAYYAN, N., RICHIE, J., ALBEITUNI, S., WAIGEL, S., WISE, A. & MITCHELL, R. A. 2016. MIF Is Necessary for Late-Stage Melanoma Patient MDSC Immune Suppression and Differentiation. *Cancer Immunology Research,* 4**,** 101-112.

YAMASHITA, J., OGAWA, M. & SHIRAKUSA, T. 1995. Free-form neutrophil elastase is an independent marker predicting recurrence in primary breast cancer. *Journal of leukocyte biology,* 57**,** 375-8.

YAN, X., ORENTAS, R. J. & JOHNSON, B. D. 2006. Tumor-derived macrophage migration inhibitory factor (MIF) inhibits T lymphocyte activation. *Cytokine,* 33**,** 188-198.

YANG, N., NIKOLIC-PATERSON, D. J., NG, Y. Y., MU, W., METZ, C., BACHER, M., MEINHARDT, A., BUCALA, R., ATKINS, R. C. & LAN, H. Y. 1998. Reversal of established rat crescentic

glomerulonephritis by blockade of macrophage migration inhibitory factor (MIF): potential role of MIF in regulating glucocorticoid production. *Molecular Medicine,* 4**,** 413-424.

YANG, Y., DEGRANPRÉ, P., KHARFI, A. & AKOUM, A. 2000. Identification of Macrophage Migration Inhibitory Factor as a Potent Endothelial Cell Growth-Promoting Agent Released by Ectopic Human Endometrial Cells1. *The Journal of Clinical Endocrinology & Metabolism,* 85**,** 4721-4727.

ZARBOCK, A. & LEY, K. 2008. Mechanisms and consequences of neutrophil interaction with the endothelium. *The American journal of pathology,* 172**,** 1-7.

ZETTER, B. R. 1998. Angiogenesis and tumor metastasis. *Annual review of medicine,* 49**,** 407-24.

ZHANG, B., QIANGBA, Y. Z., SHANG, P., WANG, Z. X., MA, J., WANG, L. Y. & ZHANG, H. 2015. A Comprehensive MicroRNA Expression Profile Related to Hypoxia Adaptation in the Tibetan Pig. *Plos One,* 10.

ZHAO, J. J., PAN, K., WANG, W., CHEN, J. G., WU, Y. H., LV, L., LI, J. J., CHEN, Y. B., WANG, D. D., PAN, Q. Z., LI, X. D. & XIA, J. C. 2012. The prognostic value of tumor-infiltrating neutrophils in gastric adenocarcinoma after resection. *PloS one,* 7**,** e33655.

ZHOU, S. L., DAI, Z., ZHOU, Z. J., WANG, X. Y., YANG, G. H., WANG, Z., HUANG, X. W., FAN, J. & ZHOU, J. 2012. Overexpression of CXCL5 mediates neutrophil infiltration and indicates poor prognosis for hepatocellular carcinoma. *Hepatology,* 56**,** 2242-54.

ZHOU, S. L., ZHOU, Z. J., HU, Z. Q., HUANG, X. W., WANG, Z., CHEN, E. B., FAN, J., CAO, Y., DAI, Z. & ZHOU, J. 2016. Tumor-Associated Neutrophils Recruit Macrophages and T-Regulatory Cells to Promote Progression of Hepatocellular Carcinoma and Resistance to Sorafenib. *Gastroenterology,* 150**,** 1646-1658 e17.

ZHU, G., TANG, Y., GENG, N., ZHENG, M., JIANG, J., LI, L., LI, K., LEI, Z., CHEN, W., FAN, Y., MA, X., LI, L., WANG, X. & LIANG, X. 2014. HIF-alpha/MIF and NF-kappaB/IL-6 axes contribute to the recruitment of CD11b+Gr-1+ myeloid cells in hypoxic microenvironment of HNSCC. *Neoplasia,* 16**,** 168-79.

APPENDIX I

Case	Age	Gender	Site	Diagnosis
1	55	M	Tongue	Normal
2	72	F	Buccal mucosa	Normal
3	69	F	Buccal mucosa	Normal
4	59	F	Buccal mucosa	Normal
5	58	F	Buccal mucosa	Normal
6	33	F	Buccal mucosa	Normal
7	57	M	Buccal mucosa	Normal
8	56	F	Buccal mucosa	Normal
9	36	F	Labial mucosa	Normal
10	16	M	Tongue	Normal
11	75	M	Lower lip	SCC mod diff
12	74	M	Tongue	SCC mod diff
13	77	F	Tongue	SCC mod diff
14	57	M	Tongue	SCC mod diff
15	73	F	Lip	SCC mod diff
16	67	M	Lip	SCC mod diff
17	76	F	Floor of mouth	SCC mod diff
18	43	M	Tongue	SCC mod diff
19	54	M	Tongue	SCC mod diff
20	37	F	Tongue	SCC mod diff
21	85	F	Tongue	SCC mod diff
22	38	M	Tongue	SCC mod diff
23	67	F	Tongue	SCC mod diff
24	62	F	Floor of mouth	SCC mod diff
25	57	M	Tongue	SCC mod diff
26	76	M	Tongue	SCC mod diff
27	72	M	Tongue	SCC mod diff

Table 1. Detection of neutrophils in healthy and cancer tissue. A panel of ten normal and seventeen HNSCC tumour tissue sections were screened for the presence of neutrophils using the neutrophil-specific marker CD66b. Abbreviations: M= Male, F=Female

Case	sex	Site	Age	Stage	Other node	Grade	Recurrence	Follow up (months)	Survival	A	Presence of Necrosis
1	F	RMT	69	T1N1mi	Yes	well	yes	9	DoD	433±211	Yes
2	M	RMT	66	T4N2b	Yes	UN	no	24	DF	14±3.4	No
3	F	FOM	59	T2N2b	Yes	UN	no	72	DF	32.75±5.9	No
4	F	AT	63	T4N1	NO	well	no	72	DF	0.041±0.041	No
5	F	PT	83	T2N2b	Yes	well	no	24	DF	944±184.4	Yes
6	M	AT	65	T1N1	NO	Mod	2nd P	48	DUR	3116±787	Yes
7	M	FOM	?	T2N2b	Yes	UN	UN	UN	UN	1240±519	Yes
8	F	AT	54	T1N1mi	NO	UN	no	24	DF	0.6±0.4	No
9	F	HP	50	T1N2c	NO	POOR	UN	UN	UN	1526±8.9	Yes
10	M	AT	50	T1N1	NO	Mod	no	60	DF	1831±392	Yes
11	M	FOM	65	T1N2c	?	UN	UN	UN	UN	2431±140	Yes
12	M	AT	71	T1N1	NO	Mod	no	96	DF	1076±382	Yes
13	F	FOM	54	T1N2c	NO	UN	UN	UN	UN	38.5±16.6	No
14	F	FOM	76	T2N1	NO	Well	no	6	DUR	692±175	Yes
15	M	FOM	60	T4N1	NO	UN	no	60	DF	15.9±5.2	No

16	M	FOM	53	T1N1mi	NO	UN	yes	36	AWD	8.5±3.7	No
17	M	AT	49	T1N1mi	NO	UN	no	96	DF	374±117	Yes
18	M	PT	57	T2N1	NO	UN	no	72	DF	1723±398	Yes
19	M	FOM	51	T1N2b	Yes	UN	yes	84	DF	9.7±4.3	No
20	F	RMT	73	T1N1	Yes	Well	Yes	12	DF	1.6±0.88	No
21	M	FOM	37	T1N2b	NO	UN	2nd P	96	AWD	127±49.9	No
22	M	FOM	62	T1N1	NO	UN	no	144	DUR	394±76.8	Yes
23	M	FOM	59	T1N2b	Yes	Mod	yes	84	DF	97.9±25.3	No
24	M	FOM	60	T4N1mi	NO	UN	2nd P	48	DUR	28.25±12	No
25	M	RMT	65	T3N1	NO	UN	UN	UN	UN	614±170	Yes
26	M	FOM	67	T4N1	NO	Mod	no	48	DF	555±87	Yes
27	M	SP	UN	T3N2b	Yes	UN	UN	UN	UN	994±250	Yes
28	M	RMT	55	T4N2b	Yes	Mod	no	72	DF	3.5±1.6	No
29	F	FOM	67	T4N1	Yes	UN	no	12	DUR	565±17.9	Yes
30	M	FOM	58	T2N1	NO	Mod	no	18	DUR	160±9	Mod

Table 2: Patient and tumour characteristics for MPO distrubtion study . Abbreviations: M= Male, F=Female, RMT=Retromolar trigone, FOM=Floor of mouth, AT=anterior tongue, PT= posterior tongue, HP= Hard palate, SP=soft palate, DoD= dead of disease, DF=disease free, DUR=dead unrelated cause, AWD=alive with disease

APPENDIX II

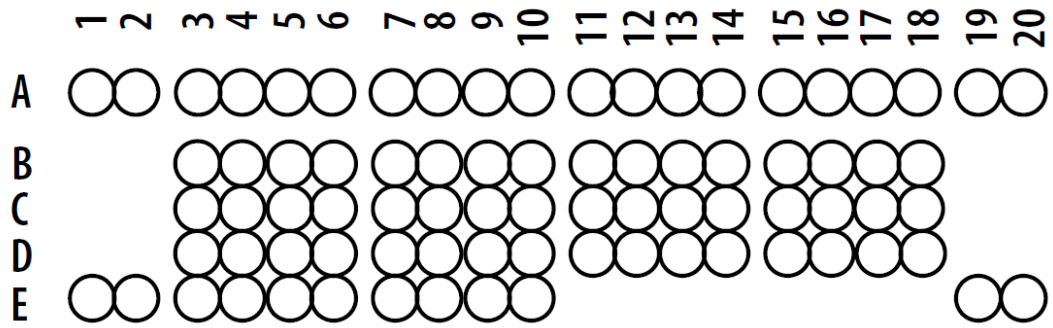

Figure 1 A human cytokines array coordinates for localizing the positive detected in the array

Coordinate	Target/Control	Alternate Nomenclature
A1, A2	Reference Spot	—
A3, A4	C5/C5a	Complement Component 5/5a
A5, A6	CD40 Ligand	CD154
A7, A8	G-CSF	CSFβ, CSF-3
A9, A10	GM-CSF	CSFα, CSF-2
A11, A12	GROα	CXCL1
A13, A14	I-309	CCL1
A15, A16	sICAM-1	CD54
A17, A18	IFN-γ	Type II IFN
A19, A20	Reference Spot	—
B3, B4	IL-1α	IL-1F1
B5, B6	IL-1β	IL-1F2
B7, B8	IL-1ra	IL-1F3
B9, B10	IL-2	—
B11, B12	IL-4	—
B13, B14	IL-5	—
B15, B16	IL-6	—
B17, B18	IL-8	CXCL8
C3, C4	IL-10	—
C5, C6	IL-12 p70	—
C7, C8	IL-13	—
C9, C10	IL-16	LCF
C11, C12	IL-17	—
C13, C14	IL-17E	—
C15, C16	IL-23	—
C17, C18	IL-27	—

Coordinate	Target/Control	Alternate Nomenclature
D3, D4	IL-32α	—
D5, D6	IP-10	CXCL10
D7, D8	I-TAC	CXCL11
D9, D10	MCP-1	CCL2
D11, D12	MIF	GIF, DER6
D13, D14	MIP-1α	CCL3
D15, D16	MIP-1β	CCL4
D17, D18	Serpin E1	PAI-1
E1, E2	Reference Spot	—
E3, E4	RANTES	CCL5
E5, E6	SDF-1	CXCL12
E7, E8	TNF-α	TNFSF1A
E9, E10	sTREM-1	—
E19, E20	Negative Control	—

Table 1: showing the cytokine/growth factor proteins detected in the array coordinates.